Évaluation de la performance métabolique et de la croissance du sébaste (*Sebastes fasciatus*) dans un contexte de changement global

Thèse présentée

dans le cadre du programme de doctorat en océanographie

en vue de l'obtention du grade de philosophiae doctor (Ph.D.)

PAR

© JOËLLE GUITARD

Avril 2026

Composition du jury :

Fanny Noisette, présidente du jury, Université du Québec à Rimouski

David Deslauriers, directeur de recherche, Université du Québec à Rimouski

Denis Chabot, codirecteur de recherche, Pêches et Océans Canada

Dominique Robert, codirecteur de recherche, Université du Québec à Rimouski

David McKenzie, examinateur externe, Université de Montpellier

Dépôt initial le 04 décembre 2025 Dépôt final le 27 avril 2026

On est esclave de ce que nous disons et maîtres de ce que nous taisons.
- Miguel Bonnefoy, Le rêve du Jaguar.

REMERCIEMENTS

J’aimerais premièrement remercier mes directeurs de thèse. Merci pour l’opportunité d’avoir entrepris ce projet, mais surtout pour la confiance que vous m’avez accordée. Merci David de m’avoir fait confiance comme ta première étudiante au doctorat. J’ai beaucoup grandi à travers ce cheminement, mais j’espère avoir pu faire la même chose pour toi. Je me considère chanceuse d’avoir pu travailler avec toi et Dominique. Mes idées et mes opinions ont toujours été écoutées et respectées. Je sentais vraiment la liberté que vous m’offriez sur ce projet, mais aussi sur les à-côtés que comporte le fait d’être une étudiante au doctorat : les conférences, le terrain, les retraites de rédaction. Mais cette équipe n’aurait pas été complète sans mon autre co-directeur, Denis. Dès que j’ai vu ton nom sur l’offre de doctorat, je savais que ce serait un projet intéressant, mais surtout avec quelqu’un de très gentil et compétent à son bord. C’est ce qui arrive quand on a une très bonne réputation ! Les gens à qui j’ai demandé conseil m’ont tous encouragée à aller essayer un projet qui avait Denis Chabot à son bord, et je ne l’ai pas regretté. Merci pour les discussions dans ton bureau, à l’IML ou chez toi, dans ton jardin ou devant R, avec ou sans bière, avec ou sans chat noir. J’ai énormément appris avec toi, non seulement sur la programmation en R, sur la respirométrie et sur le métabolisme des poissons, mais aussi sur moi-même. J’ai appris à me faire plus confiance, à ne pas avoir peur de me tromper, à oser. Même si, je l’espère, ce sont des traits normaux d’un processus de doctorat, je n’aurais pas pu rêver meilleur partenaire pour les développer.

Travailler avec Denis m’a aussi permis de réaliser ce projet au sein de Pêches et Océans Canada, à l’Institut Maurice-Lamontagne, avec tout l’équipement, mais surtout l’équipe que cela implique. Un grand merci à David Picard, qui a été une des premières personnes à me montrer les aléas de la salle des bassins et qui a non seulement réglé, mais aussi su m’apprendre à régler de multiples problèmes techniques. Merci à Tanya, qui prend toujours

aussi bien soin de nos poissons. J'ai beaucoup aimé apprendre à te connaître. Merci à Jérôme Gagnon de savoir si bien faire rouler une salle des bassins. Mes expériences à la salle des bassins n'auraient pas été les mêmes sans toutes ces personnes pour m'aider. Mais surtout, merci à Christophe Benjamin, Élodie Beaulieu et Sarah-Maude Gagnon d'avoir jeté un coup d'œil et de m'avoir assistée à pourchasser des poissons. Votre aide était précieuse. Merci à Caroline Senay d'avoir été, entre autres, à la genèse de ce projet, de m'avoir instruite et d'avoir répondu à mes multiples questions, toujours avec plaisir, sur le sébaste et sa dynamique dans son milieu naturel.

Je tiens à remercier l'équipe de plongeurs qui a récolté les sébastes en milieu naturel. Ramener de tels poissons à la surface est peut-être une tâche amusante, mais ce n'est pas une tâche simple, et je suis redevable de votre expertise sur le terrain, car grâce à elle, j'ai pu disposer d'un nombre incroyable d'organismes pour répondre aux multiples questions de recherche qui me sont passées par la tête. Merci Kathleen McGregor, Jean-Daniel Larivière-Tourangeau, Laélien Bassin, Jill Heinerth et surtout, mon meilleur attrapeur de sébastes, Frédéric Hartog. Les missions sur le terrain auxquelles j'ai participé ont créé de magnifiques souvenirs que je garderai de mon temps passé au doctorat. Merci pour votre soutien avec la respirométrie *in situ* et votre volonté d'essayer quelque chose de nouveau. Merci à Frédérick Bélanger d'avoir réussi à construire LE respiromètre *in situ* et d'avoir rendu tangible cette idée folle qui sommeillait dans la tête de David.

Un tel projet ne serait pas possible sans l'important soutien financier que nous avons reçu. Premièrement, je tiens à remercier Pêches et Océans Canada pour la subvention du projet Redtanks, qui nous a permis de récolter et de maintenir des sébastes vivants à la salle des bassins de l'Institut Maurice-Lamontagne. Ensuite, j'aimerais remercier les différents organismes qui ont soutenu mon projet, autant au niveau de bourses personnelles que pour la réalisation de projets indépendants et le financement de conférences : les bourses d'excellence au doctorat de l'Institut des sciences de la mer, les Fonds de recherche du Québec – Nature et technologies (FRQNT), le Conseil de recherches en sciences naturelles

et en génie du Canada (CRSNG), les bourses Estelle-Laberge, Ressources aquatiques Québec, PyroScience et la Fisheries Society of the British Isles.

J'aimerais prendre quelques lignes pour remercier la lignée scientifique de mon parcours pré-doctoral, qui m'a permis d'arriver au doctorat, mais surtout qui m'a fourni les outils pour le mener à bien. Merci Sandra Ann Binning de m'avoir donné une chance en tant qu'étudiante à la maîtrise. Mon parcours avec toi a été extrêmement instructif sur le monde de la science et m'a grandement aidée tout au long de mon doctorat. Je me considère extrêmement chanceuse d'avoir été une des premières diplômées du labo Binning et j'en suis ressortie avec des connaissances scientifiques et humaines qui me serviront tout au long de ma carrière. Le passage par ton labo m'a aussi permis de développer mes propres connexions dans le monde de la physiologie des poissons, ainsi qu'une confiance et une méthodologie durables. Être dans ton labo m'a aussi permis de travailler auprès de mon ami Jérémy et de rencontrer Emmanuelle qui m'ont beaucoup appris, merci Manu d'avoir toujours cru en moi et d'avoir fait partie de mon projet de maîtrise.

Ce doctorat n'aurait pas été aussi équilibré sans un entourage hors pair. Merci à Grégoire et Alexis, mes premiers amis avec qui j'ai traversé la dure épreuve de l'examen doctoral. Au moment d'écrire ces mots, vous êtes tous les deux sur la fin de votre doctorat et j'ai hâte que vous passiez de l'autre côté avec moi. Vous verrez, ça se termine un jour !

Merci Nathalia d'avoir fait partie de ma vie de bureau, d'avoir partagé rires et pleurs.

Merci aux précieuses amies que je me suis fait au long de ce parcours : Caroline Fink-Mercier, Alice Morard, Camille Brice, Camille Berthod, Juliette Girard et Kelsey Koerner. Vous êtes des femmes incroyables et je me considère chanceuse de vous avoir rencontrées durant ce parcours. Merci à Dou d'avoir répondu présente jusqu'à la fin.

Merci aussi à tous les autres amis que j'ai rencontrés. Ce serait plus facile si je remerciais la Bretagne en entier, mais je vais tout de même nommer quelques noms 😉 : Quentin, Delphine, Guillaume, Sarah, Lola, Tony, Schmutz, Océanne… j'en oublie sûrement. Merci aux Quentin, Morgane et Christian pour les magnifiques parties de tarot.

Merci à ma précieuse amie Mélissa. La vie à distance de toi est triste, mais je t'ai toujours sentie proche, toujours là pour m'écouter, pour me donner le bon conseil ou pour me dire ce que j'ai envie d'entendre. J'ai toujours senti ton soutien et l'amour que tu me portes à travers tes textos et nos interminables messages vocaux. Merci de faire partie de ma vie et d'être toujours présente.

Finalement, j'aimerais dire merci à ma famille. Merci à mes parents de m'avoir soutenue psychologiquement et financièrement. Merci d'avoir toujours soutenu mes idées et mes envies de carrière. Vous m'avez permis de croire que je pouvais devenir ce que je voulais. Même si cela a pris un peu de temps avant de me trouver réellement… Merci à ma tante Joann pour son soutien indéfectible. Merci au soutient de mes animaux de compagnie, mon chat Papoutchat qui a passé 17 ans à mes côtés, et à Apak qui a pris la relève, vos poils ont toujours été le meilleur réconfort dans les bons et les moins bons moments. Merci à mes frères et ma sœur, Robin, Roxane et Guillaume. Guillaume, tu m'as aidée dans mon parcours scolaire depuis un très jeune âge et tu as beaucoup contribué à la personne que je suis maintenant, sans même que tu t'en aperçoives, je crois. Tu es un super papa et Loïc est réellement chanceux de t'avoir.

Merci à ma famille d'adoption, celle de mon amoureux Frédéric, que je n'aurais probablement pas rencontré sans ce doctorat. Merci de m'avoir acceptée dans votre clan. Votre énergie, votre détermination et votre force m'ont grandement inspirée. Je me considère chanceuse de vous voir grandir et évoluer, et je suis aussi chanceuse, car vous me faites grandir.

AVANT-PROPOS

Ce projet de doctorat en océanographie, réalisé à l'Institut des sciences de la mer (ISMER) à l'Université du Québec à Rimouski (UQAR), s'intitule « Évaluation de la performance métabolique et de la croissance du sébaste (*Sebastes fasciatus*) dans un contexte de changements globaux ». Il visait à mieux comprendre comment les principaux facteurs environnementaux du golfe du Saint-Laurent, la température, l'oxygène dissous et l'acidification, modulent la physiologie, le métabolisme et la croissance du sébaste, une espèce d'importance écologique et commerciale dont la biomasse a fortement augmenté au cours de la dernière décennie.

Ce doctorat a été réalisé sous la supervision du professeur David Deslauriers (ISMER-UQAR), et la co-supervision de Denis Chabot (MPO–Institut Maurice-Lamontagne) et Dominique Robert (ISMER-UQAR). La biologiste Caroline Senay (MPO– Institut Maurice-Lamontagne) a également apporté une contribution importante au volet scientifique du projet ainsi qu'à la rédaction des travaux. Cette thèse s'inscrit dans le cadre du projet de recherche REDTANKS de Pêches et Océans Canada (MPO), qui visait notamment à constituer pour la première fois un cheptel vivant de sébastes, à améliorer l'estimation de leur consommation alimentaire et à préciser leurs réponses physiologiques face aux changements environnementaux. Leur rôle écologique dans le golfe du Saint-Laurent, notamment en matière de prédation et de compétition, constituait un enjeu important de ce programme.

La thèse présentée comprend une introduction générale rédigée en français, trois chapitres sous forme d'articles scientifiques rédigés en anglais, le premier publié dans *Canadian Journal of Zoology* en 2025 (DOI :10.1139/cjz-2025-0014), le second soumis à *Functional Ecology*, et le troisième destiné à être soumis au *Journal of Experimental Biology*, ainsi qu'une conclusion générale rédigée en français. Les données associées aux articles publiés ou en cours de publication ont été ou seront déposées sur la plateforme ouverte Boréalis.

Le projet doctoral a bénéficié du soutien financier de plusieurs organismes. J'ai d'abord obtenu une bourse d'excellence au doctorat de l'ISMER, avant de recevoir deux bourses majeures : la BESC-D du Conseil de recherches en sciences naturelles et en génie du Canada (CRSNG) ainsi que la bourse de doctorat du FRQ-NT. Mon parcours a également été souligné par l'attribution de deux bourses Estelle-Laberge (2021 et 2022). En parallèle, j'ai acquis une expérience en enseignement à titre d'auxiliaire pour des cours de baccalauréat et de maîtrise, tout en intervenant comme conférencière invitée dans des établissements collégiaux et universitaires

Les travaux réalisés dans le cadre de cette thèse ont donné lieu à de nombreuses présentations scientifiques, tant au Québec qu'à l'international, incluant plusieurs distinctions pour la qualité des communications. Ils ont également mené à des contributions à d'autres projets de recherche, sous forme d'articles scientifiques dans des revues internationales. Enfin, certains résultats ont fait l'objet d'efforts de vulgarisation et de couverture médiatique, permettant de sensibiliser un plus large public aux enjeux écologiques du golfe du Saint-Laurent.

Communications scientifiques :

• **Guitard J**., Chabot D., Robert D., Deslauriers D. Effet de l'exposition chronique de l'hypoxie chronique sur le métabolisme aérobique du Sébaste (*Sebastes fasciatus*). Réunion annuelle Ressources aquatiques Québec, novembre 2024, Québec, affiche. Prix de la meilleure affiche.

• Leader du comité organisateur de la session « Respfest 4: The Use of Respirometry as a Tool to Support Fisheries Conservation. 154th American Fisheries Society Annual Meeting, September 2024, Honolulu.

• **Guitard J**., Chabot D., Robert D., Deslauriers D. Metabolic rates from the bottom of the St. Lawrence, An *in situ* respirometry tale about Redfish. 154th American Fisheries Society Annual Meeting, September 2024, Honolulu, Présentation.

• **Guitard J**., Martínez-Silva MA., Coussau L. Contrôle environnemental de croissance. Conférence Horizon Sébastes, mars 2024, Mont-Joli, Présentation.

• **Guitard J**., Chabot D., Robert D., Deslauriers D. Effet de la température et du pH sur les traits métaboliques, la tolérance à l'hypoxie aiguë et la croissance du sébaste (*Sebastes* spp). Réunion annuelle Ressources aquatiques Québec, novembre 2023, Québec, affiche. *Prix de la meilleure affiche

• **Guitard J**., Chabot D., Robert D., Deslauriers D. Metabolic rates from the bottom of the Gulf of St. Lawrence, An *in situ* respirometry tale about Redfish. RespFest 3, mai 2023. Présentation en ligne.

• **Guitard J**., Chabot, D. Deslauriers D., Robert, D., Deslauriers, D. La bioénergétique du Sébaste en conditions environnementales changeantes. Réunion annuelle Ressources aquatiques Québec. Novembre 2022, Québec, Présentation 180 secondes.

• **Guitard J**., Chabot, D., Robert, D., Deslauriers D. The effect of temperature and pH on the metabolic traits and hypoxia tolerance of Redfish (*Sebastes* spp.). 152nd American Fisheries Society Annual Meeting. Conférence en ligne, août 2022. Présentation.

• **Guitard J**., Chabot, D., Robert, D., Deslauriers D. The effect of temperature and pH on the metabolic traits and hypoxia tolerance of Redfish (*Sebastes* spp.). International conference for fish biology, Juillet 2022, Montpellier, Présentation.

• **Guitard J**., Chabot, D., Robert, D., Deslauriers D. The effect of temperature and pH on the metabolic traits and hypoxia tolerance of Redfish (*Sebastes* spp.). RespFest 2, mai 2022, Rimouski. Présentation. *Prix de la meilleure présentation.

Publications en parallèle :

• Madenjian, C.P., Chipps, S.R., Deslauriers, D., **Guitard, J.J**., Daigle, N.J. (2024). Fish bioenergetics modeling. In: Alderman, S.L., Gillis, T.E. (Eds.), Encyclopedia of Fish

Physiology, vol. 2. Elsevier, Academic Press, pp. 507–518. https://dx.doi.org/10.1016/B978-0-323-90801-6.00063-X. ISBN:

- **Guitard, J. J**., Chrétien E., De Bonville J., Roche D. G., Boisclair D. and Binning S. A. (2022). Increased parasite load is associated with reduced metabolic rates and escape responsiveness in pumpkinseed sunfish. J. Exp. Biol. 225, 1–12. http://doi.org/10.1242/jeb.243160

Communications médiatiques :

- Les années lumière – 16 octobre 2022. https://urls.fr/yMI6W0

- Pêche impact - 7 juillet 2022. https://www.pecheimpact.com/hausse-des-temperatures-des-profondeurs-du-golfe-du-saint-laurent-le-sebaste-y-resistera-jusqua-une-certaine-limite/

RÉSUMÉ

Au cours des dernières décennies, le golfe du Saint-Laurent (GSL) a connu des transformations rapides marquées par un réchauffement des masses d'eau, une désoxygénation croissante et une acidification progressive des eaux. Ces changements coïncident avec une augmentation sans précédent de l'abondance des sébastes (*Sebastes mentella* et *Sebastes fasciatus)*. Ce retour spectaculaire soulève de nombreuses interrogations quant aux impacts que ces espèces ont sur leur environnement, mais aussi quant aux contraintes que les conditions environnementales actuelles et futures auront sur leur physiologie, leur croissance et leur productivité.

L'objectif général de cette thèse est de déterminer comment les facteurs environnementaux en changement dans le GSL, température, oxygène dissous et acidification, modulent le métabolisme, l'acquisition d'énergie et la croissance de *S. fasciatus*. En combinant des expérimentations contrôlées à long terme et des mesures métaboliques *in situ*, cette recherche révèle les mécanismes physiologiques susceptibles d'expliquer les ralentissements de croissance observés en milieu naturel et d'évaluer la capacité de cette espèce commerciale à faire face aux conditions à venir.

Le premier chapitre vise à quantifier les effets isolés et combinés de la température (2,5; 5,0; 7,5; 10,0 °C) et du pH (7,75 et 7,35) sur les traits métaboliques et de croissance du sébaste au cours d'une exposition de 114 jours. Les résultats montrent que la hausse de température prévue d'ici 2060 aura un impact physiologique majeur. Le métabolisme standard (TMS), le métabolisme maximal (TMM) et la capacité aérobie (CA) augmentent linéairement avec la température, traduisant à la fois un coût de maintenance plus élevé et un potentiel énergétique accru à 10 °C. Toutefois, cette hausse de CA ne s'accompagnait pas d'une augmentation proportionnelle de la consommation de nourriture, entraînant une efficacité de conversion et une croissance nettement réduites chez les poissons maintenus à 10,0 °C. Les sébastes présentaient leur meilleure performance de croissance à 2,5–5,0 °C. L'acidification prévue pour la fin du siècle (pH 7,35) a eu un effet limité : une légère augmentation du TMS suggérant un coût de régulation acido-basique plus élevé, mais sans impact détectable sur la croissance, la CA ou l'efficacité alimentaire. Ces résultats indiquent que le réchauffement, davantage que l'acidification, représente la principale contrainte pour cette espèce, du moins aux niveaux étudiés.

Le deuxième chapitre explore comment différent niveaux d'oxygène dissous (25–100% saturation) influence le métabolisme, la consommation, l'efficacité alimentaire, la croissance et la condition corporelle sur 105 jours. La réduction de l'oxygène a diminué le TMM, le TMS et la CA, tandis que les performances énergétiques déclinaient fortement sous 35–40 % saturation, indiquant une zone critique où plusieurs fonctions physiologiques sont altérées. Ces seuils, établis en conditions contrôlées, sont probablement conservateurs : en milieu naturel, où les eaux se réchauffent et la nourriture se raréfie, la sensibilité à l'hypoxie pourrait être encore plus marquée.

Ces mécanismes contribuent à expliquer les déclins récents de croissance et de condition observés chez les sébastes dans le GSL. D'autres facteurs contribuent sans doute aussi à ce ralentissement de croissance, comme l'effet additionnel de la densité-dépendance sur la disponibilité de nourriture et l'impact des mêmes variables environnementales (réchauffement, détérioration en oxygène dissous et acidification) sur les espèces de proies.

Alors que les résultats des chapitres 1 et 2 contribuent à expliquer les déclins récents de croissance dans les populations de sébaste du GSL, le chapitre 3 avait pour objectif de mesurer les taux métaboliques de cette espèce de manière *in situ*. Un système autonome a été conçu et ce dispositif, a permis d'obtenir les premières mesures de consommation d'oxygène *in situ* chez *S. fasciatus*. La comparaison entre les taux mesurés *in situ* et en laboratoire (TMS) sur les mêmes quatre individus n'a révélé aucune différence. Il convient toutefois de souligner que ces résultats reposent sur un échantillon restreint, une contrainte liée à la complexité des déploiements sur le terrain. Ces résultats suggèrent qu'en conditions stables et représentatives de leur habitat, les sébastes maintiennent un métabolisme de base comparable à celui mesuré en laboratoire après acclimatation. Cette technique novatrice ouvre la voie à de nouvelles approches intégrant davantage la variabilité environnementale dans l'étude du métabolisme des poissons.

En intégrant des expériences contrôlées et des mesures en milieu naturel, cette thèse offre une vision mécaniste de la manière dont la température, l'oxygène et l'acidification modulent la performance et la croissance du sébaste dans un GSL en rapide transformation. Les résultats montrent que la rupture de l'équilibre entre ces facteurs pourrait limiter la croissance future de cette espèce dominante. En fournissant les premières données physiologiques expérimentales de référence pour *S. fasciatus*, cette thèse contribue à éclairer la gestion durable de ce stock et à mieux comprendre les implications énergétiques des changements océaniques sur les poissons de fond du GSL.

Mots clés : Métabolisme énergétique, Réchauffement, Acidification, Hypoxie, Respirométrie *in situ*, Changements climatiques, Croissance et efficacité alimentaire, Capacité aérobie, Golfe du Saint-Laurent, Écophysiologie

ABSTRACT

Over the past decades, the Gulf of St. Lawrence (GSL) has undergone rapid transformations marked by warming water masses, increasing deoxygenation, and progressive ocean acidification. These changes coincide with an unprecedented rise in the abundance of redfish, including *Sebastes mentella* and *Sebastes fasciatus*. This remarkable resurgence raises questions not only about the impacts these species may have on their environment, but also about the constraints that present and future environmental conditions will impose on their physiology, growth, and productivity.

The overarching objective of this thesis was to determine how changing environmental factors in the GSL such as temperature, dissolved oxygen, and acidification, modulate the metabolism, energy acquisition, and growth of *S. fasciatus*. By combining long-term controlled experiments with *in situ* metabolic measurements, this research reveals the physiological mechanisms that may explain the growth declines observed in the wild and assesses the capacity of this commercially important species to cope with future conditions.

The first chapter aimed to quantify the isolated and combined effects of temperature (2.5, 5.0, 7.5, 10.0 °C) and pH (7.75 and 7.35) on metabolic traits and growth performance of redfish over a 114-day exposure. Results show that the temperature increase projected by 2060 will have a major physiological impact. Standard metabolic rate (SMR), maximum metabolic rate (MMR), and aerobic capacity (AS) all increased linearly with temperature, indicating both higher maintenance costs and a greater energetic potential at 10 °C. However, this rise in AS was not matched by an increase in food intake, leading to lower conversion efficiency and reduced growth at 10 °C. Redfish exhibited their highest growth performance between 2.5 and 5.0 °C. The level of acidification projected by the end of the century (pH 7.35) had limited effects: a slight increase in SMR suggesting a higher acid–base regulation cost, but no measurable impact on growth, AS, or feeding efficiency. These results indicate that warming, more than acidification, represents the main constraint for this species, at least within the tested levels.

The second chapter examined how different levels of dissolved oxygen (25–100% saturation) affect metabolism, consumption, feeding efficiency, growth, and condition over 105 days. Lower oxygen availability reduced MMR, SMR, and AS, while energetic performance—food intake, conversion efficiency, growth, and body condition—declined sharply below 35–40% saturation, indicating a critical zone where multiple physiological functions are impaired. These thresholds, established under controlled conditions, are likely conservative; in natural environments where waters are warming and food is becoming scarce, sensitivity to hypoxia may be even greater.

These mechanisms help explain the recent declines in growth and condition observed in redfish in the GSL. Additional factors likely also contribute to this growth slowdown, including density-dependent effects on food availability and the impact of the same environmental stressors (warming, deoxygenation, and acidification) on prey species.

The final chapter focused on developing an autonomous in situ respirometry system for estimating metabolic rates directly in the natural environment. The device, operational down to 30 m, enabled the first in situ measurements of oxygen consumption in *S. fasciatus*. Comparisons between in situ (RMR) and laboratory (SMR) rates measured in the same four individuals revealed no difference between the two. Although based on a small number of fish—a limitation tied to the logistical complexity of deployments at sea—these results suggest that under stable and representative environmental conditions, redfish maintain a baseline metabolism comparable to that measured in acclimated laboratory individuals. This innovative technique opens the door to future approaches that better integrate environmental variability into the study of fish metabolism.

By combining controlled experiments with field-based measurements, this thesis provides a mechanistic understanding of how temperature, oxygen, and acidification influence redfish performance and growth in a rapidly changing GSL. The results highlight that disruptions in the balance among these factors may limit the future growth of this dominant species. By providing the first experimental physiological baseline for *S. fasciatus*, this thesis supports the sustainable management of this stock and advances our understanding of the energetic implications of ocean change for demersal fishes in the GSL.

Keywords: Energy metabolism, Warming, Acidification, Hypoxia, *In situ* respirometry, Climate change, Growth and Feeding efficiency, Aerobic capacity, Gulf of St. Lawrence, Ecophysiology

TABLE DES MATIÈRES

LISTE DES TABLEAUX

LISTE DES FIGURES

LISTE DES ABRÉVIATIONS, DES SIGLES ET DES ACRONYMES

ACIA	Arctic Climate Impact Assessment
ADS	Action dynamique spécifique (Traduction de Specific Dynamic Action, SDA)
AIC	Akaike information criterion
AS / CA	Capacité aérobie (Aerobic Scope)
B_$\dot{M}O_2$	Background respiration rate
CAF	Capacité aérobie factorielle (Factorial Aerobic Scope)
CI	Confidence interval
CIF	Couche intermédiaire froide
CIL	Cold intermediate layer
CO_2	Dioxyde de carbone
CRF	Corticotropin-Releasing Factor (peptide lié à la réponse au stress)
DO	Dissolved oxygen
df	Degrees of freedom
DFO / MPO	Fisheries and Oceans Canada / Ministère des Pêches et Océans

DNA / ADN	Acide désoxyribonucléique
EGSL	Estuaire et Golfe du Saint-Laurent
ECA	Efficacité de conversion alimentaire
eOMP	extended Optimum Multiparameter method
FAS	Factorial aerobic scope
FCE	Food Conversion Efficiency
GAM	Generalized Additive Model
GAMM	Generalized Additive Mixed Model
GIEC	Groupe d'experts intergouvernemental sur l'évolution du climat
GSL	Golfe du Saint-Laurent
IPCC	Intergovernmental Panel on Climate Change (version anglaise du GIEC)
IQR	Interquartile range
ISMER	Institut des sciences de la mer
ISMeR	*In situ* metabolic respirometry
K	Fulton’s condition factor
ΔK	Change in Fulton’s condition factor

kPa	Kilopascals (oxygen partial pressure)
L50	Longueur où 50 % des individus sont matures
LAB-ISMeR	Laboratory respirometry on fish previously measured *in situ*
Lab-Acclim	Groupe acclimaté en laboratoire
Lmer	Linear mixed-effects models
LOL	Limiting oxygen level
MMR	Maximum Metabolic Rate
MO_2	Dépense métabolique mesurée en O_2 (mg O_2 h^{-1} ou similaire)
MR	Metabolic rate
NACW	North Atlantic Central Water (Eaux centrales de l'Atlantique Nord)
OCLTT	Oxygen- and Capacity-Limited Thermal Tolerance
O_2crit	Critical oxygen level representing hypoxia tolerance
OD	Oxygène dissous
PCO_2	Pression partielle de CO_2
PCR	Polymerase Chain Reaction (réaction en chaîne par polymérase)
Pcrit	Critical oxygen pressure

PIT-tag	Passive integrated transponder tag
REML	Restricted maximum likelihood
RMR	Resting metabolic rate
R^2	Coefficient of determination (Coefficient de détermination)
SCUBA	Self-contained underwater breathing apparatus
SD	Standard deviation (écart-type)
SMR	Standard metabolic rate
TMM	Taux métabolique maximal
TMS	Taux métabolique standard
TPC	Thermal Performance Curve (Courbe de performance thermique)
Tpejusmin	Températures de pejus inférieures
Tpejusmax	Températures de pejus supérieure
% sat.	Pourcentage saturation d'air

INTRODUCTION GÉNÉRALE

1. CHANGEMENT CLIMATIQUE : ÉVOLUTIONS DES DYNAMIQUES OCÉANIQUES

Le changement global est défini par le Groupe d'experts intergouvernemental sur l'évolution du climat (GIEC) comme un changement dans l'état du climat ou de ses propriétés et dont les variations moyennes peuvent être observées et quantifiées statistiquement sur une période de temps définie, soit des décennies ou plus (Cubash *et al.*, 2013). Au cours des dix prochaines années, les prévisions suggèrent que la Terre connaîtra une augmentation de la température moyenne de 1 à 4 °C (IPCC, 2021). Il est également prévu que les températures aux latitudes plus élevées, vers les pôles, augmentent à un rythme plus rapide qu'aux latitudes plus basses (ACIA, 2005). Parallèlement, on observe une désoxygénation progressive des océans, tant en surface qu'en profondeur. Bien que certaines zones présentent naturellement de faibles teneurs en oxygène, comme les zones de minimum d'oxygène ou les fjords profonds, l'ampleur et la fréquence des épisodes de baisse d'oxygène se sont accrues au cours des dernières décennies, notamment dans les milieux côtiers et estuariens (Diaz, 2001). Dans l'Atlantique Nord, les projections du GIEC indiquent une perte d'oxygène pouvant atteindre 4 % à 11 % d'ici la fin du siècle dans les couches intermédiaires (100–600 m), selon les différents scénarios d'émissions (Bindoff *et al.*, 2019 ; Cooley *et al.*, 2022 ; Stendardo et Gruber, 2012). Dans cette même tranche de profondeur, le pH a déjà diminué de façon mesurable au cours des dernières décennies, et les projections indiquent une baisse additionnelle de 0,3 à 0,4 unité, reflétant une acidification des eaux d'ici 2100 (Bindoff *et al.*, 2019). Outre ces changements observés dans les grandes zones océaniques, les mers semi-fermées sont encore plus vulnérables au réchauffement, à la désoxygénation et à l'acidification due à leur faible renouvellement d'eau, de leur forte stratification et de la forte influence des apports en eau douce et en nutriments (Maccracken *et al.*, 2009). Ces conditions

favorisent une augmentation et une amplification des perturbations climatiques soulignant l'importance de comprendre comment elles se manifestent et leur impact sur les ressources marines exploitées qui s'y trouvent.

2. CHANGEMENTS ABIOTIQUES DANS LE GOLFE DU SAINT-LAURENT

Le golfe du Saint-Laurent (GSL) est un vaste environnement productif et complexe. Le GSL est relié à l'océan Atlantique par deux détroits: le détroit de Belle Isle, entre le Labrador et Terre-Neuve, et le détroit de Cabot, entre Terre-Neuve et le Cap-Breton (Figure 1).

Une particularité du GSL est la formation de sa colonne d'eau et ses variations au fil des saisons. La colonne d'eau est composée de trois couches distinctes tout au long de l'été : la couche de surface, la couche intermédiaire froide (CIF) et la couche profonde. À partir du mois d'août, une combinaison du refroidissement de l'eau avec la diminution de la température ambiante et de l'augmentation des vents assure un mélange de la couche de surface jusqu'à un point où, en hiver, elle se mélange également avec la CIF (Galbraith *et al*., 2021). En hiver, la couche de surface peut atteindre 150 m de profondeur, mais sa profondeur moyenne est de 75 m. Au printemps, la température ambiante réchauffe la couche de surface, tandis que la fonte de la glace de mer et les eaux de ruissellement crégolfeent une nouvelle couche de surface à faible salinité. Cette dernière isole alors la couche de surface hivernale, qui devient la nouvelle CIF (Galbraith *et al*., 2021).

Au cours des dernières années, la dynamique de formation des différentes couches d'eau du GSL a été modulée par la modification du couvert de glace. En effet, un réchauffement des eaux et de l'air ambiant a réduit le couvert, mais aussi le temps de résidence de la glace durant l'hiver, faisant donc varier l'épaisseur et la température de la CIF durant les étés subséquents (Galbraith *et al.,* 2025).

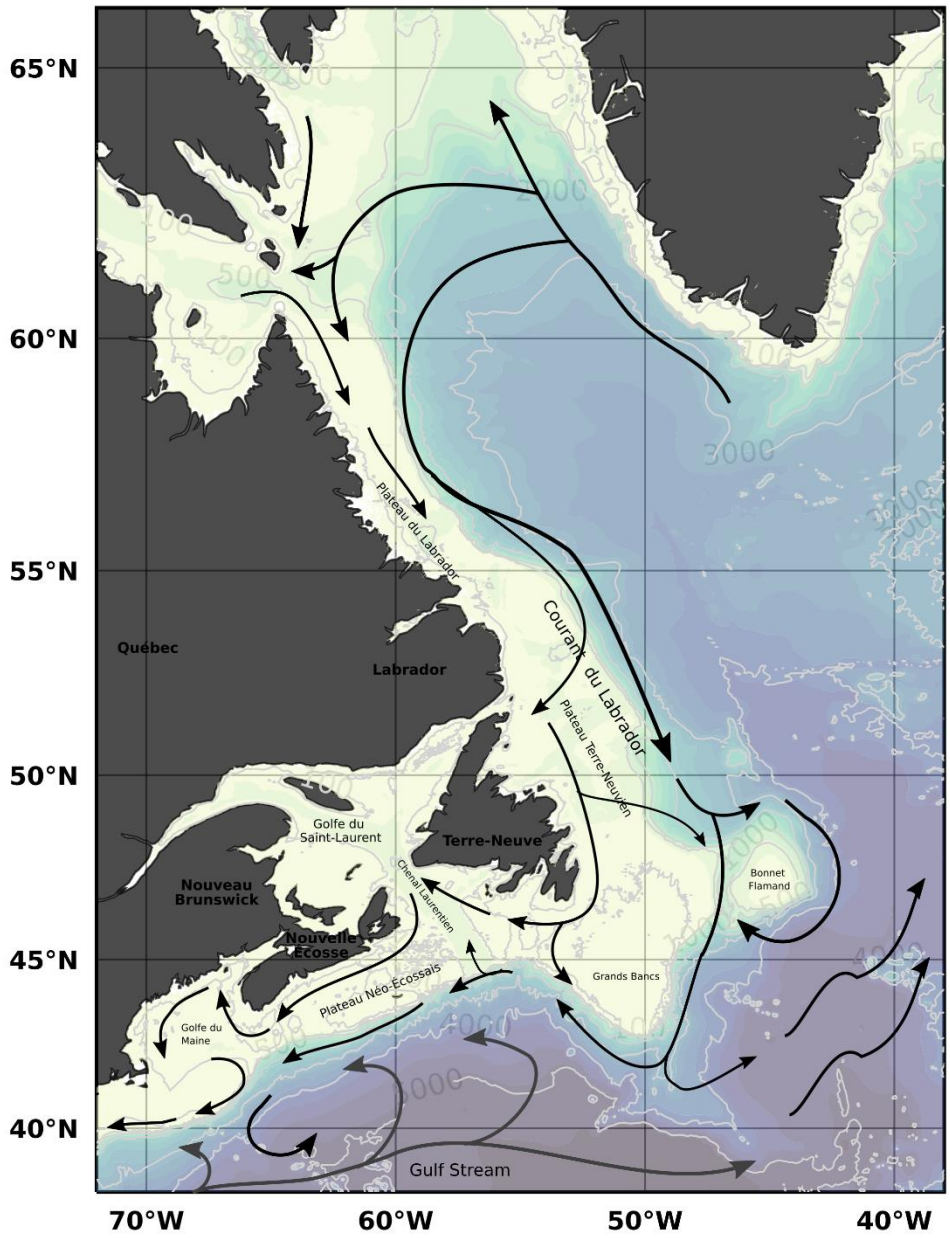

Figure 1. Carte des différents courants entrants dans le golfe du Saint-Laurent et montrant la topographie du fond de l'Atlantique nord-ouest (contours tracés en gris clair) avec un schéma des courants (flèches noires). Modifiée de Cyr *et al*., (2021)

2.1 Réchauffement rapide et réorganisation des masses d'eau profondes

La couche d'eau profonde du GSL est alimentée par un mélange de masses d'eau pénétrant par le chenal laurentien, principalement en provenance du courant du Labrador, froid et riche en oxygène (−0,7 à 3,2 °C ; 310 à 280 µmol kg^{-1} d'O_2 dissous; Jutras *et al.*, 2020), et des eaux centrales de l'Atlantique Nord (NACW), plus chaudes et moins oxygénées, transportées par le Gulf Stream (4,4 à 17,7 °C ; 155 à 250 µmol kg^{-1} d'O_2 ; Jutras *et al.*, 2020) (Figure 1). Historiquement, le courant du Labrador dominait cet apport, mais sa contribution est passée de 72 % dans les années 1930 à 53 % dans les années 1980 (Gilbert *et al.*, 2005). Les analyses des propriétés de l'eau profonde depuis les années 1930 indiquent que les changements dans la contribution relative de ces deux masses d'eau, induits par des modifications de la circulation dans l'ouest de l'Atlantique Nord, sont en grande partie responsables des tendances à long terme de désoxygénation et de réchauffement observées dans le GSL (Gilbert *et al.*, 2005 ; Jutras *et al.*, 2023). Plus récemment, des analyses suggèrent que la contribution du courant du Labrador a effectivement chuté à zéro (dans la marge d'incertitude de 5 % de la méthode eOMP ; Jutras *et al.*, 2020), ce qui implique que presque toutes les eaux entrant dans le chenal laurentien proviennent désormais du Gulf Stream (Jutras *et al.*, 2023) (Figure 1).

Selon les données récentes, la couche d'eau profonde du golfe du Saint-Laurent (>150–175 m) est aujourd'hui caractérisée par des températures variant entre 1 °C et plus de 7 °C (Galbraith *et al.*, 2025). Alors que cette couche demeurait relativement stable entre 1981 et 2010, une augmentation marquée des températures y est observée depuis 2009, tant au niveau des moyennes que des maximums (Figure 2; de 2017 à aujourd'hui). La température maximale dans les eaux profondes a ainsi atteint un record de 7,0 °C en 2022, avant de décroître légèrement à 6,7 °C en 2024, tout en demeurant nettement au-dessus des moyennes historiques (Galbraith *et al.*, 2025; Figure 2). Cette tendance au réchauffement s'est traduite par une transformation de la structure thermique des habitats profonds : à partir de 2015, la superficie occupée par les eaux à 5–6 °C a fortement diminué, au profit des eaux plus chaudes (6–7 °C), dont l'aire s'est rapidement étendue au centre et au nord-ouest du GSL entre 2017

et 2019 (Figure 2). En 2020, des températures de 7–8 °C ont été observées pour la première fois sur le fond dans le nord-est du GSL. Ces températures se sont maintenues jusqu'en 2023, mais aucune eau de fond dépassant 7 °C n'a été détectée en 2024, suggérant une anomalie plus froide, mais qui demeure tout de même au-dessus des normales saisonnières (Galbraith *et al.*, 2025; Figure 2). En parallèle, les températures moyennes à 300 m ont également atteint un maximum de 6,6 °C en 2022, soit une augmentation de plus de 1,3 °C par décennie depuis 2009, un rythme environ cinq fois supérieur à la tendance de réchauffement du siècle précédent. Ce réchauffement rapide coïncide avec une modification de la circulation régionale, notamment une contribution accrue des eaux centrales de l'Atlantique Nord (Galbraith *et al.*, 2025 ; Gilbert *et al.*, 2005 ; Jutras *et al.*, 2023).

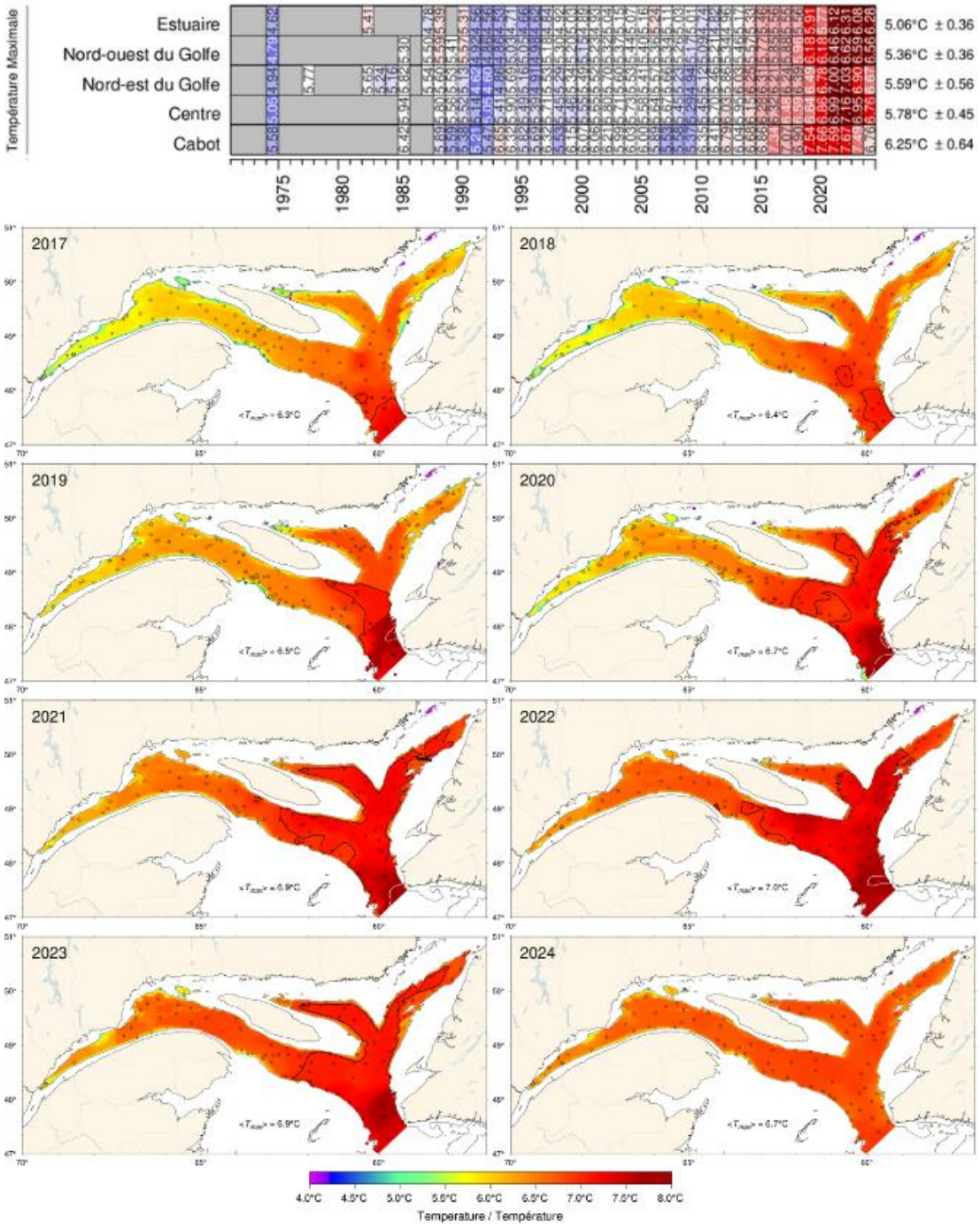

Figure 2. Hausse de la température des eaux profondes du golfe du Saint-Laurent. A) La température maximale en profondeur généralement observée entre 200 m et 300 m. Les chiffres à droite correspondent aux moyennes climatologiques et aux écarts types pour la période 1991-2020. Les chiffres dans les cases correspondent aux températures moyennes pour chaque région. Le code couleur (rouge : haute, bleue : basse) correspond à l'anomalie

de température par rapport à la climatologie 1991-2020 de chaque région et profondeur. B) Carte des températures maximales en profondeur généralement observées entre 200 m et 300 m, 2017-2024. Les cartes sont interpolées à partir des données disponibles pour chaque année entre août et septembre. Les courbes noires et blanches correspondent respectivement à 7 et 8 °C. Modifiée de Galbraith *et al.*, (2025).

2.2 Appauvrissement en oxygène et expansion de la zone hypoxique

L'augmentation des masses d'eau chaude et pauvre en oxygène pénétrant par le détroit de Cabot a entraîné un déclin marqué de l'oxygène dissous dans les couches profondes, depuis l'embouchure du chenal laurentien jusqu'à l'estuaire (Blais *et al.*, 2025). Cette transformation dans la proportion des masses d'eau joue un rôle majeur dans la désoxygénation récente, expliquant à elle seule plus de 60 % de la baisse observée des concentrations d'oxygène dissous ainsi que du réchauffement enregistré entre 2018 et 2021 dans l'estuaire et le golfe du Saint-Laurent (EGSL) (Jutras *et al.*, 2023).

À cette désoxygénation s'ajoute une intensification de la respiration bactérienne, accentuée par les températures plus élevées, qui contribue pour environ 30 % supplémentaires à la désoxygénation (Jutras *et al.*, 2023). L'eau profonde se déplaçant vers l'amont à travers le chenal laurentien perd naturellement de l'oxygène en cours de route, en raison de la respiration des organismes benthiques et de la minéralisation bactérienne de la matière organique (Gilbert *et al.*, 2005). Comme le souligne Blais *et al.*, (2025), les plus faibles niveaux d'oxygène dissous dans la couche profonde sont maintenant observés dans l'ensemble de l'estuaire et du GSL (Fig. 3B), avec une augmentation des anomalies négatives dans toutes les régions (Fig. 3A). La zone hypoxique (≤ 30 % de saturation en oxygène) est ainsi passée d'une superficie de 1300 km² en 2003 à 9400 km² en 2021 (Gilbert *et al.*, 2005 ; Jutras *et al.*, 2023), et les zones profondes où la saturation en oxygène dépasse 60 % deviennent de plus en plus rares (Fig. 3).

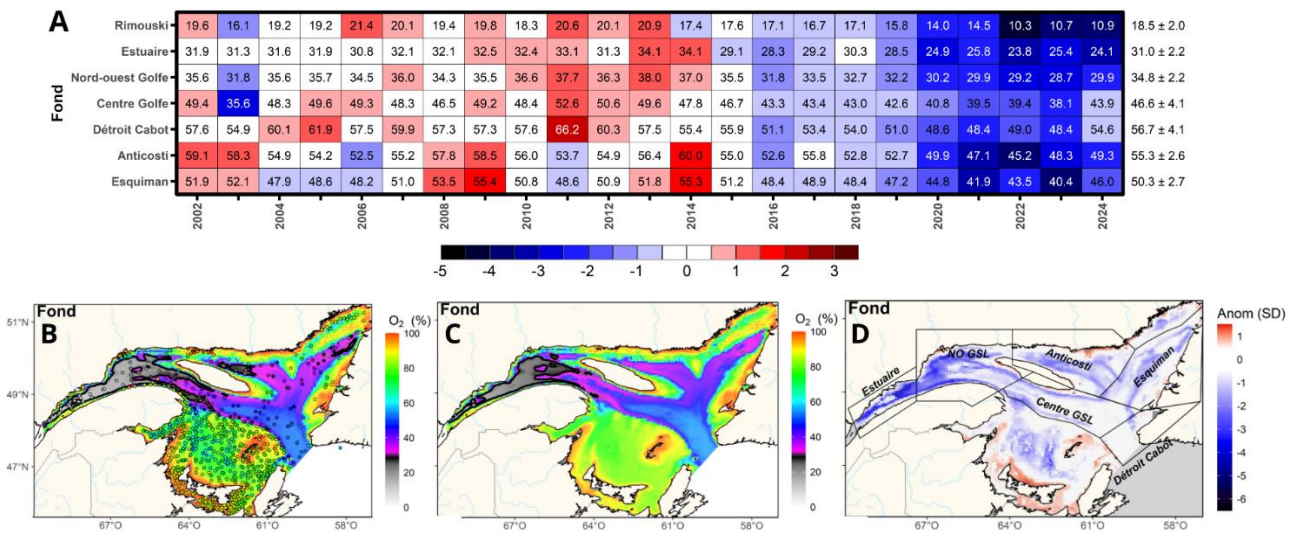

Figure 3. Moyennes annuelles de la saturation en oxygène dissous (%) au fond de l'estuaire et du golfe du Saint-Laurent pour 2024 (> 100 m). (A) Valeurs annuelles par région; les chiffres à droite indiquent les moyennes climatologiques (2002–2020 ± écart type). (B) répartition spatiale moyenne de la saturation en oxygène dissous, (C) climatologie (2002–2020) et (D) anomalies de 2024. Les zones hypoxiques (< 30 %) sont délimitées par des contours noirs. Dans (D), les teintes bleues indiquent des niveaux inférieurs à la normale, les rouges des niveaux supérieurs et le blanc des conditions normales. Les cercles ouverts montrent l'emplacement des stations en 2024. Modifiée de Blais *et al*. (2025).

2.3 Intensification des processus d'acidification

Un facteur majeur contribuant à la diminution des niveaux d'oxygène dissous est l'apport de nutriments dans la colonne d'eau. Les nutriments parviennent naturellement au fleuve du Saint-Laurent par ses affluents, depuis les Grands Lacs jusqu'au golfe, mais les apports anthropiques n'ont cessé d'augmenter depuis le début de l'industrialisation (Thibodeau *et al.*, 2010). La dégradation microbienne de la matière organique lors de son passage dans la colonne d'eau entraîne sa reminéralisation en CO_2 lorsqu'elle atteint le fond. Cet apport de nutriments et de matière organique alimente la minéralisation bactérienne et modifie la dynamique des eaux profondes du GSL. Une intensification de la minéralisation bactérienne entraîne une augmentation de la respiration métabolique, amplifiée par la hausse

des températures. Ce processus épuise l'oxygène dissous tout en libérant davantage de CO_2, contribuant ainsi à l'acidification des eaux profondes (Nesbitt et Mucci, 2021).

2.4 Un écosystème en transition : pressions abiotiques et enjeux halieutiques dans le GSL

Le GSL soutient d'importantes pêcheries ciblant une grande diversité de poissons et de crustacés. Ces espèces sont des ressources essentielles à la culture et l'économie de nombreuses communautés côtières, pour qui la pêche représente une activité centrale. Or, cette activité dépend directement de la présence, de l'abondance et de la santé de ces populations marines, qui réagissent fortement aux changements abiotiques du milieu ainsi qu'à la pression de pêche (Dulvy *et al*., 2003; Hutchings et Myers, 1994; Ward et Myers, 2005). Lorsque certaines espèces déclinent comme la crevette nordique (*Pandalus borealis*) ou le flétan du Groenland (*Reinhardtius hippoglossoides*) ou qu'une autre augmente de façon importante comme le sébaste (*Sebastes spp*.) ou le homard (*Homarus americanus*), l'équilibre écologique du golfe s'en trouve modifié, entraînant des répercussions immédiates, favorables ou défavorables, pour les pêcheries et les communautés qui en dépendent.

Dans un contexte de réchauffement, de désoxygénation et d'acidification croissante, il devient essentiel de comprendre comment ces facteurs environnementaux modifient non seulement la physiologie et la performance des individus des espèces exploitées, mais aussi la dynamique des populations exploitées (Barausse *et al*., 2011; Hutching et Myers, 1994). Dans le domaine des sciences halieutiques, qui étudient la dynamique des populations exploitées et les facteurs biologiques et environnementaux qui la modulent, ces mécanismes constituent un point d'appui essentiel pour comprendre et prédire la réponse des espèces aux pressions du milieu.

Ces transformations abiotiques profondes, réchauffement, désoxygénation et acidification, modifient rapidement les conditions physico-chimiques du GSL (Blais *et al*., 2025; Lavoie *et al*., 2020; Mucci *et al*., 2011). Ensemble, elles redéfinissent la structure et la qualité des habitats disponibles pour les organismes marins. La hausse des températures peut

accroitre la demande métabolique, tandis que la baisse de l'oxygène dissous et du pH en a pour conséquences communément décrites de réduire la tolérance physiologique (Fry, 1971; Heuer et Grosell, 2014; Schulte, 2015). Ces contraintes combinées risquent d'altérer la demande métabolique, la croissance et la survie des espèces habitant les eaux profondes du GSL, en particulier celles adaptées historiquement à des eaux froides et bien oxygénées.

3. TRAITS PHYSIOLOGIQUES ET PERFORMANCE DES POISSONS

Les traits de performance d'un individu peuvent déterminer sa capacité à réussir dans des tâches écologiquement pertinentes, telles que la quête de nourriture, la compétition avec d'autres espèces, la croissance ou la reproduction. Ces traits de performance sont définis dans cette thèse comme les traits physiologiques étudiés (Arnold, 1983 ; Bennett et Huey, 1990).

En sciences halieutiques, la croissance constitue un trait physiologique clé utilisé pour évaluer l'état de santé des individus ou des cohortes et pour prédire à quel moment une cohorte atteindra des seuils de taille critique. Ces seuils incluent la taille réglementaire minimale ou maximale de capture et la longueur à laquelle 50 % des individus sont matures (L50) et considérés comme faisant partie de la biomasse reproductrice (p. ex. Brûlé *et al*., 2024).

L'efficacité de conversion alimentaire (ECA), qui décrit l'efficacité avec laquelle un organisme transforme la nourriture ingérée en masse corporelle, est quant à elle un déterminant important de la croissance (Craig *et al.*, 2002). Elle intègre à la fois des aspects comportementaux et physiologiques de la performance, incluant la capacité de recherche de nourriture et le coût métabolique associé, et constitue ainsi un indicateur précieux de la performance globale en aquaculture et dans les études écologiques (Jobling, 1994). Ces indicateurs physiologiques sont essentiels pour comprendre l'évolution d'un stock de poissons et ainsi améliorer la prise de décisions de gestion.

En plus de la croissance comme trait de performance, la performance métabolique aérobique fournit un aperçu précieux de l'énergie potentielle disponible pour un organisme.

Il a été démontré que le niveau de consommation d'oxygène est proportionnel au niveau de dépenses énergétiques des organismes (Fry, 1971 ; Nelson et Chabot, 2024). Il s'agit donc d'un processus important, puisqu'il permet d'acquérir l'énergie nécessaire non seulement à la vie, mais à toutes autres activités demandant de l'énergie pour un organisme. L'étude des traits relatifs au métabolisme aérobique consiste donc en une approche mécaniste de l'allocation de l'énergie vers la croissance, par exemple (pour des revues, voir Chabot *et al.*, 2016b ; Nelson et Chabot, 2024).

Le métabolisme aérobique est caractérisé par des limites supérieures et inférieures. Le taux métabolique maximal (TMM) représente la capacité maximale de consommation d'oxygène (Hulbert et Else, 2000), tandis que le taux métabolique standard (TMS) reflète l'énergie minimale nécessaire pour le maintien des fonctions vitales dans un état de repos post-absorptif (Chabot *et al.*, 2016b). La différence entre le TMM et le TMS est connue sous le nom de capacité aérobie (CA), qui indique le potentiel énergétique pour des activités comme la locomotion, la digestion, la croissance et la reproduction (Claireaux et Lefrançois, 2007 ; Fry, 1948 ; Nelson, 2016). La capacité aérobie d'un animal peut aussi être représentée comme le ratio entre son TMM et son TMS, connu sous le nom de capacité aérobie factorielle (CAF). Contrairement à la CA, l'analyse de la CAF examine la capacité du système de transport de l'oxygène de l'organisme par rapport à son taux minimal de consommation d'oxygène (Halsey *et al.*, 2018). Par conséquent, la CA et la CAF peuvent fournir un aperçu de la capacité énergétique qu'un animal peut investir dans la croissance sous différentes contraintes environnementales, lorsque la nourriture n'est pas limitante.

Les traits métaboliques, tels que le TMM, le TMS et la CA, sont des traits de performance composés de différentes réactions biologiques influencées par les variables abiotiques du milieu. Par conséquent, la CA peut fournir des indications sur l'énergie potentielle qu'un animal peut investir dans sa croissance en fonction de différentes contraintes environnementales (Fry, 1971). En comprenant par quels processus les facteurs abiotiques influencent les taux de croissance des populations de poissons, nous pouvons mieux évaluer comment les activités humaines risquent d'affecter leur dynamique.

4. IMPACTS DES FACTEURS ABIOTIQUES SUR LA PHYSIOLOGIE DES POISSONS

4.1 La température comme facteur régulateur de la physiologie des poissons

Chez les ectothermes, dont la plupart des poissons, la température ambiante détermine directement la vitesse des processus physiologiques à différents niveaux d'organisation (Fry, 1971 ; Schulte, 2015), influençant ainsi leurs performances globales, leur comportement et leur écologie. L'amplitude des performances physiologiques sous un régime thermique est souvent décrite par une courbe de performance thermique (TPC), illustrant la nature limitante de la température (Fig. 4A) (Fry, 1971). Cette courbe décrit comment chaque processus physiologique a une température optimale, pour laquelle l'organisme fonctionne au maximum de ses capacités. De part et d'autre de cette température optimale, la performance diminue, formant une courbe en cloche trouvant à leurs extrémités les seuils thermiques inférieurs et supérieurs ($Tpejus_{min}$ et $Tpejus_{max}$), marquant des déclins rapides de performance (Fry, 1971 ; Pörtner, 2001). Cependant, Dell *et al*., (2011) ont montré que les TPC ont généralement une forme unimodale et asymétrique, avec une montée progressive de la performance à mesure que la température augmente, suivie d'un plateau correspondant à la température optimale, suivie d'un déclin abrupt aux températures plus élevées, comme l'ont aussi observé Clark *et al*., (2011) et Clark *et al*., (2013) (Fig. 4B). Lefevre, (2016), dans sa méta-analyse, a également rapporté une variabilité considérable de TPC entre les différentes recherches analysées. La grande variabilité des TPC observée dans la littérature peut s'expliquer par des différences interspécifiques, mais aussi par diverses formes de plasticité (acclimatation, épigénétique) au sein d'une même espèce (Lefevre, 2016 ; Schulte *et al*., 2011 ; Schulte, 2015).

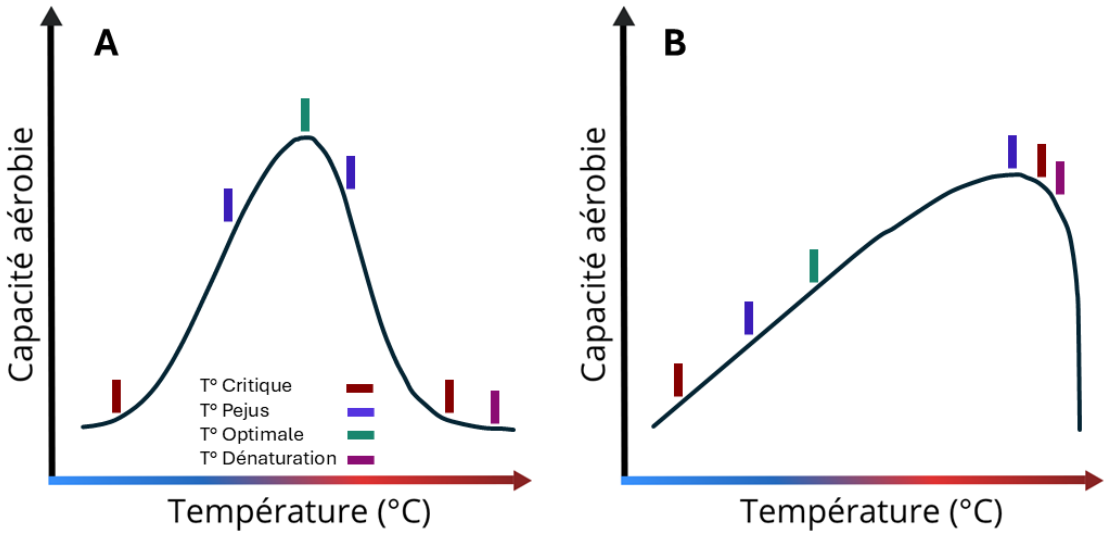

Figure 4. Représentation conceptuelle des changements de la capacité aérobie en fonction de la température. A) Suppose que la température optimale coïncide avec la capacité aérobie maximale. B) Suppose que la température optimale est inférieure à celle correspondant à la capacité maximale, laquelle est très proche de $T_{pejusmax}$. Modifiée de Clark *et al*., (2013)

Un modèle conceptuel bien connu dans la littérature, la relation entre la température et le métabolisme aérobique suit elle aussi une courbe en cloche caractéristique (Fig. 5). Le TMS augmente de manière exponentielle avec la température jusqu'à atteindre un plateau, tandis que le TMM présente généralement une courbe unimodale avec un optimum thermique. La CA tend à s'élargir jusqu'à une température optimale, puis à diminuer lorsque les coûts métaboliques de base augmentent plus rapidement que la capacité maximale à métaboliser l'oxygène. Ce modèle conceptuel constitue le fondement de plusieurs cadres théoriques visant à expliquer comment la température limite la performance physiologique (Fig. 5).

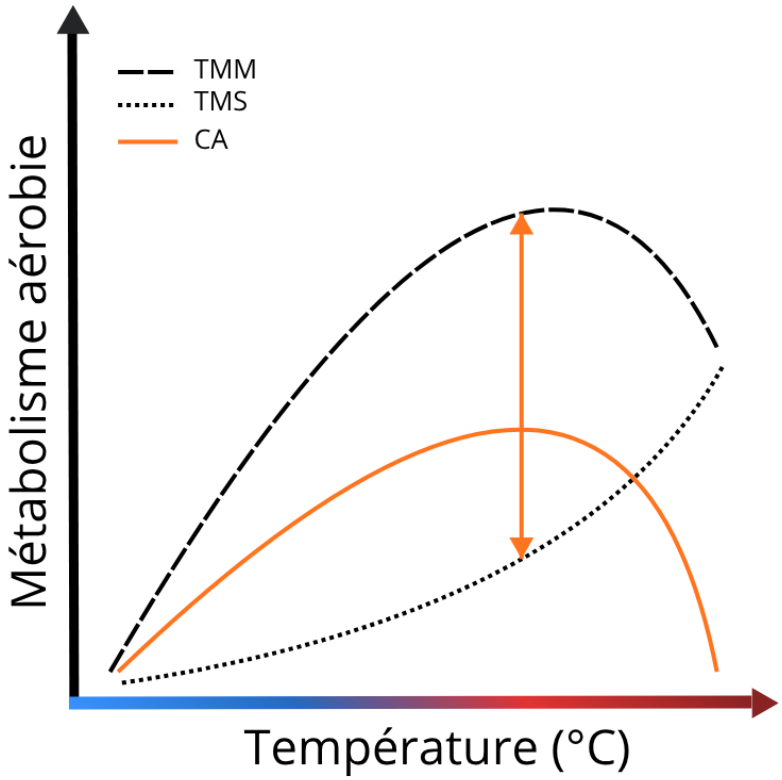

Figure 5. Schéma de l'effet de l'augmentation de la température sur le métabolisme aérobique. Taux métabolique maximal (TMM), taux métabolique standard (TMS) et la capacité aérobie (CA). Figure modifiée de Lefevre (2016)

Une hypothèse souvent invoquée pour expliquer l'effet de la température sur la relation entre la capacité aérobie (CA) et des traits de performance, comme la croissance, est celle de la tolérance thermique limitée par la capacité d'approvisionnement en oxygène (OCLTT – *oxygen- and capacity-limited thermal tolerance* ; Pörtner, 2010). Cette hypothèse stipule que, lorsque l'animal approche ses limites thermiques, sa capacité à fournir de l'oxygène aux tissus diminue, ce qui entraîne une réduction de la performance du métabolisme aérobie et, par conséquent, de la croissance. Cependant, l'hypothèse OCLTT a été critiquée pour son manque de fondement empirique. Bien que certaines études appuient certaines prédictions de l'hypothèse, notamment dans des contextes où la capacité cardiorespiratoire devient limitante (Eliason *et al*., 2011 ; Pörtner et Knust, 2007), d'autres travaux suggèrent que cette relation n'est pas universelle et que les limites thermiques peuvent résulter d'autres mécanismes physiologiques, tels qu'une baisse d'efficacité mitochondriale ou des

déséquilibres énergétiques (Gräns *et al*., 2014 ; Jutfelt *et al*., 2018 ; Schulte, 2015). Il est donc nécessaire de poursuivre les recherches de l'effet de la température sur les processus physiologiques, tout en tenant compte d'autres facteurs de stress naturel (Clark *et al*., 2013 ; Jutfelt *et al*., 2018).

L'augmentation de la température, si les apports énergétiques le permettent, peut offrir un potentiel de croissance important chez certaines espèces. Par ailleurs, une capacité aérobie (CA) élevée à des températures supérieures à la température optimale de croissance indique que ces conditions ne sont pas nécessairement létales et que les processus physiologiques peuvent encore être soutenus (Clark et al., 2013 ; Pörtner, 2010) (Fig. 4A). Toutefois, bien que la CA demeure relativement élevée au-delà de cette température optimale, la croissance diminue, suggérant que l'optimum thermique de croissance ne correspond pas nécessairement au maximum de capacité aérobie. Cette dissociation peut s'expliquer par une augmentation des coûts énergétiques d'entretien (p. ex. métabolisme de base, stress thermique), qui réduit la fraction d'énergie disponible pour la croissance malgré une capacité aérobie encore importante. Ainsi, bien que la CA fournisse une information importante sur la capacité physiologique d'une espèce, sa relation avec la croissance ou d'autres traits fonctionnels varie selon les caractéristiques propres à chaque espèce et le contexte environnemental. Une augmentation de la CA avec la température ne se traduit pas nécessairement par une augmentation de la croissance ou de la performance globale. Par exemple, Holt et Jørgensen, (2015) ont montré, à l'aide d'un modèle bioénergétique appliqué à la morue franche (*Gadus morhua*), que la température à laquelle la capacité aérobie est maximale ne correspond pas à celle où la croissance et la reproduction sont optimales. À des températures plus élevées, la hausse des coûts métaboliques, combinée à l'augmentation de certaines activités comme la ventilation ou la recherche alimentaire, réduit l'énergie disponible pour la croissance et l'investissement reproducteur (Claireaux et Lefrançois, 2007 ; Fry, 1971). Ces conséquences créent ainsi un compromis entre maintien des fonctions vitales et performance (Fry, 1971).

4.2 L'oxygène dissous comme principal facteur limitant pour les ectothermes

Tout comme la température, les niveaux d'oxygène ont des effets directs et indirects sur la physiologie et le comportement des poissons (Claireaux et Chabot, 2016 ; Killen *et al.*, 2012). Une diminution de l'oxygène dissous (OD) dans l'eau représente un facteur limitant pour les besoins physiologiques des poissons (Claireaux et Chabot, 2016 ; Fry, 1971). Comme l'oxygène est l'élément principal du métabolisme aérobique, la capacité d'un organisme à l'extraire du milieu détermine sa faculté à subvenir à ses besoins énergétiques. Quand l'oxygène devient moins disponible, l'effort pour l'extraire de l'eau et le transporter aux tissus augmente, jusqu'à atteindre un point où la demande énergétique excède cette capacité d'extraction et de transport de l'oxygène.

L'hypoxie est couramment définie comme une concentration d'oxygène dissous inférieure à 2 mg O_2 L^{-1} ou à 30 % de saturation, des seuils en deçà desquels les conséquences pour les écosystèmes peuvent être graves (Galic *et al.*, 2019 ; Rabalais *et al.*, 2010 ; Thomas et Bacher, 2018 ; Wu, 2002). Cependant, l'impact physiologique d'une diminution de l'oxygène ne dépend pas d'un seuil unique, mais plutôt de la manière dont la disponibilité en oxygène limite la capacité d'un organisme à répondre à ses besoins métaboliques. Bien que le seuil de 2 mg O_2 L^{-1} soit largement cité dans la littérature océanographique (Pollock *et al.*, 2007 ; Rabalais *et al.*, 2010 ; Vaquer-Sunyer et Duarte, 2008), il correspond à une hypoxie extrême et ne doit pas être interprété comme l'absence d'effets délétères l'OD est supérieur à ce seuil, pour la plupart des organismes aquatiques.

En réponse à une baisse de disponibilité d'oxygène dans leur milieu, plusieurs réactions dites typiques se manifestent chez les organismes aquatiques. Notamment, un phénomène appelé hyperventilation hypoxique peut être observé (Farrell et Richards, 2009). Il est caractérisé par une augmentation de la fréquence et/ou l'amplitude des mouvements operculaires par unité de temps, pour essayer d'extraire une plus grande quantité d'oxygène. Cette réponse physiologique peut être bénéfique si la diminution de l'oxygène est temporaire ou modérée, car elle retarde la transition du métabolisme aérobie vers le métabolisme

anaérobie (Perry *et al*., 2009). Cependant, cette stratégie devient coûteuse lorsque l'oxygène atteint un niveau où le coût énergétique de l'hyperventilation dépasse ses bénéfices.

Une autre réaction physiologique fréquente et observable est une réduction de la consommation de nourriture (Chabot et Claireaux, 2008 ; Lavaud *et al*., 2018) (Fig. 6). Cette réponse, observée notamment chez des poissons gardés en bassins, pourrait résulter d'une augmentation du temps de digestion. Comme la digestion représente un coût métabolique important, une réduction de la prise alimentaire permet de limiter la dépense énergétique liée au métabolisme postprandial ou action dynamique spécifique (ADS) (Chabot *et al*., 2016a). Bien que cette stratégie se traduise en une diminution de la croissance, l'énergie disponible n'est pas entièrement dépensée à digérer un repas.

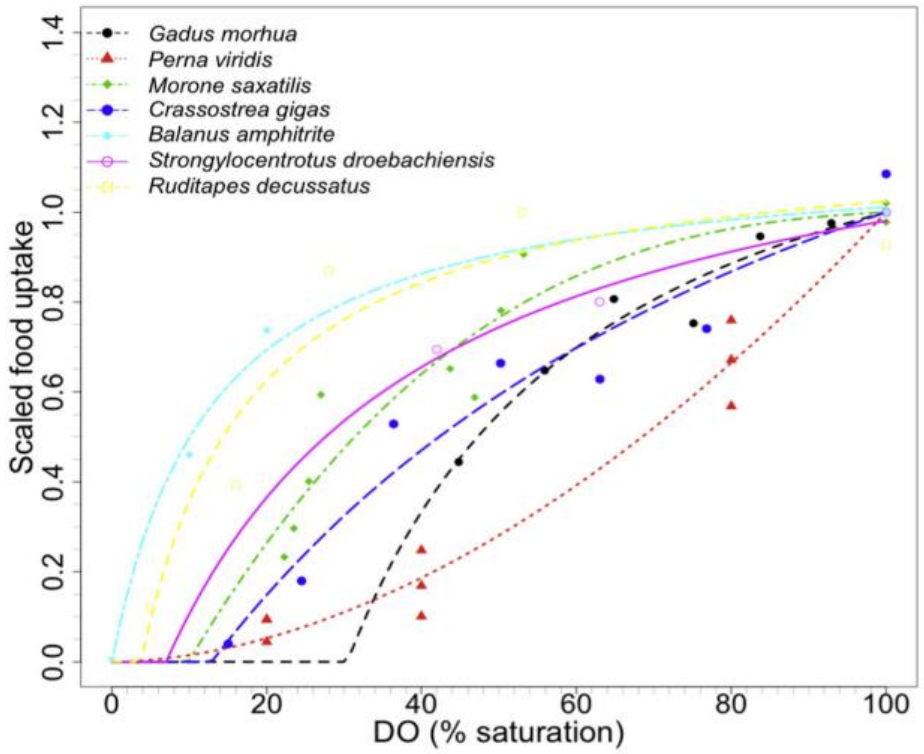

Figure 6. Taux de consommation de nourriture en fonction d'un gradient d'oxygène dissous pour différentes espèces d'invertébrés et de poissons. *Gadus morhua*, morue franche; *Perna viridis*, moule verte; *Morone saxatilis*, bar rayé; *Crassostrea gigas*, huître creuse du Pacifique; *Balanus amphitrite*, balane striée; *Strongylocentrotus droebachiensis*, oursin vert; *Ruditapes decussatus*, palourde commune. Tirée de Thomas *et al*., (2018)

À plus long terme, l'hypoxie affecte également plusieurs composantes du bilan énergétique. Par exemple, la conversion alimentaire, qui correspond à la transformation de la nourriture assimilée en masse corporelle, tend à diminuer en condition hypoxique (Jobling, 1994 ; Wang *et al*., 2009). Par exemple, chez la carpe herbivore (*Ctenopharyngodon idella*), la conversion alimentaire et la croissance semblent significativement réduites lorsque l'oxygène dissous passe sous 2 mg L^{-1} (Gan *et al*., 2013). Ce phénomène peut s'expliquer par la réduction de la capacité aérobie lorsque l'oxygène devient limitant (Claireaux et Lagardère, 1999) (Fig. 7). En condition hypoxique, le TMM diminue, ce qui réduit la disponibilité d'énergie potentielle offerte par la CA et donc la marge disponible pour la digestion. Ainsi, la digestion d'un repas, en particulier d'un repas volumineux, devient plus

coûteuse sur le plan énergétique et peut même ne plus être soutenable lorsque l'apport en oxygène est insuffisant (Claireaux et Lagardère, 1999) (Fig. 7).

Dans des situations plus extrêmes ou prolongées, certains poissons hypoxie-tolérants peuvent abaisser leur métabolisme et réduire leurs fonctions non essentielles afin de prolonger leur survie (Richards, 2011). Toutefois, cette adaptation a ses limites : si l'apport en oxygène devient insuffisant pour maintenir les processus physiologiques vitaux, des défaillances physiologiques, et donc la mort, peuvent en résulter (Richards, 2011).

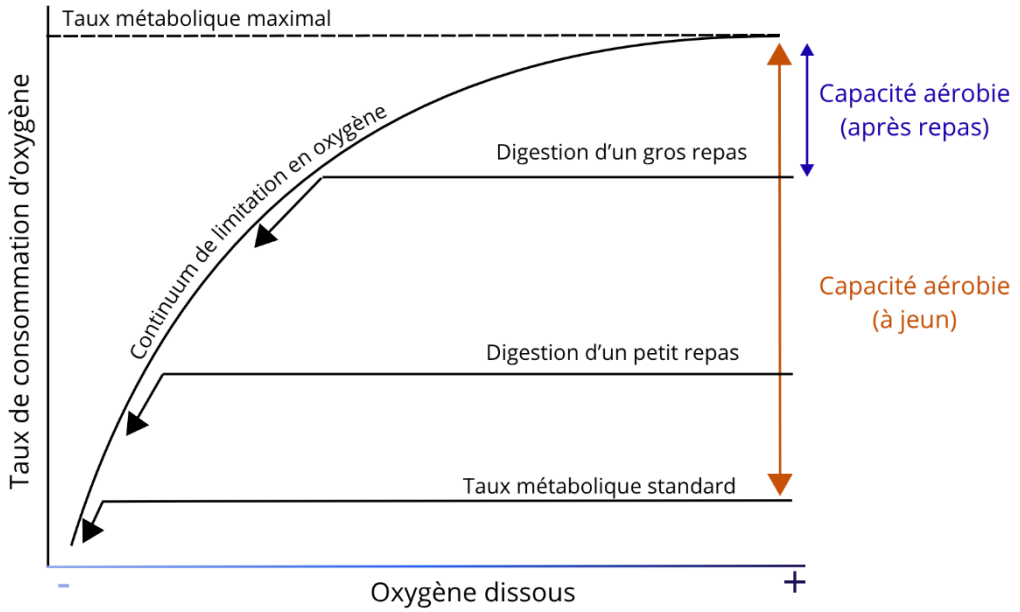

Figure 7. Représentation schématique du continuum de limitation en oxygène et de ses effets sur la capacité métabolique (courbe LOL : la courbe du niveau d'oxygène limitant). À mesure que la disponibilité en oxygène diminue, le taux métabolique maximal que les poissons peuvent atteindre est progressivement limité. La digestion augmente le taux métabolique de base proportionnellement à la taille du repas, ce qui réduit la marge d'énergie disponible pour d'autres fonctions, c'est-à-dire la capacité aérobie. Celle-ci correspond à la différence entre le taux métabolique maximal et le taux métabolique standard (à jeun) ou postprandial (après repas). Figure modifiée de Wang *et al*., (2008).

4.3 Les effets du pH et de l'acidification sur la physiologie des poissons

L'impact de l'acidification des océans sur la capacité des poissons à réguler leur équilibre acido-basique ne suit pas une tendance linéaire et peut varier selon les espèces. Une revue de la littérature par Esbaugh (2018) indique qu'une diminution du pH, correspondant à une augmentation de pCO_2 (augmentation de PCO_2 de ca. 750 à 2800 µatm) peut altérer l'homéostasie acido-basique, la survie lors des premiers stades de vie, le métabolisme, le transport de l'oxygène, la reproduction et la croissance selon l'espèce et le temps d'exposition. Or, la direction de ces effets demeure mal comprise.

À l'instar de la température et de la baisse d'oxygène dissous, le pH et les processus d'acidification peuvent moduler les traits de performance des poissons. L'acidification des océans, causée par l'augmentation des concentrations de CO_2 et la baisse du pH, peut agir différemment sur le TMS et le TMM. Elle agit typiquement comme un facteur masquant sur le TMS (Fry, 1971; Heuer et Grosell, 2014). En effet, la régulation acido-basique engendre un coût énergétique qui s'ajoute au métabolisme de base, ce qui aurait comme effet d'augmenter le TMS (Hannan et Rummer, 2018; Heuer et Grosell, 2014 ; Lefevre, 2016). Quant au TMM, de manière similaire à l'hypoxie, l'acidification peut agir comme un facteur limitant en le réduisant. Ce phénomène s'explique par la diminution de la capacité de transport de l'oxygène par l'hémoglobine, mieux connue comme « effet de Bohr » ou l'hypercapnie (Hannan et Rummer, 2018; Heuer et Grosell, 2014).

Malgré de nombreux travaux, les effets de l'acidification sur le métabolisme aérobique des poissons ne font pas consensus. Ces variations sont le reflet de leur variabilité physiologique et de leur capacité à réguler l'équilibre acido-basique (Baumann, 2019 ; Esbaugh, 2018; Heuer et Grosell, 2014; Kreiss *et al*., 2015). Selon la méta-analyse de Lefevre, (2016), les effets du CO_2 sur le métabolisme aérobique sont généralement faibles, très variables et, dans la majorité des cas, absents pour les ectothermes marins. Parmi les 125 jeux de données examinant le métabolisme de repos équivalent au TMS, seuls 18 ont révélé une augmentation significative et 25 une diminution, alors que la majorité n'a montré aucune

réponse détectable au CO_2. Cette variabilité ne s'est d'ailleurs pas traduite par une diminution systématique de la capacité aérobie : sur les 18 jeux de données portant sur la CA, seul six ont montré un effet du CO_2, un nombre très faible, et ces cas étaient majoritairement observés chez les invertébrés. Cependant, la revue systématique de Yoon *et al*., (2024) souligne que, même si les effets du pH sur le TMS, le TMM ou la CA restent souvent faibles ou incohérents, les réponses physiologiques ne sont pas pour autant négligeables. Plusieurs études rapportent une diminution de la consommation de nourriture, de l'efficacité digestive et à plus long terme, de la croissance, ce qui laisse penser que l'acidification affecte les poissons principalement par des voies indirectes, en perturbant leur bilan énergétique plutôt que leur métabolisme aérobique de manière immédiate. Yoon *et al*., (2024) insistent également sur le caractère contrasté de la littérature, marqué par des réponses parfois opposées selon les espèces, les stades de développement, la durée d'exposition ou les conditions expérimentales. Leur synthèse souligne la nécessité de mieux intégrer les différentes composantes du budget énergétique, ingestion, assimilation, dépense métabolique, croissance, pour comprendre pleinement comment le pH influence la performance des poissons dans un contexte de changements climatiques. Ainsi, même en l'absence de réponses métaboliques claires, l'étude du CO_2 demeure essentielle pour cerner ces ajustements énergétiques plus subtils et leurs répercussions potentielles sur la croissance et la survie.

5. LIMITE DES ÉTUDES EN CONDITIONS CONTRÔLÉES POUR REPRÉSENTER LA VARIABILITÉ ENVIRONNEMENTALE

La majorité des études physiologiques sur les poissons sont réalisées en conditions contrôlées, en laboratoire ou en mésocosmes, où les individus sont élevés en captivité ou transférés depuis leur milieu naturel. Ces environnements permettent un contrôle précis des variables abiotiques, comme la température, l'oxygène dissous ou le pH, et facilitent la répétabilité expérimentale. Toutefois, ils s'éloignent inévitablement des conditions naturelles, où ces mêmes variables fluctuent quotidiennement et saisonnièrement (Tableau 1). Comme l'ont mentionné Turko *et al*., (2023), les animaux maintenus en laboratoire peuvent présenter des différences physiologiques par rapport aux individus sauvages, qui

sont attribuables, entre autres, à des facteurs tels que le régime alimentaire, la charge parasitaire ou le stress lié à la captivité.

Les études menées dans des environnements stables et constants, bien qu'indispensables pour isoler des mécanismes physiologiques précis, peuvent altérer la physiologie et le comportement des organismes (Binning *et al*., 2025) et conduire à des réponses non représentatives des conditions naturelles (Calisi et Bentley, 2009). Par exemple, Beauregard *et al*., (2013) ont montré que des saumons atlantiques (*Salmo salar*) soumis à des fluctuations circadiennes de température présentaient des taux métaboliques standards (TMS) 25 à 32 % plus élevés que ceux de congénères maintenus à température constante. Ces résultats suggèrent que les protocoles expérimentaux en laboratoire, bien qu'indispensable pour isoler des effets précis, peuvent sous-estimer les coûts énergétiques associés à la vie dans des environnements naturellement variables (Tableau 1).

En revanche, les approches qui intègrent une composante de variabilité, par exemple des cycles de température, d'oxygène ou de salinité qui simulent les fluctuations naturelles, permettent de mieux représenter les pressions physiologiques réelles auxquelles les poissons sont soumis dans leur habitat (Binning *et al*., 2025). Ce type de conception expérimentale en laboratoire de plus en plus utilisé offre une vision plus écologique de la performance des organismes et améliore la pertinence des modèles bioénergétiques ou de distribution élaborés à partir de ces données, ce qui en fait un atout pour la recherche en conservation.

Tableau 1. Les avantages et désavantages des approches en laboratoire et sur le terrain. Modifié de Binning *et al*., (2025).

Approches	Avantages	Inconvénients
Approches en laboratoire	**Scientifique**	
	L'environnement de l'organisme est étroitement contrôlé et surveillé (limite les facteurs de confusion).	Ne reproduit pas la complexité des environnements naturels.
	Permets d'établir des relations de cause à effet.	Durée courte (les données représentent souvent une « image instantanée » dans le temps).
	Facile à reproduire	Implique le transfert des organismes vers un milieu artificiel.
	Accès à des outils et technologies spécialisés (microscopes, appareils PCR, incubateurs, etc.).	
	Peut fournir des preuves de concept	L'incorporation de la complexité environnementale peut réduire la puissance statistique pour détecter les différences entre traitements.
	Plus simple et moins coûteux pour tester des traitements avant les essais sur le terrain.	Limité à des expériences à plus petite échelle
		Favorise la recherche sur des espèces modèles.
		Limité aux organismes de petite taille (les contraintes d'espace restreignent la taille physique des organismes expérimentaux).
		Perte du contexte social naturel des organismes étudiés (peut induire du stress supplémentaire).
Approches en laboratoire	**Économique**	
	Réduction des besoins de déplacement (expériences souvent réalisées dans les institutions locales, réduisant les coûts de transport et d'hébergement).	Utilisation intensive de ressources (les équipements scientifiques spécialisés sont coûteux et requièrent de l'espace ainsi que du personnel technique).
Approches en laboratoire	**Social**	
	Facilite l'équilibre travail-vie personnelle en permettant aux chercheurs de résider à leur domicile (lorsque les laboratoires sont situés dans leur établissement d'attache).	Préoccupations éthiques liées à l'exposition des animaux à des conditions de laboratoire irréalistes, à l'isolement ou à des traitements potentiellement nuisibles.
Approches sur le terrain	**Scientifique**	
	Les organismes sont exposés à des interactions biotiques et abiotiques reflétant la complexité et la variabilité des écosystèmes naturels.	Manque de contrôle pouvant introduire des variables confondantes ou non mesurées.
	Données à long terme possibles (ex. suivi à distance, biotélémétrie, stations météo).	Logistique expérimentale complexe (transport, hébergement, équipement, accès aux sites).
	Pertinence accrue pour les politiques environnementales	Données variables et difficiles à reproduire
	Reflète la variabilité naturelle des populations (résultats généralisables à l'échelle de la population)	Accès aux organismes parfois limité
	Réduction du stress lié à la limitation des interactions avec les chercheurs et le milieu artificiel	Forte variation interindividuelle
Approches sur le terrain	**Économique**	
	Économie de coûts de maintien des animaux en laboratoire (bassins, enrichissement, personnel d'entretien)	Coûteux en temps et en ressources (limite le nombre de sites ou la durée du projet).
		Coûts de déplacement élevés, surtout pour les sites éloignés.
Approches sur le terrain	**Social**	
	Les interactions avec les communautés locales favorisent la confiance et la cocréation.	Risques pour la sécurité, notamment dans les sites éloignés où l'accès aux services de santé est limité.
		Préoccupations éthiques liées à la perturbation de l'environnement naturel, en particulier sur des sites ou des espèces culturellement importantes.

Les études menées directement en milieu naturel ou à l'aide d'approches *in situ* représentent une étape essentielle pour relier les réponses physiologiques observées en laboratoire aux conditions réelles rencontrées par les organismes, et comportent certains avantages et inconvénients (Binning *et al*., 2025; Tableau 1). Ces approches permettent d'évaluer la performance énergétique, la croissance ou le métabolisme aérobique des poissons dans leur environnement naturel, en tenant compte de la complexité physique des habitats, des interactions biotiques et des fluctuations spatio-temporelles de variables, telles que la température, l'oxygène ou la disponibilité alimentaire sur des traits de performance, comme la croissance ou le métabolisme.

En raison de contraintes logistiques, peu d'études ont estimé le métabolisme aérobique en milieu naturel, mais celles qui l'ont fait étaient souvent motivées par des objectifs écologiques ou de conservation, donnant lieu à des approches méthodologiques variées. Par exemple Farrell *et al*. (2003) ont utilisé un tunnel de nage mobile installé en bordure de rivière pour mesurer la consommation d'oxygène et la capacité de nage de saumons du Pacifique (*Oncorhynchus* spp.) pendant leur migration vers l'amont, intégrant ainsi les contraintes énergétiques associées à cet effort. De même, Gamperl *et al*. (2002) ont mené une expérience comparable sur des truites rouges du désert (*Oncorhynchus mykiss* ssp.) afin d'évaluer leurs adaptations physiologiques aux variations de température et de débit liées aux saisons. D'autres travaux ont conçu des respiromètres automatisés pour les profondeurs, adaptés à des espèces incapables de survivre à une remontée à la surface en raison du barotraumatisme (Drazen et Seibel, 2007 ; Drazen et Yeh, 2012). Enfin, certains dispositifs de respirométrie *in situ* ont été adaptés à des sites isolés dépourvus d'électricité, fonctionnant uniquement à partir du courant de la rivière (Mochnacz *et al*., 2017).

Ainsi, bien que les études en conditions contrôlées demeurent essentielles pour comprendre les mécanismes physiologiques de base et assurer la comparabilité des résultats, leur complémentarité avec des approches intégrant la variabilité environnementale ou des mesures effectuées *in situ* apparaît cruciale. Ensemble, ces approches permettent de mieux

relier la physiologie à l'écologie, et d'évaluer la capacité réelle des espèces à faire face aux changements rapides et multidimensionnels des milieux marins.

6. LE SÉBASTE DU GOLFE DU SAINT-LAURENT

6.1 L'écologie du sébaste

Deux espèces de sébaste dominent dans le golfe du Saint-Laurent : le sébaste atlantique (*Sebastes mentella*) et le sébaste acadien (*S. fasciatus*). Ces poissons sont considérés comme des espèces démersales, c'est-à-dire qu'ils utilisent le fond marin comme habitat et se trouvent principalement sur les pentes des bancs et dans les chenaux profonds, comme le chenal Laurentien (Senay *et al*., 2023).

Le stade adulte des deux espèces vit à de grandes profondeurs (>150 m), mais occupent des intervalles de profondeurs en moyenne distinctes. *S. mentella* occupe des profondeurs plus grandes (350-500 m) que *S. fasciatus* (<300 m). Un chevauchement de leur distribution est parfois observé en zone de sympatrie, comme dans le GSL et le chenal Laurentien à l'extérieur du GSL (Benestan *et al*., 2021 ; Senay *et al*., 2023). *S. fasciatus* est aussi largement retrouvé sur les bancs de la Côte-Nord de l'estuaire et du golfe du Saint-Laurent, parfois à des profondeurs aussi faibles que 30 mètres. Les raisons pour lesquelles certains individus occupent parfois ces zones peu profondes demeurent inconnues, mais la présence d'habitats structurés, notamment des fonds rocheux offrant des refuges adaptés aux tailles observées, constitue une explication plausible (Auster *et al*., 2003).

Des études récentes ont montré que les sébastes dont la taille est inférieure à 20 cm se nourrissent principalement de copépodes (*Calanus* sp.) et de krill (Brown-Buillemin *et al*., 2022; Brown-Vuillemin *et al*., 2023). Une transition alimentaire est observée chez les individus de 20 à 30 cm, les crevettes (*Pandalus* sp. et *Phasiphaea* sp.) et les poissons prenant une place de plus en plus importante dans leur alimentation (Brown-Vuillemin *et al*., 2022; Brown-Vuillemin *et al*., 2023). Les individus de plus de 30 cm se nourrissent quant à eux

presqu'exclusivement de crevettes et de poissons (Brown-Vuillemin *et al*., 2022; Brown-Vuillemin *et al*., 2023), des espèces qui sont elles aussi affectées par les changements opérant dans le GSL (Bourdages *et al*., 2023).

6.2 Exploitation commerciale des deux espèces et différenciation des stocks

L'exploitation commerciale des sébastes a débuté à la fin des années 1950 (Gascon, 2003). En raison de son recrutement dit « spasmodique », qui signifie qu'il connaît des épisodes de recrutement forts mais irréguliers (Licandeo *et al*., 2020), trois principales périodes d'exploitation ont été identifiées (1954-1956, 1965-1976 et 1987-1992). À la suite d'une combinaison de facteurs, notamment des conditions environnementales défavorables, incluant des épisodes de froid au début des années 1990, et la pression de la pêche, les stocks se sont effondrés à partir de 1990, menant à l'instauration d'un moratoire en 1995 pour l'Unité 1 (Fig. 8). Depuis 1999 une permission de pêche a été allouée à certains pêcheurs pour réaliser un pêche indicatrice. Cette pêche comporte toutefois plusieurs mesures mises en place pour favoriser le rétablissement des populations, notamment des protocoles qui visent à réduire les prises accessoires et à protéger les petits individus (<22 cm), la présence d'observateurs en mer mandatés par Pêches et Océans Canada (MPO), un suivi des débarquements à quai et la fermeture de certaines zones en automne et au printemps afin de protéger la reproduction (Senay *et al*., 2023).

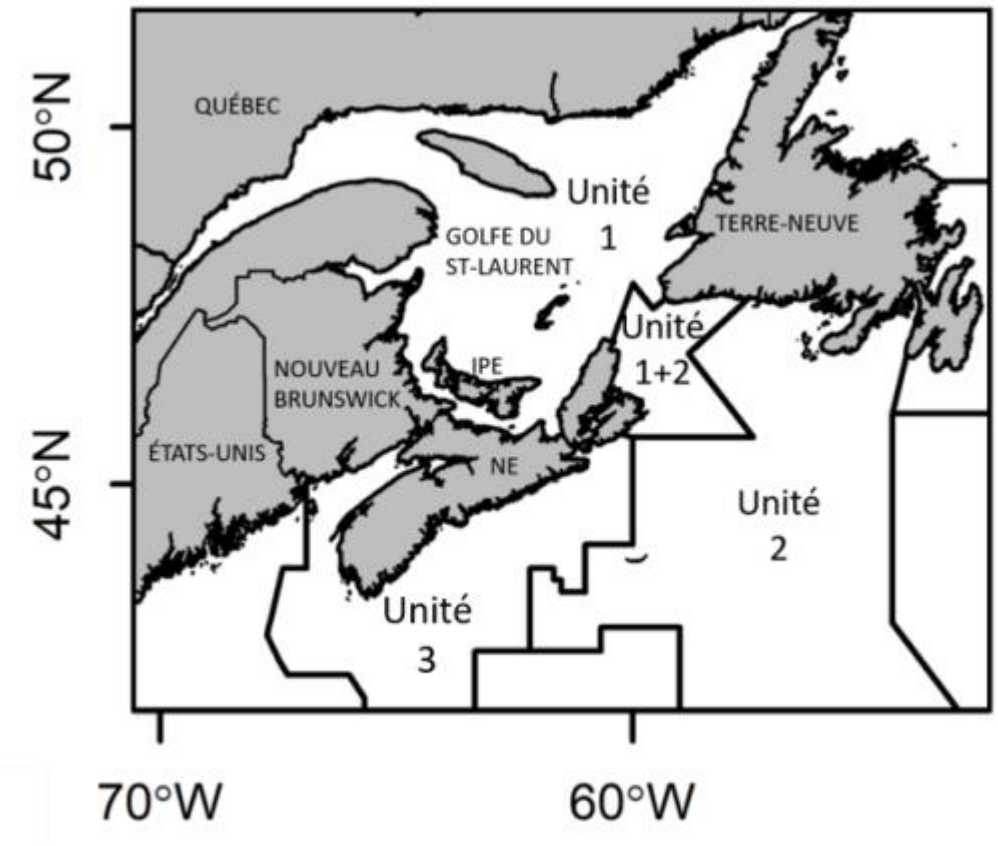

Figure 8. Unité de gestion 1, 2 et 3 (IPE = Île-du-Prince-Édouard, NE = Nouvelle-Écosse; Senay *et al*., 2021)

Les deux espèces de sébastes présentes dans le GSL sont morphologiquement très similaires, ce qui a nui à la reconnaissance de stocks distincts dans un contexte de pêche commerciale. L'absence de traits morphologiques externes permettant la discrimination des deux espèces à l'individu a mené à divers efforts afin de les distinguer, autant pour le développement d'outils utilisables sur le terrain, comme le dénombrement des rayons de la nageoire anale (Senay *et al*., 2022) que pour le développement de marqueurs génétiques nécessitant des analyses en laboratoire (Benestan *et al*., 2021 ; Roques *et al*., 2002 ; Valentin *et al*., 2014). Depuis plus de 20 ans, les analyses génétiques confirment que *S. mentella* et *S. fasciatus* sont deux espèces distinctes (Benestan *et al*., 2021 ; Valentin *et al*., 2014). Ces espèces se sont toutefois hybridées dans le passé et les études génétiques ont identifié de l'introgression historique bidirectionnelle, soit la présence d'une portion de génome de

l'autre espèce chez les deux espèces (Benestan *et al*., 2021 ; Roques *et al*., 2002). Certaines sous-composantes des deux espèces, c.-à-d. des écotypes chez *S. mentella* et des populations chez *S. fasciatus*, présentent de l'introgression historique (Benestan *et al*., 2021). En effet, l'écotype de *S. mentella* vivant dans le GSL a environ 18 % de son génome similaire à celui de *S. fasciatus* (Benestan *et al*., 2021). Plusieurs des sous-composantes des deux espèces, c.-à-d. écotypes ou populations, ne présentent toutefois pas d'introgression et l'hybridation interspécifique contemporaine semble rare (Benestan *et al*., 2021). Dans l'ensemble de leur aire de répartition de l'Atlantique nord-ouest, les deux espèces présentent une structuration spatiale importante, comparée à d'autres espèces, comme le maquereau (Bourret *et al*., 2023), ce qui suggère un faible potentiel de dispersion ou migration des espèces (Benestan *et al*., 2021).

En 2022, le sébaste représentait plus de 80 % de la biomasse capturée lors du relevé au chalut de fond du MPO dans le GSL (Fig. 9A), principalement attribuée à *S. mentella* (Senay *et al*., 2023) (Fig. 9B). L'abondance actuelle dans le GSL résulte de trois cohortes particulièrement fortes en 2011, 2012 et 2013 qui sont principalement composées de *S. mentella*, même si une augmentation des effectifs de *S. fasciatus* ont aussi été observés (Chamberland *et al*., 2025 ; Senay *et al*., 2023) (Fig. 9C). Le succès de ces cohortes pourrait être lié à des conditions environnementales favorables observées au cours de la dernière décennie.

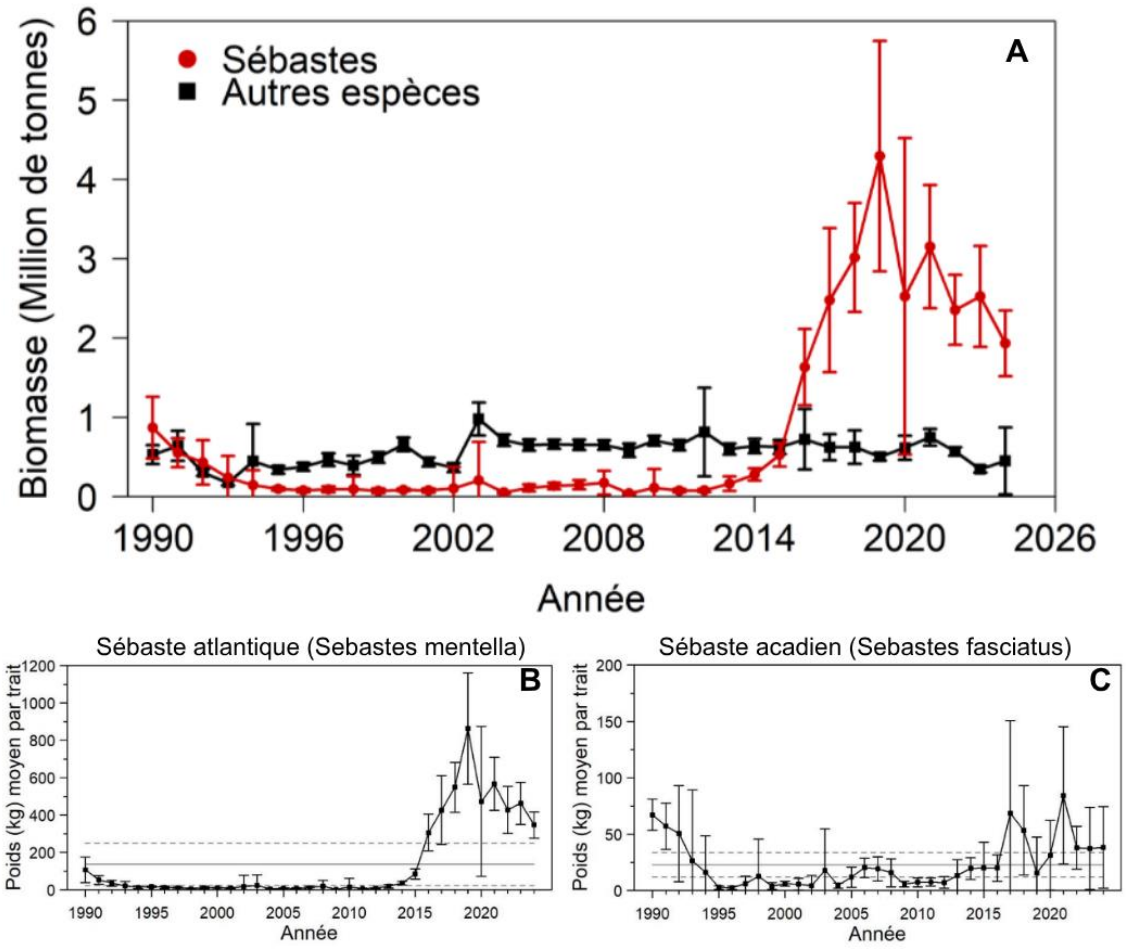

Figure 9. A) Estimations de la biomasse (en millions de tonnes) des espèces de sébaste et de toutes les autres espèces échantillonnées dans la zone d'étude. Les barres d'erreur représentent des intervalles de confiance à 95 %. Masse moyenne (kg) par trait de 15 minutes observé pendant l'étude sur le B) sébaste atlantique (*Sebastes mentella*) et C) le sébaste acadien (*Sebastes fasciatus*) dans la zone 4RST. Les barres d'erreur indiquent l'intervalle de confiance à 95 % et les lignes horizontales indiquent la moyenne pour la période 1990-2021 (ligne continue) et les limites de référence supérieure et inférieure (ligne pointillée). Tirée de Chamberland *et al*., 2025

Au moment de l'amorce de ce projet de thèse (2021), nous prévoyions que l'augmentation sans précédent de la biomasse de sébaste dans le GSL ouvrirait la porte à la réouverture de la pêche commerciale dans un avenir rapproché. Depuis le 15 juin 2024, la pêche au sébaste est effectivement rouverte dans les divisions 4RST selon le Plan de gestion du sébaste – Unité 1 (MPO), sous un Total Autorisé de Captures (TAC) de 60 000 tonnes

pour la saison 2024-2025. Pour limiter l'impact sur *S. fasciatus*, des restrictions de profondeur de chalutage ont été imposées (pêche autorisée uniquement à des profondeurs supérieures à 183 m au début de la saison).

La rentabilité des pêches dépend de la croissance des individus. Le sébaste est une espèce à croissance et à maturation lentes, avec une taille modale exploitable de 22 cm (Senay *et al*., 2023). Depuis quelques années, la taille individuelle du sébaste dans le GSL semble plafonner autour de 24–25 cm, suggérant que les cohortes récentes n'atteignent pas des tailles plus grandes; parallèlement, la biomasse totale estimée dans les unités de gestion 1 et 2 est passée de 4,3 millions de tonnes métriques en 2019 à 2,5 millions en 2024 (un déclin d'environ 40 %). Malgré cette baisse marquée, il s'agit encore d'une biomasse exceptionnelle pour le GSL, vraisemblablement au-delà de la capacité de support du milieu : ce serait donc la densité élevée qui contribuerait au ralentissement de la croissance (Brûlé *et al*., 2024; Chamberland *et al*., 2025; Coussau *et al*., 2024) (Fig. 9A).

7. PROBLÉMATIQUE ET OBJECTIFS DE LA THÈSE

La recrudescence du sébaste, tant *S. mentella* que *S. fasciatus*, constitue un évènement sans précédent dans les eaux du GSL. Cet évènement justifie qu'on s'intéresse à l'impact que ces espèces auront sur leur environnement, mais aussi quel impact l'environnement présent et futur aura sur elles.

La remontée en biomasse du sébaste, combinée à sa perte de croissance récente en comparaison aux cohortes du passé, illustre bien l'ampleur des changements déjà en cours dans le GSL. Plusieurs études montrent que les sébastes des cohortes récentes présentent des profils biologiques différents de ceux nés dans les années 1980. Par exemple, les reconstructions de croissance à partir des otolithes indiquent que les individus issus des cohortes 2011–2013 affichent une croissance plus lente et atteignent des tailles asymptotiques ou maximales plus faibles que ceux des années 1980, un phénomène attribué en grande partie à une densité-dépendance et à l'augmentation de température (Coussau *et al*., 2024). De même, ces cohortes récentes montrent une réduction marquée de la taille à la

maturité en comparaison avec celles de 1980, suggérant que les pressions de densité et les conditions environnementales changeantes influencent déjà leurs traits de vie (Brûlé *et al*., 2024). Des changements importants sont également observés dans leur écologie trophique : les individus des années 2010 n'utilisent plus les mêmes proies dominantes que ceux capturés dans les années 1990, montrant que les transformations récentes du GSL et l'arrivée massive des nouvelles cohortes influencent désormais le régime alimentaire du sébaste (Brown-Vuillemin *et al*., 2022). Enfin, les variations d'expression génique observées chez les juvéniles indiquent que leur croissance et leur métabolisme sont fortement influencés par les conditions environnementales locales, en particulier la température (Martínez-Silva *et al*., 2022). Bien que ces études portent presque qu'exclusivement sur *S. mentella*, elles démontrent que la croissance, les stratégies de reproduction, l'écologie alimentaire et la physiologie du sébaste sont en train d'être remodelées par les transformations rapides de l'environnement et de l'écosystème du GSL.

Cependant, bien que plusieurs travaux aient mis en évidence des changements de croissance, de maturité, d'alimentation ou d'expression génique, les mécanismes physiologiques qui relient les conditions environnementales du GSL aux performances du sébaste demeurent largement méconnus. La majorité des travaux portent sur *S. mentella* et reposent sur des observations en mer ou des analyses rétrospectives plutôt que sur des mesures expérimentales directes. Il manque notamment des données mécanistiques quantifiant comment la température, l'oxygène dissous et l'acidification modulent le métabolisme, l'acquisition d'énergie et la croissance, particulièrement chez *S. fasciatus*, seule espèce accessible vivante. L'absence d'expériences longues et multifactorielle, ainsi que la rareté des mesures métaboliques en conditions naturelles, empêche pour l'instant de comprendre pleinement les déclins de performance observés. Elles rendent aussi difficile l'évaluation des perspectives futures pour ces populations, qui connaissent un rebond de biomasse marqué mais demeurent vulnérables en raison d'une mortalité élevée et d'une condition physiologique fragilisée.

Malheureusement, l'accessibilité à ces deux espèces est restreinte en raison de leur habitat en grande profondeur et de leur physiologie de poissons physoclistes, c'est-à-dire que leur vessie natatoire n'est pas reliée à leur œsophage. Ils tolèrent donc mal les changements de pression associés à leur remontée vers la surface. Leur remontée rapide des profondeurs auxquelles on les retrouve entraîne donc leur mort. *S. mentella* est typiquement pêché au chalut de fond, mais les individus récoltés ne survivent pas à la remontée. Heureusement, certains groupes d'individus, maintenant identifiés comme *S. fasciatus*, utilisent des habitats moins profonds, rendant donc possible leur remontée à la surface en vie grâce à une technique élaborée et perfectionnée au sein de notre institution, soit la capture d'individus par plongeurs et leur remontée lente avec un palier à profondeur intermédiaire.

Les données recueillies dans cette thèse serviront à mieux comprendre comment les changements actuels et futurs des conditions environnementales du golfe du Saint-Laurent influencent la performance physiologique du sébaste (*S. fasciatus*). L'objectif de cette thèse était de comprendre l'effet des changements présents et futurs sur le métabolisme aérobique, la consommation de nourriture et, ultimement, la croissance de cette espèce. En estimant ces traits physiologiques sous différentes conditions de température, d'oxygène et d'acidification qui reflètent l'environnement présent et futur de cette espèce. Cette recherche permettra d'identifier certains des mécanismes sous-jacents au ralentissement de la croissance des sébastes déjà observé en conditions naturelles, et contribuera ainsi à évaluer la favorabilité des habitats profonds à long terme pour cette espèce dans un environnement changeant et à appuyer la gestion durable de la pêche commerciale récemment rouverte.

Pour ce faire, cette thèse de doctorat s'est déclinée en trois sous-objectifs, chacun associé à un chapitre :

7.1 Chapitre 1 : Le réchauffement, mais non l'acidification, augmente les taux métaboliques aérobiques et réduit la croissance du sébaste (*Sebastes fasciatus*) dans le golfe du Saint-Laurent.

L'objectif de ce chapitre était d'évaluer les effets seuls et combinés du réchauffement et de l'acidification de l'eau sur la physiologie et la croissance du sébaste (*S. fasciatus*) du golfe du Saint-Laurent. Plus précisément, nous avons (i) quantifié les traits métaboliques clés sous des combinaisons de températures (2,5, 5, 7,5, 10 °C) et de pH (7,35; 7,75), soit les taux métabolique maximal (TMM), taux métabolique standard (TMS), capacité aérobie (CA) et tolérance à l'hypoxie (O_2crit) ; (ii) évalué les composantes d'acquisition et d'utilisation de l'énergie, de consommation de nourriture, efficacité de conversion alimentaire et de croissance. Nous avons testé les hypothèses que (i) le réchauffement est le principal moteur des réponses (augmentation de TMS, altération de TMM, diminution de CA aux températures élevées, entraînant une baisse de croissance), alors que (ii) l'acidification dans l'intervalle étudiée (pH 7,35 –7,75) exerce peu d'effets et n'amplifie pas substantiellement ceux de la température. Ultimement, notre but était de lier ces réponses individuelles à des contraintes d'allocation énergétique afin d'anticiper leurs conséquences sur la performance et la productivité d'un stock d'importance écologique et commerciale sous des conditions environnementales actuelles et futures.

7.2 Chapitre 2 : Capacité aérobie et croissance réduites chez le sébaste acadien (*Sebastes fasciatus*) du golfe du Saint-Laurent soumis à une hypoxie chronique

L'objectif général de cette étude était de comprendre comment une exposition prolongée à des niveaux réduits d'oxygène dissous, représentatifs des conditions rencontrées par le sébaste acadien (*S. fasciatus*) dans le golfe du Saint-Laurent, affecte sa physiologie et sa performance de croissance. Plus précisément, nous avons exposé des poissons pendant 105 jours à huit niveaux d'oxygène dissous entre 25–100 % de saturation, à une température constante de 5 °C, afin (i) de mesurer les traits métaboliques clés, soit le taux métabolique

maximal (TMM), taux métabolique standard (TMS), capacité aérobie (CA) et tolérance à l'hypoxie (O_2crit), (ii) d'évaluer les composantes d'acquisition et d'utilisation de l'énergie, de la consommation de nourriture, efficacité de conversion alimentaire, croissance en masse et en longueur, et condition corporelle, et (iii) d'identifier des seuils/points de rupture le long du gradient d'oxygène où les effets sous-létaux émergent. Nous avons testé l'hypothèse que la diminution d'oxygène dissous réduit d'abord TMM plus que TMS, entraînant une diminution de l'énergie disponible (CA) pour les différentes activités d'importance écologique pour un individu, telle que l'alimentation et la croissance, ce qui se traduit par une baisse d'énergie disponible pour l'ingestion et la digestion de nourriture et pour la croissance, de l'efficacité alimentaire, et une perte de condition à des niveaux d'oxygène dissous à partir d'un seuil d'oxygène dissous devant être déterminé à partir des résultats. Ultimement, notre but est de relier ces réponses individuelles à des contraintes d'allocation énergétique qui pourraient limiter la performance, la répartition et la productivité du stock dans un contexte de désoxygénation croissante dans son milieu naturel.

7.3 Chapitre 3 : Du laboratoire au milieu naturel : les mesures *in situ* de consommation d'oxygène concordent avec celles obtenues en laboratoire chez *Sebastes fasciatus.*

L'objectif de cette étude était de concevoir et de tester une méthode de respirométrie *in situ* pour estimer les taux métaboliques de poissons dans leur environnement naturel, en prenant le sébaste acadien (*S. fasciatus*) comme modèle. Nous cherchions à développer un système autonome, robuste et peu invasif permettant de mesurer la consommation d'oxygène ($\dot{M}O_2$) directement en mer, tout en minimisant les manipulations et le stress liés à la capture et en évitant le transport des poissons. Le but principal qui nous a poussés à développer cette technique est de pouvoir obtenir des taux de consommation d'oxygène les plus réalistes et près de ce que les individus en milieu naturel vivront au quotidien. Le premier sous-objectif était de valider le fonctionnement technique du dispositif de respirométrie submergé et d'évaluer sa capacité à fournir des mesures précises et stables sur 24 heures dans des conditions environnementales naturelles. Le second sous-objectif visait à comparer les taux

métaboliques obtenus en milieu naturel (RMR) avec ceux mesurés en laboratoire (TMS) sur les mêmes individus ou sur des poissons de tailles comparables, afin d'évaluer la cohérence entre ces deux approches et la pertinence écologique des mesures réalisées en conditions contrôlées. Plus largement, cette étude visait à combler le fossé entre les mesures de laboratoire et les conditions naturelles, en démontrant la faisabilité et l'intérêt de la respirométrie *in situ* pour améliorer la compréhension du métabolisme et de la dépense énergétique des poissons dans leur habitat réel.

CHAPITRE 1
LE RÉCHAUFFEMENT, MAIS NON L'ACIDIFICATION, AUGMENTE LES TAUX MÉTABOLIQUES AÉROBIQUES ET RÉDUIT LA CROISSANCE DU SÉBASTE (*SEBASTES FASCIATUS*) DANS LE GOLFE DU SAINT-LAURENT.

1.1 RÉSUMÉ EN FRANÇAIS DU PREMIER ARTICLE

Comprendre les effets des changements globaux, y compris la température, le pH et la disponibilité en oxygène, sur les espèces marines d'importance commerciale est essentiel pour anticiper les conséquences sur cette ressource et les écosystèmes. Dans le golfe du Saint-Laurent (GSL), la pêche au sébaste (*Sebastes spp.)* a été soumise à un moratoire de 1995 à 2023, puis réouverte en 2024 à la suite d'un recrutement massif des cohortes 2011–2013. Malgré une forte abondance, leur physiologie métabolique et thermique demeure peu connue, rendant difficile la prédiction de leur réponse aux conditions changeantes du GSL. Nous avons quantifié les effets de quatre températures d'acclimatation (2.5, 5.0, 7.5 et 10.0 °C) et de deux niveaux de pH (7,35 et 7,75) sur les taux métaboliques standard et maximal (TMS et TMM), la capacité aérobie (CA), la capacité aérobique factorielle, la tolérance à l'hypoxie (O_2crit), la consommation de nourriture, la croissance et l'efficacité alimentaire chez les sébastes (*Sebastes fasciatus*). TMS, TMM et CA augmentaient avec la température, mais la croissance diminuait à 10.0 °C, probablement en raison de la demande métabolique accrue, tandis que la consommation alimentaire demeurait similaire de 5.0 à 10.0 °C. O_2crit était plus faible chez les poissons acclimatés à 2.5 et 5.0 °C, indiquant une moindre tolérance à l'hypoxie à des températures plus élevées. Aucun effet significatif du pH n'a été observé, sauf pour le TMS. Ces résultats suggèrent que les changements futurs dans le GSL poseront des défis aux sébastes, avec des effets potentiels à long terme sur leur croissance en raison d'une demande énergétique accrue.

Mots-clés : écophysiologie, taux métaboliques, prise de nourriture, consommation d'oxygène, tolérance à l'hypoxie, changement climatique

Cet article, intitulé « *Warming, but not acidification, increases metabolism and reduces growth of redfish (Sebastes fasciatus) in the Gulf of St. Lawrence* », a été accepté pour publication dans sa version finale en 2025 par les éditeurs de la revue *Canadian journal of zoology* (DOI : 10.1139/cjz-2025-0014). En tant que première autrice, j'ai assuré la recherche bibliographique, la conception méthodologique, la collecte et l'analyse des données, ainsi que la rédaction du manuscrit. Le chercheur Denis Chabot, deuxième auteur, est à l'origine de l'idée initiale du projet et a contribué à la conception de l'étude, au financement, à la mise à disposition des ressources matérielles, à la supervision scientifique, à l'analyse des données et à la révision du manuscrit. Caroline Senay, troisième autrice, a participé à la conceptualisation du projet, à la gestion du projet et à la révision du manuscrit. Dominique Robert, quatrième auteur, a contribué à la supervision scientifique, à la validation des analyses et à la révision du manuscrit. Enfin, le dernier auteur, David Deslauriers, a participé au développement de la méthodologie, à la mise à disposition des ressources matérielles, à la supervision et à la révision du manuscrit.

Les résultats de cette étude ont été présentés à trois occasions : d'abord à la conférence *RespFest 2* tenue à Rimouski (Canada) en mai 2022, où la présentation a remporté le prix de la meilleure communication, puis à l'*International Conference for the Biology of Fishes* tenue à Montpellier (France) à l'été 2022, et enfin à la *153rd Annual Meeting of the American Fisheries Society* (présentation en ligne) à l'automne 2023.

1.2 WARMING, BUT NOT ACIDIFICATION, INCREASES METABOLISM AND REDUCES GROWTH OF REDFISH (*SEBASTES FASCIATUS*) IN THE GULF OF ST. LAWRENCE

Joëlle J. Guitard[a], Denis Chabot[b], Caroline Senay[b], Dominique Robert[a], and David Deslauriers[a]

[a]Institut des sciences de la mer, Université du Québec à Rimouski, Rimouski, QC, Canada; [b]Maurice Lamontagne Institute, Fisheries and Oceans Canada, Mont-Joli, QC, Canada

1.3 ABSTRACT

Understanding the effects of global change, including temperature, pH, and oxygen availability, on commercially important species is crucial for anticipating consequences for these resources and their ecosystems. In the Gulf of St. Lawrence (GSL), redfish (*Sebastes spp.*) were under moratorium from 1995 to 2023, but the fishery has reopened in 2024 following massive recruitment observed in 2011–2013. Despite current high abundance, little is known about their metabolic and thermal physiology. To address this, we quantified the effects of four acclimation temperatures (2.5, 5.0, 7.5, and 10.0 °C) and two ocean acidification scenarios (current and future) on standard and maximum metabolic rates (SMR and MMR), aerobic scope (AS), factorial aerobic scope, hypoxia tolerance (O_2crit), food consumption, growth and food conversion efficiency (FCE) in redfish (*Sebastes fasciatus* Storer, 1854). SMR, MMR, and AS increased with temperature, but growth and FCE decreased with temperature, likely due to increased cost of maintenance. Food consumption was lower at 2.5 °C, but similar at higher temperatures. Redfish were less hypoxia-tolerant at higher temperatures. Except for SMR, no significant effect of pH was observed. These results suggest that future changes in the GSL will challenge redfish, with potential long-term effects on growth due to increased energy requirements.

Key words: ecophysiology, metabolic rates, food intake, oxygen uptake, hypoxia tolerance, climate change

1.4 INTRODUCTION

Global change, through biotic and abiotic factors, impacts marine species with particularly severe effects on boreal and polar species (Parmesan and Yohe 2003; Perry et al. 2005; IPCC 2023). For example, changes in temperature in the North Sea drove a northward change in mean distribution of nearly two thirds of species (Perry et al. 2005). Such periods of instability can lead to ecosystem regime shifts, which are characterized by drastic changes in food web structure and species composition within the community. One example is the collapse of several pandalid shrimp species under increasing water temperatures in the Gulf of Alaska (Anderson and Piatt 1999), which was accelerated by the resurgence of ground fish species (*Pleuronectidae*), pacific cod (*Gadus macrocephalus* Tilesius, 1810), walleye pollock (*Theragra chalcogramma* (Pallas, 1814)) as well as pleuronectid flatfishes over the course of a 10-year period (Anderson 2000).

The state of an ecosystem when a major regime shift occurs can greatly influence its resilience (Möllman and Diekmann 2012). While a stable system is typically resilient, one undergoing drastic change in abiotic factors such as temperature or pH is generally more vulnerable to similar changes in species composition and biomass (Holling 1973; Möllmann and Diekmann 2012). Georges Bank haddock illustrates how species can recover following a stock collapse (DFO 2024). A 10-fold increase in biomass over 10 years, mostly based on the sole 1999 strong year class (Platt et al. 2003; Head et al. 2005), was observed for this stock, leading to physiological changes, such as reduced growth and a below-average mean size at age (Brodziak et al. 2008). These physiological changes were driven mainly by density-dependent mechanisms and environmental factors like temperature (Wang et al. 2021) and have a major impact on resource availability to the commercial fishery (Brodziak et al. 2008). Understanding species physiological needs in a changing ecosystem through their performance traits helps to better comprehend their impact on their environment.

Performance traits of an individual can determine the ability of an individual to succeed in ecologically relevant tasks such as foraging, competing with other species, growing or

reproducing, and is defined in this study as the physiological traits investigated (Arnold 1983; Bennett and Huey 1990). In fishery science, growth is a key physiological trait used to assess the health of individuals or cohorts and to predict when a cohort will reach critical size thresholds. These thresholds include the minimum or maximum regulatory size for collection and the length at which 50% of individuals are mature (L50) and considered part of the spawning stock biomass (e.g., Brûlé et al. 2024). Food conversion efficiency (FCE), which describes how effectively an organism converts ingested food into body mass, is an important determinant of growth (Craig et al. 2002). It integrates both behavioral and physiological aspects of performance, including foraging ability and metabolic cost, and is thus a valuable indicator of overall performance in aquaculture and ecological studies (Jobling 1994). These physiological indicators are critical for making management decisions such as setting total allowable catch. In addition to growth as a performance trait, aerobic metabolic performance provides valuable insight into the potential energy available to an organism. It has been shown that the level of oxygen uptake is proportional to the amount of energy expenditures in organisms (for reviews, see Chabot et al. 2016b; Nelson and Chabot 2024). Aerobic metabolic performance is characterized by upper and lower bounds. The maximal metabolic rate (MMR) represents the maximum oxygen uptake capability (Hulbert and Else 2000), while the standard metabolic rate (SMR) reflects the minimal energy needed for maintenance in a resting, post-absorptive state (Chabot et al. 2016b). The difference between MMR and SMR is known as the aerobic scope (AS), which indicates the maximum energy capacity for activities like locomotion, digestion, growth, and reproduction (Fry 1947; Claireaux and Lefrançois 2007; Nelson 2016). However, an animal's aerobic scope can also be represented as a ratio of its MMR to SMR, known as factorial aerobic scope (FAS). In contrast to AS, FAS analysis examines the capacity of the organism's oxygen transport system in comparison to its baseline oxygen uptake rate (Halsey et al. 2018). Consequently, AS and FAS can provide insight on the potential energy capacity that an animal can invest towards growth under different environmental constraints when food is not limited.

Most environmental abiotic factors such as temperature (Schulte 2015), dissolved oxygen (Claireaux and Chabot 2016) or pH (Heuer and Grosell 2014) can have a detrimental

effect on growth by reducing aerobic scope through multiple pathways for fishes. For the majority of fishes which are ectotherms, temperature acts as a controlling factor which in the case of an increase of temperature accelerates chemical reactions. These changes in temperature can have many effects on different physiological traits of an ectotherm through those processes. While temperature has been traditionally considered a controlling factor for metabolic processes in ectotherms (Fry 1971), it does not always follow a simple bell-shaped relationship with aerobic scope, as shown by Lefevre (2016), who reported considerable variability in thermal performance curves across different studies. The effects of temperature on fish performance traits, such as metabolic rates, growth, and hypoxia tolerance (O_2crit: the minimum oxygen level required to sustain metabolic demands of maintenance (SMR); Claireaux and Chabot 2016), are well-documented (Mandic et al. 2009; Gislason et al. 2010; Schulte 2015; Ern et al. 2016). One hypothesis that attempts to explain the relationship between AS and fitness-related traits, such as growth, is the oxygen and capacity-limited thermal tolerance (OCLTT) hypothesis (Pörtner 2010). This hypothesis posits that as an animal approaches its thermal limits, its ability to supply oxygen to tissues decreases, leading to a decline in aerobic performance and, consequently, a reduction in growth. However, the OCLTT hypothesis has been criticized for its lack of empirical support, as numerous studies have demonstrated that aerobic scope does not always correlate with growth or reproductive performance (Clark et al. 2013; Jutfelt et al. 2018). Nevertheless, observing high AS values under specific environmental conditions indicates that these conditions are not lethal, and that growth remains possible (Pörtner 2010; Clark et al. 2013). Thus, while AS provides important information on the physiological capacity of a species, its relationship with fitness-related traits may vary depending on species-specific responses and environmental contexts. However, performance traits cannot only be altered by temperature, but also other abiotic factors such as pH associated with acidification processes.

Ocean acidification, caused by elevated CO_2 levels and reduced pH, can act differently on SMR and MMR. Ocean acidification is predicted to act as a masking factor for SMR, meaning that an additional energetic cost of acid-base regulation will be imposed on SMR, making it greater. (Heuer and Grosell 2014; Lefevre 2016; Hannan and Rummer 2018). As

for MMR, similarly to hypoxia, ocean acidification can act as a limiting factor and reduce MMR (Heuer and Grosell 2014). Given that fish have efficient acid-base regulation mechanisms and substantial variation in sensitivity to acidification, the increase in CO_2 in the water can, when controlled experimentally, cause contrasting effects in fish (Kreiss et al. 2015; Baumann 2019). For example, in Atlantic cod (*Gadus morhua* Linnaeus, 1758) exposed to two temperatures, 10.0 and 18.0 °C, an increase in CO_2 causing acidification induced a decrease for individuals acclimated at 10.0 °C and an increase in SMR for individuals acclimated to 18.0 °C (Kreiss et al. 2015). In spiny damselfish (*Acanthochromis polyacanthus* (Bleeker, 1855)) exposed to higher concentrations of CO_2 (946 μatm CO_2) lower resting metabolic rates and higher maximal metabolic rates were observed, resulting in a 38% increase of their aerobic scope compared to fish from the control treatment (451 μatm CO_2) (Rummer et al. 2013). A number of studies have also demonstrated no significant effect of increased CO_2 on performance traits in adult fish such as aerobic metabolism and growth (for reviews, see Lefevre 2016; Cattano et al. 2018; Yoon et al. 2024). These examples demonstrate that varying levels of CO_2 in water and changes in temperature can have distinct effects on performance traits, including metabolic rates (SMR and MMR), aerobic scope, and growth, depending on species and experimental conditions. Therefore, testing the combined effects of climate change related abiotic factors is crucial for understanding potential outcomes for fish species.

The Gulf of St. Lawrence (GSL) is warming at an alarming rate, with the average deep-layer (>200 m) temperature maximum increasing from 5.2 °C in 2009 to 7.0 °C in 2022 (Galbraith et al. 2024). In highly stratified water bodies such as the GSL, limited oxygen replenishment at depth, combined with high microbial and metabolic activity, accelerates deoxygenation and acidification through the consumption of O_2 and the release of CO_2 by bottom-dwelling organisms (Gilbert et al. 2005; Mucci et al. 2011; Nesbitt and Mucci 2021; Blais et al. 2023). Projections for the 2061–2080 period under the RCP8.5 scenario indicate an increase of about 5 °C in temperature and a decrease of 0.4 on the pH total scale (pH_T: which accounts for all hydrogen ions, including those in complexes) for the deep-layer of the GSL (Lavoie et al. 2020; IPCC 2023).

Redfish are long-lived, slow-growing, ovoviviparous fish with sporadic recruitment and strong cohorts, that can support commercial fisheries for extended periods (ca. 10 years). Two species, deep-water redfish, *Sebastes mentella* Travin, 1951 and Acadian redfish, *Sebastes fasciatus* Storer, 1854 are found in the deep-water of the GSL, distinctively *S. fasciatus* is usually found shallower than *S. mentella*, but an overlap of their vertical distribution is also observed. Visual identification of these species is challenging given their morphological similarities (Senay et al. 2022). One of the last major reproductive events occurred in 1981, supporting fisheries until the early 1990s. However, abnormally cold temperatures in the late 1980s and early 1990s, likely coupled with overfishing, led to recruitment decline and a stock collapse, resulting in the 1995 moratorium. The stock remained at low levels until three successful cohorts emerged in 2011–2013 during a period of rapid warming (Senay et al. 2023). By 2022, redfish represented nearly 82% of the total demersal biomass in Fisheries and Oceans Canada (DFO) bottom trawl surveys, compared to 15% between 1995 and 2012 (Bourdages et al. 2023). This surge not only offers a key fishing opportunity but also impacts the ecosystem through predation and competition (Brown-Vuillemin et al. 2022, 2023). Redfish are important predators of commercially valuable species such as the northern shrimp (*Pandalus borealis* Krøyer, 1838) (Brown-Vuillemin et al. 2022, 2023), which also constitutes a key prey for Atlantic cod, Atlantic halibut (*Hippoglossus hippoglossus* (Linnaeus, 1758)) and Greenland halibut (*Reinhardtius hippoglossoides* (Walbaum, 1792)) (Ouellette-Plante et al. 2020). This overlap implies a high potential for interspecific competition, which could influence trophic dynamics and resource availability. Redfish are also affected by environmental changes, with observed physiological shifts including smaller sizes at maturity (Brûlé et al. 2024) and slower growth rates (Coussau et al. 2024), resulting in redfish attaining the regulatory minimum fishing size of 22 cm at an older age (Senay and Duplisea 2024). Although the actual mechanisms behind these physiological changes remain unclear, several factors such as temperature, acidification, reduced dissolved oxygen, and density-dependent mechanisms are likely involved.

Given the close morphological and physiological similarities between *S. fasciatus* and *S. mentella*; *S. fasciatus* serves as a model species to study environmental responses in

redfish. This approach is particularly valuable because *S. mentella* typically cannot survive being brought to the surface given that they are found deeper, making comprehensive physiological studies nearly impossible.

By using *S. fasciatus* as a model, we aim to infer how both redfish species might respond to changing environmental conditions and, more broadly, how the ecosystem they inhabit may adapt to global change. Using *S. fasciatus* captured in the wild and kept in captivity, we assessed the individual and combined effects of projected warming and acidification on key performance traits, including growth rate, food consumption, FCE and metabolic parameters (MMR, SMR, AS, FAS, and O_2crit). Specifically, we examined whether growth, aerobic scope, and hypoxia tolerance would decline under these projected environmental changes, generating knowledge essential for forecasting redfish population dynamics in a changing ecosystem. Results from the present research aim to support the ongoing development of management and conservation strategies for this stock.

1.5 METHODS

1.5.1 Fish collection and housing

Redfish were successfully brought live to our aquaculture facilities using the methodology developed by Laroque (2000). Briefly, redfish were collected near les Escoumins, Québec, Canada (48.317801°N, 69.413287°W) throughout September and October 2019. SCUBA divers caught ~16–19 cm redfish with dip nets at a depth of 25–30 m and placed them into cages (52 × 31 × 31 cm), that could hold up to 30 individuals. Once full, cages were placed on the bottom higher up along the slope, at a depth of 10–15 m depending on the tide, to reduce barotrauma. The duration of this equilibration period was at least 12 h, but up to 96 h for fish caught early during each of the 5-day fishing trips. The day after the last capture, the cages were brought to the surface for transportation in oxygenated tanks to the Maurice Lamontagne Institute in Mont-Joli, Québec, Canada. Four fishing trips yielded 822 redfish.

Tableau 2. Mean seawater parameters (± standard deviation) for each ocean acidification scenario (current and future) and their targeted pH throughout the growth period for this experiment from July 2nd to October 20th, 2021, for all tanks. Salinity and pH_T (pH on the total scale) were recorded from Monday to Friday in each of the experimental tanks during the growth period, Total alkalinity was measured once a week in each of the four header tanks, pCO_2 values were estimated from pH total measurement and alkalinity.

Ocean acidification	Target pH	pH_T	Total alkalinity (mol L^{-1})	Salinity (ppt)	pCO_2 (uatm)
Current	7.75	7.70 (0.04)	2078 (10.4)	28.37 (0.31)	1988.9 (223.8)
Future	7.35	7.36 (0.05)	2078 (10.4)	28.37 (0.31)	886.2 (91.8)

Upon their arrival, fish were transferred into circular water tanks (1 m × 1.1 m, height × diameter; 760 L) supplied with 6 °C oxygenated seawater (salinity of 32 ppt). They were offered food (northern shrimp, capelin, *Mallotus villosus* Müller, 1776, and krill, *Euphausia superba* Dana, 1850) three times a week. It took about 2 weeks for redfish to acclimatize to their new environment and feed correctly. Wild fish may present various levels of parasite load, which are known to influence performance traits (Chrétien et al. 2022; Guitard et al. 2022). Hence, a week after they started eating, fish received a formaldehyde treatment (37% formaldehyde, 0.01 mL L^{-1}) for 1 h to remove possible external parasites. Furthermore, inspection of gills, muscle, and heart when fish were euthanized for tissue collection (n = 32) confirmed the absence of internal parasites.

In December 2019 and January 2020, fish were weighed and individually identified with a PIT-tag (Biomark, Idaho, USA) to allow determination of individual growth. When individuals were anesthetized (Benzocaine, 0.5 mL of solution per liter of seawater, solution = 100 g of benzocaine dissolved in 1 L of 70% ethanol) for length and weight measurements, genetic samples were taken by rubbing a sterile swab for approximately 5s in their mouth. Each swab was individually placed in a 1.5 mL Eppendorf tube and frozen at −20 °C until species identification was conducted using qPCR, as described in Brûlé et al. (2024). This method assigns individuals to either *S. fasciatus* or *S. mentella* with a 4% error rate. Of all individuals included in the experiments, 99.3% were identified as *S. fasciatus* with the

remaining 0.70% classified as *S. mentella*. Given the habitat (depth and location) where the fish were captured and our understanding of species distribution from bottom trawl surveys (Senay et al. 2023), we assumed that the individuals that were identified as *S. mentella* were in fact *S. fasciatus*, but just part of the error rate of the method. In July 2020, a 2-month experiment compared survival at two salinities, 28 and 32 (50 fish per tank, two tanks per salinity), which resulted in 100% survival in all tanks, therefore salinity was reduced from 32 to 28 (the average salinity of water pumped into the aquaculture facility) over a period of two weeks and then kept at 28 thereafter. After four months of acclimation post salinity experiment, in December 2020, fish were moved to their respective experimental tanks. Experimental methods complied with the regulations of the Canadian Council on Animal Care and were approved by the Maurice Lamontagne Institute animal care committee (Certificate 19-6 C). Fish collection in their natural habitat was done under the Parks Canada permit (SAGMP-2019-33741).

1.5.2 Experimental set-up

The experimental set-up was composed of 16 circular water tanks (1 m diameter; 760 L) arranged randomly into four temperature lines (2.5, 5.0, 7.5, and 10.0 °C). The four tanks on each line were at the same experimental temperature, with two out of four tanks randomly set to each of the experimental pH levels (7.35 and 7.75). As redfish typically live around 5 °C, the temperatures selected included both colder and warmer conditions, with the warmer conditions reflecting the 10 °C expected for 2061 from simulation for the GSL by Lavoie et al. 2020. The two ocean acidification scenarios were based on pH levels representing the current (7.75; Mucci et al. 2011; 2018) and future conditions with the −0.4 pH units decrease scenario predicted for the 2061–2080 period under an RCP8.5 scenario (7.35; Lavoie et al. 2020; IPCC 2023) of the deep layer of the GSL (Tableau 2). Water temperature was controlled using a custom-built control unit (Gell'Air, Mont-Joli, Canada) with a precision of 0.6 °C in the header tank, but close to 0.1 °C in each of the four tanks within each line. Each line was a semi-recirculating system, fluctuating between 12.5 and 15 L per minute of

new seawater being added to the header tank, and all experimental tanks draining back to the header tank.

A total of 25 fish were randomly distributed in each tank for a total of 400 fish (but see Food Consumption and Growth experiment below for a subsequent change in the number of fish per tank). Fish were fasted for 72 h, anesthetized, weighed, measured (fork length), and then randomly assigned to a tank. Fish were acclimated to the experimental tanks for a week at the same rearing conditions (5 °C). Then, temperatures were adjusted in increments of 0.5 °C per day until all experimental temperatures were reached (e.g., 2.5 weeks for 10.0 °C).

1.5.3 Monitoring of seawater carbonates

During the growth experiment, total alkalinity (TA) was monitored every week by sampling water in 104 mL glass bottles in each of the four header tanks (A, B, C, and D) for the four different temperature treatments. TA from the header tank was considered the same as that of the four experimental tanks it supplied. TA (in μmol kg^{-1} of seawater) was measured by open-cell potentiometric titration (Mintrop et al. 2000; Dickson 2010) with an automated VINDA sampling system at the Maurice Lamontagne Institute. Each 104 mL sample, warmed to 25 °C, was titrated with 0.1 mol/L hydrochloric acid to the Gran equivalence point (nonlinear curve-fitting method) using a computer-controlled Dosimat (Metrohm AG, USA) dispenser and combination glass electrode. The titrant was calibrated with a series of seawater certified reference materials (CRMs; Andrew Dickson, Scripps Institution of Oceanography, San Diego, CA). The analytical precision of TA was calculated using repeated analyses of duplicate sample and revealed a precision of <0.1%.

Using the same water samples, pH_T was determined weekly in duplicate with an Agilent Cary 60 thermoregulated spectrometer and a 10 cm quartz cell using the purified dye m cresol purple (Liu et al. 2011) provided by the laboratory of Robert H. Byrne, University of South Florida. Absorbance was measured at 730, 578, and 434 nm before and after dye addition at 25 °C (Clayton and Byrne 1993). A similar procedure was conducted before and after each set of sample measurements using a TRIS buffer prepared at a practical salinity

(S) value of approximately 30 (Millero 1986). All measurements were converted to the total proton scale (pH_T) using the measured salinity of each sample and the HSO4 association constants given by (Dickson 1990). Reproducibility and accuracy of our measurements were on the order of 0.003 pH units or better.

Both pH_T and TA measurements were then used to estimate the aragonite and calcite saturation states, pH_T *in situ* and partial pressure of carbon dioxide (pCO_2) using the CO2SYS program (Lewis and Wallace 1998), and using the dissociation constants (K1 and K2) of Mehrbach et al. (1973), as refit by Dickson and Millero (1987), the KHSO4 constant from Dickson (1990), the total boron constant from Lee et al. (2010), and KF constant from Perez and Fraga (1987).

The pCO_2 was calculated from total alkalinity from the header tank and with pH_T for all experimental tanks (Tableau 6 and 7; Figs. 12, 13, and 14). The two acidification treatments were determined based on current and future acidification scenarios are described in Tableau 2.

1.5.4 Food consumption and growth experiment

Fish were fed to satiation three times a week with capelin, northern shrimp, and krill each Monday, Wednesday, and Friday, respectively. Capelin and shrimp were cut in pieces of approximately 2–3 cm to make them easier to swallow. Food consumption for each tank was measured each feeding day. Food was offered every 5–6 min for a minimum of 1 h, to ensure that all fish fed ad libitum. Portions were weighed before feeding began and uneaten food was collected, drained, and used to correct the amount eaten.

Tableau 3. Mean mass and length with their standard deviation of redfish (*Sebastes fasciatus*) at the start of the experiment for original fish (January 25th 2021) and added fish (July 13th 2021). Mean mass and length with their standard deviation of fish just before respirometry trials.

	Mean mass (g)	SD mass (g)	Mean length (mm)	SD length (mm)
Original fish	158.44	38.94	214.79	15.30
Added fish	187.18	53.85	221.73	19.59
Respirometry	172.42	35.22	220.48	12.68

Experimental conditions were reached on 25 January 2021, and the end of the experiment was scheduled on 29 June 2021 (5 months), when all fish fasted for a minimum of 72 h, then fish were anesthetized, measured, and weighed to calculate growth rate in length and mass. However, a high occurrence of slow growth rates and mass losses were observed between January and June in all treatments, which was not observed in the fish that were not part of the experiment. This was attributed to an initial feeding protocol that did not result in ad libitum feeding (feeding stopped as soon as three food items accumulated on the bottom in this protocol) and possibly a suboptimal fish density, as redfish are gregarious and stop feeding when fewer than 10 individuals are placed in tanks of this volume (pers. obs.). Thus, on 13 July, 17 individuals (afterwards named added fish to differentiate them from the original fish) were added to each experimental tank for a total of 42 fish per tank and 672 fish for the experiment (Tableau 3) and the feeding protocol was adjusted to ensure ad libitum feeding (protocol described at the beginning of this section). Prior to the addition of fish, tanks assigned to the 10 °C treatment were gradually cooled to 8 °C over 2–3 days. Injection of CO_2 in the water was stopped for the 7.35 treatment to increase the pH and help the added fish acclimate to the experimental tanks. Twenty-four hours after the fish addition, temperature and pH were controlled again, and treatment conditions were obtained as of 16 July. Day 0 was 28 June for the original fish and 13 July for the added fish, and the growth experiment ended on 20 October, after 114 and 99 days for both groups, respectively.

Tanks were inspected every day to monitor mortality. The original fish were weighed and measured three times during the whole experiment, on 25 January, 28 June, and 20 October, whereas the added fish were measured twice, on 13 July and 20 October.

1.5.5 Respirometry trials

Two identical separate experimental water baths (200 cm length × 60 cm width × 28 cm height, 336 L) were used, each with an open circulation system. Each water bath was provided with a temperature probe (Hermetically sealed RTD probe, Omega Engineering inc., Norwalk, CT, United States), a controller (1/16 DIN Micromega autotune PID Temperature, Omega Engineering inc.), and two mixing valves (sv3109, Omega Engineering inc.) to enable mixing of the appropriate proportion of cold and warm water (total flow rates between 3.5 and 4.5 L min^{-1}) to provide each bath with seawater at the treatment temperature (Tableau 8).

Each water bath contained four resting respirometry glass chambers, two of each size (5.214 L; 33 cm, length × 15 cm, diameter or 7.016 L; 49 cm, length × 13.5 cm, diameter). The chambers were transparent but separated with an opaque panel so that fish could not see each other. Each chamber was connected to a closed water circuit to achieve adequate water mixing, made of Tygon tubing and a recirculation pump (model 1048, Eheim, Stuttgart, Germany). The volume of the recirculation loop was 48.5 mL for 5 L chambers and 60 mL for 7 L chambers. Each recirculation loop included housings for a fiber-optic oxygen probe (PyroScience Robust Oxygen) as well as a temperature sensor (PyroScience P100). These were connected to a PyroScience FireSting-O_2 4-channel oxygen meter combined with a PyroScience TEX4 (PyroScience GmbH, Aschen, Germany) to have temperature correction on each channel. Dissolved oxygen levels were measured every ~2 s. The four chambers were also connected to a single flush pump (1046, Eheim, Stuttgart, Germany) controlled by the Aquaresp software (V3, Denmark, Aquaresp.com).

At the end of the growth experiment, wet mass-specific oxygen uptake ($\dot{M}O_2$, in mg O_2 h^{-1} kg^{-1}) was measured in each respirometer by intermittent-flow respirometry (Steffensen

1989; Svendsen et al. 2016) using 11.5 min cycles consisting of a 4 min period of flush to renew the water in the respirometers followed by a 7.5 min closed period to determine oxygen consumption using the slope of the decreasing dissolved oxygen in the respirometer during the last 6 min of the closed phase, when it had become linear.

For each experimental tank, four individuals were chosen randomly among the added fish from July for respirometry trials. Respirometer size was selected as to respect a chamber to fish volume ratio between 20 and 50 (Svendsen et al. 2016) and we obtained a ratio between 29 and 52 with the two respirometer sizes. We had a total of eight individuals per treatment and 64 fish in total. The respirometry set-up was cleaned between each trial (every 4 days) with fresh water and chlorine and was rinsed thoroughly with fresh water and left to run overnight with seawater. Oxygen probes were calibrated with 100% and 0% (air sat.) solutions before each experiment. Eight trials were required to cover all eight treatments in duplicate. Treatment tanks were randomly allocated to a given respirometry experiment and water bath.

Prior to all respirometry experiments, fish were fasted for a minimum of 48 h to ensure they were in a post-absorptive state (Clark et al. 2013; Chabot et al. 2016b). Each trial lasted 5 days, including preparation and execution. On day one, the set-up was cleaned, probes were calibrated (Annexe 1), fish were selected and weighed and then isolated for the night in a basket floating in the experimental tank. On day 2, background oxygen consumption rates (B_ $\dot{M}O_2$) were estimated in each empty chamber for a minimum of 40 min before and after every respirometry trial. Then, each trial started with a chase protocol followed by 1 min of air exposure, a common method of estimating MMR in fishes (Roche et al. 2013; Rummer et al. 2016). For this, the selected fish were caught and put in a floating basket in the experimental tank the day prior to the beginning of a respirometry trial. On the day of the trial, each selected fish was individually caught, put in a circular chase area (65 cm × 15 cm, height × diameter, 50 L, depth adjusted as a function of fish height (doubling the height of the fish in water)) using a net, and chased by hand until it no longer reacted to contact and tail pinching (chase duration lasted between 1.18 and 8.68 min). The fish was then removed

from the arena and held out of the water for 1 min. The fish was thereafter placed into a respirometry chamber, which was immediately (less than 15 s) sealed. The decline in dissolved oxygen was measured constantly, without flush, until it reached ~80% air sat. to estimate MMR. Once all four fish had been chased and the MMR estimation completed, control of the system was switched to regular cycles controlled by Aquaresp running the 11.5 min loops as described above, for the next ~70 h (days 3, 4, and 5), with the fish left undisturbed, in the dark (except for a daily check-up with a red light), behind opaque curtains. Over this period, oxygen uptake rates of fish stabilized, and SMR could be estimated. Oxygen levels remained above 95% in the chambers during all cycles of SMR estimation for all trials.

After ~60 h (day 5), oxygen uptake under decreasing dissolved oxygen (DO) was quantified to estimate hypoxia tolerance (O_2crit). This was achieved by gradually injecting nitrogen in the respirometry bath. DO was lowered at a rate of approximately 5% between each cycle until DO in the chamber reached approximately 30% sat based on pilot experiments indicating that O_2crit rarely exceeded this threshold. Below 30%, DO was lowered more gradually (2%–3% between cycles) to increase the resolution of O_2crit estimates while minimizing the total duration of the trial. Aquaresp, paired with an R script, calculated $\dot{M}O_2$ in real time and the experiment lasted until the animal could not sustain SMR estimated during the previous days (Claireaux and Chabot 2016). We visually checked on the animals to make sure they were not in distress or lost equilibrium during this part of the experiment. Hypoxia tolerance trials lasted between 7 and 9 h. This protocol followed best practices for collecting and reporting respirometry data as described in Killen et al. (2021) (see Annexe 1).

1.5.6 Data extraction and analysis

1.5.6.1 Food consumption and growth rates

All data were analyzed using R v. 4.2.0 (R Foundation for Statistical Computing 2022).

Food consumption was analyzed as follows from 13 July to 20 October

(1) Food ingested per fish = (Fp − Fng − Fc) /N

where Food ingested per fish is the amount of food in grams eaten by one individual of a given tank for one meal (capelin, shrimp or krill), Fp is the amount of food prepared for that tank for that meal, Fng is the amount of food not given, Fc is the amount of food collected at the bottom of the tank at the end of the meal, and N is the number of fish in the tank during that meal.

Food consumption was calculated as the amount ingested by one fish per week. Since redfish consistently ate more capelin and less shrimp, it was preferable to calculate weekly food consumption as the sum of per capita consumption for the three meals:

(2) Weekly food consumption per fish = Σ (Food ingested per fish per meal)

Growth rates were calculated on all fish present at the end of the experiment (20 October). Specific growth rate (Jobling 1983) was calculated for each individual from 28 June for the original fish and from 13 July for the added fish to 20 October.

(3) $\log M2 - \log M1 / T \times 100$

where M2 is the mass at the end of the experiment (20 October), M1 is the mass at the beginning of the experiment (28 June or 13 July), and T the duration of the experiment (114 days for the original fish, 99 days for the added fish).

1.5.6.2 Food conversion efficiency (FCE)

The period for growth for both groups (a period of 99 days) was used to calculate Food Conversion Efficiency for each tank (FCEt) (Craig et al. 2002). First, the average growth rate for the tank (Gt) was calculated using the daily growth rate of each fish, multiplied by 99 days, to obtain their growth rate in grams. Food consumed at each meal was divided by the

number of fish in the tank, and this per capita food consumption was cumulated for each tank over the same period (Total food consumption for the tank, Ct).

(4) FCEt = Gt/Ct

1.5.6.3 Respirometry data

Wet mass-specific oxygen uptake ($\dot{M}O_2$; mg O_2 h^{-1} kg^{-1}) was calculated from the slopes of the linear regressions between oxygen concentration and time, accounting for the volume of water in the respirometer (respirometer gross volume less fish mass as an estimate of fish volume, assuming a density of 1 g mL^{-1}) for the 64 individuals tested.

Following the chase and air exposure protocol, oxygen uptake was measured during approximately 30 min without any flush/reoxygenation period because oxygen uptake changes quickly after the chase and the maximum rate could otherwise occur during a flush. To further reduce the risk of underestimating MMR, rolling regressions were used to detect the steepest part of the long decline in DO in the respirometer (Zhang et al. 2019). Contrary to sequential regressions, when one interval begins after the end of the previous interval, in rolling regressions each interval begins one point after the beginning of the previous interval. The shortest reliable interval or window width (WW) over which these regressions should be calculated was determined according to the methodology outlined by Zhang et al. (2019) and modified by Guscelli et al. (2023). This analysis gives the shortest reliable WW of 3 min.

SMR was estimated with the fishMO_2 package (Chabot 2020) as the quantile (p = 0.2) of the $\dot{M}O_2$values obtained after an acclimation period of 16 h and the start of the decline in DO used to measure O_2crit (Chabot et al. 2016b). Because we have observed night activity in this species, we have estimated SMR for each individual with and without including nights. We then have selected the lowest estimation of SMR out of these two rates. The background respiration rate (B_ $\dot{M}O_2$) was subtracted from the $\dot{M}O_2$ measurements assuming a linear increase in bacterial respiration from the start to the end of the trial.

Absolute AS was calculated as the difference between MMR and SMR (Fry 1947, 1971) and factorial aerobic scope as a ratio of MMR over SMR. O_2crit was identified with data points measured below SMR. A linear regression was fitted to the oxygen uptake values below SMR, at low values of DO, and the intersection of this line and the horizontal line representing SMR was taken to be O_2crit (Claireaux and Chabot 2016; Chabot et al. 2020).

1.5.7 Statistical analysis

Survival during the experiment was analyzed using the survival R package (Therneau and Grambsh 2000; Therneau 2020). Kaplan–Meier curves were produced first for each tank. To limit the number of curves to compare, replicate tanks within each treatment were tested using the log-rank method (Bewick et al. 2004; Everitt and Hothorn 2010) after validating the assumption of proportional hazards. The effect of temperature (using the four target temperatures) and pH on survival was studied using a Cox proportional hazards model (Bewick et al. 2004; Everitt and Hothorn 2010), checking for the assumption of proportional hazards.

To test the effect of temperature (average temperature during the growth experiment) and pH on performance traits such as food consumption and growth, and because these variables had nonlinear relationships, we used a full Generalized Additive Model (GAM) framework with the mgcv package (Wood 2017).

Food intake was measured for whole tanks, and it was not possible to distinguish the food intake of original and added fish. The full model included pH as a fixed factor and one smooth for each pH level, in addition to experimental tank as a random factor (Tableau 9, Model Food2). Food intake models and their AIC are shown in Tableau 9, with description of all terms in Tableau 10. Model selection was based on the Akaike Information Criterion (AIC) and the model with the lowest AIC was the final model.

The full model for FCE included pH as a fixed factor and one smooth for each pH level (Tableau 9, Model FCE 1). FCE models and their AIC are shown in Tableau 9, with description of all terms in Tableau 10. Model selection was based on the AIC and the model with the lowest AIC was the final model.

In the model elaboration for growth rates, as the original group of 25 fish had been subjected to experimental conditions for a longer period compared to the fish added on 13 July, group (original and added) was included as a fixed factor in the growth model. The first model tested was the full model, which included pH, group and their interaction as fixed factors and allowed for a different smooth for growth rate as a function of temperature for each combination of pH and group (Tableau 9; Growth1). Experimental tank was included as a random factor. In the final model, the interaction term was removed, retaining pH and group as fixed factors while allowing for a different smooth over temperature across groups (Tableau 9; Growth5). Selection of the final model proceeded as for food consumption models.

Preliminary models for oxygen uptake were formulated with the gam() function, but the relationship between SMR, MMR, AS, or FAS, and temperature were always linear, i.e., the effective degrees of freedom were always exactly 1, meaning that the relationships were linear and that there was no advantage in using GAM over linear models. For this reason, linear mixed effects models (lmer function in lme4 package; Bates et al. 2015; Tableau 11) were used to analyze four metabolic traits (MMR, SMR, AS, and FAS) and hypoxia tolerance (O_2crit), with temperature (average temperature during each respirometry experiment) as a continuous variable, pH as a 2-level factor, and the experimental tank and respirometry chamber as random effects. The full models included the interaction between temperature and pH as a test of homogeneity of slopes, an assumption of ANCOVAs (Tableau 11) (Quinn and Keough 2002). Reduced models without interaction were calculated when the *p*-value of the interaction was not significant, which was the case for these five response variables (Tableau 11). Marginal and conditional R-squared values for the lme models were determined using the MuMIn package (Nakagawa and Schielzeth 2013; Barton 2024). Two

fish were rejected from the models on respirometry data for two different reasons. One individual escaped from the chamber during the first night and was immediately reintroduced in the chamber the following morning. Unfortunately, this event caused added stress, and this individual did not reach SMR during the remainder of the session. Another fish was discarded because its oxygen uptake was still declining at the end of the period used to estimate SMR (Fig. 15).

Model assumptions for all models were assessed visually using diagnostic plots with the DHARMa package (Hartig 2022) and were met for all models.

1.6 RESULTS

1.6.1 Survival rate

Survival rates during the experimental period varied from 95.2 to 100% per tank (Tableau 12). In two cases, fish jumped onto the net covering their tank, seven fish developed exophthalmia and were euthanized to respect animal care procedures, and two fish were found dead in their tank. There was no effect of temperature (hazard ratio of 1.23, z = 1.725, $p = 0.09$) nor pH (hazard ratio of 0.56, z = −0.914, $p = 0.36$) on survival after pooling replicate tanks for each treatment.

1.6.2 Growth performance

1.6.2.1 Food consumption

The final simplified GAM for food consumption included pH as a fixed effect, with a smoothed effect of mean temperature (throughout the experiment). Experimental tank was included as a random effect (Tableau 9; Model Food 2).

Food consumption ranged from 0.81 g to 13.27 g fish^{-1} week^{-1} (mean 7.21 g fish^{-1} week^{-1}, SD 2.42) across all tanks. Food consumption was not influenced by pH as a categorical variable ($p = 0.215$; Tableau 4); however, it was influenced by temperature (p =

0.004; Tableau 4), being lower at 2.5 °C than at the three higher temperatures (Figure 10A). Deviance explained for this model was 31.9% (Tableau 4).

1.6.2.2 Specific growth rates in mass

The final simplified GAM for specific growth rates included pH and group as fixed effects and a smooth over mean temperature throughout the experiment, separately for each group (added and original fish). Experimental tank was included as a random effect (Tableau 9; Model Growth 5).

Across all treatments, fish had a mean mass at the beginning of the experiment (28 June for the original fish and 13 July for the added fish) of 158.44 g (SD = 38.94 g) for the original group and 187.18 g (SD = 53.85 g) for the added fish, with an overall (added and original) mean mass of 170.74 g (SD = 47.91 g) (Tableau 3).

Across all treatments, specific growth rates ranged from −0.06 to 0.20% body mass day^{-1} with a mean of 0.06% body mass day^{-1} (SD = 0.04% body mass day^{-1}) for the original fish and ranged from −0.129 to 0.149% body mass day^{-1} with a mean of 0.009% body mass day^{-1} (SD = 0.051% body mass day^{-1}) for the added fish. Growth was not influenced by pH (p = 0.293, Tableau 4), but it was influenced by the group (p < 0.0001; Tableau 4) and the temperature smooth term for each group was significant (original fish: p = 0.020; added fish: p = 0.0001; Tableau 4). Further, the shape of the relationship between growth rate and temperature differed for each group (Figure 10B). Deviance explained for this model was 40.6% (Tableau 4). Specific growth rate was highest at 5.0 °C and lowest at 10.0 °C for both groups (Figure 10B). For the original fish, which were acclimated to the treatments before the growth experiment, growth rates were significantly lower at 10.0 °C compared to the three lower temperature treatments. Added fish, which were subjected to the treatments at the beginning of the growth trial, had lower growth rates at 2.5 and 10.0 °C, peaking around 5.0 °C and a significant tank effect was observed (p < 0.0001 Tableau 4).

1.6.2.3 Influence of food ingestion on growth rate

There was a positive relationship between growth rates and food consumption and explained 40% of the variance in mean individual growth (linear model: $R_2 = 0.40$, $F(1,14) = 9.20$, $p = 0.009$; Fig. 16).

The final simplified GAM for FCE included pH as a fixed effect, with a smoothed effect of mean temperature throughout the experiment (Tableau 9; Model FCE 2). FCE ranged from −0.043 to 0.119 (mean 0.01 SD 0.040). FCE was not influenced by pH as a categorical variable ($p = 0.215$; Tableau 4), however temperature was a significant effect ($p = 0.011$; Tableau 4) and FCE was lower at 10.0 °C than at lower temperatures (Figure 10C). Deviance explained for this model was 59.5% (Tableau 4).

Tableau 4. Relationship between growth rates, food consumption, and food conversion efficiency and temperature and pH, with tank as random factor. Test statistics obtained from generalized additive model (GAM) of growth rates and food consumption as a function of temperature, pH, and group with tank treatment as a random factor for redfish. Statistically significant results are indicated in bold. edf: estimated degrees of freedom, F-value: F-statistic for the smooth term, p-value: statistical significance threshold.

Response	Predictors	edf	f-value	p-value	Deviance explained (%)
Growth rates					40.6
(% mass day $^{-1}$)	pH		1.146	0.285	
	Group		229.858	<**0.0001*****	
	Temp*added fish	2.891	6.510	**0.0002*****	
	Temp*original fish	2.034	3.583	**0.0217***	
	Tank	10.254	5.311	<**0.0001*****	
Food consumption					31.9
(g week $^{-1}$)	pH		1.626	0.204	
	Temperature	2.420	6.153	**0.005****	
	Tank	8.386	2.267	<**0.0001*****	
Food conversion efficiency					59.5
	pH		0.917	0.357	
	Temperature	2.072	6.117	**0.0001*****	

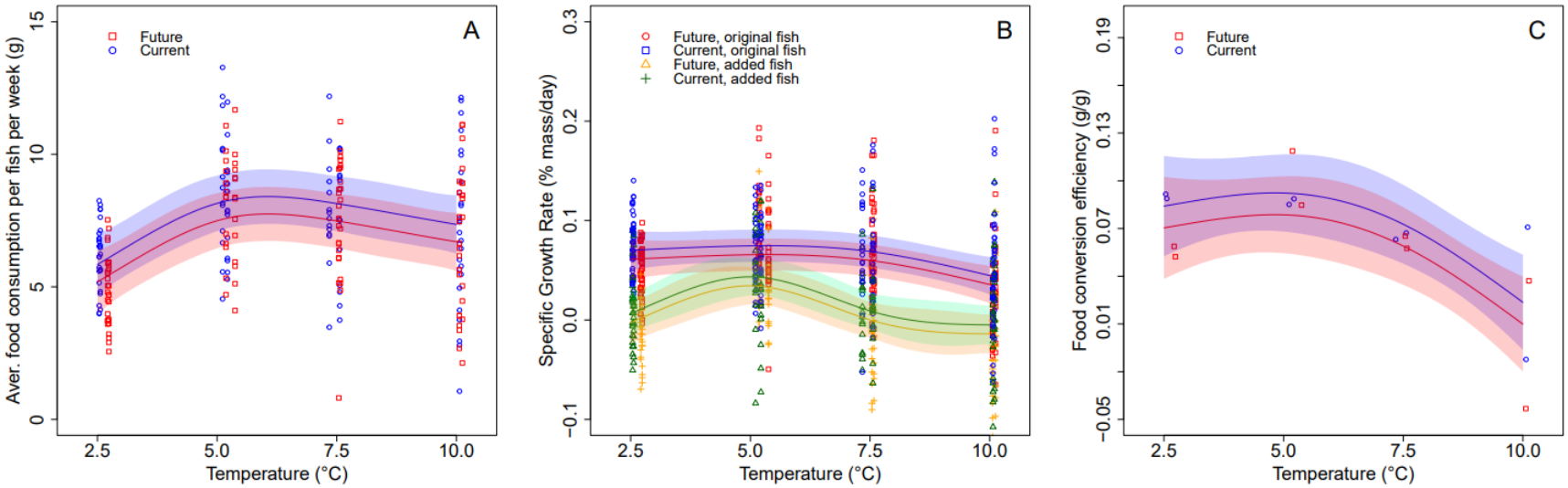

Figure 10. Effect of temperature and pH on food consumption, growth rates and food conversion efficiency. (A) Food consumption per fish in grams per week for redfish (*Sebastes fasciatus*) reared at temperature between 2.5 ◦C and 10.0 ◦C in seawater with future GSL pH (red; pH 7.35 pCO_2 ± SD: 1988.9 ± 223.8 µatm) and current Gulf of St. Lawrence (GSL) pH (blue; pH 7.75; pCO_2 ± SD: 886.2 ± 91.8 µatm). N = 208 (B) Specific growth rates in redfish after acclimation to temperature between 2.5 and 10.0 ◦C in seawater future GSL pH (red and yellow; pH 7.35; pCO_2 ± SD: 1988.9 ± 223.8 µatm) and current Gulf of St. Lawrence (GSL) pH (blue and green; pH7.75; pCO_2 ± SD: 886.2 ± 91.8 µatm) N = 662. (C) Food conversion efficiency in g/g for redfish reared at temperature between 2.5 and 10.0 ◦C in seawater with future GSL pH (red; pCO_2 ± SD: 1988.9 ± 223.8 µatm) and current Gulf of St. Lawrence (GSL) pH (blue; pCO_2 ± SD: 886.2 ± 91.8 µatm). N = 16. The shaded areas around each regression lines represents the 95% confidence intervals.

1.6.3 Aerobic metabolic performance

1.6.3.1 MMR, SMR, AS, and FAS

The final simplified LME model for metabolic traits tested the effect of temperature and pH as fixed effects and included the respirometry chamber and the experimental tank from the growth experiment, as random effects (Tableau 11; Model SMR2-MMR2-AS2-FAS2).

Mean mass of individuals before respirometry trials was 172.42 g (SD = 35.22) (Tableau 3). There was no relationship between chase duration and MMR ($p = 0.344$). MMR ranged from 104 to 216 mg O_2 h^{-1} kg^{-1} while SMR ranged from 15 to 51 mg O_2 h^{-1} kg^{-1}. MMR, AS, and FAS were not influenced by pH (pMMR = 0.851; pAS = 0.610; pFAS = 0.124; Figure 11; Tableau 5); however, SMR was significantly elevated for the pH representing future conditions (pH: 7.35; pCO_2: 1988 uatm) at all temperatures, compared with current pH (ppH = 0.0257, pTemp < 0.0001, Figure 11B, Tableau 5). There was a significant positive relationship between MMR, SMR, and AS and temperature (Figs. 2A, 2B, and 2C; Tableau 5), and a significant negative relationship between FAS and temperature (Figure 11D). The random effect "tank" added to the model was statistically significant ($p \leq 0.05$) for MMR, AS and O_2crit, meaning that factors not included in our experiment may have influenced these traits, in addition to temperature and pH.

1.6.3.2 Hypoxia tolerance (O_2crit)

Hypoxia tolerance for the temperature range of this experiment ranged between 6.5% air sat (2.5 °C) and 31.8% air sat (10.0 °C) (Figure 11E). There was no effect of pH on O_2crit ($p = 0.21$; Tableau 5), but there was a significant positive relationship between O_2crit and temperature ($p < 0.0001$, Figure 11E, Tableau 5). Individuals acclimated at 2.5 and 10.0 °C became unable to maintain SMR at an average of 14% and 22% air sat, respectively, a difference of 8% air saturation between the extreme temperatures.

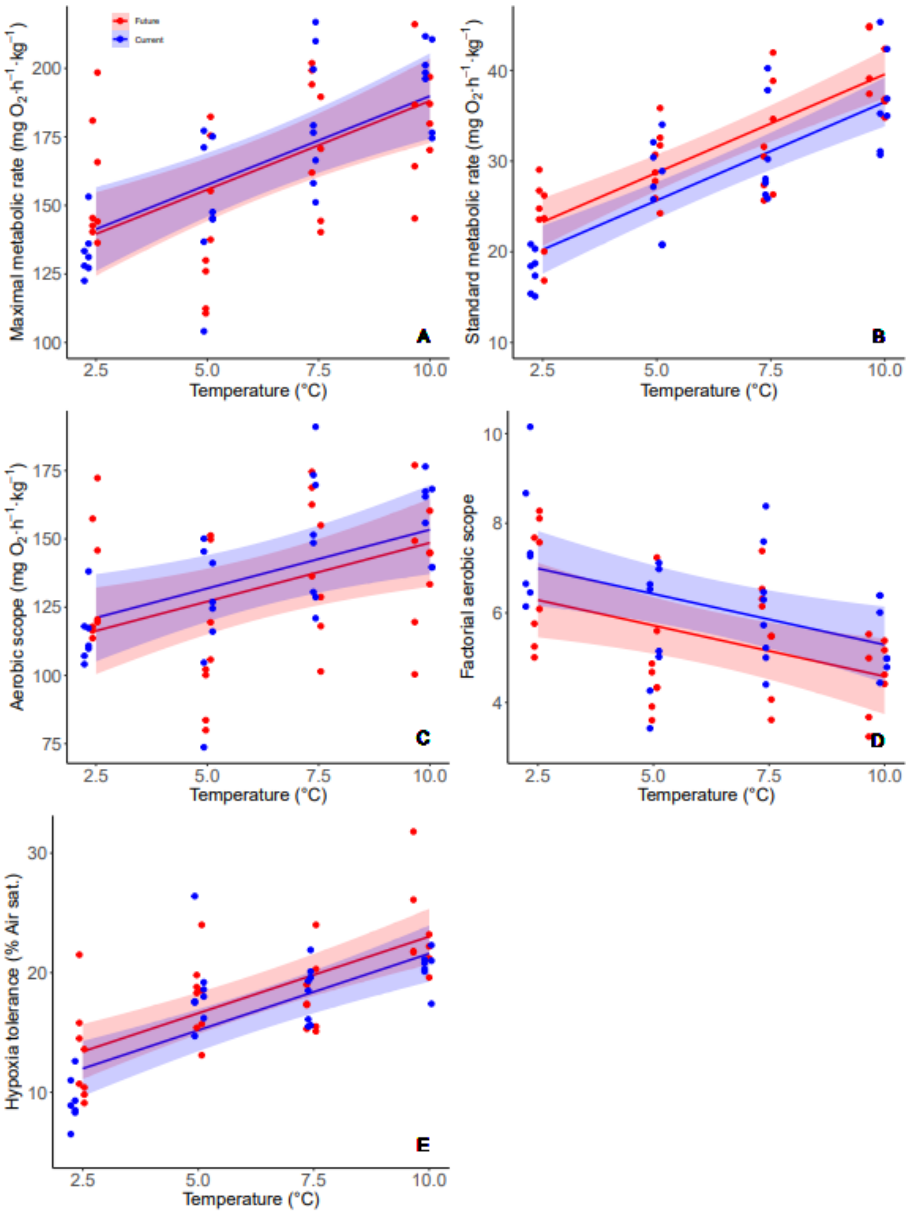

Figure 11. Effect of temperature and pH on metabolic traits. Metabolic traits of redfish (*Sebastes fasciatus*) reared at temperature between 2.5 °C and 10.0 °C in seawater with future GSL pH (red; pH 7.35; pCO_2 ± SD: 1988.9 ± 223.8 µatm) and current Gulf of St. Lawrence (GSL) pH (blue; pH 7.75; pCO_2 ± SD: 886.2 ± 91.8 µatm). Maximal metabolic rate (mg O_2 h^{-1} kg^{-1}) (A), standard metabolic rate (mg O_2 h^{-1} kg^{-1}) (B), aerobic scope (mg O_2 h^{-1} kg^{-1}) (C), factorial aerobic scope (D) and hypoxia tolerance (% air sat.) (E) (N=62). The shaded areas around each regression lines represents the 95% confidence intervals. The slopes for the two pH levels did not differ significantly in A–C-D-E.

Tableau 5. Relationship between metabolic traits estimated, temperature, pH with the tank and the respirometry chamber as random factors. Note: Test statistics obtained from linear mixed-effects model for maximum metabolic rate (MMR), standard metabolic rate (SMR), aerobic scope (AS), factorial aerobic scope (FAS) and hypoxia tolerance (O_2crit) as a function of temperature and pH treatment in redfish (*S. fasciatus*) (n = 62). Statistically significant results are indicated in bold with significance threshold of 0 "***" 0.001 "**" 0.01 "*" 0.05 "." 0.1 ' ' 1. Marginal R2 (R2M) and conditional R2 (R2C) indicate the variance explained by fixed factors and by both fixed and random factors, respectively (Nakagawa and Schielzeth 2013).

Response	Predictors	Chisq	DF	p-value	R^2M	R^2C
MMR					0.35	0.54
($mgO_2h^{-1}kg^{-1}$)	Temperature	20.687	1	> **0.0001*** **		
	pH	0.0349	1	0.8517		
SMR					0.64	0.69
($mgO_2h^{-1}kg^{-1}$)	Temperature	77.831	1	> **0.0001*** **		
	pH	4.972	1	**0.0257***		
AS					0.18	0.47
($mgO_2h^{-1}kg^{-1}$)	Temperature	8.1683	1	**0.0042****		
	pH	0.2598	1	0.6102		
					0.24	0.42
FAS	Temperature	8.5901	1	**0.0112***		
	pH	2.6917	1	0.1243		
O_2crit					0.51	0.63
(% Air sat.)	Temperature	37.2667	1	> **0.0001*** **		
	pH	1.5734	1	0.2097		

1.7 DISCUSSION

To the best of our knowledge this is the first study to conduct experimental work on redfish, given the significant challenge of bringing them to the laboratory alive and in good health. Our results showed that the predicted deep layer temperature for the GSL in 2061 (10.0 °C) affected redfish through food consumption, growth, FCE and metabolic traits, although we did not observe an effect of future acidic pH on most of the performance traits

of redfish. In this context, the lower growth rate at 10 °C was not due to reduced food consumption since it remained stable between 5.0 and 10.0 °C, but rather to a lower FCE, indicating that less growth occurred for the same amount of food eaten in comparison to lower temperatures. This is consistent with the increased maintenance costs (SMR) observed at 10 °C.

1.7.1 Energy allocation and metabolic constraints

In fish bioenergetics, when modelling energy allocation, consumed energy is first allocated to metabolism (maintenance, activity, and digestion), then to waste (feces and urine) and the leftover can be allocated to somatic or gonadal growth (Madenjian et al. 2023). As temperature increases, it is common to observe an increase in aerobic metabolism until the organism reaches a thermal threshold. Before this threshold is reached, higher temperatures can cause some functions such as postprandial increase in oxygen uptake (Specific Dynamic Action: SDA), to require more of that energy (Chabot et al. 2016a; Nelson and Chabot 2024). Consequently, other functions, such as growth, become lower energetic priorities. In recent years, Jutfelt et al. (2021) proposed the aerobic scope protection hypothesis. This hypothesis suggests that fish consuming the same size meal experience a higher SDA peak in warm water, which intensifies at even higher temperatures, potentially reducing the aerobic scope available for other oxygen-demanding activities. As Jutfelt et al. (2021) stated, animals should then ideally regulate their food intake based on their need to maintain aerobic scope under challenging conditions that temperature increase can cause. As a result, warming temperatures should result in decreased food intake as well as reduced growth, if food intake decreases while aerobic metabolism remains high. In the present experiment, SDA was not estimated for redfish under the different temperature treatments. However, given that maintenance metabolic demands (SMR) increased at the highest temperatures while food consumption remained stable, it is possible that SDA also increased so much that peak oxygen consumption is limited by the observed AS, thereby altering the time required to digest meals and eventually limiting growth. An alternate hypothesis is that, although elevated AS may be sufficient to support specific dynamic action (SDA), digestion

could be accelerated at higher temperatures. As a result, fish might not be able to consume enough food due to the physical limitation of stomach volume, especially when restricted to three meals per week. This could explain the observed results. If this hypothesis holds true, increasing the number of meals per week at higher temperatures could potentially maintain growth rates despite elevated SMR, by taking advantage of the increased AS.

Calculations of feed conversion efficiency (FCE) revealed that fish at higher temperatures had a reduced capacity to convert feed into body mass, likely because a greater proportion of ingested energy was allocated to meeting elevated maintenance costs. Although fish held at 10 °C did not consume significantly less than those at lower temperatures, they converted a smaller proportion of the ingested food into growth. As noted by Jobling (1995), the temperature at which FCE is maximized is typically slightly lower than the optimum temperature for growth. This is because maintenance costs, such as oxygen uptake and basic physiological functions, increase more rapidly with temperature than the energy allocated to growth, thereby reducing conversion efficiency at higher temperatures. In this study, no significant differences in FCE were observed between 2.5 and 5.0 °C, suggesting that this range may be optimal for feed conversion for redfish. However, growth was clearly optimized at 5.0 °C for both groups, added and original fish, as the added fish showed lower growth at 2.5 °C. This supports the idea that while lower temperatures may favor energy efficiency, slightly higher temperatures can maximize growth rates due to increased food intake and metabolic activity, despite a drop in efficiency.

Two secondary results emerged from our study. First, we have observed that for growth the two groups (original and added fish) responded similarly to the highest temperature (10 °C) but had different trends for lower temperatures. The major difference is that added fish had a lower growth rate at 2.5 °C in comparison with the 5.0 °C treatment while the original fish had similar growth rates for these two temperatures. This could be explained by the fact that the added fish had less time to acclimate to the experimental conditions compared to the original fish that were kept in these conditions for four months prior to data collection. This acclimation time difference also led to overall significantly lower growth rates for the added

fish (Tableau 4, Figure 10), but the temperature growth rate relationship showed similar conclusions for both groups when it came to predicting the effects of warmer waters expected for the second half of the Century in this region.

Second, even though growth rates were generally reduced at 10 °C, one of the four experimental tanks exposed to that temperature showed one of the best mean growth rates of all 16 tanks, causing a large variability at this temperature. This tank was also the one out of the four 10 °C treatment that had the highest food consumption (Fig. 17). The hypothesis behind the aerobic scope protection proposed by Jutfelt et al. (2021) relates to behaviour, where fish would willingly regulate their food intake based on the additional energetic costs associated to an increase in temperature. However, given that we did not observe a decline in aerobic scope at 10 °C, our results suggest that the individuals in this one tank might not have adopted this strategy, and instead simply ate more than the others resulting in faster growth rate. We thus speculate that for fish kept at 10 °C, those able to consume more food can grow faster. However, this is considering that individuals are reared in regulated tanks without any stressors such as predation risk, and that such observations might be different for fish in the wild or even in a repeated experiment. The lowest food consumption rates throughout the experiment were observed at either 10 °C for the three other tanks or 2.5 °C (Fig. 17), indicating that, at similar food quantities, temperature plays a significant role in regulating growth, particularly when comparing the two extreme treatments. Nonetheless, a significant tank effect was observed on growth performance, and this effect was not restricted to the 10 °C treatment. The variability in growth and food consumption at this temperature further highlights this effect, suggesting that factors beyond temperature and pH may have influenced growth. Although our final model, which smooths by group but ignores the effect of pH, had the best AIC and was used for our results, the full model (described earlier in the Statistical analysis section) provided some indication that pH might influence growth. Specifically, while temperature did not significantly affect growth at pH 7.75 in this full model, it had a significant effect at pH 7.35, with a peak around 6 °C for the original group and 5 °C for the added group which is also the temperatures at which potential for growth, based on gene expression, was increased in a field study on *S. mentella* (Martínez Silva et al.

2022). This suggests that fish at pH 7.35 might be more sensitive to rearing temperatures that deviate from the apparent optimal temperature of ~5 °C. However, the limited replication reduces the power of our analyses, and further experiments would be needed to confirm whether pH plays a role in modulating growth responses to temperature. Repeating the experiment would allow us to confirm whether growth is indeed reduced at 10 °C and should include higher temperatures to determine the threshold at which growth and/or survival is markedly reduced, a value that the current experiment could not establish. Given the low number of replicates, uncontrolled factors in the tank room could have influenced growth.

1.7.2 Temperature-dependent growth limitation and the role of food availability

The highest acclimation temperature in our experiment (10.0 °C) led to lower growth rates. We observed that fish maintained relatively constant food consumption at temperatures ranging from 5.0 to 10.0 °C, while experiencing increased metabolic demands. Consequently, this suggests that even when fed ad libitum, a reduction in growth is to be anticipated at high temperatures in the wild and that this is potentially attributed to a decrease in FCE at those temperatures. Moreover, in natural environments characterized by density-dependent pressures, it is highly probable that the effect of high temperature would be magnified under limited prey supply (Sánchez Lizaso et al. 2000). The current reduction in growth measured in GSL redfish in the wild (Senay et al. 2023; Coussau et al. 2024) could be partly attributable to density dependence under increasing temperatures and potentially linked to the sharp decline of the northern shrimp (Bourdages et al. 2023), recognized as an important prey (Brown-Vuillemin et al. 2022, 2023). Interestingly, the lowest food consumption in this study happened at the lowest temperature tested (2.5 °C) but this did not result in the slowest growth rate, which can be explained by the lower metabolic demand as demonstrated by a high FCE at this temperature (Figure 10). This suggests that GSL redfish are well adapted to a cold, subarctic environment and that a lower food consumption rate induced by density-dependence would not be as aggravating at low temperatures (2.5 °C) relative to those predicted for the GSL (10.0 °C).

1.7.3 Divergent effects of temperature on aerobic metabolism and growth performance

We observed that higher acclimation temperatures within our study range resulted in higher MMR, SMR, and AS accompanied by a lower FAS. Out of the hypotheses that have proposed a mechanistic understanding for the relationship between aerobic scope and growth, the OCLTT hypothesis is a widely recognized framework. The OCLTT speculates that as an animal approaches its thermal limits, its ability to supply oxygen to tissues decreases, leading to a gradual decline in aerobic performance and eventually reaching lethal temperatures (Pörtner 2010). This occurs because higher temperatures drive a continuous increase in oxygen demand, which the animal's oxygen supply system can no longer meet. This hypothesis also states that aquatic ectotherms have evolved biochemical and physiological adaptations to maximize aerobic metabolism within a specific temperature range, thereby optimizing fitness-related performance such as growth and reproduction (Pörtner 2001). Consequently, from the OCLTT point of view, the temperature at which the optimum aerobic scope is observed will also be the optimal temperature for growth (Pörtner 2010). Our results do not support this hypothesis and are more in line with that proposed by Clark et al. (2013) and Schulte et al. (2011) who demonstrated that when tested experimentally, many species' aerobic scopes and other physiological traits do not align with the thermal profiles of other critical traits like growth and reproduction (e.g., Gräns et al. 2014; Norin et al. 2014). In our study, an increase in aerobic scope did not translate into increased growth for the same temperatures suggesting that the concept of optimal temperature varies among physiological traits (Figs. 1 and 2). However, when interpreting these findings, it is important to consider potential sources of variability in our metabolic data. In particular, we acknowledge that gut transit time as a function of temperature is unknown for this species. For 7 out of 8 sessions, fasting time ranged from 72 to 119 h, which is longer than for other cold-water fish species, 48 h at 5 °C for capelin (Behrens et al. 2006), 24 h at 10 °C for two *Sebastes* species (*Sebastus caurinus* Richardson, 1844 and *Sebastus mystinus* Jordan & Gilbert, 1881; Hamilton et al.

2017), and 24 h at 10 °C for haddock and cod (Norin et al. 2019). However, fasting duration was only 48 h for the remaining session, which included treatments 2.5_7.35 and 5.0_7.35. We compared aerobic metabolic traits (MMR, SMR, AS, FAS, and O_2crit) between these treatments and their duplicates that had longer fasting periods, observing a significant difference in MMR and AS for the 5.0_7.35 treatment only, but no difference in SMR, possibly due to the extended duration of our SMR determinations. Overall, we are therefore confident that fasting duration was sufficient for our SMR determinations. The significant difference in MMR and AS between the 48 h fasting duration and another with a longer fasting duration likely reflects a tank effect, which was significant in our study, possibly due to SDA influence in one of the replicate tanks for the 5.0_7.35 treatment. However, this potential overestimation of MMR was likely too small to influence FAS, which remained consistent across sessions.

As we observed a linear increase in MMR, SMR, and AS with temperature, the acclimation temperatures used in our study did not capture the maximum thermal range for redfish aerobic metabolism. Although no previous studies have investigated the thermal limits of redfish, we are confident that these limits were not exceeded in our study, as it would have resulted in a decline in metabolic traits at higher temperatures. However, we observed a decrease in FAS, suggesting that the rising SMR is becoming more difficult to sustain, and indicating that we have likely surpassed the thermal optimum for aerobic metabolism. Temperature selection in the present study was based on knowledge of redfish distribution in the GSL, where they are systematically found at temperatures below 8 °C. We thus hypothesized that 10 °C would be sufficiently high to observe a decline in metabolic performance and a more pronounced reduction in growth rate. Although *S. fasciatus* appears to prefer water temperatures around 5–6 °C in the wild where they are found in higher densities (Kelly et al. 1972; Atkinson 1989; Senay et al. 2023), they have also been observed in warmer waters and up to 13 °C in the Gulf of Maine (Scott 1982). Future studies should expose *S. fasciatus* to higher temperatures to better define the optimum temperature range for metabolic rates and growth.

1.7.4 Ocean acidification alters aerobic metabolism but does not consistently affect growth

The effects of ocean acidification, estimated through a decrease in pH and an increase in pCO_2 (Tableau 2), on aerobic metabolic traits have been documented but have shown contrasting results in fishes (Heuer and Grosell 2014; Esbaugh 2018), including in the genus *Sebastes*. *Sebastes caurinus* that were exposed for several weeks to two pH levels (normal: 7.87 vs. low: 7.32) were characterized by a reduction in their critical aerobic swimming speed (16.8%) and aerobic scope (53.5%) under low pH comparatively with normal pH. However, no changes were observed in these traits for *S. mystinus* exposed to the same conditions and coming from the same habitat (Hamilton et al. 2017). Even though these two species are closely related and use the same habitat as adults, this difference could be explained by the fact that *S. mystinus* were exposed to high pCO_2 levels, thus a reduced pH, during early life stages, possibly leading to a better adaptation for these conditions than *S. caurinus* (Hamilton et al. 2017). Given that redfish migrate through the water column in earlier life stages, one hypothesis is that they might have been exposed to different pH levels as the water column of the deep water of the GSL is well stratified and surface layers tend to be more acidic (Lavoie et al. 2021). This exposition of redfish larvae to lower pH levels in the surface layer may result in better tolerance to low pH later in life.

As Heuer and Grosell (2014) stated, the main effect of water acidification on aerobic metabolism, when observed, is primarily that of a loading factor, sensu Fry (1971): when acidification had an effect, SMR increased (cost of acid-base regulation), driving a reduction in AS and subsequently, growth. In this study, we did observe that fish acclimated at an acidic pH had a higher SMR than those at the control or current pH, fitting this hypothesis. Therefore, in the context of ocean acidification, redfish may potentially see their AS and their growth potential decreased. Probably because of the considerable variation in SMR, MMR, AS, and FAS in this study, the increase in SMR did not have any measurable impact on aerobic scope, even when combined with an increase in temperature. In a similar study on Atlantic halibut, Gräns et al. (2014) observed elevated aerobic scope at lower pH (acidic) but

no effect on growth rates except at their lower temperature treatment. At this lower temperature treatment (5 °C) growth rates were suppressed by 24% at the low pH compared to current pH. Surprisingly, this lower temperature treatment is the temperature where these juvenile halibut are typically found in the wild (Gräns et al. 2014).

1.7.5 Temperature-dependent hypoxia sensitivity in redfish

Hypoxia tolerance, measured as O_2crit, is the ambient oxygen level at which a fish can meet its maintenance requirements but has no aerobic scope left for activity (Claireaux and Chabot 2016). In the present study, fish acclimated to higher temperatures had lower hypoxia tolerance, reflected in a higher O_2crit. As oxygen levels continue to drop, the fish is dependent on anaerobic metabolism, which is unsustainable over time. Rapid decreases in dissolved oxygen as those simulated in the laboratory are unlikely to happen in the redfish habitat, but this measurement indicates the oxygen limit that redfish can face in their environment. As redfish are a competitor to other groundfish in the GSL, O_2crit makes it possible to compare the oxygen sensitivity of redfish to that of competitors such as Atlantic cod or Greenland halibut. Plante et al. (1998), working with GSL Atlantic cod of various sizes exposed to 2 and 6 °C, observed complete mortality within hours at 10% air sat. and found that only a few individuals survived 96 h at 16% air sat., highlighting the species' sensitivity to hypoxia. Adult Greenland halibut kept at 5 °C were able to tolerate ambient dissolved oxygen down to 11% air sat., though juveniles were more sensitive to hypoxia (Dupont-Prinet et al. 2013). During our experiments, we observed that redfish had a mean O_2crit of 18.59% at 5.0 °C and 22.64% at 10.0 °C, making them more tolerant at higher temperatures than Atlantic cod, but more sensitive to hypoxia than Greenland halibut at water temperatures where all three species are frequently observed and may compete for food. Considering that dissolved oxygen levels currently range between 15% and 65% air sat. in the deep channels (Blais et al. 2023; Wallace et al. 2023), some areas, particularly the estuary, are already suboptimal habitat for redfish. Worsening of hypoxia is observed in the deep channels of the GSL and estuary (Gilbert et al. 2005; Jutras et al. 2020, 2023) and predicted to continue (Lavoie et al. 2020), likely to cause even more habitat loss for GSL redfish,

especially as this will be accompanied by warming, which makes redfish more sensitive to hypoxia based on our results.

1.7.6 Perspectives and conclusion

Results of this study are timely as the commercial fishery for GSL redfish has just reopened in 2024, which highlights the importance of a better understanding of redfish physiological responses under multiple environmental constraints. The GSL will continue to be influenced by anthropogenic inputs in multiple ways, causing warming, acidification, and low oxygen levels. Linking the growth patterns and food requirements for growth with a mechanistic approach should allow us to better predict the future of this species in its ecological role in the ecosystem and as a key resource for fisheries.

The potential redistribution of redfish within the water column, driven by warming temperatures and reduced oxygen levels, could alter their ecological role in the GSL. Adult redfish currently distribute at the bottom of the deep layer of the GSL, where waters are warming the most. The GSL waters are stratified, with a cold intermediate layer located between the relatively warm deep and surface layers. This stratification implies the possibility that redfish move up in the water column or in shallow habitats to access more favorable temperature for growth near the cold intermediate layer. Such vertical redistribution could have broad implications to cold associated species which would undergo increased predation risk from redfish.

From a fisheries perspective, anticipated future slower growth and smaller fish sizes present two challenges: a reduction in biomass, which could affect catch volume, and potential reduction in the value of the catch, as smaller fish are worth less economically than larger fish and are therefore resulting in lower landing value. Although reduced fecundity has not been directly observed, limited food availability coupled with higher metabolic demands may constrain energy allocation, potentially affecting both growth and reproduction. Since 2010, temperatures have increased markedly in the GSL, leading to environmental changes that have already affected the availability of prey for redfish. Key prey species such as

Northern shrimp, an important component of the redfish diet (Brown-Vuillemin et al. 2022, 2023), have declined in abundance, partly due to warming bottom waters and other climate-related factors. At the same time, the biomass of redfish capable of feeding on small fish and shrimp has increased substantially, and cannibalism has been increasingly observed (Brown-Vuillemin et al. 2022), further suggesting intensified intraspecific competition for food. Yet, their growth rates are lower than expected based on historical data from lower-density populations (Senay et al. 2023), indicating that current environmental conditions may already contribute to a growth reduction. This could hamper future recruitment (Burns 2022), with implications for the long-term sustainability of the population and the viability of the fishery.

Future work should investigate the species' responses to higher temperature thresholds, variable prey availability, prolonged exposure to reduced oxygen levels but also SDA under these different climate change scenarios. Developing a mechanistic understanding of these processes, particularly the impact of digestion on aerobic scope and growth, will be essential for predicting how redfish populations may adapt to the rapidly changing conditions of the GSL. This knowledge will inform conservation efforts and management strategies aimed at sustaining both the ecological and economic value of redfish in the region.

1.8 SUPPORTING INFORMATION

Tableau 6. Seawater parameters (Mean ± Standard deviation) for each experimental tank throughout the growth period (July 2nd to October 20th, 2021). Tanks represent the 16 experimental tanks in which fish were held. Treatment represents the target Temperature and pH, pH_T are the values of pH total recorded from Monday to Friday during the growth period, Total alkalinity was measured once a week in each of the four header tanks, pCO_2 values were calculated from pH_T measurements and weekly alkalinity measurements, salinity and temperature was measured from Monday to Friday.

Tank	Treatment (T°C_pH)	pH_T	Total alkalinity (mol L^{-1})	pCO_2 (uatm)	Salinity (ppt)	Temperature (°C)
A1	5_7.35	7.36 ± 0.05	2077.92 ± 11.09	1994.14 ± 237.14	28.34 ± 0.33	5.60 ± 0.37
A2	5_7.75	7.67 ± 0.04	2077.92 ± 11.09	934.54 ± 79.09	28.34 ± 0.33	5.42 ± 0.35
A3	5_7.75	7.67 ± 0.04	2077.92 ± 11.09	940.49 ± 83.20	28.34 ± 0.33	5.31 ± 0.34
A4	5_7.35	7.37 ± 0.05	2077.92 ± 11.09	1932.75 ± 247.04	28.34 ± 0.33	5.40 ± 0.35
B1	7.5_7.75	7.71 ± 0.04	2077.15 ± 10.56	861.18 ± 77.86	28.37 ± 0.31	7.57 ± 0.21
B2	7.5_7.35	7.37 ± 0.06	2077.15 ± 10.56	1942.07 ± 281.91	28.37 ± 0.31	7.58 ± 0.22
B3	7.5_7.35	7.35 ± 0.04	2077.15 ± 10.56	2047.41 ± 173.01	28.37 ± 0.31	7.60 ± 0.16
B4	7.5_7.75	7.72 ± 0.04	2077.15 ± 10.56	838.20 ± 74.68	28.37 ± 0.31	7.33 ± 0.22
C1	2.5_7.35	7.36 ± 0.05	2080.15 ± 10.02	1936.67 ± 204.21	28.36 ± 0.30	2.86 ± 0.29
C2	2.5_7.35	7.36 ± 0.04	2080.15 ± 10.02	1956.93 ± 191.92	28.36 ± 0.30	2.84 ± 0.28
C3	2.5_7.75	7.71 ± 0.05	2080.15 ± 10.02	841.72 ± 95.30	28.36 ± 0.30	2.61 ± 0.30
C4	2.5_7.75	7.71 ± 0.05	2080.15 ± 10.02	841.09 ± 92.26	28.36 ± 0.30	2.60 ± 0.27
D1	10_7.75	7.69 ± 0.03	2076.53 ± 9.89	918.63 ± 77.66	28.41 ± 0.30	10.06 ± 0.36
D2	10_7.35	7.36 ± 0.03	2076.53 ± 9.89	2049.18 ± 155.80	28.41 ± 0.30	10.10 ± 0.28
D3	10_7.75	7.69 ± 0.03	2076.53 ± 9.89	914.04 ± 75.17	28.41 ± 0.30	10.03 ± 0.30
D4	10_7.35	7.36 ± 0.05	2076.53 ± 9.89	2051.96 ± 237.44	28.41 ± 0.30	10.06 ± 0.30

Tableau 7. Seawater parameters (Mean ± Standard deviation) for each experimental tanks throughout the growth period for this experiment from January 22nd to July 1st, 2021. Tanks represent the 16 experimental tanks in which fish were held, Treatment represents the target Temperature and pH, pH_T are the values of pH total recorded from Monday to Friday during the growth period, Total alkalinity was measured once a week in each of the four header tanks, pCO_2 values were calculated from pH_T measurements and weekly alkalinity measurements, salinity and temperature was measured from Monday to Friday.

Tank	Treatment (T°C_pH)	pH_T	Temperature (°C)	Total alkalinity (mol L^{-1})	Salinity (ppt)	pCO_2 (uatm)
A1	5_7.35	7.34 ± 0.05	5.18 ± 0.23	2056.00 ± 29.60	28.95 ± 0.57	2020.66 ± 226.65
A2	5_7.75	7.73 ± 0.03	5.07 ± 0.26	2056.00 ± 29.60	28.95 ± 0.57	796.70 ± 69.64
A3	5_7.75	7.72 ± 0.04	4.97 ± 0.28	2056.00 ± 29.60	28.95 ± 0.57	821.22 ± 85.22
A4	5_7.35	7.34 ± 0.06	5.04 ± 0.23	2056.00 ± 29.60	28.95 ± 0.57	2034.19 ± 284.35
B1	7.5_7.75	7.73 ± 0.03	7.53 ± 0.27	2054.39 ± 30.07	28.95 ± 0.57	814.08 ± 57.29
B2	7.5_7.35	7.33 ± 0.04	7.53 ± 0.27	2054.39 ± 30.07	28.95 ± 0.57	2099.35 ± 217.28
B3	7.5_7.35	7.35 ± 0.06	7.49 ± 0.25	2054.39 ± 30.07	28.95 ± 0.57	2017.41 ± 223.55
B4	7.5_7.75	7.72 ± 0.03	7.37 ± 0.27	2054.39 ± 30.07	28.95 ± 0.57	820.98 ± 61.18
C1	2.5_7.35	7.34 ± 0.05	2.59 ± 0.18	2056.16 ± 28.68	28.95 ± 0.57	1991.67 ± 224.32
C2	2.5_7.35	7.34 ± 0.04	2.54 ± 0.20	2056.16 ± 28.68	28.95 ± 0.57	1979.47 ± 192.50
C3	2.5_7.75	7.73 ± 0.04	2.45 ± 0.28	2056.16 ± 28.68	28.95 ± 0.57	793.53 ± 77.86
C4	2.5_7.75	7.73 ± 0.04	2.43 ± 0.23	2056.25 ± 28.67	28.95 ± 0.57	785.98 ± 71.16
D1	10_7.75	7.72 ± 0.03	10.13 ± 0.19	2054.15 ± 29.44	28.95 ± 0.57	835.76 ± 52.40
D2	10_7.35	7.35 ± 0.04	10.15 ± 0.20	2054.15 ± 29.44	28.95 ± 0.57	2038.31 ± 171.45
D3	10_7.75	7.72 ± 0.03	10.10 ± 0.19	2054.15 ± 29.44	28.95 ± 0.57	846.08 ± 63.36
D4	10_7.35	7.35 ± 0.04	10.09 ± 0.22	2054.15 ± 29.44	28.95 ± 0.57	2028.57 ± 197.42

Tableau 8. Mean temperature and pH (± Standard error) during respirometry trials.

Tank	Treatment (T °C_pH)	Temperature (°C)	pH_T
A1	5_7.35	4.85 (0.00)	7.38 (0.00)
A2	5_7.75	5.09 (0.00)	7.73 (0.01)
A3	5_7.75	5.07 (0.00)	7.76 (0.01)
A4	5_7.35	5.11 (0.00)	7.35 (0.04)
B1	7.5_7.75	7.3 (0.00)	7.85 (0.09)
B2	7.5_7.35	7.53 (0.00)	7.38 (0.02)
B3	7.5_7.35	7.69 (0.00)	7.36 (0.02)
B4	7.5_7.75	7.39 (0.00)	7.76 (0.01)
C1	2.5_7.35	2.43 (0.00)	7.37 (0.01)
C2	2.5_7.35	2.41 (0.00)	7.35 (0.03)
C3	2.5_7.75	2.38 (0.00)	7.72 (0.02)
C4	2.5_7.75	2.35 (0.01)	7.78 (0.00)
D1	10_7.75	10.08 (0.00)	7.75 (0.01)
D2	10_7.35	10.07 (0.00)	7.33 (0.02)
D3	10_7.75	7.73 (0.00)	7.69 (0.00)
D4	10_7.35	7.31 (0.01)	7.36 (0.00)

Tableau 9. Design for best generalized additive models for each physiological trait with AIC. Model selection was based on the lowest AIC value for models of growth, food consumption and Food Conversion Efficiency.

Model	**AIC**
Growth 1 = gam(Growth rates ~ pH*group + s(Temperature, k=6, by= interaction(pH, group, drop=TRUE)) + s(Tank, bs="re"), data=Growth, method="REML")	-2286.486
Growth 2 = gam(Growth rates ~ pH + group + s(Temperature, k=9, by=interaction(pH, group, drop=TRUE)) + s(bassin, bs="re"), data=Growth, method="REML")	-2287.811
Growth 3 = gam(Growth rates ~ pH + s(Temperature, k=9, by=interaction(pH, group, drop=TRUE)) + s(bassin, bs="re"), data=Growth, method="REML")	-2261.015
Growth 4 = gam(Growth rates ~ pH + group + s(Temperature, k=9, by=pH) + s(tank, bs="re"), data= Growth, method="REML")	-2284.516
Growth 5 = gam(Growth rates ~ pH + group + s(Temperature, k=9, by=group) + s(tank, bs="re"), data= Growth, method="REML")	-2294.885
Growth 6 = gam(Growth rates ~ pH + group + s(Temperature, k=9) + s(tank, bs="re"), data= Growth, method="REML")	-2286.033
Food 1 = gam(Weekly food consumption~pH+s(Temperature, k=9, by=pH) + s(tank, bs="re"), data=Food, method="REML")	899.6192

Food 2 = gam(Weekly food consumption~pH+s(Temperature, k=9) + s(tank, bs="re"), data=Food, method="REML")	897.6241
FCE 1 = gam(Food conversion effiency ~ pH+s(Temperature, k=6, by=pH), data=FCE, method="REML")	-62.19
FCE 2 = gam(Food conversion effiency ~ pH+s(Temperature, k=6), data=FCE, method="REML")	-62.30

Tableau 10. Description and variable type of all parameters used in the generalized additive models for each physiological trait.

Parameter	Description	Variable type
Growth		
Temperature	Mean temperature during the whole growth experiment as a continuous variable	Fixed
pH	Acidification treatment as a 2 level factor (7.35-future or 7.75-current)	Fixed
Group	Group at which fish belong to during the growth experiment. Original or added	Fixed
Tank	Tank in which fish spent the whole growth experiment	Random
Food consumption (Food)		
Temperature	Mean temperature during the whole growth experiment as a continuous variable	Fixed
pH	Acidification treatment as a 2 level factor (7.35-future or 7.75-current)	Fixed
Tank	Tank in which fish spent the whole growth experiment	Random
Food conversion efficiency (FCE)		
Temperature	Mean temperature during the whole growth experiment as a continuous variable	Fixed
pH	Acidification treatment as a 2 level factor (7.35-future or 7.75-current)	Fixed
Metabolic traits		
(MMR, SMR, AS, FAS, O_{2crit})		
Temperature	Mean temperature during the respirometry trial for each treatment as a continuous variable	Fixed
pH	Acidification treatment as a 2 level factor (7.35-future or 7.75-current)	Fixed
Temperature*pH	Interaction between temperature and pH	Fixed
Tank	Tank in which fish spent the whole growth experiment	Random
Respirometry chamber	Respirometry chamber in which the fish underwent respirometry as a 8 level factor	Random

Tableau 11. Design for best linear mixed-effects models for each metabolic traits with interaction p-values. Complete models for metabolic variables included the interaction between pH and Group. The column Interaction p-value refers to the interaction term and it was never significant. This final model excludes the interactions.

Model	**Interaction p-value**
SMR 1 = lmer(SMR ~ Temperature*pH + (1 | tank + (1|respirometer), data=MR)	0.556
SMR 2 = lmer(SMR ~ Temperature + pH + (1 | tank + (1|respirometer), data=MR)	
MMR 1 = lmer(MMR ~ Temperature*pH + (1 | tank + (1|respirometer), data=MR)	0.136
MMR 2 = lmer(MMR ~ Temperature + pH + (1 | tank + (1|respirometer), data=MR)	
AS 1 = lmer(AS ~ Temperature*pH + (1 | tank + (1|respirometer), data=MR)	0.196
AS 2 = lmer(AS ~ Temperature + pH + (1 | tank + (1|respirometer), data=MR)	
FAS 1 = lmer(FAS ~ Temperature*pH + (1 | tank + (1|respirometer), data=MR)	0.968
FAS 2 = lmer(FAS ~ Temperature + pH + (1 | tank + (1|respirometer), data=MR)	
O_2crit 1 = lmer(O_2crit ~ Temperature*pH + (1 | tank + (1|respirometer), data=MR)	0.894
O_2crit 2 = lmer(O_2crit ~ Temperature + pH + (1 | tank + (1|respirometer), data=MR)	

Tableau 12. Survival rates (in %) and maximum number of individuals per tanks for the growth experiment of redfish (*Sebastes fasciatus*) from July 12th to October 20th for each tank.

Tank	Treatment	Temperature	pH	Max.nbr	Survival
A1	5_7.35	5	Future (7.35)	42	100.00
A2	5_7.75	5	Current (7.75)	42	100.00
A3	5_7.75	5	Current (7.75)	42	100.00
A4	5_7.35	5	Future (7.35)	42	100.00
B1	7.5_7.75	7.5	Current (7.75)	42	97.62
B2	7.5_7.35	7.5	Future (7.35)	42	97.62
B3	7.5_7.35	7.5	Future (7.35)	42	97.62
B4	7.5_7.75	7.5	Current (7.75)	42	97.62
C1	2.5_7.35	2.5	Future (7.35)	42	97.62
C2	2.5_7.35	2.5	Future (7.35)	42	97.62
C3	2.5_7.75	2.5	Current (7.75)	42	100.00
C4	2.5_7.75	2.5	Current (7.75)	42	100.00
D1	10_7.75	10	Current (7.75)	42	100.00
D2	10_7.35	10	Future (7.35)	40	97.50
D3	10_7.35	10	Future (7.35)	42	95.24
D4	10_7.75	10	Current (7.75)	42	95.24

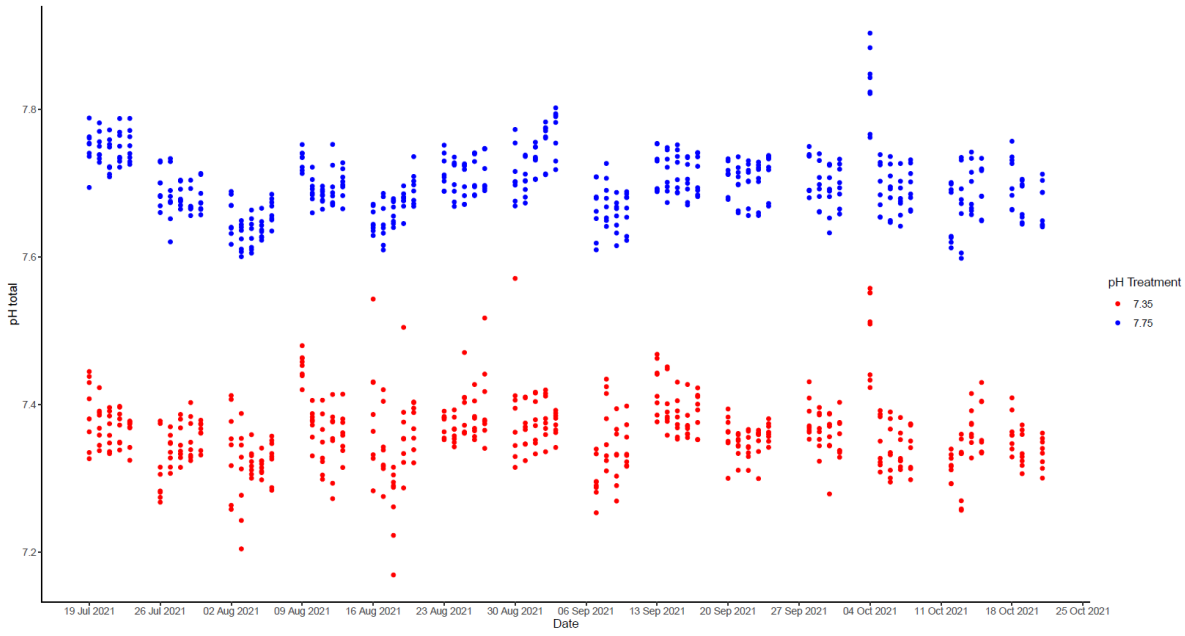

Figure 12. Values of pH total recorded from Monday to Friday in each of the experimental tanks during the growth period. In blue: tanks that were kept at a control pH treatment of 7.75. In red: tanks that were kept at an acidified pH treatment of 7.35.

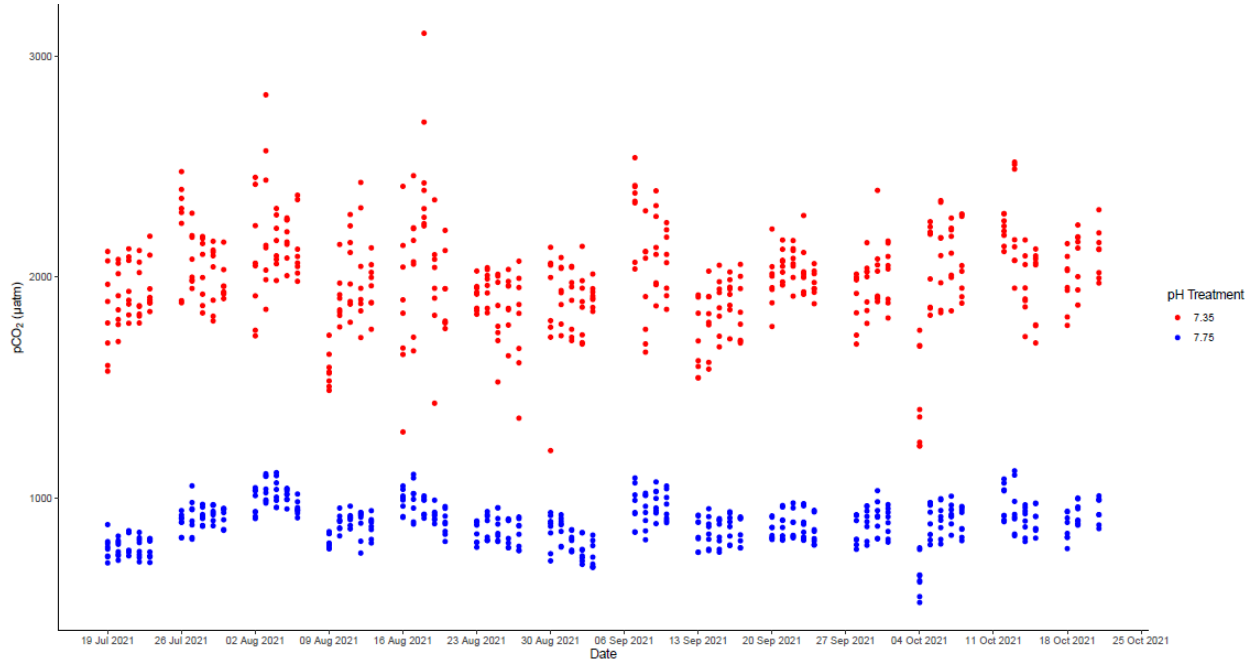

Figure 13. pCO_2 values estimated from pH total measurement and alkalinity for the period where growth was estimated for this experiment. In blue: tanks that were kept at a control pH treatment of 7.75 (current). In red: tanks that were kept at an acidified pH treatment of 7.35 (future).

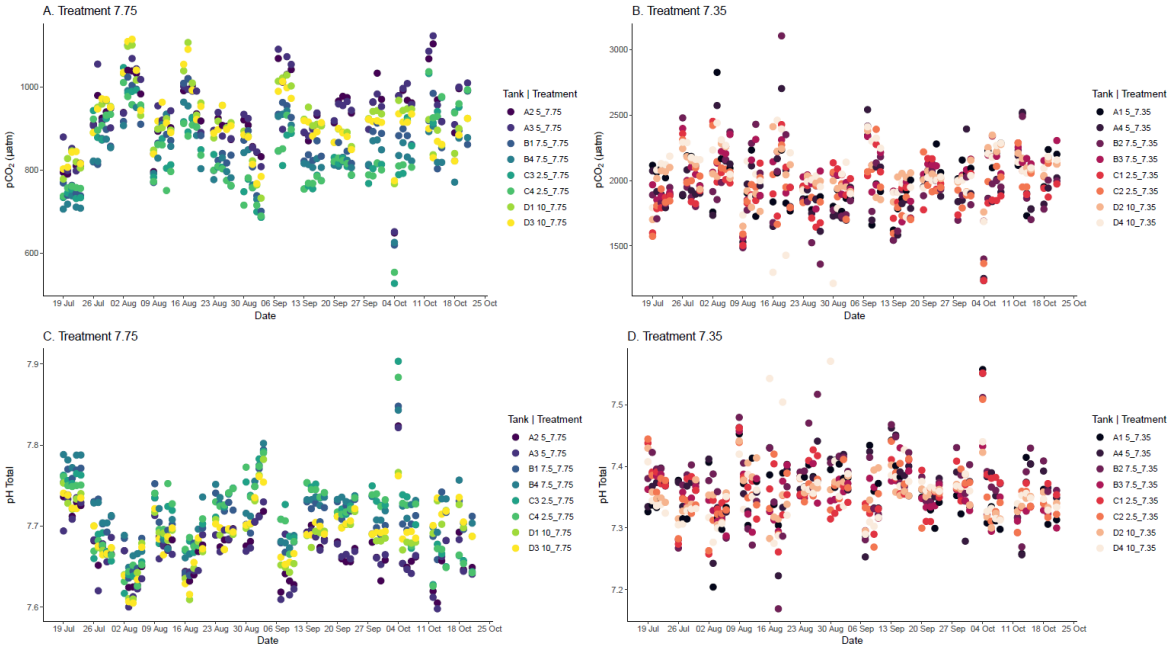

Figure 14. Seawater monitoring of the experimental tanks throughout the growth period for this experiment. A. and B. pCO_2 values estimated from pH total measurement and alkalinity for the period where growth was estimated for this experiment. A. tanks that were kept at a control pH treatment of 7.75 (current). B. tanks that were kept at an acidified pH treatment of 7.35 (future). C. and D. Values of pH total recorded everyday from Monday to Friday in each of the experimental tank during the growth period. C. tanks that were kept at a control pH treatment of 7.75 (current). D. tanks that were kept at an acidified pH treatment of 7.35 (future).

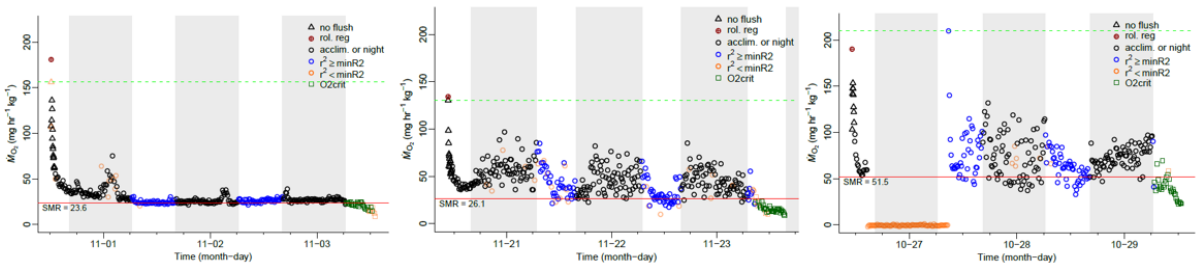

Figure 15. Evolution of oxygen uptake during 4-day experiments for 3 redfish**.** A fish which reached stable values typical of SMR during the latter part of the experiment, left figure; two fish did not reach SMR. S6S2CH1 (10.0_7.75) center figure and S1S2CH4 (2.5_7.75) right figure.

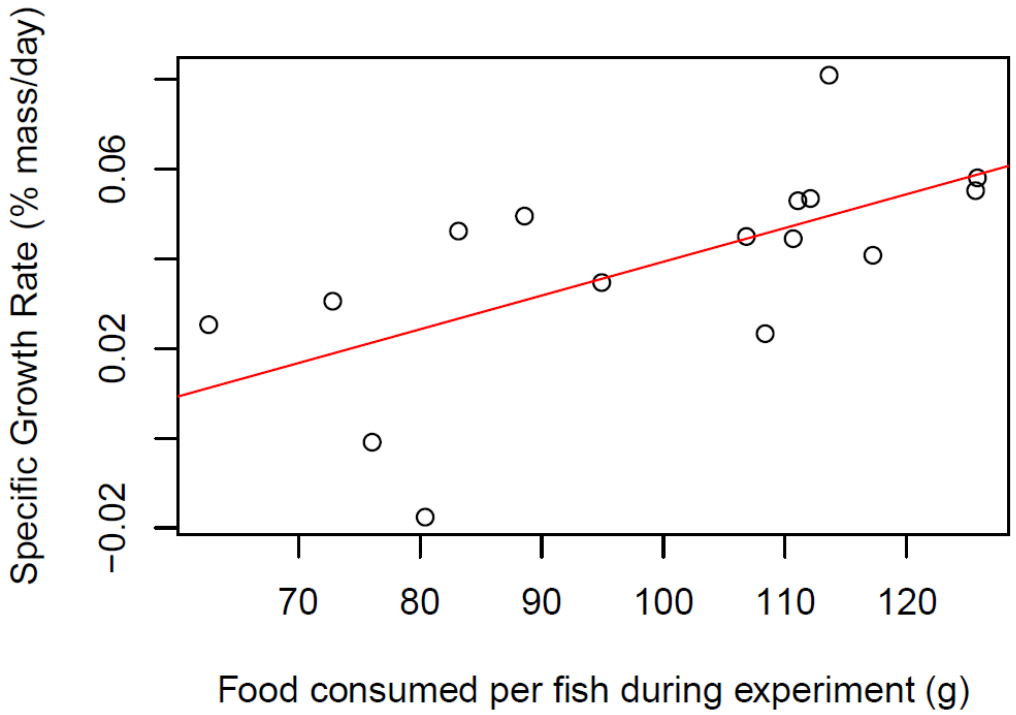

Figure 16. Relationship between food consumption and specific growth rate in redfish (*Sebastes fasciatus*). Each point represents the mean average specific growth rate (%

mass/day) of fish per tank, plotted against the total amount of food consumed per fish in that same tank (g) over the course of the experiment.

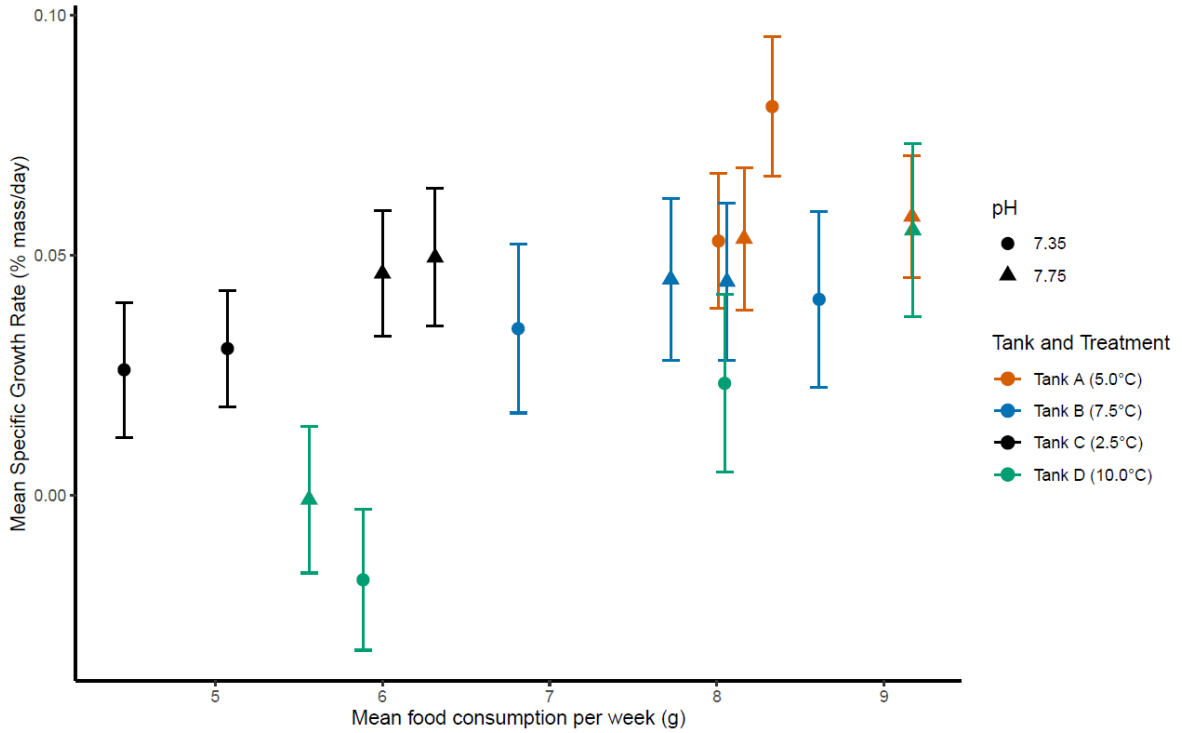

Figure 17. Mean specific growth rates in function of mean food consumption per week for all tanks. Circles are for the tank that had an acidic pH treatment of 7.35, triangles are for the tanks that had a control pH of 7.75. Each colors represents the 4 different temperature lines (A, B, C and D).

CHAPITRE 2
CAPACITÉ AÉROBIE ET CROISSANCE RÉDUITES CHEZ LE SÉBASTE ACADIEN (*SEBASTES FASCIATUS*) DU GOLFE DU SAINT-LAURENT SOUMIS À UNE HYPOXIE CHRONIQUE

2.1 RÉSUMÉ EN FRANÇAIS DU DEUXIÈME ARTICLE

Les changements climatiques en cours entraînent une baisse de l'oxygène dissous dans les systèmes marins, principalement en raison du réchauffement des eaux et de modifications de la stratification qui réduisent la solubilité de l'oxygène et le mélange vertical. Dans plusieurs régions, notamment dans le golfe du Saint-Laurent (GSL, Canada), les concentrations d'oxygène atteignent des niveaux durablement faibles, qui devraient encore diminuer à court terme, imposant des contraintes physiologiques aux organismes et modifiant ainsi la structure des écosystèmes. Le sébaste (*Sebastes fasciatus* et *S. mentella*), espèce d'importance commerciale dont l'abondance a récemment explosé dans le GSL, occupe aujourd'hui principalement des habitats où l'oxygène varie entre 20 % et 60 % de saturation. Pourtant, on connaît encore peu la manière dont ces conditions influencent leurs performances physiologiques et leur bilan énergétique. Pour pallier à cette lacune, nous avons quantifié expérimentalement les effets d'une exposition chronique (105 jours) à huit niveaux d'oxygène (25–100 % de saturation) sur la consommation de nourriture, l'efficacité de conversion alimentaire (ECA), la croissance, la condition, le métabolisme aérobique (taux métabolique standard et maximal, capacité aérobie) et la tolérance à l'hypoxie (O_2crit). La consommation de nourriture, l'ECA et les taux de croissance sont demeurés stables du traitement normoxique (95 % de saturation) jusqu'à environ 45 % de saturation, puis ont commencé à diminuer autour de 36–44 % et étaient significativement réduits à partir de 29–34 % de saturation. Le changement de condition (ΔK) n'a diminué significativement qu'à 25 % de saturation. Ce patron s'accompagne d'une diminution linéaire du métabolisme maximal (TMM) et, dans une moindre mesure, du métabolisme standard (TMS), qui, combinés, réduisent la capacité aérobie (CA). Ainsi, la stabilité des paramètres de croissance au-dessus

de 45 % de saturation reflète vraisemblablement une capacité aérobie suffisante pour soutenir l'alimentation, la digestion et la croissance en conditions contrôlées. Nos résultats indiquent que le sébaste peut maintenir son bilan énergétique sous hypoxie modérée, mais qu'il fait face à des compromis entre le maintien métabolique et la croissance lorsque les niveaux d'oxygène deviennent plus sévères (DO < 45 % de saturation). Dans le GSL, les sébastes pourraient déjà vivre à la limite de leurs capacités physiologiques pour les traits liés à la performance énergétique, et une baisse supplémentaire de l'oxygène pourrait devenir un facteur limitant majeur pour leur condition physique et leur distribution.

Mots-clés : Physiologie des poissons, limitation en oxygène, capacité aérobie, compromis énergétiques, performance métabolique, physiologie en contexte de changements climatiques, facteurs de stress environnementaux.

Cet article, intitulé « *Reduced aerobic capacity and growth performance for Gulf of St. Lawrence Acadian redfish (Sebastes fasciatus) under chronic hypoxia* », a été soumis pour publication dans cette même version à la revue *ICES Journal of Marine Science* le 7 janvier 2026. En tant que première autrice, j'ai assuré la recherche bibliographique, la conception méthodologique, la collecte et l'analyse des données, ainsi que la rédaction du manuscrit. Le chercheur Denis Chabot, deuxième auteur, est à l'origine de l'idée initiale du projet et a contribué à la conception de l'étude, au financement, à la mise à disposition des ressources matérielles, à la supervision scientifique, à l'analyse des données et à la révision du manuscrit. Caroline Senay, troisième autrice, a participé à la conceptualisation du projet, à la gestion du projet et à la révision du manuscrit. Dominique Robert, quatrième auteur, a contribué à la supervision scientifique, à la validation des analyses et à la révision du manuscrit. Enfin, le dernier auteur, David Deslauriers, a participé au développement de la méthodologie, à la mise à disposition des ressources matérielles, à la supervision et à la révision du manuscrit. Les résultats de cette étude ont été présentés lors de la conférence du chapitre Atlantique international de la *American Fisheries Society* à Québec à l'automne 2025.

2.2 REDUCED AEROBIC CAPACITY AND GROWTH PERFORMANCE FOR GULF OF ST. LAWRENCE ACADIAN REDFISH (*SEBASTES FASCIATUS*) UNDER CHRONIC HYPOXIA.

Joëlle J. Guitard[a], Denis Chabot[b], Caroline Senay[b], Dominique Robert[a], and David Deslauriers[a]

[a]Institut des sciences de la mer, Université du Québec à Rimouski, Rimouski, QC, Canada; [b]Maurice Lamontagne Institute, Fisheries and Oceans Canada, Mont-Joli, QC, Canada

2.3 ABSTRACT

Ongoing climate change is driving oxygen declines in marine systems primarily due to ocean warming and changes in stratification, reducing both oxygen solubility and vertical mixing. In many regions including the Gulf of St. Lawrence (GSL), Canada, oxygen levels have reached persistently low levels that are expected to further decrease in the short term, resulting in constraints on the physiology of organisms, which in turn affect ecosystem structure. Redfish (*Sebastes fasciatus* and *S. mentella*), commercially important species that have recently resurged in the GSL, are now found largely in habitats where oxygen levels range between 20% and 60% dissolved oxygen (DO) saturation. However, little is known about how these conditions shape their physiological performance and energy balance. To address this, we experimentally quantified the effects of chronic exposure (105 days) at eight oxygen levels (25–100% saturation) on food intake, food conversion efficiency (FCE), growth, condition, aerobic metabolism (standard and maximum metabolic rates, aerobic scope), and hypoxia tolerance (O_2crit). Food intake, FCE and growth rates remained stable to about 45% saturation, declined starting at around 36–44% saturation and were significantly reduced starting at 29–34% saturation. Change in condition (ΔK) declined significantly at 25% saturation only. This pattern corresponds to a linear decrease in maximum metabolic rate (MMR) and, to a lesser extent, standard metabolic rate (SMR), which together reduced the aerobic scope (AS). Thus, the stability of growth parameters above 45% DO likely reflects sufficient aerobic capacity to sustain feeding, digestion, and growth under laboratory conditions. These results suggest that redfish can maintain energy

balance under moderate hypoxia, but face trade-offs between metabolic maintenance and growth under more severe conditions (DO < 45% saturation). According to recent surveys carried out in August 2024, up to 55% of the biomass of *S. fasciatus* was found at DO levels that reduce growth according to our results and further oxygen declines could act as major limiting factor on their fitness and distribution.

Keywords: Fish physiology, oxygen limitation, aerobic scope, energy trade-offs, metabolic performance, climate change physiology, environmental stressors

2.4 INTRODUCTION

Oxygen is essential for the metabolism and survival of marine organisms. However, oxygen levels are declining in many ocean regions due to natural and human-induced changes, particularly increased stratification and nutrient enrichment, which stimulate microbial respiration and accelerate oxygen uptake (Rabalais et al., 2010). In particular, benthic microbial communities consume oxygen in deeper waters that are isolated from surface replenishment, leading to hypoxic conditions (Gilbert et al., 2005). Such low-oxygen zones are often more severe and persistent in semi-enclosed basins, where limited water exchange prevents the renewal of bottom waters (Caddy, 2000). Climatic factors such as ice cover and wind patterns further influence vertical mixing, thus affecting oxygen availability near the seafloor (Rabalais et al., 2010). Because oxygen availability directly limits aerobic metabolism of marine organisms (Claireaux and Chabot, 2016; Fry, 1971), declines in dissolved oxygen (DO) can impair physiological traits (Wang et al., 2009; Wu, 2002), making it critical to define hypoxia in a biologically meaningful way.

Hypoxia is commonly defined as DO concentrations below 2 mg O_2 L^{-1} or 30 % air saturation (% sat. hereafter), a threshold under which consequences for ecosystems can be severe (Galic et al., 2019; Rabalais et al., 2010; Thomas and Bacher, 2018; Wu, 2002). However, the physiological impact of reduced oxygen is not only dependent on a single threshold, but on how oxygen availability limits the capacity of an organism to meet its metabolic demands. While the 2 mg L^{-1} benchmark is widely cited in the oceanography

literature (Diaz, 2001), it reflects extreme hypoxia and may not correspond to biologically meaningful limits for most aquatic organisms (Rabalais et al., 2010; Vaquer-Sunyer and Duarte, 2008). For example, a meta-analysis of marine benthic communities revealed that while most species experience lethal effects near this value, sublethal effects are common at much higher concentrations, approaching 5 mg O_2 L^{-1} (Vaquer-Sunyer and Duarte, 2008). Reduction in food intake and growth rates at oxygen levels between 4.5 and 6.1 mg O_2 L^{-1} have been observed across freshwater, marine and anadromous fish species (Chabot and Dutil, 1999; Hrycik et al., 2017; Rosenfeld and Lee, 2022). Together, these studies highlight the need to reconsider how hypoxia is defined, using species-relevant thresholds (Hrycik et al., 2017; Rosenfeld and Lee, 2022).

As a limiting factor (Fry, 1971), hypoxia constrains activity and performance. Given that tolerance to low oxygen varies among species, the effects of hypoxia are best described using physiological indicators such as the critical oxygen pressure (Pcrit) or the critical level of oxygen saturation (O_2crit), the threshold below which aerobic metabolism cannot be sustained and a common definition of hypoxia tolerance (Chabot and Claireaux, 2008). From fully oxygenated conditions to O_2crit, aerobic scope (AS, maximum metabolic rate (MMR) – standard metabolic rate (SMR)), the portion of metabolic capacity available beyond maintenance, declines progressively (Claireaux & Chabot, 2016). Under short-term reduced DO conditions, behavioral responses such as increased ventilation rates or avoidance of hypoxic areas are typically observed (Pihl et al., 1991). Most mobile species avoid hypoxic areas, when possible, likely to preserve sufficient aerobic scope for routine and performance-related activities. However, if suboptimal conditions persist and no better oxygenated water is available to move into, other behavioral adjustments are required and physiological compensation occurs, which can include reduced movement or food intake to match energy expenditures and available aerobic scope (Claireaux and Chabot, 2016; Lavaud et al., 2018; Schurmann et al., 1994). For example, juvenile Greenland halibut (*Reinhardtius hippoglossoides*) exposed to chronic hypoxia exhibited a reduced maximum metabolic rate (MMR) and AS, along with a prolonged postprandial metabolic rate (often called specific dynamic action, SDA) compared to individuals in normoxic conditions (Dupont-Prinet et al.,

2013). Eventually, fish may reach a critical threshold, the "level of no excess activity", where MMR meets SMR (Pcrit or O_2crit, see above). Beyond this point, anaerobic metabolism is initiated to help maintain SMR, which can only be sustained briefly and increases the risk of mortality (Claireaux and Chabot, 2016). These responses, especially when hypoxia is sustained over time, can have lasting effects on growth, reproduction, and survival, ultimately reducing fitness. For example, O_2crit of Atlantic cod (*Gadus morhua*) is around 21% sat. at 4 to 6 °C, but their growth performance is reduced below 70% sat. (Chabot and Claireaux, 2008).

Redfish (*Sebastes* spp.) are demersal long-lived, slow-growing, ovoviviparous fish that display sporadic recruitment patterns, with strong cohorts that can sustain commercial fisheries for extended periods, followed by weaker cohorts (Senay et al., 2023). In the Gulf of St. Lawrence (GSL), two morphologically similar species cooccur: Acadian redfish (*Sebastes fasciatus*) and deepwater redfish (*S. mentella*). Distinctively, *S. fasciatus* is usually found in shallower waters (300 ≤ m) than *S. mentella* (350 to 500 m), with an overlap of their distribution (Senay et al., 2023). Since the late 2010s, redfish biomass has increased substantially in the GSL (Senay et al., 2023). However, this resurgence occurs in a rapidly changing environment, where redfish are exposed to multiple biotic and abiotic stressors, including rising temperatures (Guitard et al., 2025), a decline in key prey species (DFO, 2025a), and low-oxygen conditions in deep water (> 200 m), particularly at the head of deep-water channels (Blais et al., 2025). In recent years, scientific surveys report high catch rates of both species in areas with bottom DO ranging from ~25% to 60% sat., especially between 30% and 50% (Blais et al., 2025; Senay et al., 2023), suggesting that redfish regularly use low oxygen environments. In this context, redfish represent a particularly relevant study group.

To better understand how demersal fish can respond to declining oxygen levels, we conducted controlled laboratory exposures using *Sebastes fasciatus* as a model for redfish (*S. fasciatus* and *S. mentella*) in the GSL. Although *S. mentella* currently dominates the biomass in the region, it inhabits deeper waters that could not be accessed for live capture with our

collection method. On the contrary, it was possible to bring back live and healthy *S. fasciatus*, and given the close morphological and physiological similarities between the two species (Benestan et al., 2021; Brûlé et al., 2024; Gascon, 2003; Senay et al., 2022; Senay et al., 2023), the results are expected to provide relevant insights for *S. mentella* as well.

We evaluated the effects of reduced DO on key performance traits, including food intake, food conversion efficiency (FCE, the increase in mass relative to the quantity of food eaten; Craig et al., 2002), growth rates and change in condition factor, as well as metabolic traits (MMR, SMR, AS and O_2crit). Given that MMR typically declines under hypoxic conditions, we anticipated a corresponding reduction in AS, which could constrain the capacity to support aerobic processes such as digestion and growth, and, together with regulatory responses to low oxygen, contribute to reductions in food intake and FCE. We also hypothesized that the condition factor would deteriorate as oxygen levels decline, reflecting cumulative impacts on energy intake and somatic investment. By characterizing these physiological responses, we aim to determine whether hypoxia could directly constrain individual performance. These findings provide insight into the potential vulnerability of redfish to future oxygen declines and contribute to broader efforts to forecast species persistence and inform resource management under changing ocean conditions.

2.5 METHODS

2.5.1 Fish collection and housing

S. fasciatus were successfully brought live to our wet laboratory research facility using the methodology developed by Laroque (2000) and detailed in Guitard et al. (2025). Briefly, redfish were collected near Les Escoumins, Québec, Canada (48.317801°N, 69.413287°W) throughout September and October 2019 and 2021. SCUBA divers caught *S. fasciatus* with dip nets at a depth of 25–30 m and placed them in cages (33 × 34 × 23 cm), which could hold up to 30 individuals. Once full, cages were placed on the bottom higher along the slope, at a depth of 10–15 m depending on the tide, to reduce barotrauma. The duration of this

equilibration period was at least 12 h, but up to 96 h for fish caught early during each of the 5-day diving trips. The day after the last capture, the cages were brought to the surface for transportation in aerated tanks to the Maurice Lamontagne Institute in Mont-Joli, Québec, Canada. Diving trips yielded 822 *S. fasciatus* in 2019 and 192 in 2021, most of which measured between 16 and 20 cm at the time of capture.

Upon arrival, the fish were transferred to circular water tanks (1 m × 1.1 m, height × diameter; 760 L) supplied with 5 °C oxygen saturated seawater (salinity of 28 ppt). They were offered food (northern shrimp, Pandalus borealis, capelin, Mallotus villosus and krill, Euphausia superba) three times a week. It took about two weeks for *S. fasciatus* to acclimate to their new environment and feed correctly. When redfish were not used for experiments, they were maintained under optimal holding conditions (5 °C, salinity 28 ppt, 100% dissolved oxygen). Wild fish may present various levels of parasite load, which are known to influence performance traits (Chrétien et al., 2022; Guitard et al., 2022). Hence, a week after they started eating, fish received formaldehyde treatment (37% formaldehyde, 0.01 mL L-1) for 1 hour to remove possible external parasites. Inspection of the gills, muscle, and heart when some of the fish were euthanized for tissue collection (n = 32) confirmed the absence of internal parasites.

Within three months after capture, the fish were anesthetized (benzocaine, 0.5 ml solution per L of seawater; solution = 100 g of benzocaine dissolved in 1 L of 70 % ethanol), weighed (±0.01 g), measured for fork length (±1 mm) and identified with a PIT tag (Biomark, Idaho, USA) to allow determination of individual growth rates. Furthermore, genetic samples were taken by rubbing a sterile swab for approximately five seconds in their mouth. Each swab was individually placed in a 1.5 mL Eppendorf tube and frozen at -20 °C until species identification was carried out using qPCR, as described in Brûlé et al., (2024). This method assigns individuals to *S. fasciatus* or *S. mentella* with an error rate of 4%. Of all individuals included in the experiments, 99.5 % were identified as *S. fasciatus*, and the remaining 0.5 % classified as *S. mentella*. Given the habitat (depth and location) in which the fish were captured and our understanding of species distribution from bottom trawl surveys (Senay et

al., 2023), we assumed that the individuals that were identified as *S. mentella* were, in fact, *S. fasciatus* that were part of the error rate of the method.

Approximately 75 % of the fish used in this study were also used in the experiment 2021 described in Guitard et al., (2025). Briefly, these fish were exposed to four temperatures (2.5, 5.0, 7.5, and 10.0 °C) as well as two pH levels (7.35 and 7.75) for at least 99 days. No mortality associated with treatment from that experiment was observed (Guitard et al., 2025). A subset of these individuals (n=29) also underwent respirometry trials as part of the same study. Before the new experiment, all fish were maintained for at least 12 weeks at non-stressful, at 5 °C, a temperature shown to be optimal in Guitard et al. (2025) without disturbance, to ensure full recovery from previous treatments. All individuals used in the previous experiment were randomly distributed in new treatments.

Fish collection in their natural habitat was carried out under a Canada Parks permit (SAGMP-2019-33741) and was approved by the Animal Care Committees of the Maurice Lamontagne Institute (Certificate 19-7 and 21-3B). The experimental methods comply with the regulations of the Canadian Council on Animal Care and were approved by the Animal Care Committee of the Maurice Lamontagne Institute (Certificate 19-6C).

2.5.2 Experimental setup

The experimental set-up was composed of 16 circular water tanks (1 m in diameter; 760 L) arranged into four lines of four tanks, each line connected to a header tank as a semi-recirculating system, with flow rates ranging between 12.5-15 L min-1 of new seawater being added to the header tank (replenish time rate range from approximately 3 hours 33 minutes to 5 hours 20 minutes). This experimental set-up did not allow the interaction between DO and temperature with good resolution for both variables, so a single temperature was chosen for all DO treatments. Because redfish, including *S. fasciatus*, are typically captured around 2 to 7 °C in the wild (Atkinson, 1984; Senay et al., 2023), and that 5 °C has been shown to be the optimal temperature for growth in the laboratory (Guitard et al., 2025), all tanks were maintained at 5 °C. The water temperature was controlled in the header tanks using a custom-

built control unit (Gell'Air, Mont-Joli, Canada) with a precision of 0.6 °C in the header tank, but close to 0.1 °C in each of the four tanks within each line.

We selected eight DO levels, ranging from 100% to 25% sat., to reflect both the broad range of oxygen conditions currently occupied by redfish, from well-oxygenated to hypoxic habitats, and to simulate future deoxygenation scenarios. DO treatments were randomly distributed throughout the 16 tanks, with the constraint that the same treatment did not appear twice in the same line or in two adjacent tanks between lines. DO was controlled by a custom-built controller that monitored 16 optical oxygen sensors (model ODOS 5001, IKS, Karlsbad, Germany) and adjusted the proportion of air and nitrogen that was injected into the gas exchange column which served as water intake for each tank.

Temperature (°C), salinity (Profline Cond3110, WTW, Weilheim, Germany), and DO sat. (Firesting® GO2, Pyroscience, Aachen, Germany) were manually measured five times per week from Monday to Friday (Table S1). The DO target for each tank was adjusted to account for any drift of the IKS oxygen probes. In addition, DO of each tank was verified weekly with a modification of the Winkler (1888) method described by Jones et al. (1992). The correlation between GO2 probe readings and Winkler titrations was 0.997. The treatment values used in the models were based on the GO2 readings (Table S1), but in the text the target values (100% down to 25% are generally used).

2.5.3 Food intake and growth experiment

Before the beginning of the experiment, the fish were fasted for 67 h and on March 15 2022, they were anesthetized, weighed, and measured. Those measuring between 168 and 240 mm were assigned to a tank in a sequential pattern: individuals were placed in tank order from 1 to 16, then from 16 to 1, and so on, until each tank contained 34 fish, for a total of 544 *S. fasciatus*. The fish were acclimated to the experimental tanks for a week under the same rearing conditions (5 °C and 100% sat.). The oxygen levels then gradually decreased over 7 days to reach the experimental treatments on March 28. Growth was assumed to be negligible between March 15 and 28, day 0 for the calculation of growth rates. The final mass

and length were obtained at the end of the experiment on 11 July 2022 (day 105), after 72 hours of fasting.

The tanks were inspected every day from Monday to Friday to monitor mortality. The fish were fed to satiation three times a week on Monday, Wednesday and Friday with capelin, northern shrimp, and krill. The three prey were given in random order each week. Capelin and shrimp were cut into pieces of approximately 2-3 cm to make them easier to swallow. The food intake of each tank was measured for each feeding day. Food was offered every 5-6 minutes for a minimum of one hour, to ensure that all fish were fed ad libitum. Portions were weighed before feeding began and food leftover at the bottom of the tank was collected, drained, and added to the food that was not offered. The total uneaten food was measured and used to calculate the amount eaten.

2.5.4 Respirometry trials

Respirometry trials happened between July 11th and August 22nd, 2022. Treatment tanks were kept at the same temperature and DO level as during the growth experiment. The tanks were randomly assigned to a given respirometry trial and a water bath. DO during respirometry was the same as during the growth experiment and was maintained using an Aquastar controller (IKS, Karlsbad, Germany) connected to two oxygen sensors (model ODOS 5001, IKS, Karlsbad, Germany), one for each system. The controller adjusted the proportion of air and nitrogen that was injected into the gas exchange column of each respirometry tank (Table S2).

Two identical open-flow experimental water baths (200 cm in length × 60 cm in width × 28 cm in height, 336 L) were used for the respirometry trials. Each water bath was provided with a temperature probe (hermetically sealed RTD probe, Omega Engineering inc., Norwalk, CT, United States), a controller (1/16 DIN Micromega autotune PID Temperature, Omega Engineering inc.) and a mixing valve (sv3109, Omega Engineering inc.) to allow mixing of the appropriate proportion of cold and warm water (total flow rates between 3.5

and 4.5 L min-1) to provide each bath with seawater at the rearing temperature of 5.0 °C (Table S2).

Each water bath contained four resting respirometry glass chambers, two of 5.214 L (33 cm length × 15 cm diameter) and two of 7.016 L (49 cm length × 13.5 cm diameter). The chambers were transparent but separated with an opaque panel so that the fish could not see each other. Each chamber was connected to a closed water circuit to achieve adequate water mixing and measure DO. This circuit was made of Tygon tubing, a recirculation pump (model 1046, Eheim, Stuttgart, Germany) and housings for a fiber-optic oxygen probe (PyroScience Robust Oxygen) and a temperature sensor (PyroScience P100) for the first system, but only one housing for the fiber-optic oxygen probe in the second system. The volume of the recirculation loop was 48.5 mL for the 5 L chambers and 60 mL for the 7 L chambers. The oxygen and temperature probes were connected to a PyroScience FireSting-O2 4-channel oxygen meter combined with a PyroScience TEX4 (PyroScience GmbH, Aschen, Germany) for the first system, but there was a single temperature probe, placed outside the chambers, for the second system. Dissolved oxygen levels were measured every ~2 seconds. The four chambers were also connected to a single flush pump (1250, Eheim, Stuttgart, Germany) controlled by the Aquaresp software (V3, Denmark, Aquaresp.com).

The size of the respirometer was selected to respect a chamber to fish volume ratio between 20 and 50 (Svendsen et al., 2016) and this ratio for our experiment ranged from 27 to 52 (36 ± 4, mean and standard deviation). Oxygen uptake was measured for four fish per experimental tank or eight per treatment, for a total of 64 fish. The respirometry set-up was cleaned between each trial (every five days) with fresh water and chlorine, rinsed thoroughly with fresh water, and left to run overnight with seawater. Oxygen probes were calibrated with 100% and 0% sat. solutions before each experiment (Table S3). Eight trials were required to cover all eight treatments in duplicate. These were carried out between July 14 and August 22, 2022.

Wet mass-specific oxygen uptake ($\dot{M}O_2$, in mg O_2 h-1 kg-1) was measured in each respirometer by intermittent-flow respirometry (Steffensen, 1989; Svendsen et al., 2016)

using 11.5-minute cycles consisting of a 4-minute period of flush to renew the water in the respirometers followed by a 7.5 minute closed period to determine oxygen consumption using the slope of the decreasing dissolved oxygen in the respirometer during the last 6 minutes of the closed phase, when it had become linear.

Before all respirometry experiments, the fish fasted between 92 and 142 hours to ensure that they were in a post-absorptive state (Chabot et al., 2016; Clark et al., 2013). Each trial lasted five days, including preparation and execution. On day one, the set-up was cleaned, probes were calibrated, fish were selected and weighed, and then isolated for the night in a basket floating in the experimental tank. On day two, the background oxygen consumption rates ($\dot{M}O_2$ _b) were estimated in each empty chamber for a minimum of 40 minutes before and after (day five) each respirometry trial. Before introduction into the respirometer, each fish was chased to exhaustion and then exposed to air for one minute, a common method for estimating MMR in fishes (Roche et al., 2013; Rummer et al., 2016). For this, the selected fish was caught using a dip net, placed in a circular chase area (65 cm × 15 cm, height × diameter, 50 L, depth adjusted as a function of fish height [doubling the height of the fish in water]) and chased by hand until it no longer reacted to contact and tail pinching (chase duration lasted between 1 and 5.77 minutes). The fish was then removed from the arena and kept out of the water for 1 minute. Subsequently, the fish was placed in a respirometry chamber, which was immediately sealed (within less than 15 s) with no flush allowed, to ensure that the maximum rate of decline did not occur during a flush period. Once all four fish had been chased and the rate of DO decline had obviously slowed down for all four fish, control of the system was switched to regular cycles controlled by Aquaresp running the 11.5-minute loops as described above, for the next ~70 hours (days 3 to 5), with the fish left undisturbed, in the dark (except for a daily check-up with a red light), behind opaque curtains. Over this period, the oxygen uptake of fish stabilized, and the SMR could be estimated. Oxygen levels remained within 5 % sat. of the ongoing treatment in the chambers during all cycles of SMR estimation for all trials.

After ~60 hours (day 5), oxygen uptake under decreasing DO was quantified to estimate O_2crit. DO was progressively decreased by injecting nitrogen into the gas exchange column of the respirometry bath. To minimize the total duration of the trial, DO was lowered at a faster rate, approximately 5% sat. per respirometry cycle, when DO was above 30% sat. Below this level, DO was lowered more slowly (2–3 % between cycles) to increase the resolution of O_2crit estimates. Aquaresp, paired with an R script, calculated $\dot{M}O_2$ and estimated SMR in real time and the experiment lasted until the animal could not sustain SMR estimated during the previous days (Claireaux and Chabot, 2016). We visually checked on the animals to make sure they were not in distress or lost equilibrium during this part of the experiment. Hypoxia tolerance trials lasted between 2 and 6 hours. This protocol followed best practices for collecting and reporting respirometry data as described in Killen et al. (2021; see Annexe 2).

2.5.5 Data extraction and analysis

2.5.5.1 Food intake and growth rates

Food intake was analysed as follows from March 28th to July 11th:

(1) Food ingested per fish = (Fp − Fng − Fc) / N

where *Food intake per fish per meal* is the estimated amount of food in grams eaten by one individual of a given tank for one meal (capelin, shrimp or krill), Fp is the amount of food prepared for that tank for that meal, Fng is the amount of food not given, Fc is the amount of food collected at the bottom of the tank at the end of the meal, and N is the number of fish in the tank during that meal.

Weekly food intake per fish was calculated as the sum of the food intake per fish per meal for all meals of the same week. This was considered more useful and less variable because *S. fasciatus* consistently ate more capelin and less shrimp and krill.

Individual growth rates were calculated for all fish present at the end of the experiment (July 11th). Specific growth rate (Jobling, 1983) in mass (SGR_m) and length (SGR_l) was calculated for each individual from March 28th to July 11th.

(2) SGR = log M2 − log M1 / T × 100

where M2 is the mass in grams or length in millimetres at the end of the experiment (July 11th), M1 the mass or length at the beginning of the experiment (March 28th), and T the duration of the experiment (105 days).

Fulton's condition factor (K) was calculated for each individual as a proxy for body condition:

(3) K = (M / L^3) × 100

where *M* is the wet body mass (g) and L the fork length (mm) of the fish. The difference between final and initial condition factors (ΔK) was used as a measure of change in body condition over the course of the experiment.

2.5.5.2 Food conversion efficiency

FCE was calculated as the average mass gain per fish within each tank (individual final mass minus initial mass), divided by the total amount of food consumed per fish in that tank over the same period (Craig et al., 2002).

2.5.5.3 Respirometry data

Wet mass-specific oxygen uptake ($\dot{M}O_2$; mg O_2 h^{-1} kg^{-1}) was calculated from the slopes of the linear regressions between oxygen concentration and time, accounting for the volume of water in the respirometer (respirometer gross volume minus fish mass as an estimate of fish volume, assuming a density of 1g ml^{-1}) for the 64 individuals tested.

To reduce the risk of underestimating MMR, rolling regressions were used to detect the steepest part of the DO decline in the respirometer during the long closed phase that

started when the fish was placed into the respirometer (Zhang et al., 2019). Contrary to sequential regressions, when one interval begins after the end of the previous interval, in rolling regressions each interval begins one point after the beginning of the previous interval. Using the methodology outlined by Zhang et al., (2019) and modified by Guscelli et al., (2023), Guitard et al., (2025) have shown that the shortest reliable interval or window width (WW) over which these rolling regressions should be calculated to estimate MMR was three minutes for *S. fasciatus* in these respirometers.

SMR was estimated with the calcSMR function of the *fishMO2* package (Chabot, 2020), using the quantile (p = 0.2) of the $\dot{M}O_2$ values obtained after an acclimatization period of 16 hours and before the start of the decline in DO used to measure O_2crit (Chabot et al., 2016). Increases in $\dot{M}O_2$ that suggest increased spontaneous activity at night were observed (Guitard et al., 2025). Therefore, we estimated SMR for each individual with and without including data collected at night and retained the lowest estimation of SMR out of these two rates. The background respiration rate (B_ $\dot{M}O_2$) was subtracted from the $\dot{M}O_2$ measurements assuming a linear increase in bacterial respiration from the start to the end of the trial.

Absolute AS was calculated as the difference between MMR and SMR (Fry, 1948; Fry, 1971). O_2crit was identified as the intersection of the regression line obtained when oxygen uptake decreased with DO and the horizontal line corresponding to SMR, as calculated by the calcO_2crit function of the *fishMO2* package (Claireaux and Chabot, 2016).

2.5.5.4 Statistical analysis

To test the effect of DO (average DO from manual GO2 probe during the growth experiment; Tableau 15) on performance traits such as food intake, FCE, growth in mass, growth in length, and ΔK, we used a generalized additive mixed model (GAMM) framework with the mgcv package (Wood, 2017). Non-linear relationships were modeled using smooth terms and random effects were included to account for grouping structure in the data. Method REML (restricted maximum likelihood) was used for all models (Tableau 18).

The full model for weekly food intake included mean DO measured during the growth experiment (Table S1) as a smooth term, in addition to experimental tank as a random factor (Tableau 18; Model Food1).

The full model for FCE, a single measurement per tank, included only mean DO measured during the whole growth experiment as a smooth term (Tables 18; Model FCE1).

The full model for growth in mass and in length, and ΔK, included a smooth term for the mean DO measured during the growth experiment, initial length as a smooth term, and tank as a random effect (Table 18; Models Growth mass and length1, Model Condition 1).

For physiological traits that did not have a linear response to DO (food intake, FCE, growth in length and mass, ΔK), we compared predicted values and their 95% confidence intervals (CI) across the oxygen gradient to estimate the oxygen threshold below which performance became significantly lower than under moderate to high DO conditions. Specifically, we identified the highest oxygen level at which the upper bound of the 95% CI fell below the lowest point of the confidence band for the reference range (90–55% sat.), which we selected because DO had no or little influence on any of the traits within this interval and the confidence band was relatively stable. Below this threshold value, the dependent variable was significantly lower than within the reference range.

A segmented regression analysis was also performed between the same physiological traits and DO to identify the breakpoint, the DO at which the relationship between the variables changed, (segmented package in R, Muggeo, 2003). The optimal number of breakpoints was first evaluated using the selgmented function based on Akaike Information Criterion (AIC) and Davies' test for slope change. For all responses a single breakpoint was found, and the final segmented model was fitted with the segmented function, using DO as the segmented covariate. The breakpoint value and its standard error were extracted from the model output and used to characterize the physiological threshold.

Linear mixed-effects models (lmer function in the lme4 package; Bates et al., (2015); Table S6) were used to analyze four metabolic traits (MMR, SMR, AS, O_2crit), with DO

measured during each respirometry trial (Tableau 16) as a continuous predictor. Experimental (growth) tank (this effect is undistinguishable from respirometry trial, since all fish from an experimental tank were tested during the same trial in the same respirometry tank) and respirometry chamber were included as random effects to account for non-independence among individuals tested in the same setup. Models were fitted using REML and assessed using Satterthwaite's approximation for degrees of freedom via the lmerTest package (Kuznetsova et al., 2017). Preliminary analysis showed that body mass had no effect on any of the metabolic rates, likely due to the small range of masses used in this study; therefore, body mass was excluded from the full models. For all metabolic traits (MMR, SMR, AS, and O_2crit), the figures show the x-axis as decreasing DO levels from 100% sat. to 25%, illustrating declining metabolic rates with decreasing DO levels, but model outputs have positive slopes, representing increasing metabolic rates with increasing DO levels.

All models and their AIC are shown in Tableau 18 and 19, with a description of all terms in Table S4. For linear models and GAMM, combinations of terms were tested by fitting reduced models, removing one predictor at a time to evaluate their contribution. Terms were only removed if they were both non-significant and non-essential, while biologically relevant terms such as DO was always retained. Competing models were compared using AIC to identify the best-fitting structure for each response (Tableau 18-19). Model assumptions were visually assessed using residual diagnostics and DHARMa package (Hartig, 2022) diagnostic plots and were met for all models. All data were analyzed using R v. 4.2.0 (R Foundation for Statistical Computing, 2022).

2.6 RESULTS

2.6.1 Survival rate

Only one individual from the control (100 % DO) treatment had to be euthanized during the growth experiment due to exophthalmia, a problem often observed in *S. fasciatus* kept in captivity. DO levels down to 25% sat. had no effect on survival rate.

2.6.2 Food consumption and growth

2.6.2.1 Food intake

Fifteen values of weekly food consumption per fish were available for each experimental tank. Food intake declined slowly within the reference range of DO (90–55% sat.), but more rapidly below 45% sat. (Fig. 1A) with 40.6% of the deviance explained by the final model (Tableau 18). Both DO and the random variable (tank) were significant (Fig. 18A; Tableau 13). Comparison of confidence bands indicates a significantly reduced food intake at DO values below 31% sat., comparatively to the reference range. Breakpoint analysis identified a change in the relationship between DO and food intake at approximately 37.9 ± 2.6% sat. (estimated breakpoint ± standard error), indicating a shift in the response pattern above and below this level (Fig. 22).

2.6.2.2 Food conversion efficiency

A single value of FCE was available for each tank. FCE was stable within the reference range (90-55% sat) but declined rapidly below about 45% sat., with 78.7% of the deviance explained by the final model (Tableau 13; Tableau 18). The upper bound of the 95% confidence interval dropped below the lower bound of the reference range at approximately 34% sat. (Fig. 18B). Breakpoint analysis identified a change in the relationship between DO and FCE at approximately 36.2 ± 1.8% sat, (Tableau 14; Fig. 23).

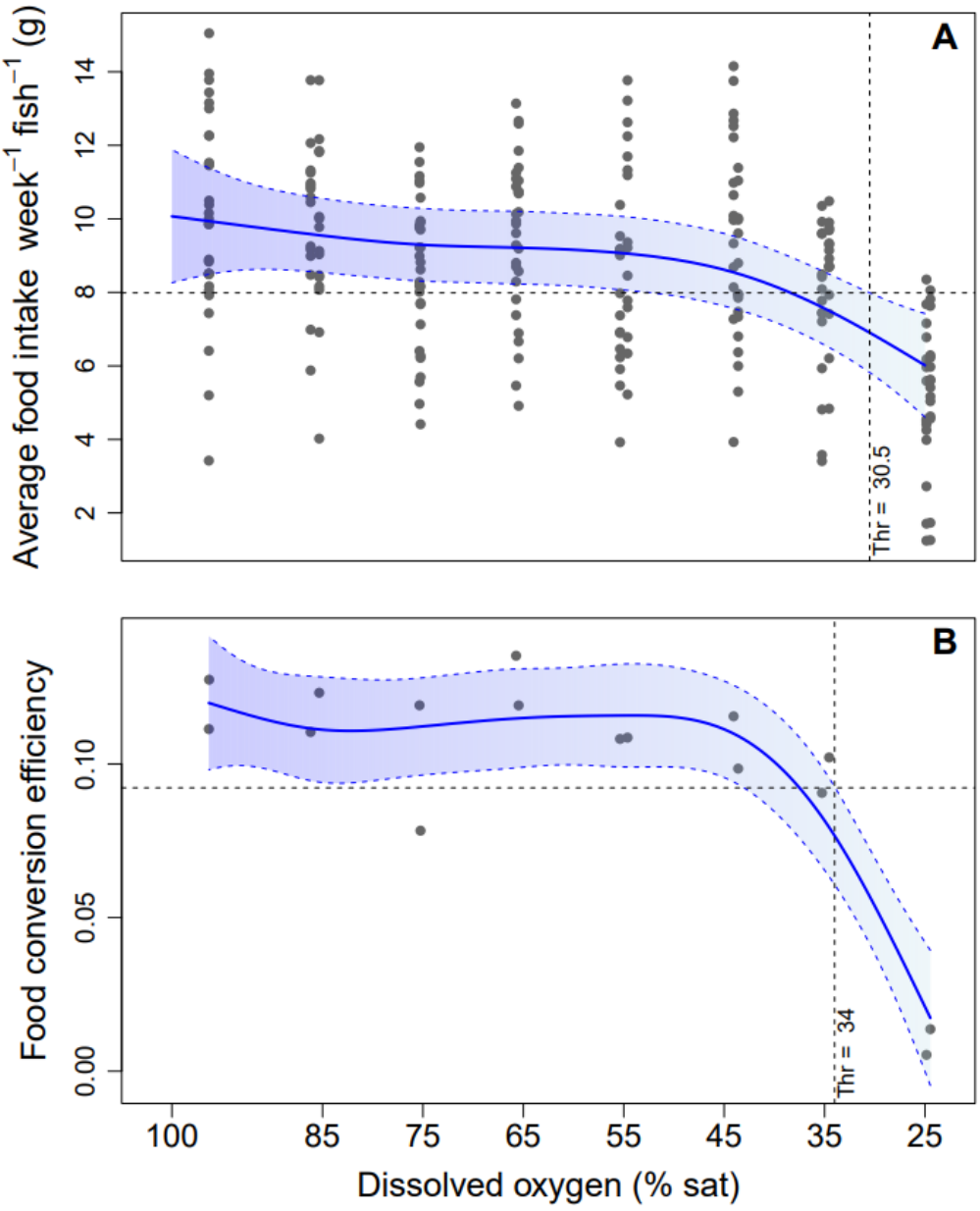

Figure 18. Effect of dissolved oxygen on food intake and food conversion efficiency (FCE) in redfish (*Sebastes fasciatus*) reared at dissolved oxygen levels between 100 and 25% saturation. (A) Food intake per week per fish (g) in each experimental tank, N = 240; and (B) food conversion efficiency. N = 16. The vertical dashed line labeled "Thr" marks the oxygen threshold where the upper 95% confidence interval falls below the lowest part of the band within the reference range (90-55% sat.), indicating a significant decline in performance under hypoxia.

Tableau 13. Relationship between food intake, food conversion efficiency (FCE), growth rates in mass and length and condition factor with dissolved oxygen for redfish (*Sebastes fasciatus*). Test statistics obtained from generalized additive model (GAMM) with initial length as a fixed effect and holding tank as a random factor for food intake, growth rates in mass and length, FCE and condition factor. Statistically significant results are indicated in bold. edf: estimated degrees of freedom, F-value: F-statistic for the smooth term, p-value: statistical significance threshold. Statistically significant results are indicated in bold.

Response	Predictors	edf	p-value	Deviance explained (%)
Food intake				40.6
(g week $^{-1}$ fish^{-1})	Dissolved oxygen	2.573	**<0.001**	
	Tank	9.925	**<0.0001**	
FCE				78.7
	Dissolved oxygen	3.438	**0.001**	
Growth rate in mass				22.4
(% mass day $^{-1}$)	Dissolved oxygen	3.425	**<0.0001**	
	Initial length	1.592	**<0.0001**	
	Tank	6.838	**0.003**	
Growth rate in length				16.8
(% length day $^{-1}$)	Dissolved oxygen	2.345	**0.01**	
	Initial length	2.539	**<0.0001**	
	Tank	8.415	**<0.0001**	
ΔK				15.1
	Dissolved oxygen	3.903	**<0.0001**	
	Initial length	1.002	**0.003**	
	Tank	3.075	0.143	

Tableau 14. Dissolved oxygen (DO) thresholds and breakpoints for physiological traits of redfish (*Sebastes fasciatus*). Thresholds represent the DO saturation (%) below which the upper bound of the 95% confidence interval (CI) of predicted values fell below the lowest part of the confidence band for the reference range (90–55% DO saturation), or the DO value below which performance was significantly reduced relative to moderate to high oxygen conditions. Break points, estimated from segmented regressions, indicate the DO value below which performance decreased faster with decreasing DO.

Physiological traits	Threshold	Breakpoint
Food intake	30.5	37.9 ± 2.6
FCE	34.0	36.2 ± 1.8
Growth rates in mass	33.5	37.2 ± 2.1
Growth rates in length	29.0	44.1 ± 4.2
ΔK	33.0	28.2 ± 8.6

2.6.2.3 Specific growth rates in mass and length

Growth rates in mass and length were significantly affected by DO, with 22.2% and 15.6% of the deviance explained by the final model, respectively (Tableau 13). Initial body length, and the random effect of tank were both significant (Tableau 13) and growth rates in both mass and length decreased with increasing initial length (slopes of -0.0009 ± 0.0002 and -0.0002 ± 0.00004 for SGR_m and SGR_l, respectively, $p < 0.0001$ in both cases). For both mass and length, estimated growth rates were fairly stable above 45% sat., but declined with decreasing oxygen saturation at lower DO. Comparison of confidence bands show that growth was significantly reduced, compared with the rates observed within the reference DO range, below 33.5% (mass) and 29% sat. (length) (Fig. 19A–B). Breakpoint analysis identified a change in the relationship between DO and growth rates, with a steeper decrease in growth with DO at 37.2% sat. ± 2.1 for mass and 44.1% sat ± 4.2 for length (Tableau 14; Fig. 24-25).

2.6.2.4 Change in condition

Change in condition factor was significantly affected by DO, with 13.1% of the deviance explained by the final model (Tableau 13; Tableau 18). Initial body length was also

significant, whereas the random effect of tank was not (Tableau 13). The relationship showed a slight decrease in ΔK with increasing initial length (slope of -0.000005 ± 0.0000018, p = 0.003). Change in fish condition during the experiment was similar within the range of 100 to about 45% sat. and was very small, with the confidence band often including zero. However, a significant lost of condition was observed below 33% sat. according to the comparison of confidence bands (Fig. 19C). Breakpoint analysis identified a change in the relationship between DO and the change in condition factor at approximately 28.2 ± 8.6 % (% ± se) (Tableau 14; Fig. 26).

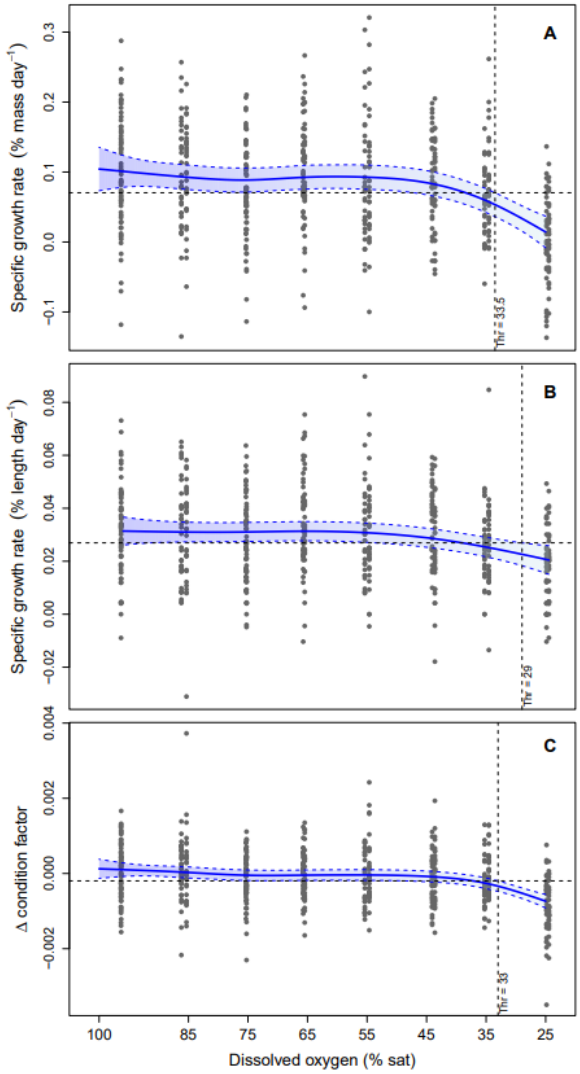

Figure 19. Effect of dissolved oxygen on growth in mass and length, and condition factor in redfish (*Sebastes fasciatus*) reared at dissolved oxygen levels between 100 and 25% saturation. (A) Specific growth rate in mass (% mass day^{-1}); (B) specific growth rate in length (% length day^{-1}); and (C) difference in condition factor (final K – initial K), all N = 541. The vertical dashed line labeled "Thr" marks the oxygen threshold below which the upper 95% confidence interval falls below the lowest part of the band within the reference range (90-55% sat.), indicating a significant decline in performance under hypoxia.

2.6.3 Aerobic metabolism

Seven fish were excluded from the models of metabolic rates due to issues during the respirometry trials (Fig. 20). One fish escaped the chamber during the first night and, despite

being reintroduced the next morning, did not reach SMR afterwards. Three were rejected because their oxygen uptake was still declining at the end of the SMR measurement period. Additionally, two fish repeatedly blocked the recirculation loop with their snout, causing stress and poor water mixing, thus resulting in non-linear oxygen declines.

Random effects (tank and respirometer) tested in the full models were consistently non-significant for MMR, SMR, AS, and O_2crit, and comparison of AIC values between models with and without random effects supported the use of simpler models (Tableau 19). As a result, final models for all metabolic traits were fitted as linear models, without random effects (Tableau 19).

Mean mass of individuals before respirometry trials was 178.5 g (SD = 36.3). Chase duration was not related to MMR ($p = 0.409$). MMR ranged from 69.9 to 221.5 mg O_2 h^{-1} kg^{-1} and decreased significantly with DO (slope = 1.25 ± 0.11, Fig. 20A). SMR ranged from 21.1 to 39.7 mg O_2 h^{-1} kg^{-1} and also declined with DO, although the relationship was weaker (slope = 0.06 ± 0.02, Fig. 20B). Despite this small lowering of SMR at low DO, AS declined significantly with decreasing oxygen availability (slope = 1.19 ± 0.11, Fig. 20C).

2.6.3.1 Hypoxia tolerance

O_2crit values declined significantly with decreasing DO (slope = 0.05 ± 0.01, Fig. 20D), indicating that hypoxia tolerance increased under low-oxygen treatments. O_2crit values ranged from 9% to 20% air sat. On average, individuals exposed to 100% and 25% DO sat. lost the ability to maintain SMR at ~15% and ~11% sat. respectively, a difference of 4% sat. across the exposition gradient.

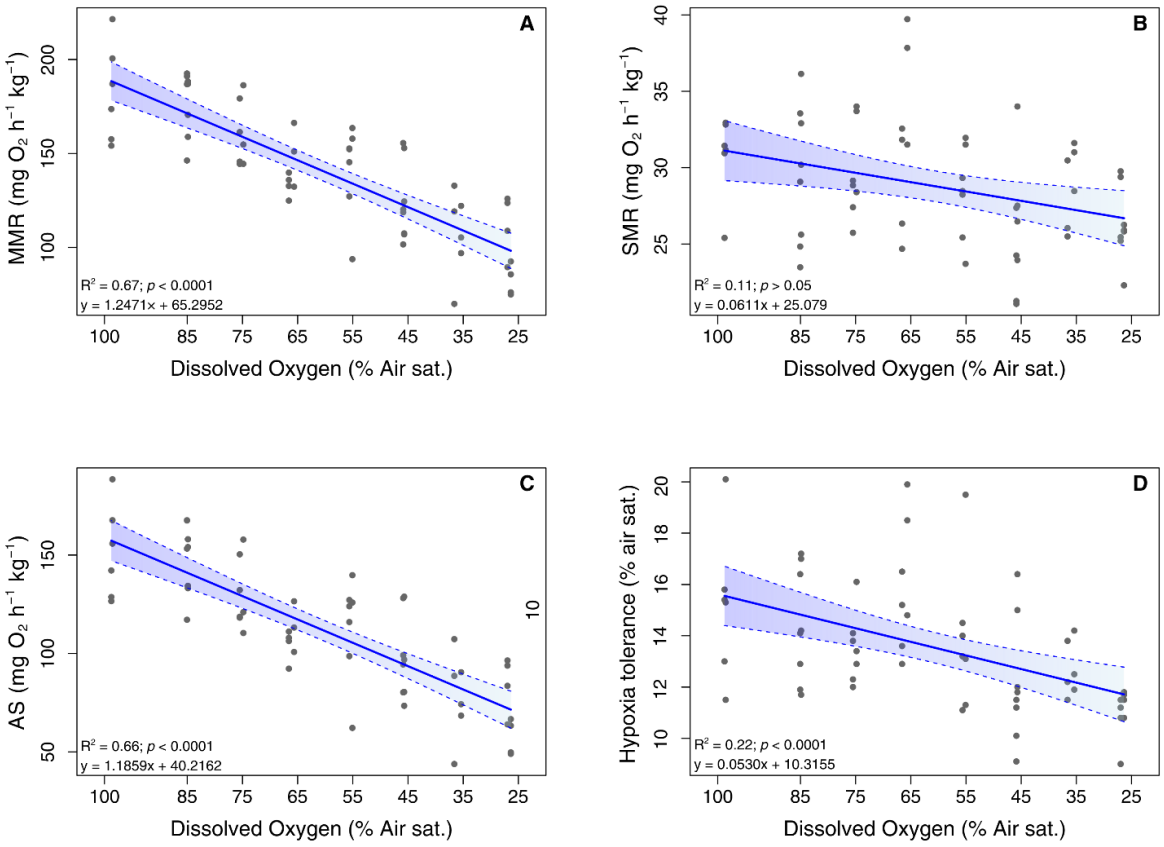

Figure 20. Effect of dissolved oxygen on metabolic traits. Metabolic traits of redfish (*Sebastes fasciatus*) reared at dissolved oxygen between 100 to 25 % DO saturation. Maximal metabolic rate (MMR, mg O_2 h^{-1} kg^{-1}) (A); standard metabolic rate (SMR, mg O_2 h^{-1} kg^{-1}) (B); aerobic scope (AS, mg O_2 h^{-1} kg^{-1}) (C); hypoxia tolerance (O_2crit, % sat.) (D). N = 57 for all panels. The shaded areas around each regression line represents the 95% confidence interval. The DO axis is inverted (high to low) to emphasize the ecological context of deoxygenation; therefore, although slopes are reported as positive in the statistical output, they represent declines in performance with decreasing DO.

2.7 DISCUSSION

The present study integrates measures of energy acquisition, such as food intake and FCE, growth rate, change in condition, and metabolic demands during a prolonged exposure to eight oxygen levels representative of current and future DO conditions in the habitat of *S. fasciatus*. Our results offer a comprehensive view of how oxygen limitation affects multiple components of the energy budget and growth rates of *S. fasciatus*. Declining oxygen reduced

aerobic metabolic capacity even above the 30% sat. threshold often used as a definition of hypoxia in the literature (Galic et al., 2019; Rabalais et al., 2010; Thomas and Bacher, 2018; Wu, 2002). Furthermore, growth rates were significantly lower around and below this threshold. The decline in growth rates, under severe reduced oxygen levels (< 30%) and at a constant temperature, was primarily driven by a combined reduction in aerobic scope and lower food intake accompanied by a reduction in FCE. Given that redfish frequently occupy habitats where DO levels approach their performance limits (Guitard et al., 2025; Senay et al., 2023), our results suggest potential trade-offs between habitat availability and physiological performance, with consequences for growth, energy balance, and potentially long-term fitness.

2.7.1 Metabolic demands and capacity

In the present study, MMR decreased more rapidly than SMR and this over the entire range of DO treatments, which considerably reduced AS at the lowest treatment. Lowered MMR and consequently reduced AS have been reported in many fish species when facing low DO treatments (Cornett et al., 2024; Mattiasen et al., 2020; Nuic et al., 2024). As DO becomes limiting, the drop in environmental PO_2 makes oxygen extraction progressively more difficult. This can trigger compensatory mechanisms aimed at either enhancing oxygen uptake or reducing energy expenditure to safeguard essential metabolic functions (Perry and Wood, 1989; Randall, 1982; Wu, 2002). Ultimately, the capacity of the gills and cardiovascular system to extract and deliver oxygen to tissues cannot be maintained as DO declines, causing MMR and consequently AS to decline (Claireaux and Chabot, 2016; Fry, 1971; Wang et al., 2009).

The limiting oxygen level curve model (Claireaux and Chabot, 2016; Claireaux and Lagardère, 1999; Wang et al., 2009) depicts a smaller decline in MMR when DO remains close to normoxia, an a progressively steeper decline as hypoxia worsens (Evans, 2007; Zhang et al., 2021). However, our results showed a strictly linear decline, similar to that of Atlantic cod (Dutil et al., 2007). In our study, both MMR and, consequently, AS, decreased

immediately after the first hypoxic treatment (85%) relative to the control (100%). As laboratory techniques make it difficult to estimate true MMR (Fu et al., 2022; Killen et al., 2017; Prinzing et al., 2021) and because wild fish rarely use their full AS (Farrell, 2016; Holt and Jørgensen, 2015), the exact shape of this decline at relatively high DO is unlikely to influence non-essential functions such as routine swimming or digestion. The observed linear decline offers new information on how this species and potentially other related species respond to decreasing oxygen availability.

The significant decrease in SMR across the range of DO was unexpected because SMR is usually interpreted as the minimum level of oxygen uptake required for maintenance, maintenance needs should remain constant even when DO levels decline. In fact, reduction in $\dot{M}O_2$ below SMR is often used to define the lethal DO level for an individual fish. (Chabot et al., 2016; Claireaux and Chabot, 2016; Nelson and Chabot, 2024). The decline in SMR observed here in fish acclimated to low DO may reflect a form of metabolic rate suppression (Richards, 2010) in which energy-saving adjustment reduces baseline maintenance cost to reduce the drop in AS that results from chronic hypoxia allowing fish to reallocate resources towards maintaining growth or other non-essential functions despite a reduced AS. However, this decline in SMR observed in low DO treatments could also be a methodological artefact related to SMR estimation. Because individual activity within the respirometer was not measured, the selection of "low values of $\dot{M}O_2$" to estimate SMR was inferred from distribution of $\dot{M}O_2$values and the fact that a comprehensive review of methods to calculate SMR found that the quantile (p= 0.2) typically succeeded in removing $\dot{M}O_2$values elevated dur to stress or activity (Chabot et al., 2016). In some species, such as Atlantic cod (Chabot and Dutil, 1999), spontaneous activity tends to decrease under hypoxia. Examination of plots of $\dot{M}O_2$ over time at constant and decreasing ambient DO in this study suggest that it was also the case in *S. fasciatus*. In other words, the proportion of $\dot{M}O_2$ values that were influenced by activity would be reduced and a p of 0.2 would underestimate SMR in fish studied at low DO treatments. We opted to keep p at 0.2 for comparability with other studies, but it is possible that true SMR was underestimated at low DO values. Although SMR was observed to decrease with DO, the difference was small. SMR ranged from 31.2 (in

normoxia) to 26.6 mg O_2 h-1 kg-1 (at ~ 25% sat.), which is comparable to the mean SMR of *S. fasciatus* reported for the same temperature for normoxia (28.6 mg O_2 h^{-1} kg^{-1}; 95 % CI = 26.3–30.9; Guitard et al., 2025). The modest size of this decrease likely has limited biological significance, although it contributes to the reduction in O_2crit, which is directly influenced by SMR.

The lowest DO treatment in the present study remained above the mean hypoxia tolerance threshold (O_2crit) reported for *S. fasciatus* at 5 °C (17.5%; Guitard et al., 2025). This was confirmed by the absence of mortality in the lowest treatment and with O_2crit values within a 5% range of the ones demonstrated by Guitard et al., (2025). Therefore, it was unlikely that individuals would rely on anaerobic metabolism to meet maintenance energy demands. O_2crit is commonly used to define the lower limit of oxygen availability at which AS reaches zero, a condition that fish should completely avoid. This has been demonstrated for Atlantic cod: mortality rate became significant at about 28% sat., even if average lethal level was 21% sat. (Plante et al., 1998). In the GSL, Atlantic cod typically avoid DO below 30% sat. (D'Amours, 1993). The same is true for *S. fasciatus* in the GSL: they are completely absent from waters with less than 70 µmol kg-1 (about 22% sat., assuming 6 °C and salinity of 34) (Senay et al. 2023, their Figure 43) regardless of temperature, a level slightly greater than the lethal level (12–16% sat.), as expected, keeping in mind that temperatures above 5 °C make *S. fasciatus* more sensitive to hypoxia (Guitard et al. 2025, their Figure 2E).

The oxygen range that limits redfish growth is ecologically relevant because it reflects the combined effects of multiple physiological processes. In this study, the breakpoint analysis show that growth rates were strongly influenced by DO below approximately 37% sat. (growth in mass) and 44% sat. (growth in length) (Figure 2; Table 2). At this DO levels, AS is about 50% of that under normoxic conditions. This is comparable to other species, where AS was halved at approximately 40% sat. (Chabot & Claireaux, 2008, their Figure 2b). This convergence suggests that the level of DO that causes a 50% reduction in AS may be an important threshold for many species of fish that should avoid such conditions. The

degree of avoidance increases with decreasing DO, as long as there are better oxygenated habitats.

Survey data (2020–2024) for *S. fasciatus* indicate that bout 60% of the biomass was found in waters between 22 and 40% sat. More precisely, just over 80% of the biomass in found below 44% sat. which corresponds to the highest threshold at which growth performance was affected for *S. fasciatus* in this study. The situation is worse for *S. mentella*: about 85% of the biomass was found in waters with 40% sat. or less (Senay et al., 2026, their Fig. 83). For both species, 100% of the biomass is found in waters of 65% and 61% for *S. fasciatus* and *S. mentella* respectively. A large proportion of the population occupied habitats that was suboptimal for growth, indicating that low-oxygen environments likely confer certain advantages. These may include increased prey availability or species-specific preference for depths where DO falls below 40% saturation, despite the associated reduction in growth rates.

2.7.2 Growth rates and condition factor

Growth in mass and length, declined under hypoxia. In fish, somatic growth and condition do not always change in the same way. Lengthening reflects structural development, whereas the changing condition reflects energy reserves. For example, a fish may invest energy in increasing length while gaining little mass, resulting in low condition, whereas surplus energy can instead be stored as lipids, improving condition without contributing to structural growth. Consequently, a decline in condition factor does not necessarily indicate a reduced capacity for growth but rather reflects depleted energy reserves. The observed decline in condition factor, with a breakpoint around 28–33% sat., accompanied by a decline in mass gain, suggests that oxygen limitation likely reduced the energy available for both tissue growth and reserve accumulation. As studies on other species show that fish can sometimes adjust to chronic low DO treatments, gradually recovering appetite and growth as an adaptation (Pichavant et al., 2000; Wang et al., 2009). What qualifies as chronic varies widely among studies, making it difficult to know whether such

adaptations apply to *S. fasciatus*. Observed reductions in mass and condition may have important ecological consequences by lowering the energy available for survival and reproduction, highlighting potential trade-offs for *S. fasciatus* occupying hypoxic habitats (< 40% sat.).

Redfish in the GSL already have smaller sizes at age, reflecting reduced growth rates (Coussau et al., 2024), smaller sizes at maturity (Brûlé et al., 2024) and lower body condition (DFO, 2025b) compared to previous cohorts. These changes are mainly attributed to the increase in temperature and the effect of density-dependence (Coussau et al., 2024; Guitard et al., 2025; Senay et al., 2023). The rising temperature levels increase the amount of food redfish need to sustain their obligatory metabolic requirements (Guitard et al., 2025), and the density-dependence observed is reducing the amount of food available for the overall stock of redfish. In addition, many GSL redfish are found in waters hypoxic enough to reduce growth rate, considering a stable temperature of 5 ˚C (60% of the biomass for *S. fasciatus* representing 134.4 kilotons), while simultaneously facing reduced prey availability and warming. These concurrent stressors suggest that redfish are already facing energetic constraints that could further compromise growth, condition, and long-term population productivity.

2.7.3 Food intake and assimilation

In this study, the decrease in growth was driven primarily by reduced food intake, which started around 38% sat. and was significant at 31% sat. Other studies reported that a reduction in food intake is a major contributor to the reduction in growth rates under hypoxia (Abdel-Tawwab et al., 2019; Chabot and Claireaux, 2008; Pichavant et al., 2001; Rosenfeld and Lee, 2022; Wang et al., 2009). Reduction in AS throughout the DO gradient likely limits the energy available for activities beyond maintenance, such as digestion. The reduction in food intake under hypoxia appears to be linked to prolonged time required for energy assimilation, as suggested by the increasing duration of SDA when fish digest in hypoxia (Eliason and Farrell, 2014; Jordan and Steffensen, 2007; Zhang et al., 2010). This increased

SDA duration reflects energy-saving strategies to keep this activity within the reduced aerobic capacity and adjustments to sustain oxygen delivery to tissues (Jordan and Steffensen, 2007).

Under hypoxia, reduced food intake rates can be viewed as a means of lowering energy demand and, in turn, oxygen requirements. Appetite regulation relies on a coordinated series of signals: from hunger hormones such as ghrelin, to leptin-mediated suppression at the gene-expression level (Bernier and Craig, 2005; Bernier et al., 2012), to stress hormones such as cortisol, and finally to satiety signals produced by the digestive tract (Gorissen et al., 2006; Volkoff and Rønnestad, 2020). Hypoxia can slow digestion, keeping these satiety signals active for longer, further reducing food intake. These mechanisms were not investigated, but these immediate and longer-term responses could explain the decline in feeding at DO levels below ~40% sat.

FCE dropped sharply at the lowest treatment (25%), representing a 95% decrease in efficiency compared to all other treatments combined. The decline in FCE is consistent with the strong reduction in mass growth observed at low DO levels. The particularly low FCE under severe hypoxia suggests that the digestive and assimilative processes became increasingly constrained at 25% DO. This loss in efficiency could be due to decreased gastrointestinal blood flow, altered digestive enzymes, or increased relative allocation to maintenance metabolism (Wang et al., 2009; Wu, 2002). For example, in Atlantic cod under hypoxia treatment (19-25% sat.), coeliac and mesenteric blood flow decreased by more than 40% and 60%, respectively (Axelsson and Fritsche, 1991). In juvenile cobia (Rachycentron canadum), prolonged exposure to hypoxia (~3.15 mg O_2 L^{-1} or ~48% sat. for 28 days) reduced digestive enzyme activities, altered intestinal morphology, and downregulated tight junction protein expression (Yang et al., 2021). Such changes likely alter nutrient assimilation and contribute to reduced growth efficiency.

In our experiments, fish were held in tanks without prey or predator interactions, and food was easily accessible and non-limiting. In the wild, individuals would need to allocate a larger portion of their AS to swimming and foraging, leaving less energy available for SDA

when AS is reduced. Consequently, the level of DO at which growth begins to decline is likely higher under natural conditions than the ~38% observed in the laboratory. At DO levels below this value, the effect on growth would probably be more pronounced due to additional biotic and abiotic modulators.

2.7.4 Limitations

A significant tank effect was detected for food intake, growth and condition, reflecting uncontrolled factors such as social dynamics, food competition, or small differences in water flow and equipment. Such variations can reduce the power to detect treatment effects, and therefore, limited replication remains the main constraint of this experiment. The available space limited the number of treatments and the number of replicates, and we opted for eight DO levels to improve the resolution of threshold estimates. Although additional replicates would have been desirable, strong and consistent DO effects across tanks indicate that tank-level noise did not obscure the main patterns of interest.

Initial body length also influenced all growth metrics and ΔK, reflecting the expected size-dependent pattern in which larger individuals grow more slowly and show smaller changes in condition. Although this effect was not the main focus of the experiment, body length shaped individual growth responses and should be considered when assessing the effects of DO on the physiology of *S. fasciatus*.

Further investigations of SDA, blood-flow dynamics, and digestive enzyme activity would refine our understanding of how DO constrains digestion and growth. Integrating hypoxia with different temperature regimes will be essential, because O_2crit decreases with temperature in *S. fasciatus* (Guitard et al., 2025) and thermal conditions likely modify both digestive costs and physiological traits. Such multi-stressor experiments would clarify how oxygen and temperature jointly shape energy allocation.

2.7.5 Perspectives and conclusions

Despite the clear decline in growth and condition observed below ~40% DO in the present study, a large proportion of redfish biomass in the GSL remains concentrated in deep-water channels where oxygen sat. ranges between 25–60%. In these areas, approximatively 60% of *S. fasciatus* and 85% of *S. mentella* biomass are found (Blais et al., 2025; Senay et al., 2026). This suggests that the apparent recovery of redfish stocks could mask underlying declines in individual productivity. Smaller and leaner fish contribute less to yield and recruitment (Saborido-Rey et al., 2004), even if biomass remains high. With climate change further intensifying deoxygenation and warming in the GSL, the carrying capacity of deep habitats for redfish is likely to decrease, a trend that has been observed since 2020 (Chamberland et al., 2025). Therefore, understanding how habitat use, predator pressure, and prey availability interact with oxygen constraints will be critical to predict future trajectories of redfish populations and to ensure sustainable management of the fishery. Management will need to consider not only biomass but also environmental constraints, since low-oxygen habitats can reduce growth, and likely reproduction, and the overall productivity of stocks.

2.8 SUPPORTING INFORMATION

Tableau 15. Seawater parameters (Mean ± Standard deviation) for each experimental tank throughout the growth period (March 28th to July 11th, 2022). Tanks represent the 16 experimental tanks, separated in four lines of for tanks, in which fish were held. Treatment represents the target dissolved oxygen, DO manual are the values of dissolved oxygen recorded from Monday to Friday during the growth period and DO Winkler are the values from the Winkler method, salinity (in the header tank of the four lines) and temperature (in each tank) were measured from Monday to Friday.

Tank	Treatment	DO manual	DO Winkler	Temperature	Salinity
A1	65	64.60 ± 2.12	66.78 ± 1.60	5.09 ± 0.39	28.39 ± 0.53
A2	85	83.47 ± 1.97	85.24 ± 1.92	5.05 ± 0.38	28.39 ± 0.53
A3	55	54.64 ± 1.19	55.60 ± 0.87	5.02 ± 0.31	28.39 ± 0.53
A4	75	73.86 ± 1.65	75.56 ± 0.92	5.05 ± 0.31	28.39 ± 0.53
B1	35	35.29 ± 1.29	35.29 ± 0.88	4.97 ± 0.08	28.41 ± 0.52
B2	100	94.05 ± 2.00	96.43 ± 1.34	4.95 ± 0.08	28.41 ± 0.52
B3	25	25.27 ± 1.29	25.08 ± 0.29	4.84 ± 0.06	28.41 ± 0.52
B4	45	43.32 ± 1.65	49.80 ± 15.42	4.86 ± 0.06	28.41 ± 0.52
C1	45	43.76 ± 1.24	43.85 ± 0.73	5.11 ± 0.09	28.41 ± 0.52
C2	75	73.76 ± 1.45	74.91 ± 1.04	5.16 ± 0.07	28.41 ± 0.52
C3	65	64.36 ± 1.65	66.16 ± 0.99	5.16 ± 0.07	28.41 ± 0.52
C4	100	94.02 ± 1.97	97.08 ± 1.39	5.14 ± 0.07	28.41 ± 0.52
D1	25	24.90 ± 1.42	24.73 ± 1.53	4.84 ± 0.06	28.41 ± 0.52
D2	55	53.92 ± 1.37	54.95 ± 0.67	4.80 ± 0.05	28.41 ± 0.52
D3	35	34.60 ± 1.29	34.79 ± 0.89	4.85 ± 0.07	28.41 ± 0.52
D4	85	84.29 ± 2.05	86.36 ± 1.57	4.84 ± 0.06	28.41 ± 0.52

Tableau 16. Mean dissolved oxygen and mean temperature (± Standard error) during respirometry trials. The mean was calculated from the four median values obtained from the four respirometry chambers for each session × system combination, excluding the period of diminishing DO used to calculate O_2crit.

Session	System	Treatment	Dissolved oxygen	Temperature
1	1	35	35.38 ± 0.16	4.83 ± 0.06
1	2	100	98.76 ± 0.30	4.97 ± 0.04
2	1	65	66.58 ± 0.15	4.85 ± 0.09
2	2	75	75.49 ± 0.40	4.93 ± 0.18
3	1	100	98.56 ± 0.59	4.95 ± 0.04
3	2	45	45.69 ± 0.35	4.86 ± 0.13
4	1	65	65.64 ± 0.23	4.83 ± 0.04
4	2	45	45.87 ± 0.17	4.82 ± 0.12
5	1	55	55.63 ± 0.14	5.08 ± 0.05
5	2	25	26.37 ± 0.17	4.89 ± 0.10
6	1	75	74.84 ± 0.49	4.78 ± 0.07
6	2	55	55.08 ± 0.38	4.84 ± 0.12
7	1	85	84.88 ± 0.23	5.09 ± 0.06
7	2	25	26.97 ± 0.25	4.87 ± 0.11
8	1	85	85.05 ± 0.28	4.98 ± 0.05
8	2	35	36.60 ± 0.19	4.99 ± 0.14

Tableau 17. Description and variable type of all parameters used in the generalized additive and linear models for each physiological trait

Parameter	Description	Variable type
Growth rates		
DO	Mean dissolved oxygen measured during the whole growth experiment as a continuous variable	Fixed
Initial length	Length of individuals when the experiment started	Fixed
Tank	Tank in which fish spent the whole growth experiment	Random
Food consumption		
DO	Mean dissolved oxygen measured during the whole growth experiment as a continuous variable	Fixed
Tank	Tank in which fish spent the whole growth experiment	Random
Food conversion efficiency (FCE)		
DO	Mean dissolved oxygen measured during the whole growth experiment as a continuous variable	Fixed
Change in condition (ΔK)		
DO	Mean dissolved oxygen measured during the whole growth experiment as a continuous variable	Fixed
Initial length	Length of individuals when the experiment started	Fixed
Tank	Tank in which fish spent the whole growth experiment	Random
Metabolic traits		
(MMR, SMR, AS, FAS, O_{2crit})		
DO	Mean dissolved oxygen measured during the whole growth experiment as a continuous variable	Fixed
Tank	Tank in which fish spent the whole growth experiment	Random
Respirometer	Respirometry chamber in which the fish underwent respirometry as an 8 level factor	Random

Tableau 18. Models tested for each of food consumption, FCE, growth in mass and length, and change in condition factor (ΔK), along with their AIC value. For the first four dependent variables, all predictors were significant and no simplified model was tested.

Model	AIC
Food 1 = gam(Weekly food consumptions ~ s(DO) + s(tank, bs="re"), data= Food, method="REML")	1057.101
FCE 1 = gam(Food conversion efficiency ~s(DO), data=FCE, method="REML")	-79.29
Growth mass 1 = gam(Growth rates ~ s(DO) + s(Initial length) + s(tank, bs="re"), data= Growth, method="REML")	-1350.3
Growth length 1 = gam(Growth rates ~ s(DO) + s(Initial length) + s(tank, bs="re"), data= Growth, method="REML")	-2946.48
ΔK 1 = gam(Δ Condition ~ s(DO) + s(Initial length) + s(tank, bs="re"), data= Growth, method="REML")	-6305.11
ΔK 2 = gam(Δ Condition ~ s(DO) + s(Initial length) , data= Growth, method="REML")	-6308.26

Tableau 19. Design for best linear mixed-effects models for each metabolic traits with interaction p-values.

Model	**AIC**
MMR 1 = lmer(MMR ~ Dissolved oxygen + (1 | tank) + (1| respirometer), data=MR)	511.2
MMR 2 = lmer(MMR ~ Dissolved oxygen + (1 | tank), data=MR)	508.9
MMR 3 = lmer(MMR ~ Dissolved oxygen + (1| respirometer), data=MR)	508.8
MMR 4 = lm(MMR ~ Dissolved oxygen, data=MR)	506.5
SMR 1 = lmer(SMR ~ Dissolved oxygen + (1 | tank) + (1| respirometer), data=MR)	320.2
SMR 2 = lmer(SMR ~ Dissolved oxygen + (1 | tank), data=MR)	317.8
SMR 3 = lmer(SMR ~ Dissolved oxygen + (1| respirometer), data=MR)	320.7
SMR 4 = lm(SMR ~ Dissolved oxygen, data=MR)	318.4
AS 1 = lmer(AS ~ Dissolved oxygen + (1 | tank) + (1| respirometer), data=MR)	511.3
AS 2 = lmer(AS ~ Dissolved oxygen + (1 | tank), data=MR)	508.9
AS 3 = lmer(AS ~ Dissolved oxygen + (1| respirometer), data=MR)	508.9
AS 4 = lm(AS ~ Dissolved oxygen, data=MR)	506.6
FAS 1 = lmer(FAS ~ Dissolved oxygen + (1 | tank) + (1| respirometer), data=MR)	163.8
FAS 2 = lmer(FAS ~ Dissolved oxygen + (1 | tank), data=MR)	161.4
FAS 3 = lmer(FAS ~ Dissolved oxygen + (1| respirometer), data=MR)	161.5
FAS 4 = lm(FAS ~ Dissolved oxygen, data=MR)	159.2
O_2crit 1 = lmer(O2crit ~ Dissolved oxygen + (1 | tank) + (1| respirometer), data=MR)	261.5
O2crit 2 = lmer(O2crit ~ Dissolved oxygen + (1 | tank), data=MR)	259.9
O2crit 3 = lmer(O2crit ~ Dissolved oxygen + (1| respirometer), data=MR)	259.7
O2crit 4 = lm(O2crit ~ Dissolved oxygen, data=MR)	258.2

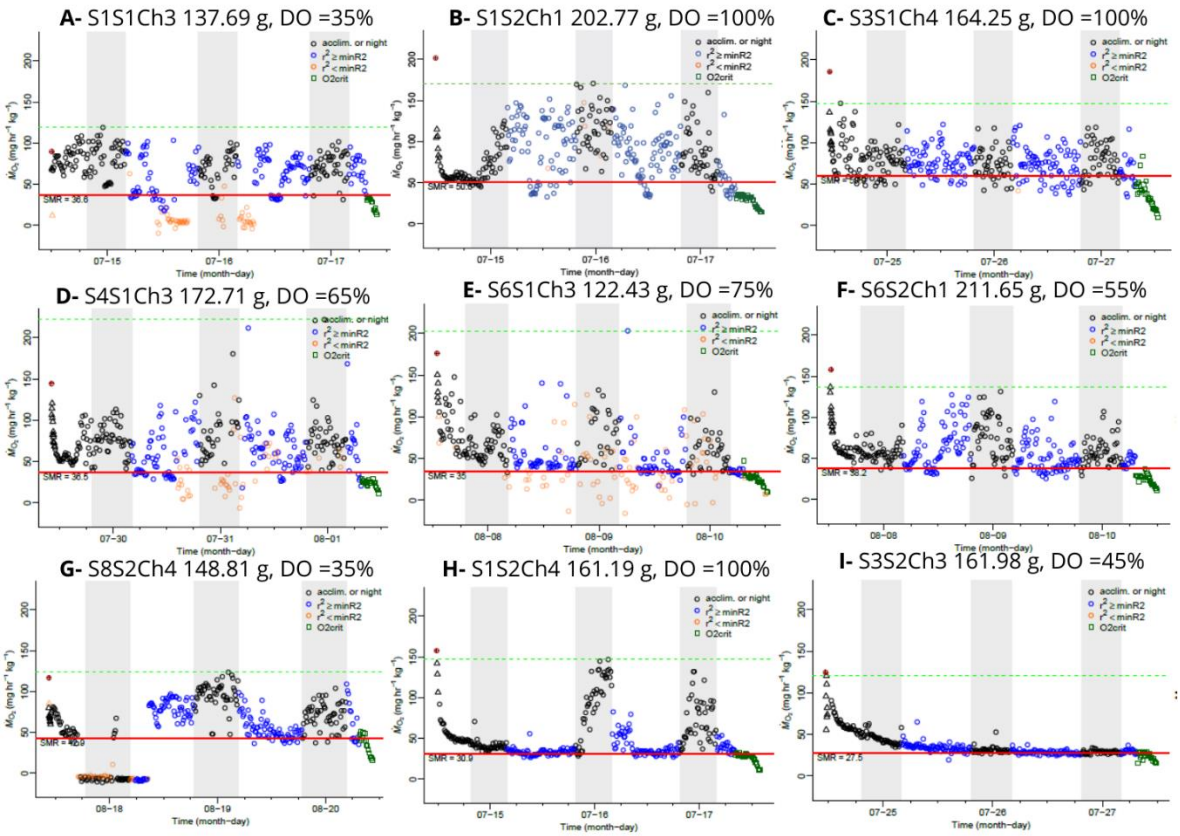

Figure 21. Time series of oxygen uptake over 4-day respirometry trials. Panels A–G show the seven redfish excluded from the metabolic trait analysis, while panels H and I illustrate two cases retained in the dataset: one exhibiting night activity (H) and one without night activity (I).

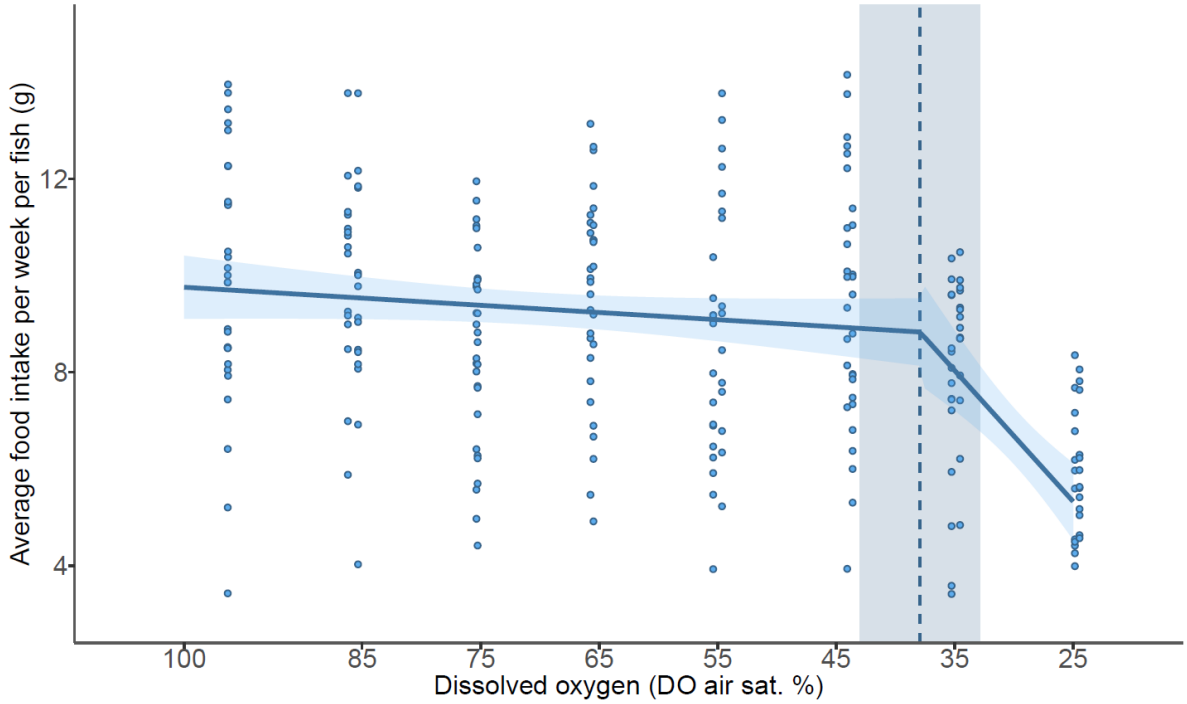

Figure 22. Breakpoint analysis of average food intake per week per fish of redfish (*Sebastes fasciatus*) in response to dissolved oxygen (DO) availability. Blue points represent observed values, and the solid line shows model predictions from the segmented regression. The dashed vertical line indicates the estimated oxygen breakpoint, below which average food intake per week per fish declined significantly. The shaded dark blue rectangle represents the 95% confidence interval of the breakpoint estimate. The light blue shaded band illustrates the 95% confidence interval around the predicted values. Together, these features highlight the oxygen threshold at which condition factor transitions from relatively stable values under moderate–high DO to significantly reduced values at low DO.

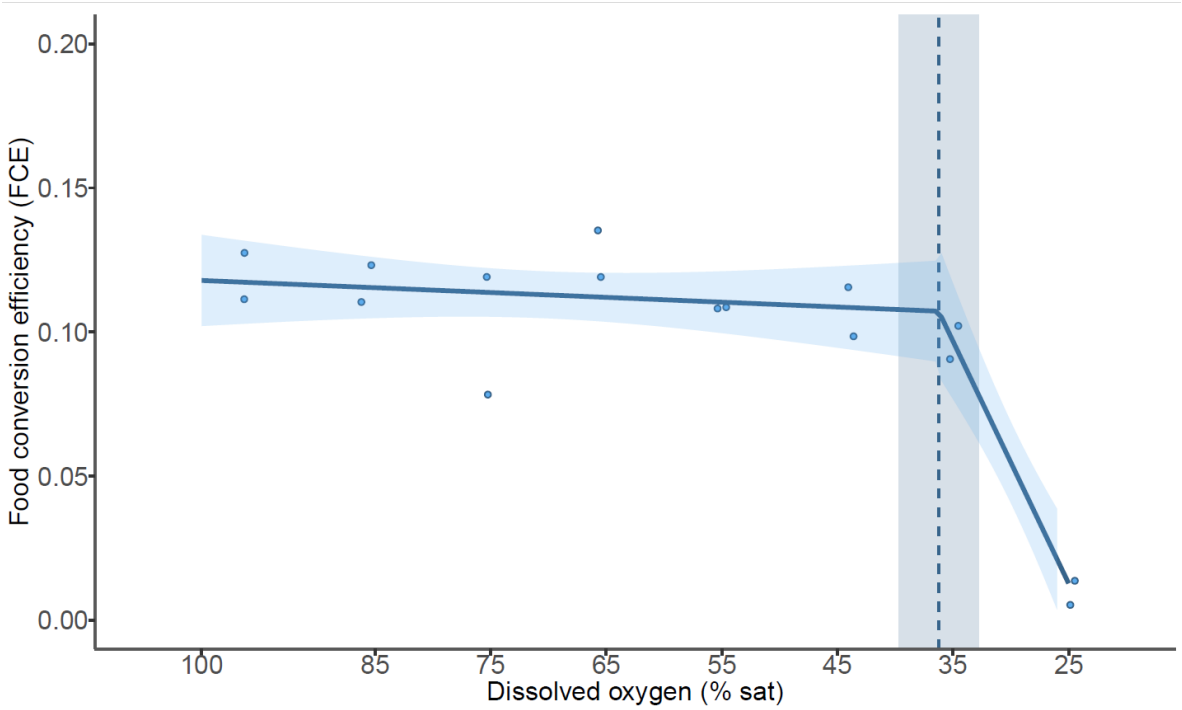

Figure 23. Breakpoint analysis of food conversion efficiency (FCE) of redfish (*Sebastes fasciatus*) in response to dissolved oxygen (DO) availability. Blue points represent observed values, and the solid line shows model predictions from the segmented regression. The dashed vertical line indicates the estimated oxygen breakpoint, below which FCE declined significantly. The shaded dark blue rectangle represents the 95% confidence interval of the breakpoint estimate. The light blue shaded band illustrates the 95% confidence interval around the predicted values. Together, these features highlight the oxygen threshold at which condition factor transitions from relatively stable values under moderate–high DO to significantly reduced values at low DO.

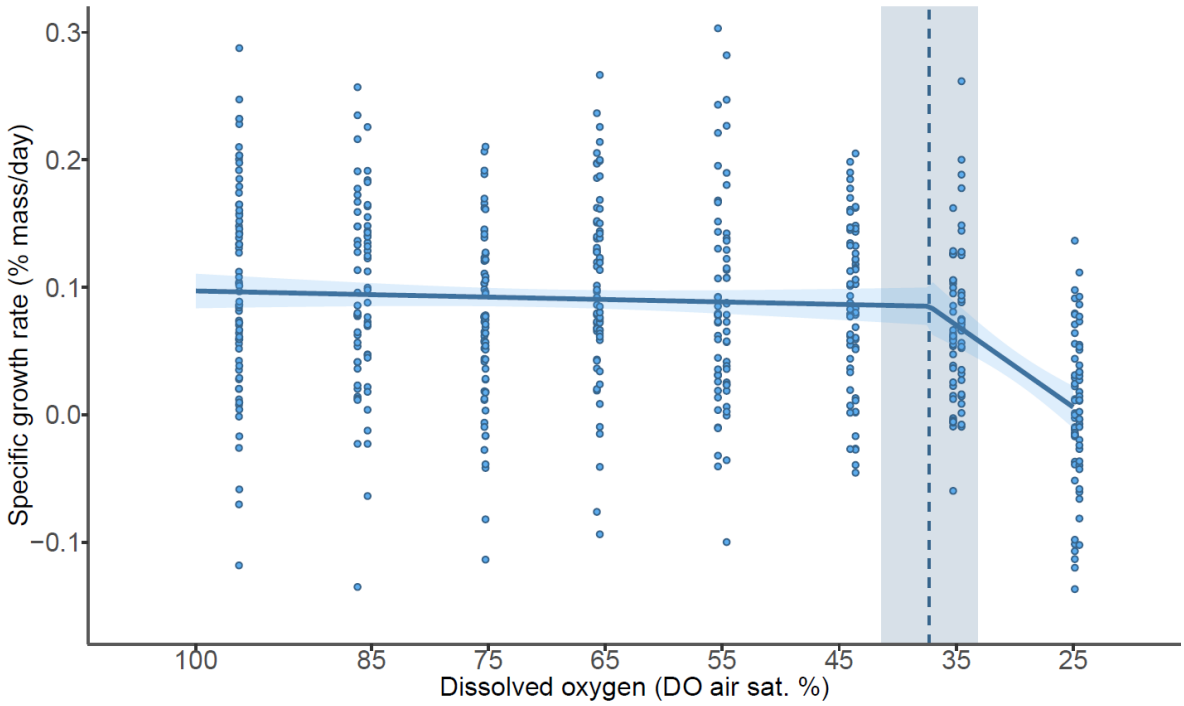

Figure 24. Breakpoint analysis of specific growth rate in mass of redfish (*Sebastes fasciatus*) in response to dissolved oxygen (DO) availability. Blue points represent observed values, and the solid line shows model predictions from the segmented regression. The dashed vertical line indicates the estimated oxygen breakpoint, below which specific growth rate in mass declined significantly. The shaded dark blue rectangle represents the 95% confidence interval of the breakpoint estimate. The light blue shaded band illustrates the 95% confidence interval around the predicted values. Together, these features highlight the oxygen threshold at which condition factor transitions from relatively stable values under moderate–high DO to significantly reduced values at low DO.

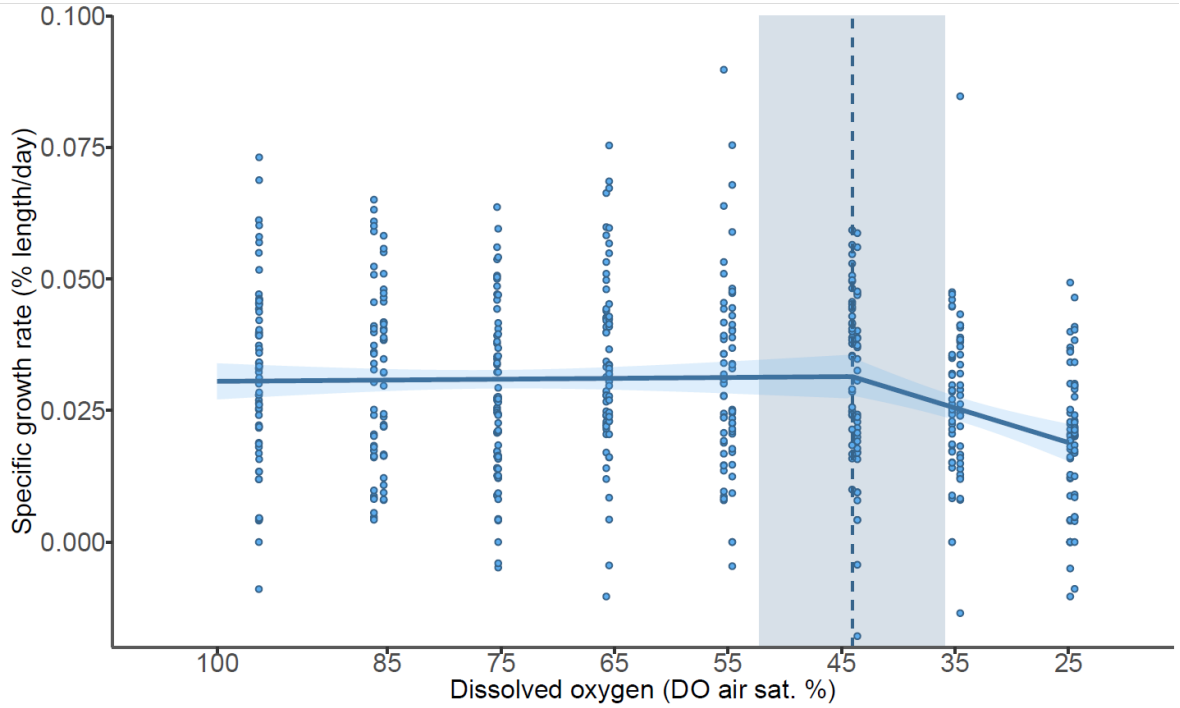

Figure 25. Breakpoint analysis of specific growth rate in length of redfish (*Sebastes fasciatus*) in response to dissolved oxygen (DO) availability. Blue points represent observed values, and the solid line shows model predictions from the segmented regression. The dashed vertical line indicates the estimated oxygen breakpoint, below which specific growth rate in length declined significantly. The shaded dark blue rectangle represents the 95% confidence interval of the breakpoint estimate. The light blue shaded band illustrates the 95% confidence interval around the predicted values. Together, these features highlight the oxygen threshold at which condition factor transitions from relatively stable values under moderate–high DO to significantly reduced values at low DO.

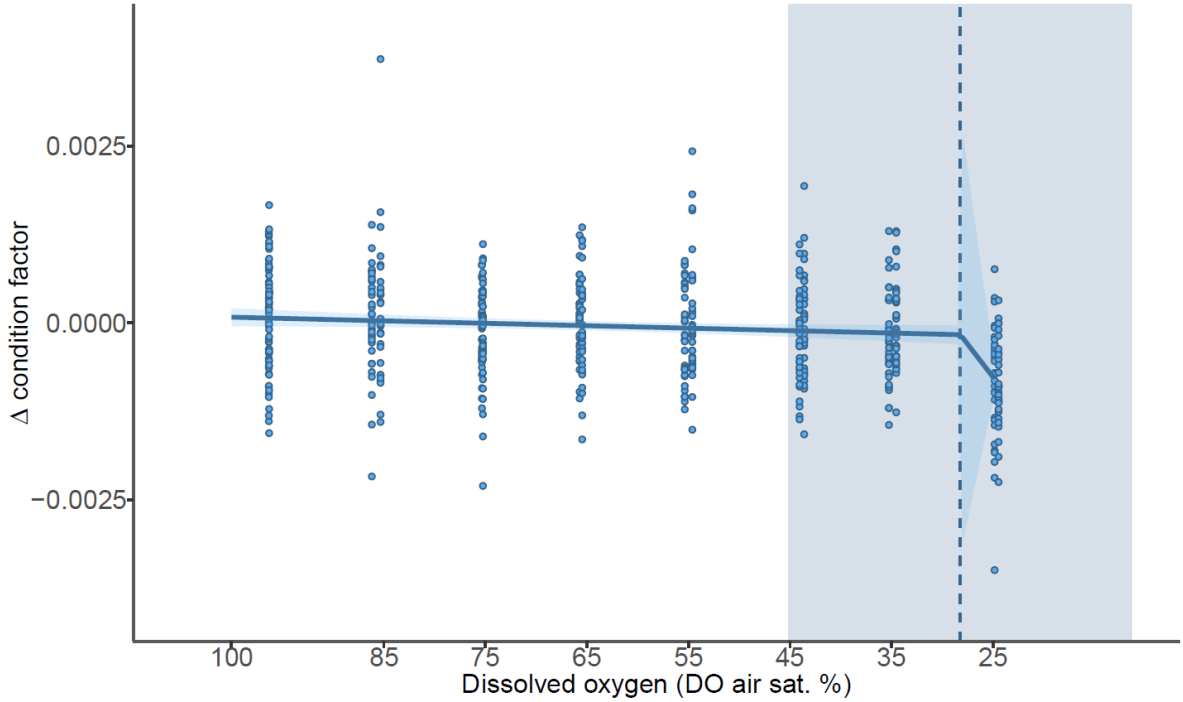

Figure 26. Breakpoint analysis of changes in condition factor of redfish (*Sebastes fasciatus*) in response to dissolved oxygen (DO) availability. Blue points represent observed values, and the solid line shows model predictions from the segmented regression. The dashed vertical line indicates the estimated oxygen breakpoint, below which condition factor declined significantly. The shaded dark blue rectangle represents the 95% confidence interval of the breakpoint estimate. The light blue shaded band illustrates the 95% confidence interval around the predicted values. Together, these features highlight the oxygen threshold at which condition factor transitions from relatively stable values under moderate–high DO to significantly reduced values at low DO.

CHAPITRE 3
DU LABORATOIRE AU MILIEU NATUREL : LES MESURES *IN SITU* DE CONSOMMATION D'OXYGÈNE CONCORDENT AVEC CELLES OBTENUES EN LABORATOIRE CHEZ *SEBASTES FASCIATUS*

3.1 RÉSUMÉ EN FRANÇAIS DU TROISIÈME ARTICLE

En conditions contrôlées, la mesure de la consommation d'oxygène constitue un indicateur fiable du taux métabolique. Toutefois, cette approche exige de capturer les poissons et de les transporter au laboratoire, ce qui peut influencer leur physiologie, et les conditions expérimentales peuvent différer du milieu naturel, réduisant ainsi la pertinence des tests pour la recherche en conservation. L'objectif de cette étude était de développer une méthode peu invasive permettant d'estimer les taux métaboliques de poissons directement *in situ*. Deux respiromètres construits sur mesure ont été déployés à 30 mètres de profondeur dans l'estuaire du Saint-Laurent (Canada) afin de mesurer la consommation d'oxygène de sébastes acadiens (*Sebastes fasciatus*) en milieu naturel sur une période de 24 heures (n = 10). Pour valider la méthode, le taux métabolique de routine (TMR) mesuré *in situ* a été comparé au taux métabolique standard (TMS) obtenu en laboratoire chez les mêmes individus (n = 4) ainsi que chez des *S. fasciatus* de taille similaire acclimatés en laboratoire (n = 11). Malgré les variations naturelles de température, de luminosité, de remplissage stomacal et les stimuli biotiques potentiels, les valeurs de RMR mesurées en milieu naturel concordaient étroitement avec les TMS obtenus en laboratoire. Ces résultats démontrent la faisabilité de la respirométrie *in situ* pour estimer la consommation d'oxygène tout en conservant une pertinence écologique.

Mots-clés : variabilité environnementale, respirométrie à débit intermittent, taux métaboliques, respirométrie de terrain, dispositif autonome

Cet article, intitulé « Bridging lab and field*: In situ* oxygen uptake measurements match laboratory-derived values in *Sebastes fasciatus* », sera soumis pour publication comme un article de méthodes dans la revue *Journal of Experimental Biology*. En tant que première autrice, j'ai assuré la recherche bibliographique, la conception méthodologique, la collecte et l'analyse des données, ainsi que la rédaction du manuscrit. Le chercheur Denis Chabot, deuxième auteur, à la mise à disposition des ressources matérielles, à la supervision scientifique, à l'analyse des données et à la révision du texte. Dominique Robert, troisième auteur, a contribué à la supervision scientifique, à la validation des analyses et à la révision du manuscrit. Enfin, le dernier auteur, David Deslauriers, est à l'origine de l'idée initiale du projet et a contribué à la conception de l'étude, a participé au développement de la méthodologie, à la mise à disposition des ressources matérielles, à la supervision et à la révision du manuscrit.

Les résultats de cette étude ont été présentés en ligne lors de la conférence *Respfest 3* qui avait lieu à La Rochelle au printemps 2023. Ces résultats ont aussi été présentés lors de la session « *Respfest 4 : the use of respirometry as a tool to support fisheries conservation* » à la 154[e] rencontre annuelle de la *American Fisheries Society* à Honolulu, HI en septembre 2024.

3.2 BRIDGING LAB AND FIELD: *IN SITU* OXYGEN UPTAKE MEASUREMENTS MATCH LABORATORY-DERIVED VALUES IN *SEBASTES FASCIATUS*

Joëlle J. Guitard[a*], Denis Chabot[b], Dominique Robert[a], et David Deslauriers[b]

[a] Institut des sciences de la mer, Université du Québec à Rimouski, Rimouski, QC, Canada

[b] Maurice Lamontagne Institute, Fisheries and Oceans Canada, Mont-Joli, QC, Canada

3.3 ABSTRACT

Under laboratory conditions, measuring oxygen uptake provides a reliable proxy for metabolic rate. However, this require that fish are captured and transported to the laboratory, which may influence their physiology, and laboratory conditions may differ from the wild

render the tests less relevant for conservation research. The objective of the present study was to develop a minimally invasive method to estimate metabolic rates *in situ* of fish. Two custom-built respirometers were deployed at a depth of 30 meters in the St. Lawrence Estuary (Canada) to measure oxygen uptake in wild redfish (*Sebastes fasciatus*) over a 24-hour period (n=10). To validate the method, *in situ* routine metabolic rate (RMR) was compared to standard metabolic rate (SMR) measured on the same individuals in the laboratory (n=4) and on laboratory acclimated *S. fasciatus* (n=11). Despite natural fluctuations in temperature, light, gut fullness and potential biotic stimuli, RMR measured in the wild were consistently similar to laboratory-derived SMR. These findings demonstrate the feasibility of *in situ* respirometry for estimating oxygen uptake while maintaining ecological relevance.

Key-words: Environmental variability, intermittent flow respirometry, metabolic rates, field respirometry, autonomous instrumentation

3.4 INTRODUCTION

Understanding metabolic rates has long been a cornerstone of physiological research, as it provides insights into the energetic demand of organisms (Nelson, 2016; Nelson and Chabot, 2024). Historically, direct calorimetry, the measurement of heat production, was the most accurate method for quantifying metabolic rate. However, its complexity and the requirement for specialized equipment made it challenging to apply broadly, particularly for aquatic organisms such as fishes (Nelson, 2016). The development of indirect calorimetry methods, which estimate metabolic activity through measurements oxygen uptake and/or CO_2 release, provided a more practical alternative (Nelson, 2016). As measuring CO_2 in water presents significant challenges, particularly in sea water (Nelson, 2016), most studies on fish rely on oxygen uptake as a proxy for metabolic rate a valid approach as their rate of energy expenditure is closely tied to oxygen uptake (Nelson, 2016; Nelson and Chabot, 2024). By measuring oxygen uptake, respirometry offers a reliable proxy for metabolic rate, enabling to study the energetic needs of aquatic species in both laboratory and natural settings.

Metabolic rate is a fundamental ecological process, as it governs energy assimilation, transformation, and allocation, directly shaping key functions for maintenance, resource use, growth, and reproduction (Brown et al., 2004). Estimating metabolic rates through oxygen uptake in fishes provides insight on the potential energy available to an organism and can be achieved with minimal laboratory equipment (e.g., Ern and Jutfelt, 2024). However, determining meaningful levels of metabolic rate from the collected data can be more challenging. Standard metabolic rate in fishes (SMR: the lowest metabolic rate needed to sustain life in a resting, fasting, and non-stressed condition) is ecologically significant because it provides a basis for determining aerobic scope (AS)—the energy available for activities like movement, digestion, and reproduction, beyond basal metabolic needs (Chabot et al., 2016; Claireaux and Lefrançois, 2007). SMR also constitutes a valuable input into bioenergetic models predicting energy allocation. To estimate SMR, the fish must be in a post-absorptive state and exhibit minimal activity or movement. Even though most of these measurements are obtained in the laboratory, such strict conditions cannot always be met, and the resulting oxygen uptake is then referred to as routine metabolic rate (RMR). RMR includes the small, spontaneous activities that fish typically display in a respirometer—such as maintaining position or occasional fin movements, and therefore represents a broader, less strictly defined measure of baseline metabolism (Chabot et al., 2016). Because the level of activity is not quantified, RMR can fall anywhere between SMR and much higher values, although appropriate respirometer design generally keeps it close to SMR (Chabot et al., 2016). This variability in the literature reflects the practical reality that RMR is used when true resting conditions cannot be confirmed.

Most respirometry studies are conducted in controlled laboratory environments, where animals are either bred in captivity or transported from their natural habitats. As mentioned by Turko et al. (2023), laboratory animals can differ from wild animals, due to differences in diet, parasite load and stress exposure. In addition, bringing animals in the laboratory often involves various interventions, such as antiparasitic measures and rearing in conditions that do not fully reflect their natural environment (Turko et al., 2023). These conditions may also result in the loss of individuals that do not adjust well to captivity, meaning that the animals

remaining in experiments may not fully reflect the physiological diversity found in the wild. Studying fishes in the lab can also lead to overestimation or underestimation of certain metabolic traits. For example, maintaining fishes at constant temperatures in the lab may not be relevant if wild individuals live where temperature fluctuates daily. Beauregard et al. (2013) showed that Atlantic salmon (*Salmo salar*) exposed to circadian fluctuations in water temperature had SMRs 25–32% higher than conspecifics kept at a constant temperature, suggesting that standard lab protocols may underestimate metabolic rates of fish from variable natural environments. These findings highlight the importance of accurate metabolic measurements obtained in environmental conditions relevant for the target species, particularly when such data are used in bioenergetic models intended to simulate growth under natural, fluctuating conditions.

While minimizing stressors in laboratory experiments can improve the precision of metabolic rate estimates (Auer et al., 2016), measurements taken directly in natural habitats could offer more ecologically relevant insight into physiological responses, which would thus be highly valuable for developing accurate models. Few studies have estimated metabolic rates in natural environments due to logistical constraints, however those that did were driven by ecological and conservation objectives, leading to different methodological approaches. For instance, Farrell et al. (2003) deployed a mobile streamside swim tunnel to estimate the oxygen uptake and swimming capacity of migrating Pacific salmon (*Oncorhynchu*s spp.), including the energetic challenges of upstream migration. Another example is the streamside experiment on desert Redband trout (*Oncorhynchus mykiss* ssp.) testing for physiological adaptations to variability in seasonal flow and diel water temperature (Gamperl et al., 2002). Both studies highlight the motivation to assess oxygen uptake or physiological traits in conditions that reflect ecological challenges faced by these species, thereby linking physiology more directly to conservation and other management issues. Other studies have designed automated deep-sea respirometers for species that cannot survive being brought to the surface due barotrauma (Drazen and Seibel, 2007; Drazen and Yeh, 2012). While these systems have provided metabolic data for previously unstudied species, they do not allow control over which individuals enter the respirometer. Additionally, some field respirometry

setups have been adapted for remote locations without electricity and rely only on the natural current of the stream to flush the respirometer where the experiment is taking place (Mochnacz et al., 2017). These methodological advancements have improved data collection for metabolic and conservation research but require extensive logistics, such as transporting large tanks, expertise in deploying sophisticated deep-sea systems, and relying on natural water flow instead of pumps in intermittent-flow respirometry (Drazen and Yeh, 2012; Farrell et al., 2003; Mochnacz et al., 2017).

In the present study, we aimed to build and use a simple and autonomous *in situ* respirometer that allows the study of fish in their natural, probably fluctuating environment, while minimizing handling stress. This system is of particular interest for species that cannot easily be brought back to the laboratory. The first objective was to test a new respirometry setup that allows the measurement of oxygen uptake ($\dot{M}O_2$) for Acadian redfish (*Sebastes fasciatus*) in their natural environment. The second objective was to evaluate how $\dot{M}O_2$ measurements taken *in situ* compare to those obtained in a controlled laboratory setting, both with the same individuals and with other *S. fasciatus* of similar size. Because *in situ* respirometry trials (ISMeR) involve greater environmental variability, shorter acclimation and measurement periods, and an inability to assess whether fish are fully post-absorptive, we predicted that metabolic rates measured *in situ* would exceed laboratory-derived SMR values.

3.5 METHODS

3.5.1 Study site, sampling and collection

S. fasciatus were sampled (*in situ* respirometry: ISMeR) or captured (Lab) near Les Escoumins, Québec, Canada (48.317801°N, 69.413287°W) in September–November 2019, November 2021 and September 2022. The collection site was at a depth of 25 to 30 meters accessible to SCUBA divers. Collected *S. fasciatus* underwent an *in situ* respirometry trial (ISMeR) that lasted ca. 24 hrs (see *In situ* respirometry trials section). *S. fasciatus* that

underwent *in situ* respirometry and other collected *S. fasciatus* (ca. 800 in 2019, 200 in 2021 and 100 in 2022) were successfully brought live to our aquaculture facilities using the methodology developed by Larocque (2000) and successfully used in Guitard et al. (2025 and chapter 2 of this thesis). Briefly, SCUBA divers caught *S. fasciatus* with dip nets and placed them into cages (33 × 34 × 23 cm) that could hold up to 30 individuals. Most fish measured between 16 and 20 cm at the time of capture. Once full, cages were placed higher up along the slope, at a depth of 10–15 m depending on the tide, to reduce barotrauma. The duration of this equilibration period was at least 12 h, but up to 96 h for fish caught early during each of the 5-day fishing trips. The day after the last capture, the cages were brought to the surface for transportation in aerated tanks to the Maurice Lamontagne Institute in Mont-Joli, Québec, Canada (48.580002°N, 68.180000°W).

Upon their arrival, fish were transferred into circular water tanks (1 m height × 1.1 m diameter; 760 L) supplied with 5 ℃ oxygenated seawater (salinity of 28 ppt). Fish that underwent respirometry trials were kept in separated tanks from the other fish brought to our facilities for our collection. All fish were offered food (northern shrimp, *Pandalus borealis*, capelin, *Mallotus villosus*, and krill, *Euphausia superba*) three times a week. It took about two weeks for the individuals to acclimatize to their new environment and feed correctly. Wild fish may present various levels of parasite load, which are known to influence performance traits (Chrétien et al., 2022; Guitard et al., 2022). Hence, a week after they started eating, fish received a formaldehyde treatment (37% formaldehyde, 0.01 ml L^{-1}) for 1 hour to remove possible external parasites. In order to minimize stress, this preventive treatment was not applied to fish used for *in situ* respirometry before they underwent laboratory respirometry. One month after they started eating, fish were anesthetized (Benzocaine, 0.5 ml of solution per liter of seawater, solution = 100 g of benzocaine dissolved in 1 L of 70 % ethanol) weighed, measured and individually identified with a PIT-tag (Biomark, Idaho, USA).

3.5.2 Layout of experiments

This study generated three sets of respirometry data, 1) *In situ* respirometry (ISMeR), 2) controlled laboratory respirometry using fish that underwent *in situ* respirometry (Lab-ISMeR) and 3) controlled laboratory respirometry on acclimated fish (Lab-Acclim). *In situ* respirometry or ISMeR was conducted over two consecutive years, in November 2021 and in September 2022. Controlled laboratory respirometry on individuals that underwent *in situ* respirometry or Lab-ISMeR was performed only on some individuals from September 2022 trials, after 54 days in captivity. Controlled laboratory respirometry or Lab-Acclim on acclimated individuals took place in August and September 2021 and in June 2022, for fish collected in fall 2019 and 2021, respectively (Tableau 20).

Tableau 20. Summary of fish groups included in *in situ* (ISMeR) and laboratory (Lab-ISMeR, Lab-Acclim) respirometry experiments on redfish (*Sebastes fasciatus*). Collection details specify, depth, equipment, and acclimation time in captivity. Experimental year indicates the testing period. N (tested fish) shows the number of individuals initially tested, while N (usable fish) indicates the number of individuals retained for analysis after excluding trials technical malfunction. Notes provide additional details on equipment failures, subsequent mortalities, and relationships between groups (e.g., same individuals retested after laboratory acclimation).

Group / Dataset	Collection details	Experimental year	N (tested fish)	N (usable fish)	Notes
ISMeR 2021	*In situ* trials at 25–30 m depth, HOBO probe	**2021 (Nov)**	7	5	One pump failure → 3 fish lost; survivors later died after PIT-tagging → no Lab-ISMeR follow-up
ISMeR 2022	*In situ* trials at 25–30 m depth, PyroScience probe	**2022 (Sep)**	7	5	2 fish discarded for technical malfunction, 1 fish escaped = no ISMeR-Lab comparison
Lab-ISMeR	Same fish from ISMeR 2022, tested in lab after ~54 d in captivity	**2022 (Nov)**	6	6 (4 with a paired ISMeR)	4 individuals paired with ISMeR, plus 2 Lab-only
Lab-Acclim	Collected fall 2019	**2021**	3	3	~2 years in captivity
Lab-Acclim	Collected fall 2021,	**2022**	4	4	~9 months in captivity

3.5.3 *In situ* respirometry trials (ISMeR)

In situ respirometry trials were conducted in November 2021 and September 2022 using an *in situ* respirometry setups designed specifically for this study. Two respirometers were available each year, with only the oxygen probe and its chamber differing each year.

The assembly guide is provided in supporting information (SI). Briefly, each setup was equipped with two acrylic respirometry chambers to hold the fish during respirometry (Loligo, Systems, Viborg, Denmark, 1.2 L; 30 cm length × 7.2 cm diameter) and hold the oxygen probe (Loligo, 0.77 L; 25 cm length × 6.2 cm diameter in 2021; and 1.2 L; 30 cm length × 7.2 cm diameter in 2022). Both chambers were connected to a closed loop (54 mL), made of Tygon tubing and a recirculation pump (model AD20P-1230A, Brushless DC 12V submersible pump, TCT electronics, Shenzhen, China, 4 L min^{-1}) to achieve adequate water mixing between the two chambers. A third plexiglass cylinder housed batteries and electronics. This intermittent flow respirometry setup was fixed on an 84 cm × 54 cm fiberglass grating using PVC sheets and stainless-steel hardware to ensure that it stayed on the bottom with as little disturbance as possible (Figure 27; Assembly guide in SI).

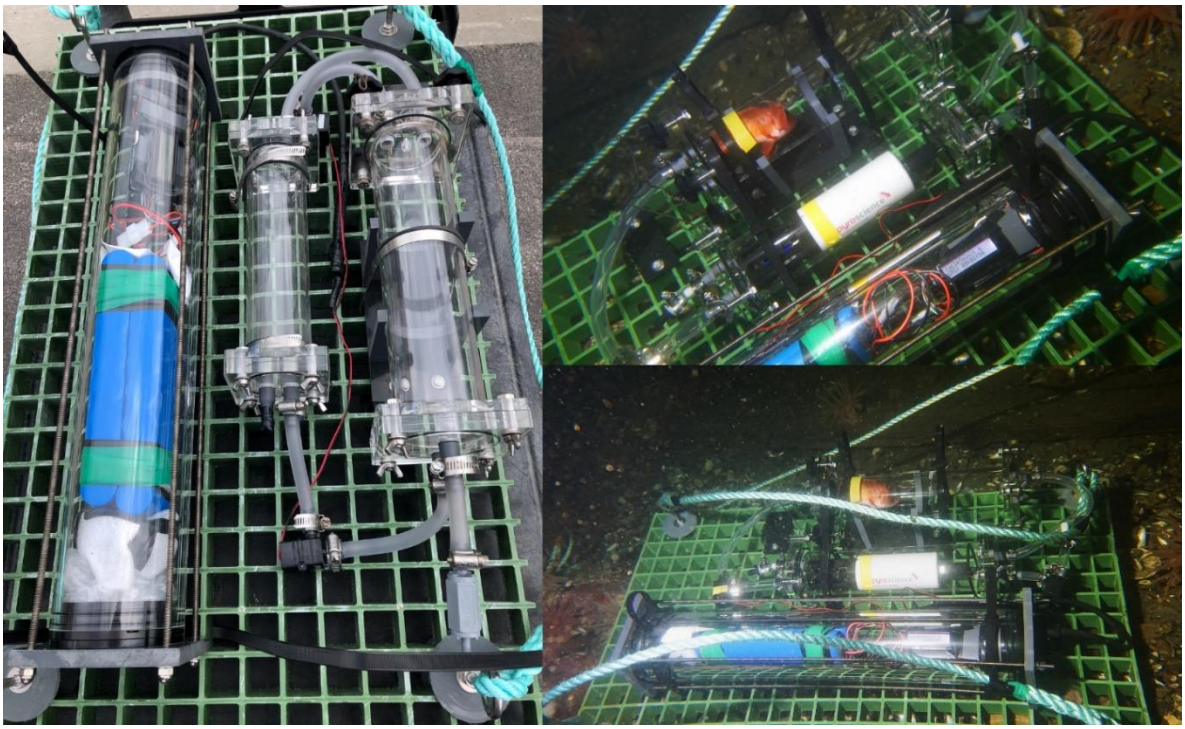

Figure 27. Picture of the 2021 assembled setup outside of water (left). Pictures of the 2022 setup in use underwater (right).

In 2021, a HOBO dissolved oxygen logger (U26-001, Onset computer Corporation, Bourne, MA, USA) measured both dissolved oxygen and temperature. Dissolved oxygen

concentration (mg L^{-1}) was measured every minute. For the first two days, dissolved oxygen (DO) was measured using 14-minute cycles consisting of a 7-min period of flush to renew the water in the respirometers followed by a 7-min closed period of which the last 6 minutes were used to determine oxygen uptake. Since the HOBO probe only allowed one measurement every minute, we reassessed the duration of the recirculation period, as shorter closed periods yielded fewer data points and longer periods therefore allowed more robust slope estimates. The two subsequent days, cycles lasted 20 minutes, with a 10-min period of flush followed by a 10-min closed period, of which the last 9 minutes were used to determine oxygen uptake. Considering the volume of the chamber and all parts included in the recirculation loop, we obtained a chamber to fish volume ratio between 23 and 52, depending on fish size. The oxygen probes used were calibrated with 100% and 0% (air sat.) solutions before going to the field (Annexe 3).

In 2022, an AquapHOx dissolved oxygen logger (Pyroscience GmbH, Aschen, Germany) was used to estimate the oxygen uptake (hPa) with data being collected every second. During each trial day, DO was measured using 10-minute cycles consisting of a 4-min period of flush to renew the water in the respirometers followed by a 6-min closed period of which the last 5 minutes were used to determine oxygen uptake. Considering the volume of the chamber and all parts included in the recirculation loop, we obtained a chamber to fish volume ratio between and 24 and 66. The oxygen probes used were calibrated with 100% and 0% (air sat.) solutions before going to the field (Annexe 3).

Divers installed the *in situ* respirometry setups at the bottom of the collection site, fish chambers were opened, and pumps were activated to ensure that all chambers and tubes were correctly filled with water. Once the setup was stabilized and functional, two fish of appropriate size were captured with dip nets and placed as quickly as possible into the respirometry chambers. Chambers were closed and oxygen uptake recording began as soon as fish were inside chambers. Oxygen uptake was monitored for ca. 24 hrs. Following that period, divers took the fish out of the respirometry chambers and place them in individual cages at mid-depth relative to the capture site, to allow for decompression of the swim

bladder as described above. At the end of the recording period for a given pair of fish, the *in situ* respirometry setups was brought back to the surface, data from the oxygen loggers were downloaded to a computer, batteries were changed, and divers brought back the setup to the bottom and repeated the procedures with a new pair of individuals. Respirometry trials were performed on four pairs of fish each year.

In 2021, one of the recirculation pumps failed on day 2, resulting in unusable data for three out of four fish for that setup. On the fifth day, when all fish were brought up to the surface for transport, the fish used for respirometry trials were anesthetized and identified with PIT-tag (Biomark, Idaho, USA) associated with their *in situ* respirometry trials. Unfortunately, this additional handling caused excessive stress, and all individuals died within hours or days after arrival to the rearing facilities. Moreover, two individuals that underwent *in situ* respirometry were accidentally discarded without obtaining their mass. As no fish survived, no laboratory respirometry data were available for comparison with the *in situ* measurements of the 2021 cohort.

In 2022, one of the batteries had a connection problem, resulting in only one functioning setup being available for the second day. The issue was resolved the following day. Finally, one fish escaped from its individual cage at the end of the *in situ* trial, making it impossible to bring it back to the laboratory for subsequent respirometry and mass measurements.

For the two individuals with unknown mass in 2021 and the one which escaped in 2022, we assigned a body mass representing the mean for all individuals tested in the same year (Tableau 22).

3.5.4 Lab respirometry trials (Lab-ISMeR and Lab-Acclim)

3.5.4.1 Lab-ISMeR

Laboratory oxygen uptake was measured for six fish brought back alive from the 2022 ISMeR deployment (Tableau 20: Lab-ISMeR). They were acclimated for 54 days and tested in November 2022 at a constant temperature of 6 °C and a salinity of 28.

The setup included three glass chambers placed inside a rectangular tank (200 cm length × 60 cm width × 28 cm height, 336 L) with an open circulation system. Temperature was controlled by mixing cold and warm seawater. Temperature of the incoming seawater was measured with a temperature probe (Hermetically sealed RTD probe, Omega Engineering inc., Norwalk, CT, United States) and fed to a controller (1/16 DIN Micromega autotune PID Temperature, Omega Engineering inc.) connected to a mixing valve (sv3109, Omega Engineering inc.) to obtain the appropriate ratio of cold and warm (flow rate between 3.5 and 4.5 L min^{-1}).

The chambers were transparent but separated by opaque panels so that fish could not see each other. To achieve adequate water mixing, each chamber was connected to a recirculation loop made of Tygon tubing and a recirculation pump (3 L chamber: model 1046, Eheim, Stuttgart, Germany, 5 L min^{-1}; 1.5 L chamber: model AD20P-1230A, Brushless DC 12V submersible pump, 4 L min^{-1}). The volume of the recirculation loop was 16 mL for 1.5 L chambers and 52 mL for 3 L chambers. Each recirculation loop included housings for a fiber-optic oxygen probe (PyroScience Robust Oxygen Probe) as well as a temperature sensor (PyroScience P100). These were connected to a PyroScience FireSting-O_2 4-channel oxygen meter combined with a PyroScience TEX4 to have temperature correction on each channel. Dissolved oxygen levels were measured every ~2 seconds. The three chambers were also connected to a single flush pump (model 1048, Eheim, Stuttgart, Germany, 10 L min^{-1}) controlled by the Aquaresp software (V3, Denmark, Aquaresp.com).

Wet mass-specific oxygen uptake ($\dot{M}O_2$, in mg O_2 h^{-1} kg^{-1}) was measured in each respirometer by intermittent-flow respirometry (Steffensen, 1989, Svendsen et al. 2016) using 11.5-minute cycles consisting of a 4-min period of flush to renew the water in the respirometers followed by a 7.5 minute closed period to determine oxygen uptake using the slope of the decreasing dissolved oxygen in the respirometer during the last 6 minutes of the closed phase, when it had become linear.

Respirometer size was selected as to respect a chamber to fish volume ratio between 20 and 50 (Svendsen et al., 2016) and we obtained ratios between 41 and 56. The respirometry setup was cleaned before each trial with fresh water and chlorine and was rinsed thoroughly with fresh water and left to run over night with seawater. The oxygen probes used were calibrated with 100% and 0% (air sat.) solutions before each experiment (Annexe 4). Fish were fasted for a minimum of 72 hours prior to all respirometry experiments to ensure they were in a post-absorptive state (Clark et al., 2013; Chabot et al., 2016). Each trial lasted 4 days, including preparation and execution. On day one, the setup was cleaned, probes were calibrated, fish were selected and weighted and then isolated for the night in a basket floating in the holding tank. On day two, background oxygen uptake rates ($\dot{M}O_2$_b) were estimated in each empty chamber for a minimum of 40 minutes before and after every respirometry trial. Each trial started with a chase protocol followed by one minute of air exposure, a common method of estimating MMR in fishes (Roche et al., 2013; Rummer et al., 2016) and tested on *S. fasciatus* (Guitard et al., 2025). For this, fish were transferred one at the time to a circular chase arena (65 cm height × 15 cm × diameter, 50 L, depth adjusted as a function of fish height [doubling the height of the fish in water]) using a net and chased by hand until it no longer reacted to contact and tail pinching (chase duration lasted between 70 and 131 second). The fish was then removed from the arena and held out of the water for 1 minute. It was thereafter placed into a respirometry chamber, which was immediately (less than 15 s) sealed until the oxygen level reach ~ 80 % air sat. to estimate MMR. Once the MMR estimation was completed for all individuals, control of the system was switched to regular cycles controlled by Aquaresp running the 11.5-minute loops as described above, for the following ~70 hours (days 3 and 4), with the fish left undisturbed, in the dark (except for a

daily check-up with red lights), behind opaque curtains. Over this period, oxygen uptake rates of fish stabilized, and SMR could be estimated. Oxygen levels remained above 95% in the chambers during all cycles of all trials. The trials were ended at the end of day 4, when the fish were brought back to their holding tank. This protocol follows best practices for collecting and reporting respirometry data as described in Killen et al., 2021 (see Annexe 4).

3.5.4.2 Lab-Acclim trials

Laboratory estimates of SMR were also obtained from *S. fasciatus* of similar size (Tableau 22) which were captured from the same site for other projects, had not been studied *in situ*, but had been exposed to laboratory conditions for up to two years (Tableau 20). These fish were classified into two groups according to the date of their capture and thus the length of their stay in captivity. The first group of fish was captured in Fall of 2019 and subjected to respirometry trials in August and September of 2021. The second group of fish was captured in November 2021, and their oxygen uptake was studied in June 2022 (Tableau 20).

Laboratory-based respirometry was performed in two experimental water baths (including the temperature control system) identical to the one described for Lab-ISMeR. Each bath was fitted with a combination of different respirometer sizes to measure oxygen uptake of different sizes of fish while keeping the volume of water to fish between 20 and 50 (Svendsen et al., 2016). These experiments involved fish of very different sizes, but only seven *S. fasciatus* of similar size to those studied with ISMeR were retained here (Tableau 22), using the same respirometer chambers and recirculation loops used for Lab-ISMeR.

3.5.5 Data extraction

For all trials (*in situ* and laboratory) $\dot{M}O_2$ were calculated from the slopes obtained from the linear regression between oxygen uptake, in kPa, and time (h), accounting for the volume of the respirometer and its recirculation loop, adjusted for the volumes of fish and probe. Fish mass was used as an estimate of fish volume, assuming a density of 1 g mL^{-1}.

3.5.5.1 *In situ* data extraction

For each sensor type, custom R scripts were developed to extract, clean, and structure the data. Raw files were batch-processed using metadata entries that included the time of fish placement into and removal from the respirometer, as well as the durations of flush, wait, and measurement phases for each trial.

To determine the timepoints corresponding to oxygen uptake measurements, an automated routine first identified a reliable anchor point (a clear end of a measurement slope), from which previous and subsequent cycles were generated based on the known cycle duration. All extracted cycles were visually inspected using automatically generated plots to verify the positioning of slope boundaries. This step was more challenging for the 2021 HOBO data because fewer data points were available during each measurement period as the probe recorded DO only once per minute rather than every two seconds in 2022 with the PyroScience system. During this step, two fish from the 2022 trials were rejected because there were apparent signs of a malfunctioning system likely due to air remaining in the setup when the fish was introduced into the respirometer.

To obtain $\dot{M}O_2$ for each fish, only the periods corresponding to the closed measurement phases were retained. In 2021, with the HOBO logger the DO concentration was measured with salinity set to zero. Average salinity during the trials (HOBO U24-Conductivity logger) was 30 ppt, which was used to convert oxygen concentration and temperature into oxygen partial pressure (PO_2) in kPa. PO_2 was measured in 2022.

Summary statistics of DO and temperature at the end of the flush period were used to estimate ambient sea water oxygenation and temperature (Tableau 21).

Oxygen uptake rates were computed using the fishMO2 package (Chabot, 2020; Chabot et al., 2016). The calcSMR function of fishMO2 was used to calculate a low and repeatable level of metabolic rates in the respirometers (quantile p=0.2) of the $\dot{M}O_2$ values obtained for a period of ca. 24 hours of data after 3 hours acclimation. We refer to this value

as resting metabolic rate (RMR), since the trials were relatively short and the fish were not necessarily fasted. Background respiration was not measured or subtracted, as it was logistically impossible to obtain. We expected it to be negligible due to the short duration of the trials and the low water temperatures. This assumption is supported by independent laboratory measurements under similar conditions, where microbial respiration accounted for only a minimal fraction of total $\dot{M}O_2$. Low R^2 slopes in the *in situ* trials were typically associated with unsettled fish or air intrusions. To avoid excluding valid low $\dot{M}O_2$ values, each decline was visually inspected, and the minimum R^2 was chosen (between 0.7 and 0.95) using the diagnostic approach of Chabot et al. (2021), selecting a minimum R^2 that rejected non-linear declines in DO but retained linear ones.

3.5.5.2 Laboratory data extraction

Wet mass-specific oxygen uptake rates ($\dot{M}O_2$; mg O_2 h^{-1} kg^{-1}) were calculated from the slopes of linear regressions between DO (kPa) and time. Background respiration was estimated from empty respirometers before and after the fish trial and subtracted assuming a linear increase from start to end of the experiment. Using the same diagnostic evaluation of R^2 values recommended by Chabot et al. (2021), we selected an R^2 threshold of 0.85 for the laboratory trials. All slopes exceeded this value for every individual except one, which had a rejection rate of 2.84%.

SMR was estimated with the fishMO2 package (Chabot 2016; Chabot et al., 2016b) as the quantile ($p = 0.2$) of the $\dot{M}O_2$ values obtained for a period of ca. 72 hours after an acclimatation period of 10 hours. Because we have observed night activity in this species, we have estimated SMR for each individual with and without nights, retaining the lower estimate as our best estimate of SMR.

3.5.6 Statistical analysis

3.5.6.1 Comparison of RMR for ISMeR between both years

To test whether routine metabolic rates differed between the 2021 and 2022 *in situ* trials, we first confirmed normality (Shapiro–Wilk test, $p > 0.3$ for both years) and homogeneity of variance (Levene's test, $p = 0.08$). Because the assumption of equal variances was not strictly met, we applied Welch's t-test, which is robust to unequal variances, to compare RMR between years.

3.5.6.2 Comparison of SMR for Lab-ISMeR and Lab-Acclim fish

To evaluate whether standard metabolic rates (SMR) differed between laboratory fish that had never undergone *in situ* respirometry (Lab-Acclim) and those measured in the laboratory after *in situ* respirometry (Lab-ISMeR), we used Welch's t-test. This test was chosen because sample sizes were small and unequal (Lab-Acclim: $n = 7$; Lab-ISMeR: $n = 6$) and the assumption of equal variances could not be guaranteed.

3.5.6.3 Comparison of RMR from ISMeR to SMR in the lab

To extend comparisons beyond individuals measured in both settings, we compared metabolic rates between fish measured *in situ* (ISMeR) and those measured in the laboratory (Lab). The ISMeR group comprised four individuals from 2021 (unpaired) and four individuals from 2022 which were also tested in the laboratory and paired for this analysis. The Lab group comprised six Lab-ISMeR fish (four paired, see above, and two individuals measured successfully in the lab but with no valid RMR obtained *in situ* because of technological issues) and seven Lab-Acclim fish. Because the dataset contained both paired observations (2022 ISMeR–Lab-ISMeR) and independent observations (ISMeR 2021 and Lab-ISMeR-only + Lab-Acclim), we applied the partially overlapping samples t-test using the R package "Partiallyoverlapping" (Derrick et al., 2017a; Derrick et al., 2017b). This test combines information from paired and unpaired data without discarding observations and

interpolates between the paired t-test and Welch's test depending on the data structure. We used the Welch-type version (i.e., not assuming equal variances), which is Type I error robust.

3.5.6.4 Comparison of RMR from ISMeR and SMR from Lab-ISMeR

To compare metabolic rates measured *in situ* (ISMeR) and in the laboratory (Lab-ISMeR) for the same individuals sampled in 2022, we used a paired t-test. This test evaluates whether the mean within-individual difference between ISMeR and Lab measurements differs from zero. Given the small sample size (n = 4 pairs), assumptions of equal variance could not be reliably evaluated; thus, Welch's adjustment for unequal variance was applied. Body mass was also compared between the two experiments using the same paired test structure.

3.6 RESULTS

3.6.1 Abiotic factors variability

Median temperatures recorded during *in situ* respirometry trials ranged from 3.87 °C to 5.46 °C, with temperature remained close to 5 °C during most of the time, for most of the trials. Mean temperatures were similar, varying from 3.90 °C to 5.30 °C, and the standard deviations remained low (0.21 °C to 1.04 °C), reflecting limited thermal fluctuation during individual trials. These results indicate that, despite minor inter-individual differences, the thermal environment was generally stable during measurements, which is reflected by the low interquartile range for most individuals (Fig. 28; Tableau 21). Most fish experienced steady conditions throughout the measurements, with values staying close to the average and showing little variation over time. However, the thermal range in 2022 was broader than in 2021, with maximum values reaching 7.10 °C for some individuals and generally higher IQRs (interquartile range). Individuals tested in 2022 experienced higher and more variable temperatures than those tested in 2021, which influenced RMR within 2022 (Figure 31) but did not affect the comparison between years (Figure 29).

For DO, medians ranged from 79.56% to 89.44% sat. and mean DO saturation ranged between 81.30% and 89.65% sat. Standard deviations were generally low (1.42% to 6.09% sat.), indicating that most fish experienced steady oxygen conditions during the respirometry trials, at levels known not to affect SMR (Chapter 2, this thesis). Nevertheless, a few exceptions were observed in 2022, with SDs of ambient DO reaching up to 6.09% sat.

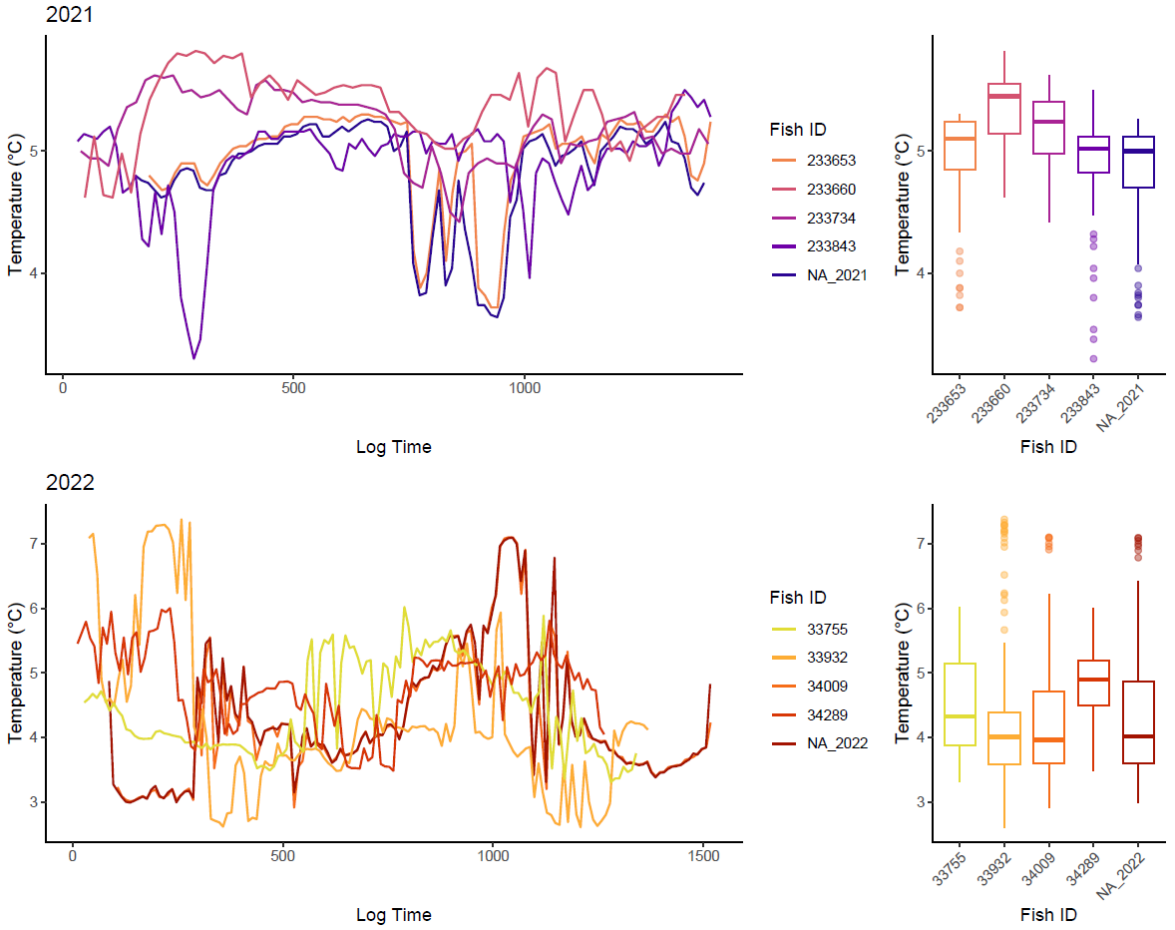

Figure 28. Temperature recorded during *in situ* respirometry trials in 2021 (top panel) and 2022 (bottom panel) for redfish (*Sebastes fasciatus*). Each line represents an individual fish, identified by its own color

Tableau 21. Summary of temperature (mean ± standard deviation, median, interquartile range (IQR), minimum, and maximum) recorded during *in situ* respirometry trials and dissolved oxygen saturation (mean ± standard deviation, median, minimum, and maximum) obtained from the end of the flushing period during respirometry trials for each individual fish (ID) in 2021 and 2022.

	Temperature					Dissolved oxygen			
ID	Mean ± SD	Median	IQR	Min	Max	Mean ± SD	Median	Min	Max
233653_2021	4.88 ± 0.46	5.12	0.25	3.72	5.30	81.43 ± 1.43	81.63	77.70	84.31
233660_2021	5.30 ± 0.21	5.46	0.34	4.92	5.68	89.65 ± 1.49	89.44	87.09	92.76
233734_2021	5.04 ± 0.23	5.25	0.42	4.42	5.38	88.15 ± 2.09	87.97	84.26	92.48
233843_2021	5.00 ± 0.26	5.02	0.26	3.96	5.50	86.36 ± 2.60	86.05	78.71	91.94
NA_2021	4.67 ± 0.52	5.04	0.40	3.64	5.24	85.12 ± 1.42	85.42	81.69	87.95
33755_2022	4.71 ± 0.74	4.31	0.62	3.31	6.02	81.30 ± 4.48	80.50	75.55	92.04
33932_2022	3.90 ± 0.71	3.87	1.17	2.61	5.94	82.22 ± 6.09	80.50	77.38	107.13
34009_2022	4.55 ± 1.04	4.04	0.75	3.20	7.10	81.44 ± 5.37	79.56	76.54	98.69
34289_2022	4.70 ± 0.61	4.83	0.40	3.48	5.81	82.40 ± 2.85	82.59	76.97	90.83
NA_2022	4.28 ± 0.99	4.02	1.26	2.99	7.10	84.35 ± 5.49	81.90	79.83	102.46

3.6.2 Comparison of RMR for ISMeR between both years

Among the individuals successfully tested *in situ*, five individuals were tested using the HOBO probe in 2021 and five with the PyroScience probe in 2022 for a total of ten individuals included in this comparison. Greater variability was observed among the five individuals measured with the HOBO probe compared to those measured with the PyroScience probe. However, RMR did not differ significantly between fish measured *in situ* in 2021 (mean = 32.65 mg O_2 h^{-1} kg^{-1}) and those measured in 2022 (mean = 34.40 mg O_2 h^{-1} kg^{-1}; Welch's t-test: t = -0.33, df = 7.89, p = 0.746; Fig. 29A).

3.6.3 Comparison of SMR for Lab-ISMeR and Lab-ACCLIM fish

Standard metabolic rates did not differ significantly between Lab-Acclim fish (n = 7, mean = 35.6 mg O_2 h^{-1} kg^{-1}) and Lab-ISMeR fish (n = 6, mean = 43.7 mg O_2 h^{-1} kg^{-1}; Welch's t-test: t = –1.78, df = 10.5, p = 0.10; Fig. 29B).

3.6.4 Comparison of RMRs from ISMeR in both years and SMRs in the lab

The partially overlapping Welch t-test indicated no significant difference in metabolic rates between RMR measured *in situ* and SMR measured in the lab (t = –1.27, df = 10.4, p = 0.23; Fig. 29C). The global dataset included ten ISMeR fish (five in 2021 and five in 2022) and 13 lab fish (six Lab-ISMeR, including four paired with ISMeR, plus seven Lab-Acclim).

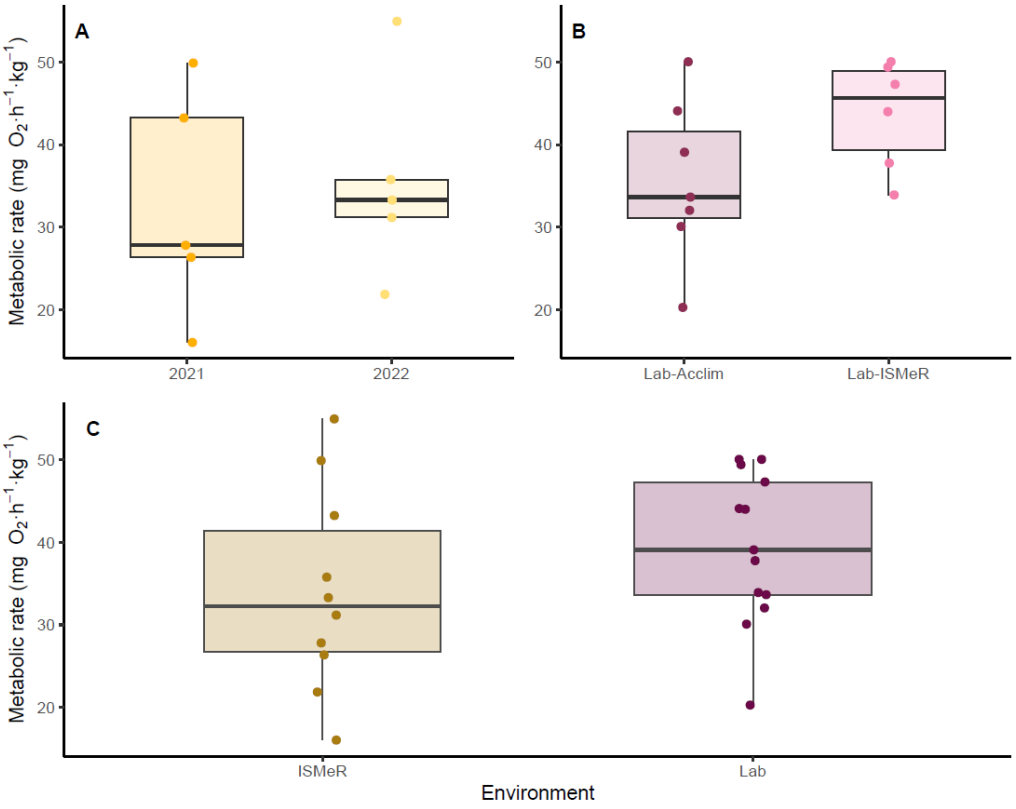

Figure 29. $\dot{M}O_2$ (mg O_2 h^{-1} kg^{-1}) of redfish (*Sebastes fasciatus*). **A)** *In situ* respirometry in 2021 using the HOBO probe (dark yellow; *n* = 5) vs. 2022 using the Pyroscience probe (yellow; *n* = 5) **B)** Laboratory measurements for acclimated lab fish (Lab-Acclim; dark red; n=7) vs the subset tested *in situ* in 2022 (Lab-ISMeR; pink; *n* = 6). **C)** $\dot{M}O_2$ across environments (ISMeR vs Lab), pooling years within ISMeR and pooling Lab-Acclim with Lab-ISMeR within Lab. All panels show basic boxplots (median, interquartile range, and 1.5×IQR whiskers) with individual fish plotted as points; no mean/CI overlays are shown. For statistical analysis, data were grouped by environment (ISMeR vs Lab), with both paired and unpaired observations accounted for using a partially overlapping samples t-test.

3.6.5 Comparison of RMR from ISMeR and SMR from Lab-ISMeR

Out of the fish tested during *in situ* respirometry and lab respirometry in 2022, four individuals had paired data for both. Their mean RMR was 30.52 ± 6.07 mg $O_2 \cdot h^{-1} \cdot kg^{-1}$ (mean mass: 58.83 ± 20.55 g), while their mean lab SMR was 43.65 ± 6.86 mg $O_2 \cdot h^{-1} \cdot kg^{-1}$ (mean mass: 61.38 ± 20.24 g). The difference between the two means was not significant (paired Welch t-test, t = –2.15, df = 3, p = 0.12; Fig. 30).

Body mass did not differ significantly between *in situ* and laboratory measurements of the same individuals (mean difference = 2.6 g; paired t-test: t = –0.32, df = 3, p = 0.77).

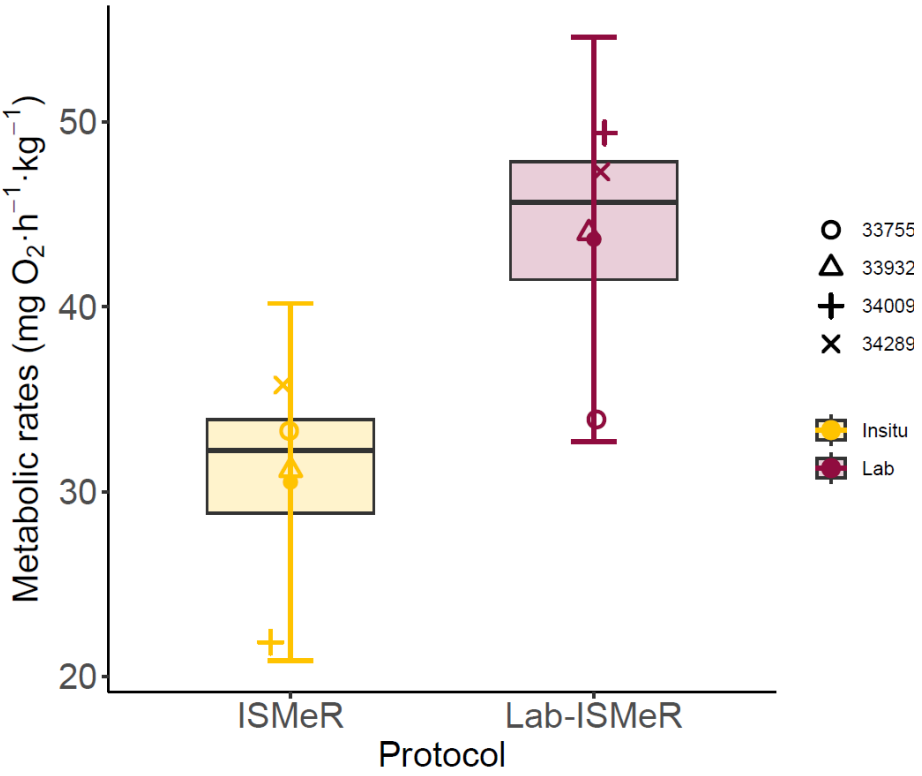

Figure 30. $\dot{M}O_2$ (mg O_2 h^{-1} kg^{-1}) for redfish (*Sebastes fasciatus*) that were measured during *in situ* respirometry (ISMeR, yellow) and on the same fish in the laboratory (Lab-ISMeR, burgundy) n = 4. Boxplots show medians, interquartile ranges, and 1.5×IQR whiskers; overlaid symbols give group means ± 95% CI. Point shape denotes PIT tag to visualize repeated measures.

3.7 DISCUSSION

To the best of our knowledge, this is the first study to measure $\dot{M}O_2$ in *S. fasciatus in situ*, offering a rare alternative to laboratory-based approaches that are often limited by the challenges of capturing and transporting this physoclistous species alive and in good condition. This is also the first study in fish to compare *in situ* and laboratory-based $\dot{M}O_2$ measurements on the same individuals, hinting on how experimental conditions may influence aerobic metabolic performance relative to the natural environment.

We initially predicted that metabolic rates measured *in situ* would exceed lab-based SMR values due to uncontrolled abiotic (temperature, oxygenation, salinity) and biotic variables (digestion, spontaneous activity, and environmental stimuli) and to the relatively short duration of field trials, which means that the fish may not have had time to acclimate to the respirometer and display $\dot{M}O_2$ values typical of SMR. However, no significant differences were detected between the best possible estimation of RMR obtained *in situ* and SMR in the lab on some of the same individuals and other similar size fish acclimated to laboratory conditions. This suggests that metabolic data collected *in situ* can provide reliable estimates of maintenance cost for *S. fasciatus* in the field. Nonetheless, the limited sample size and the inclusion of three individuals with estimated mass (two in 2021 and one in 2022; not part of the same-individual comparison) highlight the need for further replication to confirm these findings. Despite these limitations, the consistency observed on repeated individuals supports the potential of *in situ* respirometry as a valuable approach to estimate the rate of energy expenditures under relevant environmental conditions, and this approach is particularly useful for species that are difficult to transport or maintain in captivity. *In situ* respirometry offers clear benefits and applications in conservation physiology and the study of sensitive taxa.

The absence of statistical differences between field and lab estimates of maintenance metabolic rates should, however, be interpreted cautiously, as the small sample size for the ISMeR vs. Lab-ISMeR comparison strongly limited statistical power. Contrary to our initial

hypothesis, *in situ* RMR showed a trend for lower values than laboratory derived SMR. This result suggests that a larger number of observations or longer *in situ* trials could bring the current trend to statistical significance. Indeed, in our previous work on *S. fasciatus* (Guitard et al., 2025), a stable SMR was rarely reached within the first 24 h of measurement. In Guitard et al., (2025), more reliable estimates were obtained after 48 h, as $\dot{M}O_2$ gradually declined and stabilized under controlled laboratory conditions. These long periods with elevated $\dot{M}O_2$ were likely partly due to the fish being chased to elicit MMR just before placement in the respirometer. A similar period was required before low and stable values of $\dot{M}O_2$ were observed in some of the *in situ* trials as well. We couldn't dissociate whether these variable rates were caused by the stress of handling, confinement, or digestion but it is likely that extended *in situ* trials would reveal further declines in $\dot{M}O_2$, resulting in lower estimates of RMR.

As noted in our predictions, capturing fish directly from their natural habitat prevented us from assessing their digestive state, which may have influenced the $\dot{M}O_2$ measured during the early phase of the trials. Longer *in situ* respirometry trials would help reduce this uncertainty by allowing time for digestion to be completed. Another possible approach would be to control food intake prior to respirometry, for example by equipping respirometers with bait to lure fish inside and automatic closing doors, as suggested by Drazen and Yeh, (2012). This technique would reduce handling because fish would enter the chambers on their own, but it introduces new challenges, fish may not consume all the bait, and uneaten food could increase bacterial respiration. Even with such methods, extended *in situ* trial durations would remain essential to obtain reliable RMR estimates.

An additional consideration is the abiotic environment in which our trials were conducted. At Les Escoumins in the St. Lawrence Estuary, bottom temperature (~30 m: 5 °C on average) and dissolved oxygen (80–90% saturation) remained relatively stable during the *in situ* measurements despite the possible effect of tide-induced movements of water masses. At these depths, fish likely remained below the seasonal thermocline, where temperatures are consistently cold and less affected by rapid surface fluctuations. In early fall, although surface

waters start to cool, waters at ~30 m remain stable between 2 and 7 °C, a pattern maintained by seasonal stratification and the persistent cold intermediate layer (Galbraith et al., 2024). Although less variable than surface waters, temperatures at ~30 m still fluctuate seasonally, typically ranging from near 0 °C in winter to around 6–7 °C in late summer and early fall, depending on local mixing and stratification (Galbraith et al., 2024). In addition to this seasonal pattern, the area is known for tidally driven upwelling events caused by strong currents and complex bottom topography, which can bring deeper, colder water toward mid-depths (Bluteau et al., 2021; Cyr et al., 2015). These events may cause occasional short-term drops in temperature, even in warmer months. Overall, the thermal environment was consistent and representative of the cold, near-bottom conditions typically encountered by *S. fasciatus* in late fall at Les Escoumins, providing stable yet realistic conditions for metabolic measurements during that period.

In laboratory settings, fish metabolic rates usually increase with temperature across the species' natural range. In contrast, natural environments are rarely thermally constant. Work on Atlantic salmon (*Salmo salar*) has shown that diel temperature fluctuations can influence SMR depending on acclimation temperature and population origin (Oligny-Hébert et al., 2015), and more broadly, that environmental variability can substantially shape metabolic responses in ways that differ from stable laboratory settings (Enders and Boisclair, 2016). In our trials, mean bottom temperature was near 5 °C, but natural variations between 3 and 7 °C occurred during *in situ* trials. *In situ* measurements occasionally showed short increases in $\dot{M}O_2$ that coincided with small temperature peaks (Fig. 31). When examining each year separately, the relationship between RMR and temperature showed no significant variation in 2021, whereas a positive relationship was detected within the temperature range experienced by fish in 2022 (Fig. 31). However, this within-year effect was small and did not translate into differences in overall RMR between years: mean RMR did not differ significantly between all fish tested in 2021 and all fish tested in 2022 (Fig. 29A). This indicates that the quantile-based approach effectively captures resting metabolic rates despite minor within-trial temperature variation, and that *S. fasciatus* maintained stable maintenance costs under the relatively constant thermal conditions encountered *in situ*. Thus, while *in situ*

conditions at the study site facilitated comparison with laboratory experiments under stable conditions, this type of comparison may be more complex if *in situ* conditions were more variable, possibly necessitating comparison with laboratory experiments under variable biotic conditions. Caution is warranted when extending these findings to species or habitats with greater environmental variability. For example, in freshwater environments or shallow marine habitats, temperature and oxygen can fluctuate rapidly due to diel cycles, river inflows, or seasonal changes. Such variability can complicate the interpretation of *in situ* respirometry data, but it also provides valuable insight into how fish cope with unstable environmental conditions.

3.7.1 Future improvement of the setup

Few studies have successfully measured the metabolic rate of fishes *in situ* (Drazen and Seibel, 2007; Drazen and Yeh, 2012; Farrell et al., 2003), and our work represents a rare attempt to do so. However, within the context of high complexity and cost of such experiment, several technical challenges resulted in a reduced number of observations relative to the initial plan. In particular, the setup built sometimes required on-site repairs, and some valuable data were likely lost to the retention of air in the circuit. To minimize the occurrence of such issues in the future, the use of sturdier pumps would provide more consistent water flow to effectively flush out any residual air and thus decrease the risk that air remains trapped in the chambers or tubing, while helping prevent damage from debris. Visual inspection to confirm the absence of air when the setup is brought under the surface would also help in preventing this problem.

Another important source of variability was the choice of oxygen probe. In the present experiment, we tested two probes: a HOBO probe characterized by a minimum recording frequency of one measurement per minute, and a PyroScience probe, which provided recordings every second. This comparison highlighted the trade-off between affordability and data quality. While metabolic rates could be extracted from both probes, the PyroScience system generated more robust and reliable data. We did not see a statistical difference

between the two probes (as shown by the 2021 vs. 2022 comparison; Fig. 29A), but the Pyroscience data (2022) showed less variation overall. Also, the higher acquisition frequency of the Pyroscience probe made data extraction easier and more consistent by providing a greater number of datapoints for calculating reliable slopes. Since the completion of this experiment, newer probes have become available from PyroScience and other manufacturers. Based on our experience, we strongly recommend investing in high-frequency, high-precision sensors, as the quality of the oxygen signal is fundamental to the success of *in situ* respirometry.

In conclusion, our study provides the first comparison between *in situ* and lab-based aerobic metabolic rates on fish. This comparison showed that this new *in situ* respirometry setup yields estimates consistent with laboratory-based SMR. While our limited sample size prevents strong inference, the approach is promising for generating ecologically relevant metabolic data in species where traditional laboratory respirometry is impractical, such as in physoclist species. Future studies should focus on increasing sample size, extending the duration of *in situ* trials, and controlling for digestive state in order to better capture baseline metabolic demand. These improvements will help refine *in situ* respirometry as a conservation-oriented tool for studying the physiology of hard-to-access marine species.

3.8 SUPPORTING INFORMATION

Tableau 22. Metadata for redfish individuals used across all respirometry trials. Shown are the experiment type (*in situ* ISMeR using HOBO or Pyro probes, and laboratory-acclimated respirometry), individual identification (PIT-tag), wet mass at the time of testing, year of collection, and year of measurement. Grey-highlighted masses correspond to individuals for which body mass was not recorded and subsequently assigned as the mean mass of all other individuals tested in the same year.

Experiment	ID	Mass (g)	Collection year	Testing year
ISMeR - HOBO	233653	54.35	2021	2021
ISMeR - HOBO	NA	54.35	2021	2021
ISMeR - HOBO	233843	60.5	2021	2021
ISMeR - HOBO	233734	67.97	2021	2021
ISMeR - HOBO	233660	32.1	2021	2021
ISMeR - Pyro	34009	31.42	2022	2022
ISMeR - Pyro	NA	55.81	2022	2022
ISMeR - Pyro	33932	57.91	2022	2022
ISMeR - Pyro	33755	80.54	2022	2022
ISMeR - Pyro	34289	65.46	2022	2022
Lab-ISMeR	34009	34.65	2022	2022
Lab-ISMeR	34289	66.14	2022	2022
Lab-ISMeR	33871	72.5	2022	2022
Lab-ISMeR	34088	33.26	2022	2022
Lab-ISMeR	33932	61.18	2022	2022
Lab-ISMeR	33755	83.56	2022	2022
Lab-Acclim	234092	95.55	2019	2021
Lab-Acclim	233922	72.96	2019	2021
Lab-Acclim	234126	71.74	2019	2021
Lab-Acclim	33721	57.18	2021	2022
Lab-Acclim	33640	72.57	2021	2022
Lab-Acclim	33738	32.2	2021	2022
Lab-Acclim	33599	82.44	2021	2022

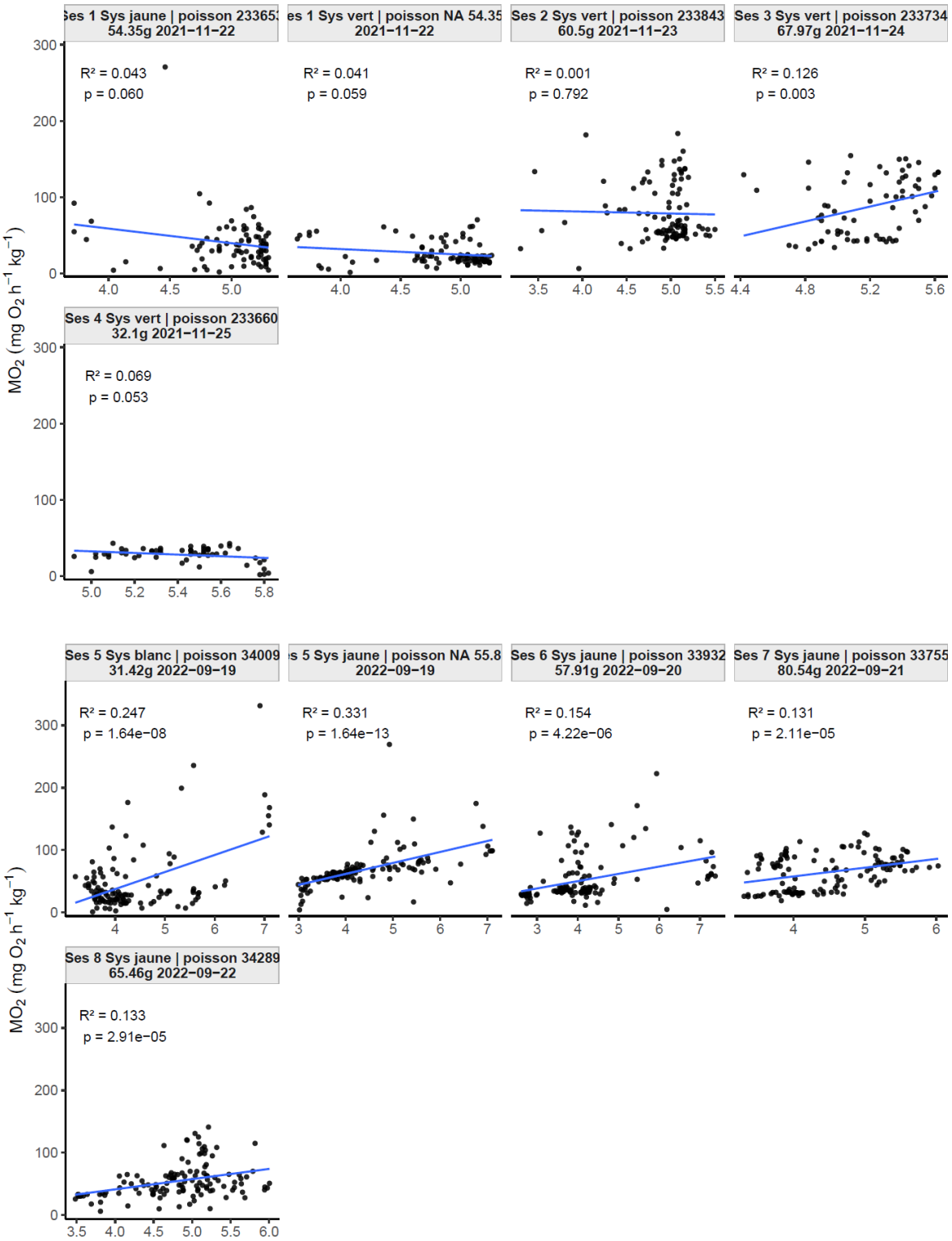
Ses 1 Sys jaune | poisson 233653
54.35g 2021−11−22
R² = 0.043
p = 0.060
es 1 Sys vert | poisson NA 54.35
2021−11−22
R² = 0.041
p = 0.059
Ses 2 Sys vert | poisson 233843
60.5g 2021−11−23
R² = 0.001
p = 0.792
Ses 3 Sys vert | poisson 233734
67.97g 2021−11−24
R² = 0.126
p = 0.003
Ses 4 Sys vert | poisson 233660
32.1g 2021−11−25
R² = 0.069
p = 0.053
Ses 5 Sys blanc | poisson 34009
31.42g 2022−09−19
R² = 0.247
p = 1.64e−08
s 5 Sys jaune | poisson NA 55.8
2022−09−19
R² = 0.331
p = 1.64e−13
Ses 6 Sys jaune | poisson 33932
57.91g 2022−09−20
R² = 0.154
p = 4.22e−06
Ses 7 Sys jaune | poisson 33755
80.54g 2022−09−21
R² = 0.131
p = 2.11e−05
Ses 8 Sys jaune | poisson 34289
65.46g 2022−09−22
R² = 0.133
p = 2.91e−05
MO2 (mg O2 h−1 kg−1)

Figure 31. Relationship between individual mass-specific oxygen consumption rate ($\dot{M}O_2$, mg O_2 h^{-1} kg^{-1}) and water temperature (°C) for all non-excluded *in situ* respirometry trials on redfish (*Sebastes fasciatus*). Panels are grouped by year (2021 first, then 2022); each panel shows one fish (session–system and PIT label). The x-axis is adaptive per panel; the y-axis is fixed within each year to aid visual comparison across individuals. A linear model ($\dot{M}O_2 \sim$ temperature) is fit per panel (solid line); the printed *p*-value is the two-sided t-test for the slope (H_0: $\beta_1 = 0$), and R^2 is the coefficient of determination from that model.

ASSEMBLY GUIDE RESPIROMETER V1.0

Author: Frédérik Bélanger

Project: Respirometer V1.0

This assembly guide presents the general steps to assemble the respirometer V1.0. It does not include all dimensions and steps to fully build the system but is directed to explaining the general steps and resources to assemble the respirometer. To find more information about the different parts used for this system, refer to the parts lists and the manufacturer's specification sheets.

First, the underwater housing from Blue Robotics was assembled following the manufacturer's instruction on their website. This housing has a custom acrylic tube length to accommodate for the batteries used to power the system. It includes an electronic tray to mount all the electronics. The underwater bulkhead connector, the underwater switch, the two blank bulkheads, and the vent bulkhead were mounted on the endcap of the housing. The bulkhead connector was installed by taping the hole on the endcap to the proper thread size. The pumps were connected to the in-line underwater connector using an underwater splicing kit from 3M and following the pin out presented on Tableau 23.

The electronics were then mounted in the housing. This includes the Arduino board, the relay mountable board, the 12V-5V power supply, the potentiometer, the Subcon connectors, the underwater switch, the batteries, the real-time clock, and the LCD screen. The electronics were connected following the following schematics (Figure 32). The Arduino

is powered by the 12V to 5V converter from Blue Robotics and the power is controlled by the underwater switch. The LCD screen and real-time clock are powered from the Arduino 3.3V and communicate using the I2C (SDA and SCL) pins in parallel. The LCD screen is used to display the start time of the cycles and the cycle time. The potentiometer is connected to 3.3V and ground of the Arduino. The cursor pin is then connected to analog pin 0 of the Arduino. The voltage measure on pin 0 is used to control the cycle times before it starts. The pumps are powered directly by the battery and controlled by the relays on the Arduino. The bulkhead connector pin out is presented in Tableau 23. The charging pins are meant to connect another in-line connector to the bulkhead so that the batteries can be charged without opening the housing. A fuse holder and fuse were added on the VCC+ lead from the batteries. More information about the programming of the Arduino can be found in the file itself.

Once the electronics were completed, a clamp system was made using the threaded rods, stainless steel hardware and PVC sheets to hold the housing shut since there is no safety on the housing and it relies only on outside pressure to stay closed. In the next version of the housings from blue robotics, this is not necessary since the housing comes with a retaining nylon ring.

The 2 Loligo chambers, the underwater housing, the pumps, and the lifting hardware were installed on the fibreglass grating using PVC sheets and stainless-steel hardware. Pump 2 was then connected using Tygon tubing to the organism chamber and one check valve so that it would flush the water from the chambers. A check valve was added to the output of the organism chamber so that the water could not go back inside. Pump 1 was mounted in between the two chambers so that the sensor chamber would get water from the organism chamber. A tube was then installed in between the two chambers to complete the loop. Plastic knobs were added to the organism chamber to make it easier for divers to open the chamber. Those knobs were attached using a small wire to make sure they wouldn’t get lost

underwater. All the tubing was secured using hose clamps. The full assembly of the respirometer is shown in Figure 33.

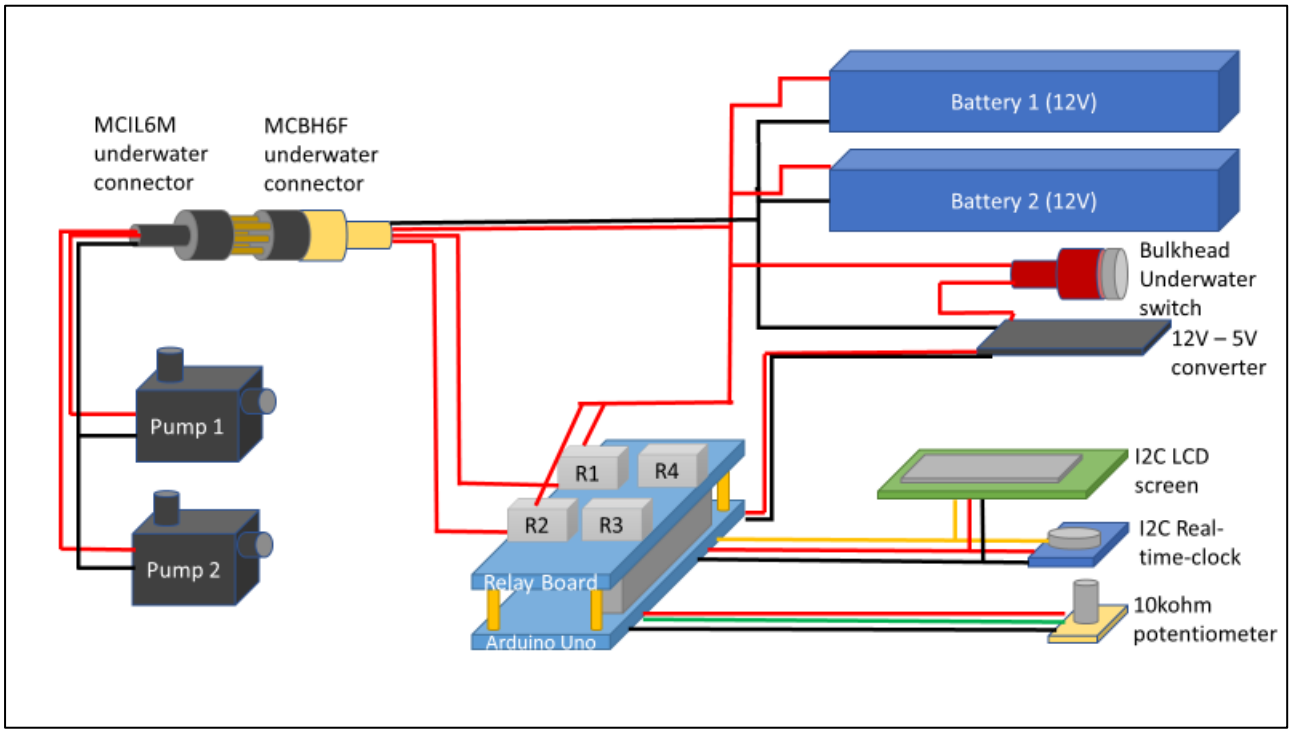

Figure 32. Electronics schematics

Tableau 23. Underwater connectors pin out

Inside housing connections	**Bulkhead and in-line pins**	**Outside housing connections**
Relay 1 VCC	1 (black)	Pump 1 (sensor) VCC
GND	2 (white)	Pump 1 and 2 GND
Relay 2 VCC	3 (red)	Pump 2 (flush) VCC
GND	4 (green)	GND charging pin
Battery VCC	5 (orange)	VCC charging pin

Battery VCC	6 (blue)	VCC charging pin

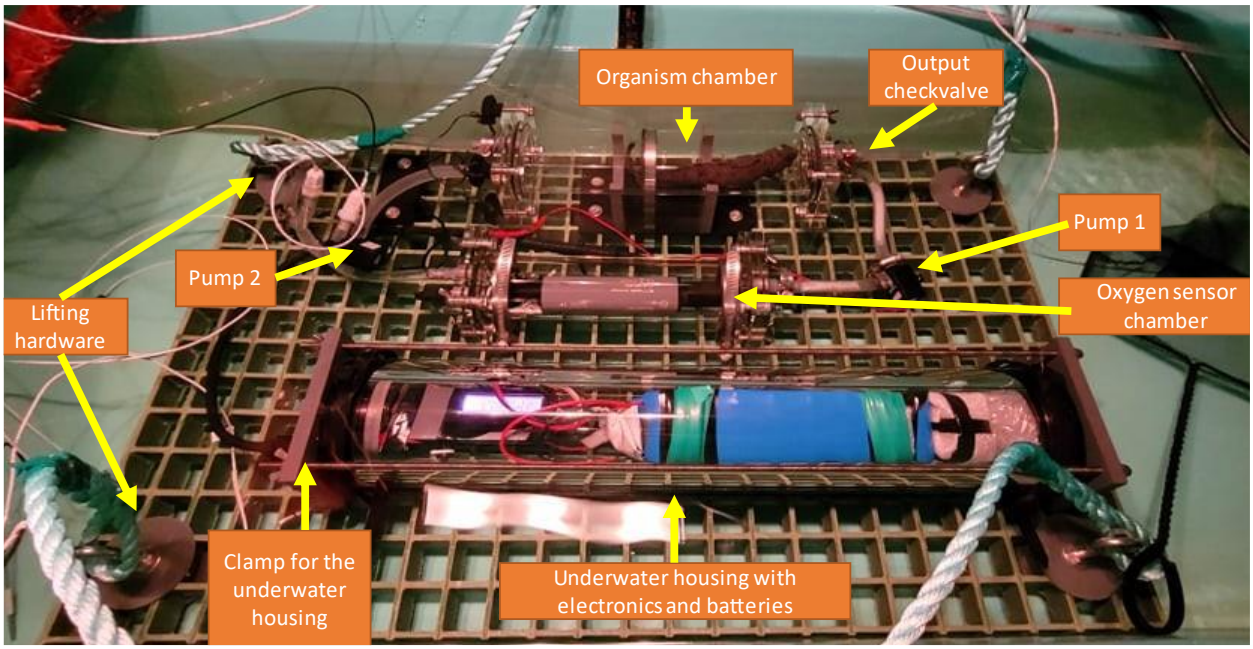

Figure 33. Assembled system

CONCLUSION GÉNÉRALE

La présente thèse avait pour objectif principal d'évaluer l'influence des conditions environnementales actuelles et futures du golfe du Saint-Laurent (GSL) sur les performances physiologiques du sébaste (*Sebastes fasciatus*). Le GSL est en plein changement, marqué par un réchauffement (Galbraith *et al*., 2025), une acidification (Mucci *et al*., 2011 ; Nesbitt et Mucci, 2021) et une diminution de l'oxygène dissous (Blais *et al*., 2025) de ses eaux profondes déjà observables. Ce type de changements physico-chimiques affectent les espèces marines, autant au niveau physiologique que populationnel (Breitburg *et al*., 2018 ; Kroeker *et al*., 2013 ; Pörtner et Farrell, 2008). Des études récentes montrent d'ailleurs que les cohortes abondantes de sébaste de 2011–2013 diffèrent nettement de celles des années 1980, avec une croissance réduite (Coussau *et al*., 2024), une taille à la maturité plus faible (Brûlé *et al*., 2024), des changements trophiques marqués (Brown-Vuillemin *et al*., 2022) et des réponses physiologiques modulées (Martínez-Silva *et al*., 2022) par les conditions environnementales. Ces tendances confirment que les transformations du GSL influencent déjà la biologie du sébaste, ce qui renforce la pertinence des résultats présentés dans cette thèse.

Malgré cette importance écologique et halieutique, les connaissances expérimentales sur la physiologie du sébaste demeurent très limitées, en grande partie en raison des difficultés associées à la capture et au maintien d'individus vivants en laboratoire. À ce jour, une seule étude a documenté le maintien de sébastes en captivité, avec un nombre restreint d'individus et des mesures limitées à la croissance et à des observations qualitatives de l'alimentation (Kohler, 1966). Dans ce contexte, les résultats présentés dans cette thèse contribuent à combler un manque important en fournissant une caractérisation quantitative et intégrée des réponses physiologiques du sébaste à des conditions environnementales actuelles et futures.

En milieu naturel, divers facteurs abiotiques peuvent moduler la croissance et la physiologie des individus (Claireaux et Lefrançois, 2007 ; Fry, 1971). Toutefois, la performance physiologique et la croissance des poissons résultent souvent de l'interaction complexe entre de multiples facteurs biotiques et abiotiques. Pour mieux comprendre les mécanismes sous-jacents à ces changements, les travaux de ce doctorat ont cherché à isoler certains des principaux facteurs abiotiques, comme la température, le pH et la saturation en oxygène dissous, et à en évaluer les effets directs dans un environnement expérimental contrôlé. Cette approche mécaniste a permis de préciser le rôle de ces contraintes environnementales dans la performance du sébaste et d'éclairer leur importance relative dans un contexte de changements climatiques. Enfin, une partie de cette recherche a visé à valider la portée des mesures effectuées sur le métabolisme en laboratoire par le développement d'une méthode de respirométrie *in situ*, permettant d'estimer les taux métaboliques directement dans l'habitat naturel des poissons, sous l'influence des conditions environnementales réelles. Ainsi, par l'entremise de cette thèse, j'ai fourni des pistes de réponses aux questions suivantes et qui sont synthétisées dans la Figure 34:

1. Les températures plus élevées et la baisse de pH prévue pour le golfe du Saint-Laurent d'ici 2061 affecteront-elles le métabolisme aérobique, la consommation de nourriture, l'efficacité de conversion alimentaire et la croissance du sébaste ?

2. Comment les niveaux d'oxygène observés et futurs de l'habitat du sébaste du GSL affectent-ils le métabolisme aérobique, la consommation de nourriture, la conversion alimentaire et comment contribuent-ils à la baisse de croissance observée du sébaste.

3. Est-il possible de développer et valider une méthode de respirométrie *in situ* permettant d'estimer les taux métaboliques du sébaste dans son environnement naturel, et dans quelle mesure ces estimations reflètent-elles celles obtenues en laboratoire ?

Les sections qui suivent présentent les principales contributions de chacun des chapitres à la littérature scientifique, les limitations des études ainsi que les perspectives qu'elles ouvrent pour de recherches futures.

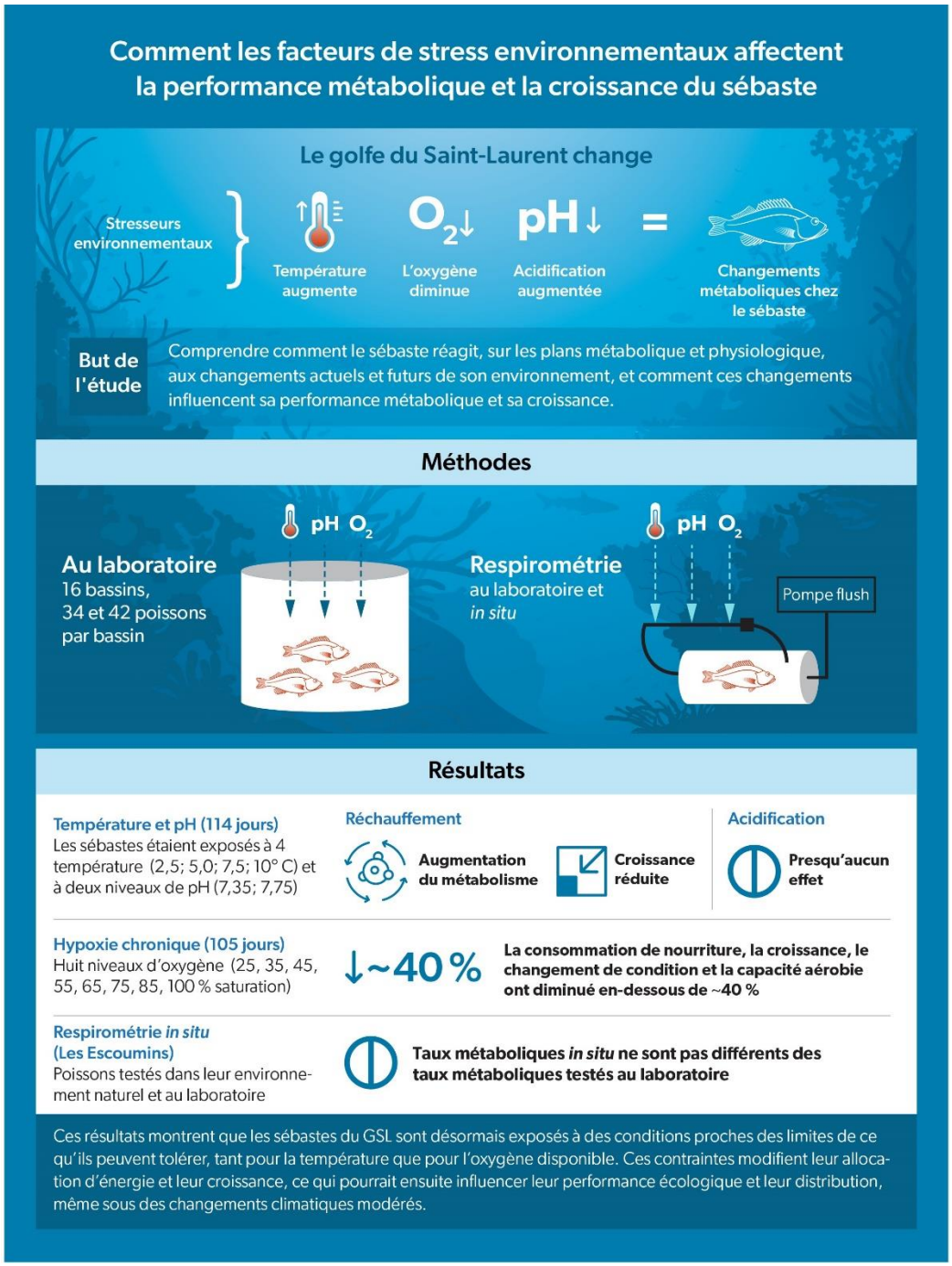

Figure 34. Schéma résumé de l'objectif, des méthodes et des principaux résultats de cette thèse.

3.9 LA FENÊTRE THERMIQUE OPTIMALE POUR LE SÉBASTE

Le Chapitre 1 avait pour objectif d'évaluer l'effet de la température et de l'acidification, séparément et de manière combinée, sur plusieurs traits physiologiques du sébaste, soit le métabolisme aérobique, la consommation de nourriture, l'efficacité de conversion alimentaire et la croissance. L'étude couvrait un gradient allant des eaux froides où l'espèce est présente dans l'estuaire et le golfe du Saint-Laurent (2,5 et 5,0 °C), une température intermédiaire (7,5 °C) et une température future de 10 °C, projetée pour la période 2061-2080 (Lavoie *et al.*, 2020). Elle incluait également deux niveaux de pH : l'un correspondant aux conditions actuelles (7,75), et l'autre à l'acidification prévue pour la seconde moitié du siècle (7,35; Mucci *et al.*, 2011). Pour ce faire, nous avons mené des expériences en bassins en exposant *S. fasciatus* à ces variables abiotiques pour une durée de 114 jours. Suite à ces expositions, les taux métaboliques ont pu être estimés par respirométrie à débit intermittent, et ce, aux mêmes conditions d'exposition. Toutes les autres variables physiologiques, telles que la consommation de nourriture et la croissance ont été mesurées durant et après l'exposition prolongée des individus.

Les résultats du **Chapitre 1** ont révélé que la hausse de température prévue pour la fin du siècle lorsqu'extrapolée aux conditions naturelles pourrait engendrer un effet marqué sur la physiologie et la croissance du sébaste, tandis que la réduction de pH testée n'a montré aucun effet détectable. Le métabolisme standard (TMS), le métabolisme maximal (TMM) et la capacité aérobie (CA) ont tous augmenté de manière linéaire avec l'exposition aux températures plus élevées. Cela indique un coût de maintenance accru (TMS), avec une augmentation plus rapide du TMM aux températures les plus élevées, se traduisant en une augmentation du potentiel énergétique (CA), c'est-à-dire de la capacité à soutenir une production aérobie d'ATP, sans pour autant refléter directement l'énergie disponible pour la croissance. au traitement le plus chaud. Cependant, la hausse de la CA ne s'est pas accompagnée d'une augmentation proportionnelle de la consommation de nourriture. Ainsi, les individus maintenus à la température la plus élevée (10 °C) ont présenté à la fois une croissance plus faible et une efficacité de conversion alimentaire réduite comparativement à

ceux des traitements plus froids. Autrement dit, même si leur capacité métabolique était augmentée, ces poissons n'ont pas consommé suffisamment de nourriture pour soutenir une croissance équivalente, ils ont aussi transformé cette nourriture en biomasse de façon moins efficace. Les résultats de ce chapitre ont donc démontré qu'une capacité aérobie élevée ne garantit pas une disponibilité élevée pour la croissance. Les résultats de ce **Chapitre 1** ont aussi montré qu'aux quatre températures d'exposition utilisées, *S. fasciatus* a performé le mieux à 2,5 et 5,0 °C. À ces températures, les poissons présentaient les taux de croissance les plus élevés, la meilleure efficacité de conversion alimentaire et une consommation de nourriture proportionnelle aux besoins métaboliques, ce qui permettait de soutenir efficacement leur croissance, contrairement aux autres traitements. La baisse du pH, simulant une acidification prévue d'ici 2100, n'a eu d'effet mesurable sur aucun des traits mesurés, excepté pour le taux métabolique standard. Dans le Chapitre 1, un pH plus faible (7,35) représentant les conditions futures, a entraîné un TMS plus élevé, ce qui suggère un coût énergétique de base accru probablement causé par la régulation acido-basique supplémentaire. Cette hausse du TMS ne s'est pas traduite par des effets mesurables sur les autres traits de performance, comme la capacité aérobie ou la croissance.

La réalisation des travaux de recherche dans le cadre du **Chapitre 1** a mené à plusieurs contributions à la littérature. Premièrement, ce fut la première expérience réussie de capture, de transport et de maintien à long terme de sébastes acadiens (*S. fasciatus*) permettant l'étude directe de leur performance physiologique. Deuxièmement, cette réussite a mené à la première analyse des réponses physiologiques de *S. fasciatus* à des conditions environnementales actuelles et futures de son habitat naturel, le golfe du Saint-Laurent. Troisièmement, bien qu'il soit difficile d'affirmer que nous avons trouvé la fenêtre thermique optimale pour la croissance, nous avons maintenant une meilleure idée des températures auxquelles ce poisson performe mieux et celles qui risquent de poser un problème dans le futur.

Un résultat surprenant de cette étude a été de constater que, bien que la croissance fût plus faible à 10 °C, l'un des bassins à cette température présentait tout de même la meilleure

croissance observée. Nous avons proposé que cette baisse de croissance pour les individus exposés à 10 °C, malgré une capacité aérobie accrue, puisse s'expliquer par l'hypothèse de la protection de la capacité aérobie (*Aerobic scope protection hypothesis*; Jutfelt *et al*., 2021). Selon cette hypothèse, des poissons consommant un repas de taille équivalente présenteraient un pic d'énergie attribué à la digestion (ADS : action dynamique spécifique ou métabolisme postprandial) plus élevé en eau chaude. Ce pic s'intensifierait à des températures encore plus élevées, réduisant ainsi le potentiel aérobie disponible pour d'autres activités. Contrairement à cette hypothèse, pour le cas spécifique de ce bassin, nous avons pu observer que les poissons capables de consommer davantage de nourriture pouvaient croître plus rapidement, considérant que leur CA était à son plus haut à la température de 10 °C. Toutefois, notre hypothèse implique que les individus sont élevés dans des bassins contrôlés, sans aucun facteur de stress, tel que le risque de prédation ou de coûts associés à la recherche de nourriture. Les résultats pourraient donc différer chez des poissons en milieu naturel ou même lors d'une expérience répétée. Afin de tester cette hypothèse chez *S. fasciatus* il serait pertinent de répéter l'expérience en adoptant une stratégie de distribution de nourriture différente, et possiblement en incluant des températures plus élevées. De plus, il serait important de monitorer l'activité des poissons dans les bassins. Les poissons aillant eu une meilleure croissance dans un des bassins à 10 °C ont su tirer avantage de la température plus chaude avec une augmentation de leur consommation de nourriture qui s'est reflété en croissance accrue, mais il est possible que leur activité générale était aussi diminuée en comparaison aux autres bassins. Dans les expériences du **Chapitre 1**, les poissons étaient nourris trois fois par semaine *ad libitum*. Offrir des repas plus fréquents, ce qui éviterait qu'ils soient limités par la capacité de leur estomac à chaque prise alimentaire, pourrait ainsi aider à tester cette hypothèse, particulièrement si l'on y ajoute des mesures de l'ADS aux différentes températures.

La baisse de croissance des sébastes observée en milieu naturel pourrait être en partie attribuable au phénomène de densité-dépendance dans un contexte de réchauffement (Coussau *et al*., 2024 ; Senay *et al*., 2023) et possiblement liée à la baisse d'un apport énergétique important : le déclin de la crevette nordique (Bourdages *et al*., 2023), identifiée

comme une proie importante (Brown-Vuillemin *et al*., 2022 ; Brown-Vuillemin *et al*., 2023). Le **Chapitre 1** a permis de démontrer que la hausse de température, même lorsque la nourriture est disponible à volonté, entraîne une diminution de la croissance aux températures les plus élevées. Dans ce contexte, les recherches futures devraient s'intéresser aux effets combinés de la température, de la limitation alimentaire et de l'oxygène dissous, afin de mieux reproduire les conditions naturelles actuelles du GSL. Sur la base des résultats des Chapitres 1 et 2, on peut prédire que l'effet de la température sur la croissance sera exacerbé sous conditions hypoxiques, de sorte que des températures intermédiaires, pour lesquelles les effets étaient limités en condition normoxique (p. ex. 7.5 °C), pourraient entraîner une diminution plus marquée de la croissance lorsque l'oxygène devient limitant.

De manière complémentaire, il est attendu que les seuils d'oxygène identifiés au **Chapitre 2** soient modulés par la température, avec l'apparition d'effets négatifs à des niveaux d'oxygène plus élevés lorsque la température augmente. Autrement dit, des niveaux d'oxygène n'ayant pas d'effet mesurable à 5 °C pourraient devenir limitants à des températures plus élevées, en raison de l'augmentation concomitante des coûts métaboliques et de la réduction de la capacité aérobie.

Une telle approche permettrait de mieux comprendre la dynamique actuellement observée, soit des taux de croissance plus faibles, une maturité sexuelle à plus petite taille et, selon les récentes évaluations, une mortalité accrue au sein du stock (Chamberland et al., 2025 ; Senay et al., 2023), en intégrant explicitement les interactions entre contraintes énergétiques et environnementales.

L'expérience élaborée pour permettre de répondre à la question posée dans le **Chapitre 1** a permis en parallèle l'investigation de l'influence des températures d'exposition sur le génome du sébaste, menée par la chercheuse Christelle Leung. Une publication sous forme d'article révisé par les pairs en a découlé (Leung *et al*., 2025). Cette étude transcriptomique a montré que l'expression génique varie significativement en fonction de la température, avec des profils relativement similaires entre 2.5 et 5.0 °C, et des différences plus marquées aux températures plus élevées. Les résultats indiquent également que la réponse

transcriptionnelle dépend à la fois des conditions d'exposition à long terme et des variations à court terme, ainsi que de leur interaction. Enfin, les poissons acclimatés à des températures plus élevées présentent une réponse plus importante aux changements thermiques aigus, notamment associée à des fonctions liées au stress, ce qui suggère que l'environnement thermique passé influence la réponse aux fluctuations de température.

3.10 MISE EN ÉVIDENCE D'UN SEUIL CRITIQUE D'OXYGÈNE POUR LA PERFORMANCE DU SÉBASTE

Le **Chapitre 2** avait pour objectif de déterminer comment une exposition prolongée à des niveaux réduits d'oxygène dissous, représentatifs des conditions rencontrées par les sébastes (*S. fasciatus* et *S. mentella*) dans le golfe du Saint-Laurent, influence leurs traits physiologiques et leurs performances de croissance. L'étude couvrait un gradient de saturation en oxygène allant de 25 à 100 % (25, 35, 45, 55, 65, 75, 85 et 100 % air sat.) (Blais *et al*., 2025 ; Senay *et al*., 2023). Pour ce faire, nous avons exposé des *S. fasciatus* à ces conditions pendant 106 jours dans des bassins contrôlés. Les taux métaboliques ont ensuite été mesurés par respirométrie à débit intermittent aux mêmes niveaux d'oxygène que ceux imposés durant l'exposition, pour les autres variables physiologiques, consommation de nourriture, efficacité de conversion alimentaire, croissance et condition corporelle, elles ont été suivies pendant et après cette exposition prolongée.

Les résultats du **Chapitre 2** ont révélé que la réduction en oxygène dissous a eu des effets négatifs clairs sur la consommation de nourriture, l'efficacité de conversion alimentaire, la croissance, le changement de leur condition. Les seuils critiques, qui sont les niveaux à partir desquels nos modèles prédisent une baisse significative de performance se situent entre 36 et 44 % de saturation (Tableau 14), marquant une zone où les capacités physiologiques des sébastes commencent à être fortement compromises. Sur le plan du métabolisme aérobique, la baisse d'oxygène dissous ambiante s'est traduite par une diminution du taux métabolique maximal (TMM) et à moindre mesure du taux métabolique standard (TMS), entraînant une réduction importante de la capacité aérobie (CA). Ces changements indiquent un affaiblissement de la capacité aérobie à soutenir la production

d'énergie pour l'activité, incluant la croissance, un effet attendu selon la littérature (Fry, 1971). Cependant, la forme de cette relation s'écarte nettement du patron prédictif de la courbe LOL (Figure 7). Plutôt qu'une baisse graduelle du TMM suivie d'un seuil abrupt, *S. fasciatus* a présenté un déclin strictement linéaire dès le premier traitement de baisse d'oxygène dissous. Ce patron, rarement documenté, hormis chez la morue franche (Dutil *et al*., 2007), met en évidence une réponse métabolique différente de celle généralement anticipée face à la diminution d'oxygène disponible.

La réalisation des travaux de recherche dans le cadre du **Chapitre 2** a mené à plusieurs contributions importantes à la littérature. Premièrement, ces travaux de recherches ont pu mettre en évidence une zone critique entre 30 et 35% de saturation en oxygène en dessous de laquelle plusieurs fonctions physiologiques sont significativement altérées. Deuxièmement, l'exposition prolongée à l'hypoxie entraîne non seulement une réduction du métabolisme aérobique, mais une cascade d'effets sur les performances énergétiques incluant la consommation alimentaire, l'efficacité de conversion, la croissance et la condition physique. Peu d'études avaient jusqu'ici examiné ces relations de manière intégrée et sur une période d'exposition aussi longue. Le **Chapitre 2** a permis de mieux comprendre la sensibilité du sébaste aux faibles saturations en oxygène, un aspect jusqu'ici peu documenté pour cette espèce. Les résultats qui découlent de ces travaux permettent de mieux prédire les performances physiologiques de *S. fasciatus* dans un milieu changeant. Les résultats indiquent que tous les traits physiologiques déclinent avec la baisse de l'oxygène dissous à partir d'un certain seuil, et ce, dans des conditions contrôlées de température et de nourriture. Ces seuils sont donc probablement sous-estimés par rapport à ceux rencontrés en milieu naturel, où les eaux se réchauffent et la nourriture se raréfie. Dans ce contexte, l'effet du réchauffement devrait accentuer cette sensibilité à l'hypoxie. En effet, les résultats du **Chapitre 1** montrent que l'augmentation de la température entraîne une hausse du métabolisme de base ainsi qu'une élévation de la tolérance à l'hypoxie (O_2crit), ce qui réduit la marge de tolérance à de faibles concentrations en oxygène. Il est donc probable que les seuils identifiés dans cette étude se déplacent vers des saturations en oxygène plus élevées à des températures au-dessus de 5 °C, rendant les individus plus sensibles à l'hypoxie que ce

qui a été observé ici à 5 °C. Dans un contexte naturel où ces conditions se combinent également à une limitation potentielle de la ressource alimentaire, les effets négatifs de l'hypoxie sur les performances physiologiques du sébaste pourraient ainsi être amplifiés.

Pour mieux comprendre comment les faibles saturations en oxygène rencontrées par les sébastes en milieu naturel influencent leur physiologie, deux grandes avenues de recherche émergent des résultats du **Chapitre 2** : (1) approfondir l'étude de l'hypoxie à différents niveaux d'organisation biologique et (2) examiner les effets combinés de l'hypoxie et de la température.

La première avenue consiste à explorer plus finement les réponses induites par l'hypoxie, du niveau moléculaire à l'organisme entier, afin de mieux relier les ajustements internes aux effets physiologiques observés, comme la croissance ou la consommation de nourriture (Zhu *et al*., 2013). Cette approche soulève ainsi des questions plus mécanistes. Par exemple, quels sont les mécanismes intrinsèques de régulation de l'appétit chez les individus exposés à de faibles niveaux d'oxygène dissous ? Quels processus internes sont déclenchés lorsqu'un seuil critique est atteint ? Certaines études menées sur d'autres espèces se sont intéressées à ces aspects, notamment en examinant les réponses transcriptomiques associées à la régulation de l'appétit dans le cerveau des poissons (Bernier *et al*., 2012 ; Bernier et Craig, 2005) ou encore l'activité de certaines enzymes digestives (Wang *et al*., 2009 ; Wu, 2002 ; Yang *et al*., 2021). Étudier ces mécanismes chez le sébaste constituerait ainsi une prochaine étape logique. De plus, il serait pertinent d'examiner la réponse postprandiale en conditions hypoxiques, notamment l'amplitude et la durée de l'action dynamique spécifique (SDA) en relation avec la capacité aérobique disponible. Dans la lignée de l'hypothèse proposée par Jutfelt et al. (2021), on peut s'attendre à ce que, sous hypoxie, le pic de SDA soit réduit afin de ne pas mobiliser l'ensemble de la capacité aérobique. Cette contrainte se traduirait par une digestion plus étalée dans le temps, plutôt que par une augmentation du pic métabolique. Ainsi, à des niveaux d'oxygène proches des seuils critiques (p. ex. ~40 % de saturation), où la consommation de nourriture demeure comparable à celle observée en normoxie mais tend à diminuer, on prédirait un SDA caractérisé par une amplitude plus faible

mais une durée prolongée, ce qui pourrait correspondre aux tendances observées aux plus faibles saturations en oxygène dans cette étude.

La seconde avenue touche aux interactions entre hypoxie et température. Les expériences du **Chapitre 2** ont été réalisées à une température stable et contrôlée de 5 °C, choisie spécifiquement pour éviter tout stress thermique (Chapitre 1 de cette thèse; Guitard *et al*., 2025). Or, nous avons montré que les traits métaboliques, incluant la tolérance à l'hypoxie aiguë (O_2crit), varient fortement avec la température, notamment avec une diminution d'O_2crit à des températures plus chaudes. Ce résultat indique que les températures d'exposition modulent le point auquel l'oxygène devient limitant (Fry, 1971). Par conséquent, combiner différentes saturations en oxygène à différents régimes de température pourrait modifier de façon importante les traits mesurés ici et influencer à la fois l'amplitude et la durée de la ADS dans le cadre d'une expérience multistresseurs. Les connaissances actuelles ouvrent ainsi la voie à des recherches intégrant les conditions hypoxiques typiques du GSL aux températures actuelles et futures, afin d'évaluer leurs effets combinés sur la physiologie du sébaste.

Une comparaison qualitative entre certaines conditions expérimentales des Chapitres 1 et 2 permet également de mettre en perspective les performances observées chez *S. fasciatus*. En considérant les conditions les plus favorables de chaque étude, soit les bassins à 5 °C dans le Chapitre 1 et ceux à 100 % de saturation en oxygène dans le Chapitre 2, il apparaît que les performances physiologiques (p. ex. croissance, efficacité de conversion alimentaire) semblent globalement supérieures dans l'expérience sur l'oxygène. Il convient toutefois de souligner que cette comparaison repose sur une évaluation visuelle des résultats et ne s'appuie pas sur des analyses statistiques formelles.

Plusieurs facteurs pourraient expliquer ces différences apparentes entre les deux expériences. D'abord, des différences dans la taille initiale des individus pourraient avoir influencé les performances mesurées, en raison de variations allométriques des taux métaboliques et de croissance. Ensuite, la variabilité naturelle entre groupes expérimentaux, ainsi que des effets saisonniers liés au moment des expériences (début vs fin de l'été),

pourraient avoir modulé l'appétit et les taux de croissance. Enfin, les conditions de pH différaient entre les deux études : le Chapitre 1 incluait des niveaux de pH plus faibles et contrôlés (7.35–7.75), alors que le Chapitre 2 se déroulait à un pH plus élevé et plus proche des conditions naturelles (~7.85–7.9). À cet égard, une diminution de l'appétit avait été observée de manière anecdotique lors de la mise en place du contrôle du pH, suggérant que ce facteur pourrait avoir contribué à réduire les performances dans le Chapitre 1.

Ces éléments mettent en évidence l'importance de considérer l'ensemble du contexte expérimental lors de l'interprétation des résultats et soulignent le potentiel d'interactions entre facteurs abiotiques, même dans des conditions considérées comme optimales.

3.11 DÉVELOPPEMENT D'UNE NOUVELLE MÉTHODE D'ESTIMATION DES TAUX MÉTABOLIQUES

L'objectif du **Chapitre 3** était de concevoir et de valider une méthode de respirométrie *in situ* pour le sébaste acadien (*S. fasciatus*), permettant d'obtenir des mesures précises et stables de la consommation d'oxygène et, ainsi, des taux métaboliques représentatifs des conditions naturelles. Cette méthode a ensuite été évaluée en comparant les taux obtenus *in situ* à ceux mesurés en laboratoire, à la fois chez les mêmes individus et chez d'autres poissons testés uniquement en laboratoire, afin d'examiner la cohérence des réponses métaboliques entre environnements. En somme, cette approche permet de rapprocher les observations issues du laboratoire des conditions naturelles et d'améliorer notre compréhension des taux métaboliques des poissons dans leur habitat naturel. De telles études sont essentielles pour améliorer notre compréhension des processus physiologiques en milieu naturel et renforcer la pertinence des travaux en conservation. Comme le soulignent Binning *et al*. (2025), combiner les données obtenues en laboratoire, les observations sur le terrain et les méthodes qui se situent entre les deux permet d'obtenir une vision plus complète et de tirer des conclusions écologiquement plus robustes.

La réalisation des travaux de recherche du **Chapitre 3** a mené à plusieurs contributions importantes à la littérature, tant sur le plan méthodologique que physiologique. Sur le plan

méthodologique, ce chapitre a permis le développement et la validation d'une méthode d'estimation des taux métaboliques directement *in situ,* adaptée à une espèce physocliste vivant à plus de 30 m de profondeur. Dans ce contexte, nous avons conçu et opéré avec succès un système simple, autonome et déployable jusqu'à 30 m, capables d'enregistrer la consommation d'oxygène de poissons vivants dans leur habitat naturel.

Ces travaux ont également permis d'identifier les améliorations techniques nécessaires pour optimiser la fiabilité du dispositif, notamment la gestion de l'air résiduel, la robustesse des pompes et la fréquence d'acquisition de données des sondes d'oxygène, tout en soulignant la supériorité des capteurs à haute fréquence (PyroScience) sur les sondes plus économiques (HOBO). Le déploiement de ce dispositif a permis la première collecte de taux métaboliques *in situ* chez *S. fasciatus*, et à la première comparaison directe entre les taux mesurés *in situ* et ceux obtenus en laboratoire sur les mêmes individus. À notre connaissance, il s'agit d'une approche inédite chez les poissons, qui ouvre la voie à de futures études comparatives entre conditions contrôlées et naturelles.

Sur le plan physiologique, les résultats du **Chapitre 3** ont montré que les taux métaboliques mesurés *in situ* étaient comparables à ceux obtenus en laboratoire, suggérant que, dans un environnement stable et représentatif de leur habitat naturel, *S. fasciatus* maintient un métabolisme de base similaire à celui observé à jeun et après acclimatation en laboratoire. Ces résultats appuient la validité écologique des mesures *in situ* et démontrent le potentiel de cette approche pour estimer les coûts énergétiques réels d'espèces difficiles à maintenir en captivité. Plus largement, ils renforcent le lien entre la physiologie expérimentale et l'écologie de terrain, offrant un nouvel outil pour intégrer la variabilité environnementale dans les études bioénergétiques et de conservation.

Malgré ces avancées méthodologiques, la respirométrie *in situ* et les résultats qui en découlent comportent certaines limites. Le petit nombre d'individus mesurés, principalement dû à la complexité du déploiement en mer et aux défis techniques rencontrés sur le terrain, réduit la puissance statistique de l'étude et limite la portée des conclusions. De plus, bien que le dispositif ait bien fonctionné, il n'est pas encore entièrement optimisé. La présence

occasionnelle d'air résiduel dans le circuit, la fragilité de certaines composantes et la différence de fréquence d'échantillonnage entre les sondes d'oxygène ont pu ajouter de la variabilité aux estimations. Ces limites ne remettent pas en question la pertinence de l'approche, mais permettent d'identifier les améliorations à faire pour ensuite la tester sur un plus grand nombre d'individus. Avec ces ajustements, la respirométrie *in situ* pourra devenir un outil encore plus robuste pour mesurer le métabolisme en milieu naturel.

Le dispositif développé dans le **Chapitre 3** représentait une première étape importante vers la validation d'une méthode permettant d'estimer les taux métaboliques directement en milieu naturel. Les résultats obtenus confirment la faisabilité de la technique et la précision du système. La prochaine étape consisterait à augmenter le nombre d'individus afin d'améliorer la robustesse des données et de mieux caractériser la variabilité interindividuelle. Un échantillonnage plus long permettrait également d'explorer plus finement le lien entre les taux métaboliques mesurés *in situ* et ceux obtenus en conditions contrôlées au laboratoire.

Pour des travaux dans des eaux plus chaudes, l'utilisation de techniques de plongée avancées permettraient le déploiement et l'utilisation de ce système à des profondeurs supérieurs à 30 m, augmentant considérablement la gamme d'espèces et d'habitats pouvant être étudiés. La mise en œuvre de ce type d'approche à de telles profondeurs requiert toutefois une équipe hautement qualifiée en plongée scientifique, en raison des contraintes logistiques et de sécurité associées à ces manipulations. Néanmoins, le dispositif développé demeure adaptable à des profondeurs plus faibles, où son déploiement peut être réalisé plus facilement, sans nécessairement recourir à des opérations de plongée spécialisées.

Une fois cette phase de validation complétée, le dispositif pourrait être utilisé dans divers contextes expérimentaux et écologiques. Par exemple, il pourrait servir à étudier la dépense énergétique d'individus exposés à des gradients abiotiques naturels (température, oxygène, courant), à mesurer le coût métabolique associé à l'ingestion d'une proie, ou encore à examiner l'influence du contexte environnemental immédiat, comme la présence de congénères, de proies ou de prédateurs. À plus long terme, un système de respirométrie *in situ* fonctionnel et robuste pourrait ainsi contribuer à répondre à une grande variété de

questions écophysiologiques, allant de l'effet des conditions naturelles sur la performance énergétique à l'évaluation du coût d'un combat avec une ligne de pêcheur.

3.12 LIMITES DE L'ÉTUDE ET PRÉCAUTIONS D'INTERPRÉTATIONS

3.12.1 Limite de l'espèce

Une limite importante de cette thèse concerne la portée des conclusions obtenues à partir d'expériences menées exclusivement sur *S. fasciatus*, alors que plusieurs des motivations de ce projet découlaient de préoccupations liées à l'avenir de *S. mentella* dans le GSL. Bien que ces deux espèces partagent un grand nombre de traits morphologiques, écologiques et physiologiques (Brown-Vuillemin *et al*., 2022 ; Brown-Vuillemin *et al*., 2023 ; Brûlé *et al*., 2024 ; Senay *et al*., 2023), elles présentent aussi des différences notables de répartition en profondeur (Stefánsson *et al*., 2009), de structuration génétique (Benestan *et al*., 2021 ; Valentin *et al*., 2014) et d'histoire démographique (Cadrin *et al*., 2010), susceptibles d'influencer leurs réponses respectives aux changements environnementaux.

La distinction entre les deux espèces a longtemps été difficile, en l'absence de critères externes fiables pour l'identification individuelle (Senay *et al*., 2022). Avant l'adoption généralisée des analyses génétiques, l'attribution des individus à l'une ou l'autre espèce reposait sur des critères imparfaits. Dans le cadre de cette thèse, l'utilisation de poissons pour lesquels l'espèce avait été confirmée génétiquement minimise ce risque, mais il demeure essentiel de souligner que les résultats obtenus ne peuvent être appliqués à *S. mentella* qu'avec prudence.

Les deux espèces ont par ailleurs connu des épisodes d'hybridation et d'introgression génétique, dont l'ampleur varie selon les populations et les écotypes (Benestan *et al*., 2021). Certains groupes intraspécifiques présentent une portion du génome de l'autre espèce, tandis que d'autres n'en montrent aucune signature. Par exemple, l'écotype de *S. mentella* présent dans le GSL porte environ 18 % du génome d'origine *S. fasciatus* (Benestan *et al*., 2021). Ces processus historiques n'impliquent pas une hybridation actuelle, mais ils soulignent que

les deux espèces n'ont pas évolué de manière totalement indépendante, ce qui pourrait influencer certains traits physiologiques ou adaptatifs (Benestan *et al*., 2021). Ils rappellent également que les réponses observées chez *S. fasciatus* pourraient refléter partiellement des traits hérités d'une histoire évolutive partagée.

Enfin, la forte structuration spatiale observée chez les deux espèces de sébastes du nord-ouest atlantique, et leur faible potentiel de dispersion, suggèrent que les réponses physiologiques pourraient varier d'une population à l'autre (Benestan *et al*., 2021). Les résultats expérimentaux obtenus ici représentent donc les réponses d'une population côtière de *S. fasciatus* du GSL, et ne doivent pas être extrapolés sans nuance à *S. mentella* ou à des populations de *S. fasciatus* provenant d'autres unités géographiques.

Dans l'ensemble, bien que *S. fasciatus* constitue un modèle pertinent pour comprendre les contraintes physiologiques auxquelles les sébastes du GSL sont exposés, les différences spatiales, génétiques et historiques entre espèces et entre écotypes ou populations invitent à une interprétation prudente.

Bien que ces éléments invitent à la prudence, plusieurs caractéristiques communes à *S. fasciatus* et *S. mentella*, notamment leur écologie, leur utilisation d'habitats soumis à de faibles saturations en oxygène et certaines similitudes physiologiques rapportées dans la littérature, suggèrent que les mécanismes mis en évidence dans cette thèse pourraient également s'appliquer, au moins en partie, à *S. mentella*. En particulier, les contraintes liées à la limitation en oxygène et à l'équilibre énergétique devraient affecter de manière comparable des espèces occupant des niches écologiques similaires dans le GSL. Ainsi, bien que la portée des résultats doive être interprétée avec prudence, ils fournissent un cadre mécaniste pertinent pour formuler des hypothèses testables chez *S. mentella*. Les travaux futurs gagneraient à inclure explicitement différentes populations et, idéalement, des individus de *S. mentella*, afin d'évaluer dans quelle mesure les tendances observées ici se généralisent à l'ensemble du complexe *Sebastes* du GSL. Toutefois, la récolte d'individus de *S. mentella* vivants demeure extrêmement difficile avec les méthodes actuelles, ce qui

explique leur absence dans nos expériences et souligne la nécessité de développer des approches d'échantillonnage adaptées, d'où le fort potentiel des mesures *in situ*.

3.12.2 Limites des études expérimentales

Il est important de souligner les limites propres à l'application des résultats expérimentaux à des conditions environnementales naturelles. Les expériences contrôlées permettent d'isoler les effets de variables spécifiques, mais elles ne reproduisent pas l'ensemble des interactions biotiques et abiotiques présentes dans le milieu. En milieu naturel, les poissons sont soumis à des fluctuations dynamiques de température, d'oxygène, de salinité et de disponibilité alimentaire, ainsi qu'à des pressions de prédation, de compétition et de densité qui peuvent modifier leur physiologie ou leur comportement énergétique. Ainsi, bien que les tendances observées en laboratoire fournissent une base robuste pour comprendre les mécanismes physiologiques sous-jacents, leur ampleur et leurs conséquences écologiques doivent être interprétées avec prudence lorsqu'on les transpose à l'échelle du GSL.

Des effets de bassin ont également été observés dans les deux études expérimentales, suggérant que certaines variations non contrôlées entre unités expérimentales ont pu influencer les réponses mesurées. Bien que l'inclusion du bassin comme effet aléatoire permette de tenir compte statistiquement de cette variabilité, elle ne permet pas d'en identifier les causes précises. Plusieurs facteurs pourraient y contribuer, notamment des différences fines dans les conditions physico-chimiques (micro-variations d'oxygène, de température ou de circulation de l'eau), des effets liés à la structure sociale ou à la densité locale, ou encore des différences dans le comportement alimentaire entre groupes.

Des approches alternatives, telles qu'une augmentation du nombre de réplicats indépendants, une redistribution plus fréquente des individus entre bassins ou l'utilisation de dispositifs expérimentaux individualisés (p. ex. chambres ou systèmes à compartiments indépendants), pourraient permettre de mieux dissocier les effets liés au traitement de ceux associés à l'unité expérimentale. Néanmoins, ces approches impliquent souvent des

compromis importants, notamment en termes de logistique, de stress pour les individus ou de perte de réalisme écologique. Dans ce contexte, le design utilisé dans cette thèse représente un compromis entre contrôle expérimental et conditions d'élevage permettant d'obtenir des réponses physiologiquement pertinentes.

Par ailleurs, une variabilité individuelle importante a été observée pour plusieurs des traits mesurés, suggérant que les réponses physiologiques ne sont pas homogènes au sein des groupes expérimentaux. Bien que les analyses reposent principalement sur des valeurs moyennes afin de dégager des tendances générales, cette variabilité pourrait refléter des différences comportementales entre individus, notamment en termes d'activité, d'accès à la nourriture ou de hiérarchie sociale.

Dans ce contexte, l'hypothèse d'une alimentation *ad libitum* uniforme mérite d'être nuancée. Bien que la nourriture ait été offerte en quantité non limitante, il est probable que tous les individus n'y aient pas eu accès de manière équivalente ou n'aient pas consommé des rations similaires. Ces différences individuelles peuvent ainsi contribuer à la variabilité observée dans les performances de croissance et d'efficacité de conversion alimentaire.

Plutôt que de constituer uniquement une source de bruit, cette variabilité pourrait représenter une composante biologique importante, reflétant la diversité des stratégies individuelles face aux contraintes environnementales. Son intégration explicite dans de futurs travaux, notamment par le suivi individuel des comportements alimentaires ou des traits physiologiques, permettrait de mieux comprendre les mécanismes sous-jacents aux réponses observées.

De plus, les différences observées entre les deux expériences de cette thèse, même dans des conditions considérées comme optimales, illustrent que des variations dans le contexte expérimental (p. ex. taille des individus, saison, conditions physico-chimiques) peuvent influencer les performances mesurées. Cela souligne que les résultats obtenus en laboratoire ne dépendent pas uniquement des variables ciblées, mais également de l'ensemble des conditions dans lesquelles les organismes sont maintenus. De futurs travaux en laboratoire

devraient intégrer des fluctuations des conditions environnementales similaires à celles observées en milieu naturel.

3.13 INTÉGRATION ET PORTÉE DES RÉSULTATS

Dans l'ensemble, les résultats issus de cette thèse s'articulent de manière cohérente autour d'un même objectif : comprendre comment les principaux facteurs de changements environnementaux du GSL (température, oxygène et acidification) influencent la performance énergétique et la croissance de *S. fasciatus*.

Cette thèse met en évidence que la capacité aérobie, bien qu'informative sur le potentiel métabolique des individus, ne constitue qu'une composante de la performance énergétique globale, celle-ci étant également contrainte par l'acquisition et l'assimilation de l'énergie ainsi que par les compromis d'allocation. Dans l'ensemble, ces travaux offrent une vision intégrée du fonctionnement physiologique du sébaste face à des conditions environnementales changeantes tout en constituant les premières données expérimentales de référence sur la physiologie de cette espèce, jusque-là pratiquement inconnue en laboratoire. Ils démontrent que la croissance et la performance métabolique du sébaste reposent sur un équilibre étroit entre la température, l'oxygène et l'accès à la nourriture, et que la rupture de cet équilibre, par réchauffement ou désoxygénation, pourrait limiter sa croissance future et possiblement sa survie dans le GSL. Ces mécanismes contribuent d'ailleurs à expliquer les ralentissements de croissance et les déclins de condition déjà observés chez les sébastes en milieu naturel au cours des dernières années (Senay *et al*., 2023). De tels changements ne sont pas anodins pour l'industrie de la pêche : une croissance réduite signifie que les poissons atteignent plus lentement les tailles commercialement recherchées, affectant à la fois la qualité du produit, la valeur économique et la capacité des pêcheurs à cibler des individus de grande taille.

Un point important à considérer concerne la pertinence de tester des conditions environnementales futures, notamment celles projetées pour la période 2060–2080, alors que la distribution du sébaste dans le golfe du Saint-Laurent pourrait évoluer en réponse aux

changements climatiques. La migration vers des zones plus nordiques constitue en effet un mécanisme d'ajustement potentiel, ce qui pourrait limiter l'exposition de l'espèce aux conditions les plus extrêmes dans le GSL. Toutefois, les résultats obtenus demeurent pertinents dans la mesure où ils permettent de caractériser les limites physiologiques et les mécanismes sous-jacents aux réponses du sébaste face à ces contraintes. Ces approches expérimentales offrent ainsi un cadre mécaniste utile pour anticiper les réponses de l'espèce, que ce soit dans le GSL ou dans d'autres habitats futurs présentant des conditions similaires.

Sur le plan écologique, ces résultats suggèrent qu'un ralentissement généralisé de la croissance pourrait entraîner des répercussions à l'échelle de la population et de l'écosystème. En modifiant la structure d'âge et de taille, notamment via des changements des traits d'histoire de vie comme la taille à maturité (Brûlé *et al*., 2024), et en renforçant les effets de densité au sein de cohortes abondantes, la croissance influence directement la dynamique démographique des stocks (Coussau *et al*., 2024). Par ailleurs, ces modifications peuvent se répercuter sur les interactions trophiques, comme en témoigne l'évolution récente du régime alimentaire du sébaste et l'augmentation de la pression de prédation sur certaines proies clés dans le golfe du Saint-Laurent (Brown-Vuillemin *et al*., 2022).

Pris ensemble, ces éléments suggèrent que les contraintes sur la croissance ne se limitent pas à une réponse individuelle aux conditions environnementales, mais participent à une cascade d'effets écologiques susceptibles de réduire la résilience du stock face à la variabilité environnementale, et ultimement, de compromettre sa capacité à soutenir le recrutement futur.

En combinant des expériences contrôlées et des mesures *in situ*, cette recherche établit un pont entre la physiologie expérimentale et l'écologie de terrain, contribuant ainsi à une compréhension plus réaliste du coût énergétique des poissons dans leur habitat naturel.

Les paramètres physiologiques et les seuils identifiés dans cette thèse offrent également un potentiel important pour des approches de modélisation visant à prédire les réponses du sébaste aux changements environnementaux. Les relations établies entre température,

oxygène dissous et performance énergétique pourraient notamment être intégrées dans des modèles bioénergétiques, afin de mieux représenter les compromis entre acquisition, allocation et utilisation de l'énergie.

L'intégration de ces approches constituerait une étape importante pour relier les mécanismes physiologiques mis en évidence ici à des prédictions à l'échelle des individus et des populations.

ANNEXES

Annexe 1. Checklist of 53 essential criteria for the reporting of methods for aquatic intermittent-flow respirometry by Killen et al., 2021.

Number	Criterion and Category	Response	Value (where required)	Units
	EQUIPMENT, MATERIALS, AND SETUP			
1	Body mass of animals at time of respirometry	Yes		
2	Volume of empty respirometers	Yes	5 and 7 liters	
3	How chamber mixing was achieved	Yes, with a pump through recirculation loop		
4	Ratio of net respirometer volume (plus any associated tubing in mixing circuit) to animal body mass	Yes chamber/fish		
5	Material of tubing used in any mixing circuit	Yes, Tygon		
6	Volume of tubing in any mixing circuit	Yes	48.5 ml for 5 L and 60 ml for 7 L	
7	Confirm volume of tubing in any mixing circuit was included in calculations of oxygen uptake	YES		
8	Material of respirometer (e.g. glass, acrylic, etc.)	Yes, glass		

9	Type of oxygen probe and data recording	Yes		
10	Sampling frequency of water dissolved oxygen	Yes	2	seconds
11	Describe placement of oxygen probe (in mixing circuit or directly in chamber)	Yes, mixing circuit		
12	Flow rate during flushing and recirculation, or confirm that chamber returned to normoxia during flushing	Yes		
13	Timing of flush/closed cycles	Yes.		
14	Wait (delay) time excluded from closed measurement cycles	Yes		
15	Frequency and method of probe calibration (for both 0 and 100% calibrations)	Yes	Once every trial	Sodium sulphite was used to obtain a 0% solution for calibration. Bubblers were used to calibrate for 100%, Calibrations were done before each trial at the temperature of the trial.
16	State whether software temperature compensation was used during recording of water oxygen concentration			
	MEASUREMENT CONDITIONS			
17	Temperature during respirometry	Yes and included in model		
18	How temperature was controlled	Yes		
19	Photoperiod during respirometry	Yes. No photoperiod. Behind black		

		curtains throughout		
20	If (and how) ambient water bath was cleaned and aerated during measurement of oxygen uptake (e.g. filtration, periodic or continuous water changes)	Yes	Once between every trial	
21	Total volume of ambient water bath and any associated reservoirs	Yes	336	Liters
22	Minimum water oxygen dissolved oxygen reached during closed phases	yes	80	% air sat
23	State whether chambers were visually shielded from external disturbance	Yes		
24	How many animals were measured during a given respirometry trial (i.e. how many animals were in the same water bath)	Yes	4 in the same water bath, 2 separated bath, total of 8	
25	If multiple animals were measured simultaneously, state whether they were able to see each other during measurements	Yes.	They could not see each other. Panel separating them	
26	Duration of animal fasting before placement in respirometer	yes	72	Hours
27	Duration of all trials combined (number of days to measure all animals in the study)	Yes	8 trials of 5 days	
28	Acclimation time to the laboratory (or time since capture for field studies) before respirometry measurements	Yes	See: Growth experiment	

	BACKGROUND RESPIRATION			
29	State whether background microbial respiration was measured and accounted for, and if so, method used (e.g. parallel measures with empty respirometry chamber, measurements before and after for all chambers while empty, both)	Yes	Before and after trials	
30	State if background respiration was measured at beginning and/or end, state how many slopes and for what duration	Yes	Beginning and end	5 slopes minimum on each end
31	State how changes in background respiration were modelled over time (e.g. linear, exponential, parallel measures)	Yes	linear	
32	Level of background respiration (e.g. as a percentage of SMR)			
33	Method and frequency of system cleaning (e.g. system bleached between each trial, UV lamp)	Yes, specified in methods		
	STANDARD OR ROUTINE METABOLIC RATE			
34	Acclimation time after transfer to chamber, or alternatively, time to reach beginning of metabolic rate measurements after introduction to chamber	Yes	16	Hours
35	Time period, within a trial, over which oxygen uptake was measured (e.g. number of hours)	Yes	3 ½	days
36	Value taken as SMR/RMR (e.g. quantile, mean of lowest 10 percent, mean of all values)	Yes	0.2 quantile (Chabot et al., 2016)	

37	Total number of slopes measured and used to derive metabolic rate (e.g. how much data were used to calculate quantiles)	Between 0 and 10% of slopes were rejected during the period estimated for SMR		
38	Whether any time periods were removed from calculations of SMR/RMR (e.g. data during acclimation, periods of high activity [e.g. daytime])	Due to some nocturnal spontaneous activity, nights were excluded for 44 individuals		
39	r^2 threshold for slopes used for SMR/RMR (or mean)	0.93 in one case but mostly 0.95		
40	Proportion of data removed due to being outliers below r-squared threshold	No outliers		
	MAXIMUM METABOLIC RATE			
41	When MMR was measured in relation to SMR (i.e. before or after)	Yes, before		
42	Method used (e.g. critical swimming speed respirometry, swim to exhaustion in swim tunnel, or chase to exhaustion)	Yes, chase + air		
43	Value taken as MMR (e.g. the highest rate of oxygen uptake value after transfer, average of highest values)	Yes, highest rate of oxygen uptake over the trial		

44	If MMR measured post-exhaustion, length of activity challenge or chase (e.g. 2 min, until exhaustion, etc.)	Yes		
45	If MMR measured post-exhaustion, state whether further air-exposure was added after exercise	Yes	1	minute
46	If MMR measured post-exhaustion, time until transfer to chamber after exhaustion or time to start of oxygen uptake recording	Yes		
47	Duration of slopes used to calculate MMR (e.g. 1 min, 5 min, etc.)	Yes		
48	Slope estimation method for MMR (e.g. rolling regression, sequential discrete time frames)	Yes. Rolling regression		
49	How absolute aerobic scope and/or factorial aerobic scope is calculated (i.e. using raw SMR and MMR, allometrically mass-adjusted SMR and MMR, or allometrically mass-adjusting aerobic scope itself)	Yes		
	DATA HANDLING AND STATISTICS			
50	Sample size	**Yes**	64	
51	How oxygen uptake rates were calculated (software or script, equation, units, etc.)	Yes		
52	Confirm that volume (mass) of animal was subtracted from respirometer volume when calculating oxygen uptake rates	Yes		
53	State whether analyses accounted for variation in body mass and describe any allometric mass-corrections or adjustments	Yes		

Annexe 2. Checklist of 53 essential criteria for the reporting of methods for aquatic intermittent-flow respirometry by Killen et al., 2021.

Number	Criterion and Category	Response	Value (where required)	Units
	EQUIPMENT, MATERIALS, AND SETUP			
1	Body mass of animals at time of respirometry	Y	Mean (± SD) 178.51 (36.25)	
2	Volume of empty respirometers	Y	5.214; 7.016	
3	How chamber mixing was achieved	Y	Closed circuit with Tygon loop + recirculation pump (Eheim 1048)	
4	Ratio of net respirometer volume (plus any associated tubing in mixing circuit) to animal body mass	Y	27-52 (mean 36, SD 4)	
5	Material of tubing used in any mixing circuit	Y	Tygon	
6	Volume of tubing in any mixing circuit	Y	48.5 (5 L chambers); 60 (7 L chambers)	
7	Confirm volume of tubing in any mixing circuit was included in calculations of oxygen uptake	Y		
8	Material of respirometer (e.g. glass, acrylic, etc.)	Y	Glass	

9	Type of oxygen probe and data recording	Y	PyroScience Robust fiber optic Oxygen probes; FireSting-O2 (4-ch) + TEX4	
10	Sampling frequency of water dissolved oxygen	Y	~ every 2 s	
11	Describe placement of oxygen probe (in mixing circuit or directly in chamber)	Y	In recirculation loop	
12	Flow rate during flushing and recirculation, or confirm that chamber returned to normoxia during flushing	Y		
13	Timing of flush/closed cycles	Y	11.5-min cycles: 4-min flush; 7.5-min closed	
14	Wait (delay) time excluded from closed measurement cycles	Y	First 1.5 min excluded; slope over last 6 min	
15	Frequency and method of probe calibration (for both 0 and 100% calibrations)	Y	0% and 100% DO calibrations before each experiment	Sodium sulphite was used to obtain a 0% solution for calibration. Bubblers were used to calibrate for 100%, Calibrations were done before each trial at the

				temperature of the trial
16	State whether software temperature compensation was used during recording of water oxygen concentration	Y		
	MEASUREMENT CONDITIONS			
17	Temperature during respirometry	Y	5°C	See table S2
18	How temperature was controlled	Y	Omega RTD probe + PID controller; mixing valves (sv3109) blending cold/warm seawater (3.5-4.5 L min-1 supply)	
19	Photoperiod during respirometry	Y	Dark (opaque curtains); daily check with red light	
20	If (and how) ambient water bath was cleaned and aerated during measurement of oxygen uptake (e.g. filtration, periodic or continuous water changes)	Y	System cleaned each trial with freshwater + chlorine; rinsed; overnight seawater run; open-circulation system	
21	Total volume of ambient water bath and any associated reservoirs	Y	336	L
22	Minimum water oxygen dissolved oxygen reached during closed phases		A diminution of between 9 and 20% maximum depending on the treatment	

23	State whether chambers were visually shielded from external disturbance	Y	They were with partitions	
24	How many animals were measured during a given respirometry trial (i.e. how many animals were in the same water bath)	Y	4 per bath (8 total when both baths used)	
25	If multiple animals were measured simultaneously, state whether they were able to see each other during measurements	Y	They were not	
26	Duration of animal fasting before placement in respirometer	Y	Between 96 and 142	hours
27	Duration of all trials combined (number of days to measure all animals in the study)	y	8 trials of 5 days, 40 days	days
28	Acclimation time to the laboratory (or time since capture for field studies) before respirometry measurements	Y	Between 1 and 3 years	
	BACKGROUND RESPIRATION			
29	State whether background microbial respiration was measured and	Y	Empty-chamber measures before and after each trial	

	accounted for, and if so, method used (e.g. parallel measures with empty respirometry chamber, measurements before and after for all chambers while empty, both)			
30	State if background respiration was measured at beginning and/or end, state how many slopes and for what duration	Y	40 min per chamber before (day 2) and after (day 5)	
31	State how changes in background respiration were modelled over time (e.g. linear, exponential, parallel measures)	Y	linear	
32	Level of background respiration (e.g. as a percentage of SMR)	Y	Mean of 3.71% Range of 0.02 to 16.9 %	
33	Method and frequency of system cleaning (e.g. system bleached between each trial, UV lamp)	Y	Between each trial: freshwater + chlorine; rinse; overnight seawater	
	STANDARD OR ROUTINE METABOLIC RATE			

34	Acclimation time after transfer to chamber, or alternatively, time to reach beginning of metabolic rate measurements after introduction to chamber	Y	~>24 h post-transfer; SMR estimated during days 3 to 5	
35	Time period, within a trial, over which oxygen uptake was measured (e.g. number of hours)	Y	~70	
36	Value taken as SMR/RMR (e.g. quantile, mean of lowest 10 percent, mean of all values)	Y	0.2 quantile	
37	Total number of slopes measured and used to derive metabolic rate (e.g. how much data were used to calculate quantiles)	Y	An average of 199 slopes with a range from 122 to 284 slopes	
38	Whether any time periods were removed from calculations of SMR/RMR (e.g. data during acclimation, periods of high activity [e.g. daytime])	Periods of high activity at night		
39	r^2 threshold for slopes used for SMR/RMR (or mean)	Y	0.90	
40	Proportion of data removed due to being	Y	Between 0 and 0.03 mean = 0.006	

	outliers below r-squared threshold			
	MAXIMUM METABOLIC RATE			
41	When MMR was measured in relation to SMR (i.e. before or after)	Y	Before	
42	Method used (e.g. critical swimming speed respirometry, swim to exhaustion in swim tunnel, or chase to exhaustion)	Y	Chase and air exposition	
43	Value taken as MMR (e.g. the highest rate of oxygen uptake value after transfer, average of highest values)	Y	Highest rate	
44	If MMR measured post-exhaustion, length of activity challenge or chase (e.g. 2 min, until exhaustion, etc.)	Y	1 to 5.77	minutes
45	If MMR measured post-exhaustion, state whether further air-exposure was added after exercise	Y	yes	
46	If MMR measured post-exhaustion, time until transfer to chamber after exhaustion or time to	Y	<15	seconds

	start of oxygen uptake recording			
47	Duration of slopes used to calculate MMR (e.g. 1 min, 5 min, etc.)	Y		
48	Slope estimation method for MMR (e.g. rolling regression, sequential discrete time frames)	Y	Rolling regression	
49	How absolute aerobic scope and/or factorial aerobic scope is calculated (i.e. using raw SMR and MMR, allometrically mass-adjusted SMR and MMR, or allometrically mass-adjusting aerobic scope itself)	Y		Using mass specific MMR and SMR
	DATA HANDLING AND STATISTICS			
50	Sample size	**Y**	8 per treatment N= 64	
51	How oxygen uptake rates were calculated (software or script, equation, units, etc.)	Y	With fish MO2 package in R	
52	Confirm that volume (mass) of animal was subtracted from respirometer volume	Y	yes	

	when calculating oxygen uptake rates			
53	State whether analyses accounted for variation in body mass and describe any allometric mass-corrections or adjustments	Y		The range of fish body masses used in this study resulted in scaling relationships close to 1 for all traits. Therefore, mass-specific metabolic rates were analysed without including body mass as a covariate in the models.

Annexe 3. Checklist of 53 essential criteria for the reporting of methods for aquatic intermittent-flow respirometry by Killen et al., 2021 adapted for *in situ* respirometry

Number	Criterion	Response	Value
1	Body mass of animals at time of respirometry	Yes	Mean assigned for unknown masses; size-appropriate individuals used; Table 22
2	Volume of empty respirometers	Yes	1.2 L (fish chamber); probe chamber 0.77 L (2021) or 1.2 L (2022)

3	How chamber mixing was achieved	Yes	Closed loop with Tygon tubing + 12V submersible pump
4	Ratio of net respirometer volume to animal body mass	Yes	23–52 (2021); 24–66 (2022)
5	Material of tubing used in any mixing circuit	Yes	Tygon
6	Volume of tubing in any mixing circuit	Yes	54 mL closed loop
7	Tubing volume included in calculations?	Yes	Included in chamber-to-fish ratio
8	Material of respirometer	Yes	Acrylic
9	Type of oxygen probe and data recording	Yes	2021: HOBO U26-001; 2022: AquapHOx (PyroScience)
10	Sampling frequency of water dissolved oxygen	Yes	2021: 1/min; 2022: 1/s
11	Placement of oxygen probe	Yes	In dedicated probe chamber connected to loop
12	Flow rate during flushing and recirculation	Yes	Recirc pump 4 L min^{-1}; flush durations described but no flow rate given
13	Timing of flush/closed cycles	Yes	2021: 7/7 min then 10/10 min; 2022: 4/6 min
14	Wait time excluded from closed measurement cycles	Yes	Last 6 min (2021 first cycles), last 9 min (2021 long cycles), last 5 min (2022)

15	Probe calibration	Yes	Sodium sulphite was used to obtain a 0% solution for calibration. Was done once before going to the field, so once before four days of use.
16	Software temperature compensation	2022 only	AquapHOx has integrated temp compensation (implicit)
17	Temperature during respirometry	Yes	Natural variability measured by both probes
18	How temperature was controlled	Yes	Ambient seawater; Natural variability
19	Photoperiod during respirometry	Yes	Natural darkness at depth
20	Ambient water bath cleaning/aeration	Not applicable	In situ seawater environment
21	Total volume of ambient water bath	Not applicable	Open ocean environment
22	Minimum dissolved oxygen during closed phases	Yes	Table 1; determined from probe readings
23	Chambers visually shielded?	No	Animals had access to the open water
24	Animals per trial	Yes	1 fish per setup, 2 setup per trial
25	Animals able to see each other?	yes	They could see all other organisms around them, but not the other respirometry setup
26	Duration of fasting before placement	Not stated	Impossible to know the state of the fish
27	Duration of all trials combined	Yes	~24 h per pair; 4 pairs per week, one week per year
28	Acclimation time before respirometry	Not applicable	Wild fish; immediate measurement after capture

29	Background respiration measured?	No	
30	Duration/number of background slopes	No	
31	Model for background respiration	No	
32	Background respiration level	No	
33	System cleaning	Not applicable	In situ deployment
34	Acclimation time after transfer	Yes	3 hours before using data for RMR
35	Time period over which oxygen uptake was measured	Yes	~24 hours
36	Value taken as SMR/RMR	Yes	RMR derived from closed-cycle slopes
37	Number of slopes used	Not stated	
38	Time periods removed	Yes	3 hours before using data for RMR
39	r^2 threshold for slopes	Yes	between 0.7 and 0.95
40	Proportion of slopes removed	Yes	
41	When MMR measured	Not applicable	
42	Method for MMR	Not applicable	
43	Value taken as MMR	Not applicable	
44	Chase duration	Not applicable	
45	Air exposure added	Not applicable	
46	Transfer time to chamber	Not applicable	

47	Duration of slopes for MMR	Not applicable	
48	Slope estimation method for MMR	Not applicable	
49	Aerobic scope calculation	Not applicable	
50	Sample size	Yes	4 pairs per year (8 fish/year) minus losses; see table 1
	How oxygen uptake was calculated	Yes	Slope of DO decline during closed phase
52	Animal mass subtracted from volume?	Yes	Mass included in chamber-to-fish ratio
53	Mass-correction/allometry	Partial	Missing masses replaced with yearly mean

Annexe 4. Checklist of 53 essential criteria for the reporting of methods for aquatic intermittent-flow respirometry by Killen et al., 2021, used for laboratory fish in the chapter 3.

Number	Criterion and Category	Response	Value (where required)	Units
	EQUIPMENT, MATERIALS, AND SETUP			
1	Body mass of animals at time of respirometry	Y	Table 22	
2	Volume of empty respirometers	Y	1.5 L and 3 L chambers	

3	How chamber mixing was achieved	Y	Tygon tubing + recirculation pump	
4	Ratio of net respirometer volume (plus any associated tubing in mixing circuit) to animal body mass	Y	41-56	
5	Material of tubing used in any mixing circuit	Y	Tygon	
6	Volume of tubing in any mixing circuit	Y	16 mL (1.5 L); 52 mL (3 L)	
7	Confirm volume of tubing in any mixing circuit was included in calculations of oxygen uptake	Y	Yes	
8	Material of respirometer (e.g. glass, acrylic, etc.)	Y	Glass	
9	Type of oxygen probe and data recording	Y	PyroScience Robust probe; FireSting-O2 + TEX4	
10	Sampling frequency of water dissolved oxygen	Y	~ every 2 s	
11	Describe placement of oxygen probe (in mixing circuit or directly in chamber)	Y	In recirculation loop	
12	Flow rate during flushing and recirculation, or confirm that chamber returned to normoxia during flushing	Y	4–5 L/min recirc; 10 L/min flush	

13	Timing of flush/closed cycles	Y	4-min flush; 7.5-min closed	
14	Wait (delay) time excluded from closed measurement cycles	Y	First 1.5 min excluded; slope over last 6 min	
15	Frequency and method of probe calibration (for both 0 and 100% calibrations)	Y	Before each experiment (0% & 100%)	Sodium sulphite was used to obtain a 0% solution for calibration.
16	State whether software temperature compensation was used during recording of water oxygen concentration	y	Yes (via TEX4)	
	MEASUREMENT CONDITIONS			
17	Temperature during respirometry	Y	6	°C
18	How temperature was controlled	Y	RTD probe + PID controller + mixing valve	
19	Photoperiod during respirometry	Y	Dark; red-light daily check	

20	If (and how) ambient water bath was cleaned and aerated during measurement of oxygen uptake (e.g. filtration, periodic or continuous water changes)	Y	Freshwater+chlorine; rinse; overnight seawater	
21	Total volume of ambient water bath and any associated reservoirs	Y	336	L
22	Minimum water oxygen dissolved oxygen reached during closed phases	Y	~80% for MMR, >95% for SMR	
23	State whether chambers were visually shielded from external disturbance	Y		
24	How many animals were measured during a given respirometry trial (i.e. how many animals were in the same water bath)	Y	3	
25	If multiple animals were measured simultaneously, state whether they were able to see each other during measurements	Y	No	
26	Duration of animal fasting before placement in respirometer	Y	≥72	hours
27	Duration of all trials combined (number of days to measure all animals in the study)	Y	4 days per trial	
28	Acclimation time to the laboratory (or time since capture for field studies) before respirometry measurements	Y	54	

	BACKGROUND RESPIRATION			
29	State whether background microbial respiration was measured and accounted for, and if so, method used (e.g. parallel measures with empty respirometry chamber, measurements before and after for all chambers while empty, both)	Y	Empty chamber before & after	
30	State if background respiration was measured at beginning and/or end, state how many slopes and for what duration	Y	≥40 min before & after	
31	State how changes in background respiration were modelled over time (e.g. linear, exponential, parallel measures)	Y	Linear	
32	Level of background respiration (e.g. as a percentage of SMR)			
33	Method and frequency of system cleaning (e.g. system bleached between each trial, UV lamp)	Y	Freshwater + chlorine; overnight seawater between each trials	
	STANDARD OR ROUTINE METABOLIC RATE			
34	Acclimation time after transfer to chamber, or alternatively, time to reach beginning of metabolic	Y	>24 h	

	rate measurements after introduction to chamber			
35	Time period, within a trial, over which oxygen uptake was measured (e.g. number of hours)	Y	~70	
36	Value taken as SMR/RMR (e.g. quantile, mean of lowest 10 percent, mean of all values)	Y	0.2 quantile, Chabot et al., 2016a	
37	Total number of slopes measured and used to derive metabolic rate (e.g. how much data were used to calculate quantiles)			
38	Whether any time periods were removed from calculations of SMR/RMR (e.g. data during acclimation, periods of high activity [e.g. daytime])	Y	Nights were excluded	
39	r^2 threshold for slopes used for SMR/RMR (or mean)	Y	Between 0.7 and 0.95	
40	Proportion of data removed due to being outliers below r-squared threshold	y	One individual had a R2 rejection % of 2.89%	
	MAXIMUM METABOLIC RATE			
41	When MMR was measured in relation to SMR (i.e. before or after)	Y	Before SMR	
42	Method used (e.g. critical swimming speed respirometry,	Y	Chase + 1-min air exposure	

	swim to exhaustion in swim tunnel, or chase to exhaustion)			
43	Value taken as MMR (e.g. the highest rate of oxygen uptake value after transfer, average of highest values)	Y	Highest oxygen uptake rate	
44	If MMR measured post-exhaustion, length of activity challenge or chase (e.g. 2 min, until exhaustion, etc.)	Y	70–131	seconds
45	If MMR measured post-exhaustion, state whether further air-exposure was added after exercise	Y	1	minute
46	If MMR measured post-exhaustion, time until transfer to chamber after exhaustion or time to start of oxygen uptake recording	Y	<15	Seconds
47	Duration of slopes used to calculate MMR (e.g. 1 min, 5 min, etc.)	NA		
48	Slope estimation method for MMR (e.g. rolling regression, sequential discrete time frames)	NA		
49	How absolute aerobic scope and/or factorial aerobic scope is calculated (i.e. using raw SMR and MMR, allometrically mass-adjusted SMR and MMR, or allometrically mass-adjusting aerobic scope itself)	NA		

	DATA HANDLING AND STATISTICS			
50	Sample size	**Y**	Table 1	
51	How oxygen uptake rates were calculated (software or script, equation, units, etc.)	y	Linear decline during closed phase	
52	Confirm that volume (mass) of animal was subtracted from respirometer volume when calculating oxygen uptake rates	Y		
53	State whether analyses accounted for variation in body mass and describe any allometric mass-corrections or adjustments	Y		

RÉFÉRENCES BIBLIOGRAPHIQUES

Abdel-Tawwab, M., Monier, M. N., Hoseinifar, S. H., & Faggio, C. (2019). Fish response to hypoxia stress: Growth, physiological, and immunological biomarkers. Fish Physiology and Biochemistry, 45, 997–1013.

ACIA. (2005). Arctic climate impact assessment - Scientific report. Cambridge University Press.

Anderson, P. J. (2000). Pandalid shrimp as indicators of ecosystem regime shift. Journal of Northwest Atlantic Fishery Science, 27, 1–18. https://doi.org/10.2960/J.v27.a1

Anderson, P. J., & Piatt, J. F. (1999). Community reorganization in the Gulf of Alaska following ocean climate regime shift. Marine Ecology Progress Series, 189, 117–123. https://doi.org/10.3354/meps189117

Arnold, S. J. (1983). Morphology, performance and fitness. American Zoologist, 23, 347–361.

Atkinson, D. B. (1984). Distribution and abundance of beaked redfish in the Gulf of St. Lawrence, 1976–1981. Journal of Northwest Atlantic Fishery Science. 5, 189–197.

Auster, P. J., Lindholm, J., & Valentine, P. C. (2003). Variation in habitat use by juvenile Acadian redfish, Sebastes fasciatus. Environmental Biology of Fishes, 68(4), 381–389. https://doi.org/10.1023/B:EBFI.0000005751.30906.d5

Axelsson, M., & Fritsche, R. (1991). Effects of exercise, hypoxia and feeding on the gastrointestinal blood flow in the Atlantic cod Gadus morhua. Journal of Experimental Biology, 158, 181–198.

Baumann, H. (2019). Experimental assessments of marine species sensitivities to ocean acidification and co-stressors: How far have we come? Canadian Journal of Zoology, 97(5), 399–408. https://doi.org/10.1139/cjz-2018-0198

Barausse, A., Michieli, A., Riginella, E., Palmeri, L., & Mazzoldi, C. (2011). Long-term changes in community composition and life-history traits in a highly exploited basin (Northern Adriatic Sea): The role of environment and anthropogenic pressures. Journal of Fish Biology, 79(6), 1453–1486.

Barton, K. (2024). MuMIn: Multi-model inference (R package version 1.48.4). https://CRAN.R-project.org/package=MuMIn

Bates, D., Mächler, M., Bolker, B., & Walker, S. (2015). Fitting linear mixed-effects models using lme4. Journal of Statistical Software, 67, 1–48.

Beauregard, D., Enders, E., & Boisclair, D. (2013). Consequences of circadian fluctuations in water temperature on the standard metabolic rate of Atlantic salmon parr (Salmo salar). Canadian Journal of Fisheries and Aquatic Sciences, 70(7), 1072–1081. https://doi.org/10.1139/cjfas-2012-0342

Behrens, J. W., Præbel, K., & Steffensen, J. F. (2006). Swimming energetics of the Barents Sea capelin (Mallotus villosus) during the spawning migration period. Journal of Experimental Marine Biology and Ecology, 331(2), 208–216. https://doi.org/10.1016/j.jembe.2005.10.012

Benestan, L. M., Rougemont, Q., Senay, C., Normandeau, E., Parent, E., Rideout, R., Bernatchez, L., Lambert, Y., Audet, C., & Parent, G. J. (2021). Population genomics and history of speciation reveal fishery management gaps in two related redfish species (Sebastes mentella and Sebastes fasciatus). Evolutionary Applications, 14(2), 588–606. https://doi.org/10.1111/eva.13143

Bennett, A. F., & Huey, R. B. (1990). Studying the evolution of physiological performance. Oxford Surveys in Evolutionary Biology, 7, 251–284.

Bernier, N. J., & Craig, P. M. (2005). CRF-related peptides contribute to stress response and regulation of appetite in hypoxic rainbow trout. American Journal of Physiology: Regulatory, Integrative and Comparative Physiology, 289, 982–990. https://doi.org/10.1152/ajpregu.00668.2004

Bernier, N. J., Gorissen, M., & Flik, G. (2012). Differential effects of chronic hypoxia and feed restriction on the expression of leptin and its receptor, food intake regulation and the endocrine stress response in common carp. Journal of Experimental Biology, 215(13), 2273–2282. https://doi.org/10.1242/jeb.066183

Bewick, V., Cheek, L., & Ball, J. (2004). Statistics review 12: Survival analysis. Critical Care, 8(5), 389–394. https://doi.org/10.1186/cc2955

Bindoff, N. L., Cheung, W. W. L., Kairo, J. G., Arístegui, J., Guinder, V. A., Hallberg, R., Hilmi, N., Jiao, N., Karim, M. S., Levin, L., O'Donoghue, S., Purca Cuicapusa, S. R., Rinkevich, B., Suga, T., Tagliabue, A., & Williamson, P. (2019). Changing ocean, marine ecosystems, and dependent communities. In H.-O. Pörtner et al. (Eds.), IPCC special report on the ocean and cryosphere in a changing climate.

Binning, S. A., Ackerly, K. L., Cooke, S. J., Fusi, M., Isaza, D. F. G., Schwieterman, G. D., Rummel, A., Hardison, E. A., Martin, S., Munson, A., & Pineda, M. (2025). The lab-field continuum in conservation physiology research: Leveraging multiple approaches to inform policy and practice. Conservation Physiology, 13, 1–14. https://doi.org/10.1093/conphys/coaf063

Blais, M., Galbraith, P. S., & Starr, M. (2025). Chemical and biological oceanographic conditions in the Gulf of St. Lawrence during 2024. Canadian Technical Report of Hydrography and Ocean Sciences, 405, vi + 87 p. https://doi.org/10.60825/gmbq-jf70

Bluteau, C. E., Galbraith, P. S., Bourgault, D., Villeneuve, V., & Tremblay, J.-É. (2021). Nutrient transport pathways in the Lower St. Lawrence Estuary: Seasonal perspectives from winter observations. Ocean Science, 17, 1509–1525.

Bourdages, H., Brassard, C., Desgagnés, M., Galbraith, P. S., Gauthier, J., Nozères, C., Scallon-Chouinard, P.-M., & Senay, C. (2023). Preliminary results from the ecosystemic survey in August 2022 in the estuary and northern Gulf of St. Lawrence. DFO Canadian Science Advisory Secretariat Research Document, 2023/074.

Bourret, A., Smith, A., Van Beveren, E., Plourde, S., Curti, K. L., Jansen, T., Richardson, D. E., Castonguay, M., Rodriguez-Ezpeleta, N., & Parent, G. J. (2023). Quantifying genetic differentiation and population assignment between two contingents of Atlantic mackerel (*Scomber scombrus*) in the Northwest Atlantic. Canadian Journal of Fisheries and Aquatic Sciences, 80, 1084–1097. https://doi.org/10.1139/cjfas-2022-0232

Breitburg, D., Levin, L. A., Oschlies, A., Grégoire, M., Chavez, F. P., Conley, D. J., Garçon, V., Gilbert, D., Gutiérrez, D., Isensee, K., Jacinto, G. S., Limburg, K. E., Montes, I., Naqvi, S. W. A., Pitcher, G. C., Rabalais, N. N., Roman, M. R., Rose, K. A., Seibel, B. A., Telszewski, M., Yasuhara, M., & Zhang, J. (2018). Declining oxygen in the global ocean and coastal waters. Science, 359. https://doi.org/10.1126/science.aam7240

Brodziak, J., Traver, M. L., & Col, L. A. (2008). The nascent recovery of the Georges Bank haddock stock. Fisheries Research, 94, 123–132. https://doi.org/10.1016/j.fishres.2008.03.009

Brown, J. H., Gillooly, J. F., Allen, A. P., Savage, V. M., & West, G. B. (2004). Toward a metabolic theory of ecology. Ecology, 85, 1771–1789.

Brown-Vuillemin, S., Chabot, D., Nozères, C., Sirois, P., & Robert, D. (2022). Diet composition of redfish (Sebastes sp.) during periods of population collapse and massive resurgence in the Gulf of St. Lawrence. Frontiers in Marine Science, 9, 963039. https://doi.org/10.3389/fmars.2022.963039

Brown-Vuillemin, S., Robert, D., Tremblay, R., Chabot, D., & Sirois, P. (2023). Feeding ecology of redfish (*Sebastes* sp.) inferred from the integrated use of fatty acid profiles as complementary dietary tracers to stomach content analysis. Journal of Fish Biology, 102, 1049–1066. https://doi.org/10.1111/jfb.15348

Brûlé, C., Benhalima, K., Roux, M.-J., Parent, G., Chavarria, C., & Senay, C. (2024). Updating knowledge of redfish (*Sebastes fasciatus*) reproduction in a changing environment, the Gulf of St. Lawrence and Laurentian Channel, Canada. Journal of Fish Biology. https://doi.org/10.1111/jfb.15677*Sebastes mentella* and

Burns, C. M. (2022). Régime alimentaire, croissance, et facteurs de recrutement des larves de sébaste (*Sebastes mentella*) dans le golfe du Saint-Laurent (Thèse de doctorat). Université du Québec à Rimouski.

Caddy, J. F. (2000). Marine catchment basin effects versus impacts of fisheries on semi-enclosed seas. ICES Journal of Marine Science, 57, 628–640.

Cadrin, S. X., Bernreuther, M., Daníelsdóttir, A. K., Hjörleifsson, E., Johansen, T., Kerr, L., Kristinsson, K., Mariani, S., Nedreaas, K., Pampoulie, C., Planque, B., Reinert, J., Saborido-Rey, F., Sigurdsson, T., & Stransky, C. (2010). Population structure of beaked redfish, Sebastes mentella: Evidence of divergence associated with different habitats. ICES Journal of Marine Science, 67(8), 1617–1630. https://doi.org/10.1093/icesjms/fsq046

Calisi, R. M., & Bentley, G. E. (2009). Lab and field experiments: Are they the same animal? Hormones and Behavior, 56, 1–10. https://doi.org/10.1016/j.yhbeh.2009.02.010

Cattano, C., Claudet, J., Domenici, P., & Milazzo, M. (2018). Living in a high CO_2 world: A global meta-analysis shows multiple trait-mediated fish responses to ocean acidification. Ecological Monographs, 88(3), 320–335. https://doi.org/10.1002/ecm.1297

Chabot, D. (2020). fishMO2: Calculate and plot the standard metabolic rate (SMR), the critical oxygen level (O_2crit) and the specific dynamic action (SDA) and related variables in fishes and crustaceans (Version 0.46).

Chabot, D., & Claireaux, G. (2008). Environmental hypoxia as a metabolic constraint on fish: The case of Atlantic cod, Gadus morhua. Marine Pollution Bulletin, 57, 287–294. https://doi.org/10.1016/j.marpolbul.2008.04.001

Chabot, D., & Dutil, J. D. (1999). Reduced growth of Atlantic cod in non-lethal hypoxic conditions. Journal of Fish Biology, 55, 472–491.

Chabot, D., Koenker, R., & Farrell, A. P. (2016a). The measurement of specific dynamic action in fishes. Journal of Fish Biology, 88(1), 152–172. https://doi.org/10.1111/jfb.12836

Chabot, D., Steffensen, J. F., & Farrell, A. P. (2016b). The determination of standard metabolic rate in fishes. Journal of Fish Biology, 88(1), 81–121. https://doi.org/10.1111/jfb.12845

Chabot, D., Zhang, Y., & Farrell, A. P. (2021). Valid oxygen uptake measurements: Using high r2 values with good intentions can bias upward the determination of standard metabolic rate. Journal of Fish Biology.

Chamberland, J.-M., Bourdages, H., Desgagnés, M., Galbraith, P. S., Isabel, L., Ouellette-Plante, J., Roux, M.-J., Scallon-Chouinard, P.-M., & Senay, C. (2025). Résultats préliminaires du relevé écosystémique d'août 2024 dans l'estuaire et le nord du golfe du Saint-Laurent. DFO Canadian Science Advisory Secretariat Research Document, 2025/032.

Chrétien, E., De Bonville, J., Guitard, J., Binning, S. A., Melis, É., Kack, A., Côté, A., Gradito, M., Papillon, A., Thelamon, V., et al. (2022). Few studies of wild animal performance account for parasite infections: A systematic review. Journal of Animal Ecology, 1–13.

Claireaux, G., & Chabot, D. (2016). Responses by fishes to environmental hypoxia: Integration through Fry's concept of aerobic metabolic scope. Journal of Fish Biology, 88(1), 232–251. https://doi.org/10.1111/jfb.12833

Claireaux, G., & Lagardère, J. P. (1999). Influence of temperature, oxygen and salinity on the metabolism of the European sea bass. Journal of Sea Research, 42(2), 157–168. https://doi.org/10.1016/S1385-1101(99)00019-2

Claireaux, G., & Lefrançois, C. (2007). Linking environmental variability and fish performance: Integration through the concept of scope for activity. Philosophical Transactions of the Royal Society B: Biological Sciences, 362(1487), 2031–2041. https://doi.org/10.1098/rstb.2007.2099

Clark, T. D., Jeffries, K. M., Hinch, S. G., & Farrell, A. P. (2011). Exceptional aerobic scope and cardiovascular performance of pink salmon (*Oncorhynchus gorbuscha*) may underlie resilience in a warming climate. Journal of Experimental Biology, 214(18), 3074–3081. https://doi.org/10.1242/jeb.060517

Clark, T. D., Sandblom, E., & Jutfelt, F. (2013). Aerobic scope measurements of fishes in an era of climate change: Respirometry, relevance and recommendations. Journal of Experimental Biology, 216(15), 2771–2782. https://doi.org/10.1242/jeb.084251

Clayton, D. H., & Byrne, R. H. (1993). Spectrophotometric seawater pH measurements: Total hydrogen ion concentration scale calibration of m-cresol purple and at-sea results. Deep-Sea Research Part I: Oceanographic Research Papers, 40, 2115–2129. https://doi.org/10.1016/0967-0637(93)90048-8

Cooley, S., Schoeman, D., Bopp, L., Boyd, P., Donner, S., Ghebrehiwet, D. Y., Ito, S.-I., Kiessling, W., Martinetto, P., Ojea, E., Racault, M.-F., Rost, B., & Skern-Mauritzen, M. (2022). Oceans and coastal ecosystems and their services. In H.-O. Pörtner et al. (Eds.), Climate change 2022: Impacts, adaptation and vulnerability.

Cornett, J. C., Hamilton, S. L., & Logan, C. A. (2024). Physiological sensitivities to hypoxia differ between co-occurring juvenile flatfishes. Journal of Experimental Marine Biology and Ecology, 578, 152033.

Coussau, L., Morissette, O., Robert, D., & Sirois, P. (2024). Drivers of growth in strong year classes of the deepwater redfish (*Sebastes mentella*) population from the Gulf of St. Lawrence derived from otolith increment-based growth chronologies. Journal of Fish Biology. https://doi.org/10.1111/jfb.15903

Craig, S., Maryland, V., & Helfrich, L. A. (2002). Understanding fish nutrition, feeds, and feeding. Virginia Cooperative Extension, 1–4.

Cubash, U., Wuebbles, D., Chen, D., Facchini, M. C., Frame, D., Mahowald, N., & Winther, J.-G. (2013). Introduction. In T. F. Stocker, D. Qin, G.-K. Plattner, M. Tignor, S. K. Allen, & J. Boschung (Eds.), Climate change 2013: The physical science basis. Contribution of Working Group I to the Fifth Assessment Report of the Intergovernmental Panel on Climate Change (pp. 1–5, xix–xx).

Cyr, F., Bourgault, D., Galbraith, P. S., & Gosselin, M. (2015). Turbulent nitrate fluxes in the Lower St. Lawrence Estuary, Canada. Journal of Geophysical Research: Oceans, 120, 2308–2330.

Cyr, F., Snook, S., Bishop, C., Galbraith, P. S., Pye, B., Chen, N., & Han, G. (2021). Conditions océanographiques physiques sur le plateau continental de Terre-Neuve-et-Labrador en 2019. DFO Canadian Science Advisory Secretariat Research Document, 2021/017.

Dell, A. I., Pawar, S., & Savage, V. M. (2011). Systematic variation in the temperature dependence of physiological and ecological traits. Proceedings of the National Academy of Sciences of the United States of America, 108(26), 10591–10596. https://doi.org/10.1073/pnas.1015178108

Derrick, B., Toher, D., & White, P. (2017a). How to compare the means of two samples that include paired observations and independent observations: A companion to Derrick, Russ, Toher and White (2017). Quantitative Methods for Psychology, 13, 120–126.

Derrick, B., Toher, D., Russ, B., & White, P. (2017b). Test statistics for the comparison of means for two samples that include both paired and independent observations. Journal of Modern Applied Statistical Methods, 16, 137–157.

DFO. (2024). Eastern Georges Bank haddock (*Melanogrammus aeglefinus*) assessment to 2023.

DFO. (2025a). Estuary and Gulf of St. Lawrence northern shrimp (*Pandalus borealis*) stock status update in 2024. DFO Canadian Science Advisory Secretariat Science Response, 2025/002.

DFO. (2025b). Units 1 and 2 redfish (*Sebastes mentella* and *Sebastes fasciatus*) stocks assessment in 2024. DFO Canadian Science Advisory Secretariat Science Advisory Report, 2025/014.

Diaz, R. J. (2001). Overview of hypoxia around the world. Journal of Environmental Quality, 30, 275–281. https://doi.org/10.2134/jeq2001.302275x

Dickson, A. G., & Millero, F. J. (1987). A comparison of the equilibrium constants for the dissociation of carbonic acid in seawater media. Deep-Sea Research Part A. Oceanographic Research Papers, 34, 1733–1743.

Dickson, A. G. (1990). Thermodynamics of the dissociation of boric acid in synthetic seawater from 273.15 to 318.15 K. Deep Sea Research Part A. Oceanographic Research Papers, 37, 755–766. https://doi.org/10.1016/0198-0149(90)90004-F

Dickson, A. G. (2010). The carbon dioxide system in seawater: Equilibrium chemistry and measurements. In U. Riebesell, V. J. Fabry, & L. Hansson (Eds.), Guide to best practices for ocean acidification research and data reporting (pp. 17–52). Publications Office of the European Union.

Drazen, J. C., & Seibel, B. A. (2007). Depth-related trends in metabolism of benthic and benthopelagic deep-sea fishes. Limnology and Oceanography, 52(5), 2306–2316. https://doi.org/10.4319/lo.2007.52.5.2306

Drazen, J. C., & Yeh, J. (2012). Respiration of four species of deep-sea demersal fishes measured in situ in the eastern North Pacific. Deep-Sea Research Part I: Oceanographic Research Papers, 60, 1–6. https://doi.org/10.1016/j.dsr.2011.09.007

Dulvy, N. K., Sadovy, Y., & Reynolds, J. D. (2003). Extinction vulnerability in marine populations. Fish and Fisheries, 4(1), 25–64.

Dupont-Prinet, A., Vagner, M., Chabot, D., & Audet, C. (2013). Impact of hypoxia on the metabolism of Greenland halibut (*Reinhardtius hippoglossoides*). Canadian Journal of Fisheries and Aquatic Sciences, 70, 461–469.

Dutil, J. D., Sylvestre, E. L., Gamache, L., Laroque, R., & Guderley, H. (2007). Burst and coast use, swimming performance and metabolism of Atlantic cod (*Gadus morhua*) in sub-lethal hypoxic conditions. Journal of Fish Biology, 71, 363–375. https://doi.org/10.1111/j.1095-8649.2007.01487.x

Eliason, E. J., & Farrell, A. P. (2014). Effect of hypoxia on specific dynamic action and postprandial cardiovascular physiology in rainbow trout (*Oncorhynchus mykiss*). Comparative Biochemistry and Physiology Part A: Molecular & Integrative Physiology, 171, 44–50.

Eliason, E. J., Clark, T. D., Hague, M. J., Hanson, L. M., Gallagher, Z. S., Jeffries, K. M., Gale, M. K., Patterson, D. A., Hinch, S. G., & Farrell, A. P. (2011). Differences in thermal tolerance among sockeye salmon populations. Science, 332(6025), 109–112. https://doi.org/10.1126/science.1199158

Enders, E. C., & Boisclair, D. (2016). Effects of environmental fluctuations on fish metabolism: Atlantic salmon (*Salmo salar*) as a case study.

Ern, R., & Jutfelt, F. (2024). The OptoReg system: A simple and inexpensive solution for regulating water oxygen. Conservation Physiology, 12, 1–8.

Ern, R., Norin, T., Gamperl, A. K., & Esbaugh, A. J. (2016). Oxygen dependence of upper thermal limits in fishes. Journal of Experimental Biology, 219(21), 3376–3383. https://doi.org/10.1242/jeb.143495

Esbaugh, A. J. (2018). Physiological implications of ocean acidification for marine fish: Emerging patterns and new insights. Journal of Comparative Physiology B, 188(1), 1–13. https://doi.org/10.1007/s00360-017-1105-6

Evans, D. O. (2007). Effects of hypoxia on scope-for-activity and power capacity of lake trout (*Salvelinus namaycush*). Canadian Journal of Fisheries and Aquatic Sciences, 64, 345–361.

Everitt, B. S., & Hothorn, T. (2010). A handbook of statistical analyses using R (2nd ed.). Chapman and Hall/CRC.

Farrell, A. P. (2016). Pragmatic perspective on aerobic scope: Peaking, plummeting, pejus and apportioning. Journal of Fish Biology, 88, 322–343.

Farrell, A. P., Lee, C. G., Tierney, K., Hodaly, A., Clutterham, S., Healey, M., Hinch, S., & Lotto, A. (2003). Field-based measurements of oxygen uptake and swimming performance with adult Pacific salmon using a mobile respirometer swim tunnel. Journal of Fish Biology, 62(1), 64–84. https://doi.org/10.1046/j.1095-8649.2003.00010.x

Farrell, A. P., & Richards, J. G. (2009). Defining hypoxia: An integrative synthesis of the responses of fish to hypoxia. In C. J. Brauner (Ed.), Fish physiology (Chap. 11, pp. 487–503). Academic Press.

Fry, F. E. J. (1948). Effects of the environment on animal activity. Publications of the Ontario Fisheries Research Laboratory No. 68. University of Toronto Press.

Fry, F. E. J. (1971). The effect of environmental factors on the physiology of fish. Fish Physiology, 6, 1–98. https://doi.org/10.1016/S1546-5098(08)60146-6

Fu, S. J., Dong, Y. W., & Killen, S. S. (2022). Aerobic scope in fishes with different lifestyles and across habitats: Trade-offs among hypoxia tolerance, swimming performance and digestion. Comparative Biochemistry and Physiology Part A: Molecular and Integrative Physiology, 272, 111277.

Galbraith, P. S., Chassé, J., Caverhill, C., Nicot, P., Gilbert, D., Lefaivre, D., & Lafleur, C. (2021). Conditions océanographiques physiques dans le golfe du Saint-Laurent en 2020. DFO Canadian Science Advisory Secretariat Research Document, 2021/045.

Galbraith, P. S., Chassé, J., Shaw, J.-L., Dumas, J., Lefaivre, D., & Bourassa, M. (2025). Physical oceanographic conditions in the Gulf of St. Lawrence during 2024. Canadian Technical Report of Hydrography and Ocean Sciences, 397.

Galic, N., Hawkins, T., & Forbes, V. E. (2019). Adverse impacts of hypoxia on aquatic invertebrates: A meta-analysis. Science of the Total Environment, 652, 736–743.

Gamperl, A. K., Rodnick, K. J., Faust, H. A., Venn, E. C., Bennett, M. T., Crawshaw, L. I., Keeley, E. R., Powell, M. S., & Li, H. W. (2002). Metabolism, swimming performance, and tissue biochemistry of high desert Redband trout (*Oncorhynchus mykiss*): Evidence for phenotypic differences in physiological function. Physiological and Biochemical Zoology, 75(5), 413–431.

Gan, L., Liu, Y. J., Tian, L. X., Yue, Y. R., Yang, H. J., Liu, F. J., Chen, Y. J., & Liang, G. Y. (2013). Effects of dissolved oxygen and dietary lysine levels on growth performance, feed conversion ratio and body composition of grass carp (*Ctenopharyngodon idella*). Aquaculture Nutrition, 19(6), 860–869.

Gascon, D. (2003). Redfish multidisciplinary research zonal program (1995–1998): Final report. Canadian Technical Report of Fisheries and Aquatic Sciences, 2462.

Gilbert, D., Sundby, B., Gobeil, C., Mucci, A., & Tremblay, G. H. (2005). A seventy-two-year record of diminishing deep-water oxygen in the St. Lawrence estuary: The northwest Atlantic connection. Limnology and Oceanography, 50(5), 1654–1666.

Gislason, H., Daan, N., Rice, J. C., & Pope, J. G. (2010). Size, growth, temperature and the natural mortality of marine fish. Fish and Fisheries, 11(2), 149–158.

Gorissen, M. H. A. G., Flik, G., & Huising, M. O. (2006). Peptides and proteins regulating food intake: A comparative view. Animal Biology, 56, 447–473.

Gräns, A., Jutfelt, F., Sandblom, E., Jönsson, E., Wiklander, K., Seth, H., Olsson, C., Dupont, S., Ortega-Martinez, O., Einarsdottir, I., Björnsson, B. T., Sundell, K., & Axelsson, M. (2014). Aerobic scope fails to explain the detrimental effects on growth resulting from warming and elevated CO_2 in Atlantic halibut. Journal of Experimental Biology, 217(5), 711–717.

Guitard, J. J., Chrétien, E., De Bonville, J., Roche, D. G., Boisclair, D., & Binning, S. A. (2022). Increased parasite load is associated with reduced metabolic rates and escape responsiveness in pumpkinseed sunfish. Journal of Experimental Biology, 225.

Guitard, J. J., Chabot, D., Senay, C., Robert, D., & Deslauriers, D. (2025). Warming, but not acidification, increases metabolism and reduces growth of redfish (*Sebastes fasciatus*) in the Gulf of St. Lawrence. Canadian Journal of Zoology, 103. doi: 10.1139/cjz-2025-0014

Guscelli, E., Noisette, F., Chabot, D., Blier, P. U., Hansen, T., Ros, M. C., Pepin, P., Skanes, K. R., & Calosi, P. (2023). Northern shrimp from multiple origins show similar sensitivity to global change drivers, but different cellular energetic capacity. Journal of Experimental Biology, 226. https://doi.org/10.1242/jeb.245400

Halsey, L. G., Killen, S. S., Clark, T. D. et Norin, T. (2018). Exploring key issues of aerobic scope interpretation in ectotherms: absolute versus factorial. Reviews in Fish Biology and Fisheries, 28(2), 405-415. https://doi.org/10.1007/s11160-018-9516-3

Hamilton, S. L., Logan, C. A., Fennie, H. W., Sogard, S. M., Barry, J. P., Makukhov, A. D., et al. (2017). Species-specific responses of juvenile rockfish to elevated pCO_2: From behavior to genomics. PLoS ONE, 12(1), 1–23. https://doi.org/10.1371/journal.pone.0169670

Hannan, K. D., & Rummer, J. L. (2018). Aquatic acidification: A mechanism underpinning maintained oxygen transport and performance in fish experiencing elevated carbon dioxide conditions. Journal of Experimental Biology, 221(5). https://doi.org/10.1242/jeb.154559

Hartig, F. (2022). DHARMa: Residual diagnostics for hierarchical (multi-level/mixed) regression models (R package version 0.4.6). https://CRAN.R-project.org/package=DHARMa

Head, E. J. H., Brickman, D., & Harris, L. R. (2005). An exceptional haddock year class and unusual environmental conditions on the Scotian Shelf in 1999. Journal of Plankton Research, *27*(6), 597–602. https://doi.org/10.1093/plankt/fbi019

Heuer, R. M., & Grosell, M. (2014). Physiological impacts of elevated carbon dioxide and ocean acidification on fish. American Journal of Physiology: Regulatory, Integrative and Comparative Physiology, 307(9), R1061–R1084. https://doi.org/10.1152/ajpregu.00064.2014

Holling, C. S. (1973). Resilience and stability of ecological systems. Annual Review of Ecology and Systematics, 4, 1–23.

Holt, R. E., & Jørgensen, C. (2015). Climate change in fish: Effects of respiratory constraints on optimal life history and behaviour. Biology Letters, 11. https://doi.org/10.1098/rsbl.2014.1032

Hrycik, A. R., Almeida, L. Z., & Höök, T. O. (2017). Sub-lethal effects on fish provide insight into a biologically relevant threshold of hypoxia. Oikos, 126, 307–317.

Hulbert, A. J., & Else, P. L. (2000). Mechanisms underlying the cost of living in animals. Annual Review of Physiology, 62, 207–235.

Hutchings, J. A., & Myers, R. A. (1994). What can be learned from the collapse of a renewable resource? Atlantic cod (*Gadus morhua*) of Newfoundland and Labrador. Canadian Journal of Fisheries and Aquatic Sciences, 51(9), 2126–2146.

IPCC. (2021). Summary for policymakers. In Climate change 2021: The physical science basis. Contribution of Working Group I to the Sixth Assessment Report of the Intergovernmental Panel on Climate Change.

IPCC. (2023). Climate change 2023: Synthesis report. Contribution of Working Groups I, II and III to the Sixth Assessment Report of the Intergovernmental Panel on Climate Change.

Jobling, M. (1983). Growth studies with fish: Overcoming the problems of size variation. Journal of Fish Biology, 153–157.

Jobling, M. (1994). Fish bioenergetics. Chapman & Hall, London, UK. https://doi.org/10.1016/0044-8486(95)90056-x

Jordan, A. D., & Steffensen, J. F. (2007). Effects of ration size and hypoxia on specific dynamic action in cod. Physiological and Biochemical Zoology, 80, 178–185.

Jutfelt, F., Norin, T., Åsheim, E., Rowsey, L., Andreassen, A., Morgan, R., Clark, T., & Speers-Roesch, B. (2021). Aerobic scope protection reduces ectotherm growth under warming. Functional Ecology. https://doi.org/10.1111/1365-2435.13811

Jutfelt, F., Norin, T., Ern, R., Overgaard, J., Wang, T., McKenzie, D. J., Lefevre, S., Nilsson, G. E., Metcalfe, N. B., Hickey, A. J. R., Brijs, J., Speers-Roesch, B., Roche, D. G., Gamperl, A. K., Raby, G. D., Morgan, R., Esbaugh, A. J., Gräns, A., Axelsson, M., Ekström, A., Sandblom, E., Binning, S. A., Hicks, J. W., Seebacher, F., Jorgensen, C., Killen, S. S., Schulte, P., Clark, T. D. (2018). Oxygen- and capacity-limited thermal tolerance: Blurring ecology and physiology. Journal of Experimental Biology, 221(1), 2016–2019. https://doi.org/10.1242/jeb.169615

Jutras, M., Dufour, C. O., Mucci, A., Cyr, F., & Gilbert, D. (2020). Temporal changes in the causes of the observed oxygen decline in the St. Lawrence Estuary. Journal of Geophysical Research: Oceans, 125(12), 1–20. https://doi.org/10.1029/2020JC016577

Jutras, M., Mucci, A., Chaillou, G., Nesbitt, W. A., & Wallace, D. W. R. (2023). Temporal and spatial evolution of bottom-water hypoxia in the St. Lawrence estuarine system. Biogeosciences, 20(4), 839–849. https://doi.org/10.5194/bg-20-839-2023

Kelly, G. F., Earl, P. M., & Kaylor, J. D. (1972). Redfish. In NOAA NMFS Extension Fish Facts Publication (No. 1).

Killen, S. S., Marras, S., Ryan, M. R., Domenici, P., & McKenzie, D. J. (2012). A relationship between metabolic rate and risk-taking behaviour is revealed during hypoxia in juvenile European sea bass. Functional Ecology, 26(1), 134–143. https://doi.org/10.1111/j.1365-2435.2011.01920.x

Killen, S. S., Norin, T., & Halsey, L. G. (2017). Do method and species lifestyle affect measures of maximum metabolic rate in fishes? Journal of Fish Biology, 90, 1037–1046.

Killen, S. S., Christensen, E. A. F., Cortese, D., Závorka, L., Norin, T., Cotgrove, L., Crespel, A., Munson, A., Nati, J. J. H., Papatheodoulou, M., et al. (2021). Guidelines for reporting methods to estimate metabolic rates by aquatic intermittent-flow respirometry. Journal of Experimental Biology, 224.

Kohler, A. C. (1966). Feeding and growth of redfish (Sebastes) in captivity. Journal of the Fisheries Research Board of Canada, 23(10), 1621–1623.

Kreiss, C. M., Michael, K., Lucassen, M., Jutfelt, F., Motyka, R., Dupont, S., & Pörtner, H. O. (2015). Ocean warming and acidification modulate energy budget and gill ion regulatory mechanisms in Atlantic cod (*Gadus morhua*). Journal of Comparative Physiology B, 185(7), 767–781. https://doi.org/10.1007/s00360-015-0923-7

Kroeker, K. J., Kordas, R. L., Crim, R., & Hendriks, I. E. (2013). Impacts of ocean acidification on marine organisms: Quantifying sensitivities and interaction with warming. Global Change Biology, 19, 1884–1896. https://doi.org/10.1111/gcb.12179

Kuznetsova, A., Brockhoff, P., & Christensen, R. (2017). lmerTest package: Tests in linear mixed effects models. Journal of Statistical Software, 82, 1–26.

Laroque, R. (2000). A SCUBA technique for collecting live Sebastes spp. specimens. Canadian Technical Report of Fisheries and Aquatic Sciences, 2309, v + 13 p.

Lavaud, R., Thomas, Y., Pecquerie, L., Benoît, H. P., Guyondet, T., Flye-Sainte-Marie, J., & Chabot, D. (2018). Modeling the impact of hypoxia on the energy budget of Atlantic cod in two populations of the Gulf of St. Lawrence, Canada. Journal of Sea Research, 143, 243–253. https://doi.org/10.1016/j.seares.2018.07.001

Lavoie, D., Lambert, N., Rousseau, S., Dumas, J., Chassé, J., Long, Z., Perrie, W., Starr, M., Brickman, D., & Azetsu-Scott, K. (2020). Projections of future physical and biogeochemical conditions in the Gulf of St. Lawrence, on the Scotian Shelf and in the Gulf of Maine. Canadian Technical Report of Hydrography and Ocean Sciences, 334.

Lavoie, D., Lambert, N., Starr, M., Chassé, J., Riche, O., Le Clainche, Y., Azetsu-Scott, K., Béjaoui, B., Christian, J. R., & Gilbert, D. (2021). The Gulf of St. Lawrence biogeochemical model: A modelling tool for fisheries and ocean management. Frontiers in Marine Science, 8, 1–29. https://doi.org/10.3389/fmars.2021.732269

Lee, K., Kim, T., Byrne, R. H., Millero, F. J., Feely, R. A., & Liu, Y. (2010). The universal ratio of boron to chlorinity for the North Pacific and North Atlantic oceans. Geochimica et Cosmochimica Acta, 74(6), 1801–1811. https://doi.org/10.1016/j.gca.2009.12.027

Lefevre, S. (2016). Are global warming and ocean acidification conspiring against marine ectotherms? A meta-analysis of the respiratory effects of elevated temperature, high CO_2 and their interaction. Conservation Physiology, 4, 1–31. https://doi.org/10.1093/conphys/cow009

Leung, C., Guitard, J. J., Senay, C., Bourret, A., Chabot, D., & Parent, G. J. (2025). Past environments modulate response to fluctuating temperatures in a marine fish species, Sebastes fasciatus. Journal of Experimental Biology, 228(21). https://doi.org/10.1242/jeb.251288

Licandeo, R., Duplisea, D. E., Senay, C., Marentette, J. R., & McAllister, M. K. (2020). Management strategies for spasmodic stocks: A canadian atlantic redfish fishery case study. Canadian Journal of Fisheries and Aquatic Sciences, 77(4), 684–702. https://doi.org/10.1139/cjfas-2019-0210

Liu, X., Patsavas, M. C., & Byrne, R. H. (2011). Purification and characterization of meta-cresol purple for spectrophotometric seawater pH measurements. Environmental Science & Technology, 45(11), 4862–4868. https://doi.org/10.1021/es200665d

Maccracken, M., Briones, E. E., Gilbert, D., Korotaev, G., Naqvi, W., Perillo, G. M. E., Rixen, T. I. M., Stanev, E., Sundby, B., Thomas, H., Unger, D., & Urban, E. R. (2009). Vulnerability of semi-enclosed marine systems to environmental disturbances. In E. R. Urban, G. Sundbeck, & H. Kremer (Eds.), (pp. 7–34). Island Press.

Madenjian, C. P., Chipps, S. R., Deslauriers, D., Guitard, J. J., & Daigle, N. J. (2023). Fish bioenergetics modeling. In Reference module in life sciences (2nd ed.). Elsevier. https://doi.org/10.1016/b978-0-323-90801-6.00063-x

Martínez-Silva, M. A., Vagner, M., Senay, C., & Audet, C. (2022). Using gene expression to identify the most suitable environmental conditions for growth and metabolism of juvenile deepwater redfish (*Sebastes mentella*) in the estuary and the Gulf of St. Lawrence. ICES Journal of Marine Science, 79(2), 382–393. https://doi.org/10.1093/icesjms/fsab269

Mattiasen, E. G., Kashef, N. S., Stafford, D. M., Logan, C. A., Sogard, S. M., Bjorkstedt, E. P., & Hamilton, S. L. (2020). Effects of hypoxia on the behavior and physiology of kelp forest fishes. Global Change Biology, 26, 3498–3511.

Mehrbach, C., Culberson, C. H., Hawley, J. E., & Pytkowicz, R. M. (1973). Measurement of the apparent dissociation constants of carbonic acid in seawater at atmospheric pressure. Limnology and Oceanography, 18, 897–907. https://doi.org/10.4319/lo.1973.18.6.0897

Millero, F. J. (1986). The pH of estuarine waters. Limnology and Oceanography, 31(4), 839–847. https://doi.org/10.4319/lo.1986.31.4.0839

Mintrop, L., Pérez, F. F., González-Dávila, M., Santana-Casiano, M., & Körtzinger, A. (2000). Alkalinity determination by potentiometry: Intercalibration using three different methods. Ciencias Marinas, 26, 23–27. https://doi.org/10.7773/cm.v26i1.573

Mochnacz, N. J., Kissinger, B. C., Deslauriers, D., Guzzo, M. M., Enders, E. C., Anderson, W. G., Docker, M. F., Isaak, D. J., Durhack, T. C., & Treberg, J. R. (2017). Development and testing of a simple field-based intermittent-flow respirometry system for riverine fishes. Conservation Physiology, 5(1). https://doi.org/10.1093/conphys/cox048

Möllmann, C., & Diekmann, R. (2012). Marine ecosystem regime shifts induced by climate and overfishing: A review for the Northern Hemisphere. In G. Woodward, U. Jacob, & E. J. O'Gorman (Eds.), Advances in ecological research (pp. 303–347). Academic Press. https://doi.org/10.1016/B978-0-12-398315-2.00004-1

Mucci, A., Starr, M., Gilbert, D., & Sundby, B. (2011). Acidification of lower St. Lawrence estuary bottom waters. Atmosphere-Ocean, 49(3), 206–218. https://doi.org/10.1080/07055900.2011.599265

Muggeo, V. M. R. (2003). Estimating regression models with unknown break-points. Statistics in Medicine, 22, 3055–3071.

Nakagawa, S., & Schielzeth, H. (2013). A general and simple method for obtaining R2 from generalized linear mixed-effects models. Methods in Ecology and Evolution, 4(2), 133–142. https://doi.org/10.1111/j.2041-210x.2012.00261.x

Nelson, J. A. (2016). Oxygen consumption rate v. rate of energy utilization of fishes: A comparison and brief history of the two measurements. Journal of Fish Biology, 88(1), 10–25. https://doi.org/10.1111/jfb.12824

Nelson, J. A., & Chabot, D. (2024). Energy consumption: Metabolism. In S. L. Alderman & T. E. Gillis (Eds.), Encyclopedia of fish physiology (Vol. 2, pp. 482–492). Elsevier. https://doi.org/10.1016/B978-0-323-90801-6.00084-7

Nesbitt, W. A., & Mucci, A. (2021). Direct evidence of sediment carbonate dissolution in response to bottom-water acidification in the Gulf of St. Lawrence, Canada. Canadian Journal of Earth Sciences, 58(1), 84–92. https://doi.org/10.1139/cjes-2020-0020

Norin, T., Canada, P., Bailey, J. A., & Gamperl, A. K. (2019). Thermal biology and swimming performance of Atlantic cod (*Gadus morhua*) and haddock (*Melanogrammus aeglefinus*). PeerJ, 2019(10), 1–25. https://doi.org/10.7717/peerj.7784

Norin, T., Malte, H., & Clark, T. D. (2014). Aerobic scope does not predict the performance of a tropical eurythermal fish at elevated temperatures. Journal of Experimental Biology, 217(2), 244–251. https://doi.org/10.1242/jeb.089755

Nuic, B., Bowden, A., Franklin, C. E., & Cramp, R. L. (2024). Atlantic salmon (*Salmo salar*) do not prioritize digestion when energetic budgets are constrained by warming and hypoxia. Journal of Fish Biology, 104, 1718–1731

Oligny-Hébert, H., Senay, C., Enders, E. C., & Boisclair, D. (2015). Effects of diel temperature fluctuation on the standard metabolic rate of juvenile Atlantic salmon (*Salmo salar*): Influence of acclimation temperature and provenience. Canadian Journal of Fisheries and Aquatic Sciences, 72, 1306–1315

Ouellette-Plante, J., Chabot, D., Nozères, C., & Bourdages, H. (2020). Diets of demersal fish from the CCGS Teleost ecosystemic surveys in the estuary and northern Gulf of St. Lawrence, August 2015–2017. Canadian Technical Report of Fisheries and Aquatic Sciences, 3383, v + 121 p.

Parmesan, C., & Yohe, G. (2003). A globally coherent fingerprint of climate change. Nature, 421, 37–42. https://doi.org/10.1038/nature01286

Perez, F. F., & Fraga, F. (1987). Association constant of fluoride and hydrogen ions in seawater. Marine Chemistry, 21, 161–168. https://doi.org/10.1016/0304-4203(87)90036-3

Perry, S. F., Jonz, M. G. et Gilmour, K. M. (2009). Oxygen sensing and the hypoxic ventilatory response. Dans A. P. Farrell, C. J. Brauner et J. G. Richards (dir.), Fish Physiology (Academic P, chap. Chapter 5, p. 193-253). Academic Press.

Perry, S. F., & Wood, C. M. (1989). Control and coordination of gas transfer in fishes. Canadian Journal of Zoology, 67, 2961–2970

Pichavant, K., Person-Le-Ruyet, J., Le Bayon, N., Sévère, A., Le Roux, A., Quéméner, L., Maxime, V., Nonnotte, G., & Boeuf, G. (2000). Effects of hypoxia on growth and metabolism of juvenile turbot. Aquaculture, 188, 103–114

Pichavant, K., Person-Le-Ruyet, J., Le Bayon, N., Severe, A., Le Roux, A., & Boeuf, G. (2001). Comparative effects of long-term hypoxia on growth, feeding and oxygen consumption in juvenile turbot and European sea bass. Journal of Fish Biology, 59, 875–883

Pihl, L., Baden, S. P., & Diaz, R. J. (1991). Effects of periodic hypoxia on distribution of demersal fish and crustaceans. Marine Biology, 108, 349–360

Plante, S., Chabot, D., & Dutil, J. D. (1998). Hypoxia tolerance in Atlantic cod. Journal of Fish Biology, 53, 1342–1356

Platt, T., Fuentes-Yaco, C., & Frank, K. T. (2003). Spring algal bloom and larval fish survival. Nature, 423, 398–399. https://doi.org/10.1038/423398b

Pollock, M. S., Clarke, L. M. J., & Dubé, M. G. (2007). The effects of hypoxia on fishes: From ecological relevance to physiological effects. Environmental Reviews, 15, 1–14. https://doi.org/10.1139/a06-006

Pörtner, H. (2001). Climate change and temperature-dependent biogeography: Oxygen limitation of thermal tolerance in animals. Naturwissenschaften, 88(4), 137–146. https://doi.org/10.1007/s001140100216

Pörtner, H. O. (2010). Oxygen- and capacity-limitation of thermal tolerance: A matrix for integrating climate-related stressor effects in marine ecosystems. Journal of Experimental Biology, 213(6), 881–893. https://doi.org/10.1242/jeb.037523

Pörtner, H. O., & Farrell, A. P. (2008). Physiology and climate change. Science, 322, 690–692

Pörtner, H. O., & Knust, R. (2007). Climate change affects marine fishes through the oxygen limitation of thermal tolerance. Science, 315, 95–97

Prinzing, T. S., Zhang, Y., Dulvy, N. K., & Wegner, N. C. (2021). Analytical methods matter too: Establishing a framework for estimating maximum metabolic rate for fishes. Ecology and Evolution, 9987–10003

Quinn, G. P., & Keough, M. J. (2002). Experimental design and data analysis for biologists. Cambridge University Press

Rabalais, N. N., Díaz, R. J., Levin, L. A., Turner, R. E., Gilbert, D., & Zhang, J. (2010). Dynamics and distribution of natural and human-caused hypoxia. Biogeosciences, 7(2), 585–619. https://doi.org/10.5194/bg-7-585-2010

Randall, D. (1982). The control of respiration and circulation in fish during exercise and hypoxia. Journal of Experimental Biology, 100, 275–288

Richards, J. G. (2011). Metabolic rate suppression as a mechanism for surviving hypoxia. In A. P. Farrell (Ed.), Encyclopedia of fish physiology (pp. 1767–1775). Academic Press. https://doi.org/10.1016/B978-0-12-374553-8.00208-4

Roche, D. G., Binning, S. A., Bosiger, Y., Johansen, J. L., & Rummer, J. L. (2013). Finding the best estimates of metabolic rates in a coral reef fish. Journal of Experimental Biology, 216, 2103–2110

Roques, S., Sévigny, J. M., & Bernatchez, L. (2002). Genetic structure of deep-water redfish, *Sebastes mentella*, populations across the North Atlantic. Marine Biology, 140(2), 297–307. https://doi.org/10.1007/s002270100705

Rosenfeld, J., & Lee, R. (2022). Thresholds for reduction in fish growth and consumption due to hypoxia: Implications for water quality guidelines to protect aquatic life. Environmental Management, 70, 431–447

Rummer, J. L., Binning, S. A., Roche, D. G., & Johansen, J. L. (2016). Methods matter: Considering locomotory mode and respirometry technique when estimating metabolic rates of fishes. Conservation Physiology, 4, 1–13

Rummer, J. L., Stecyk, J. A. W., Couturier, C. S., Watson, S. A., Nilsson, G. E., & Munday, P. L. (2013). Elevated CO_2 enhances aerobic scope of a coral reef fish. Conservation Physiology, 1(1), cot023. https://doi.org/10.1093/conphys/cot023

Saborido-Rey, F., Garabana, D., & Cerviño, S. (2004). Age and growth of redfish (*Sebastes marinus*, *S. mentella*, and *Sebastes fasciatus*) on the Flemish Cap (Northwest Atlantic). ICES Journal of Marine Science, 61, 231–242.

Sánchez Lizaso, J. L., Goñi, R., Reñones, O., García Charton, J. A., Galzin, R., Bayle, J. T., Sánchez Jerez, P., Perez Ruzafa, A., & Ramos, A. A. (2000). Density dependence in marine protected populations: A review. Environmental Conservation, 27(2), 144–158. https://doi.org/10.1017/S0376892900000187

Schulte, P. M. (2015). The effects of temperature on aerobic metabolism: Towards a mechanistic understanding of the responses of ectotherms to a changing environment. Journal of Experimental Biology, 218(12), 1856–1866. https://doi.org/10.1242/jeb.118851

Schulte, P. M., Healy, T. M., & Fangue, N. A. (2011). Thermal performance curves, phenotypic plasticity, and the time scales of temperature exposure. Integrative and Comparative Biology, 51(5), 691–702. https://doi.org/10.1093/icb/icr097

Schurmann, H., Steffensen, J. F., & Bushnell, P. G. (1994). Oxygen consumption in four species of teleosts from Greenland: No evidence of metabolic cold adaption. Polar Biology, 14, 49–54.

Scott, J. S. (1982). Depth, temperature and salinity preferences of common fishes of the Scotian Shelf. Journal of Northwest Atlantic Fishery Science, 3, 29–39. https://doi.org/10.2960/j.v3.a2

Senay, C., & Duplisea, D. (2024). Potential removals of redfish (*Sebastes mentella* and *Sebastes fasciatus*) in unit 1. DFO Canadian Science Advisory Secretariat Research Document, 2024/031, iv + 11 p.

Senay, C., Bermingham, T., Parent, G. J., Hugues, P., Parent, É., & Bourret, A. (2022). Identifying two redfish species, *Sebastes mentella* and *S. fasciatus*, in fishery and survey catches using anal fin ray count in units 1 and 2. Canadian Technical Report of Fisheries and Aquatic Sciences, 3445, viii + 46 p.

Senay, C., Rousseau, S., Brûlé, C., Chavarria, C., Isabel, L., Parent, G. J., Chabot, D., & Duplisea, D. (2023). Unit 1 redfish (*Sebastes mentella* and *Sebastes fasciatus*) stock status in 2021. DFO Canadian Science Advisory Secretariat Research Document, 2023/036, xi + 125 p.

Stefánsson, M., Reinert, J., Sigurðsson, Þ., Kristinsson, K., Nedreaas, K., & Pampoulie, C. (2009). Depth as a potential driver of genetic structure of *Sebastes mentella* across the North Atlantic Ocean. ICES Journal of Marine Science. https://doi.org/10.1093/icesjms/fsp059

Steffensen, J. F. (1989). Some errors in respirometry of aquatic breathers: How to avoid and correct for them. Fish Physiology and Biochemistry, 6, 49–59.

Stendardo, I., & Gruber, N. (2012). Oxygen trends over five decades in the North Atlantic. Journal of Geophysical Research: Oceans, 117(11), 1–18. https://doi.org/10.1029/2012JC007909

Svendsen, M. B. S., Bushnell, P. G., & Steffensen, J. F. (2016). Design and setup of intermittent-flow respirometry system for aquatic organisms. Journal of Fish Biology, 88, 26–50.

Therneau, T. M. (2020). A package for survival analysis in R (R package version 3.1-12).

Therneau, T. M., & Grambsch, P. M. (2000). The Cox model. In Modeling survival data: Extending the Cox model (pp. 39–77). Springer.

Thibodeau, B., Lehmann, M. F., Kowarzyk, J., Mucci, A., Gélinas, Y., Gilbert, D., Maranger, R., & Alkhatib, M. (2010). Benthic nutrient fluxes along the Laurentian Channel: Impacts on the N budget of the St. Lawrence marine system. Estuarine, Coastal and Shelf Science, 90(4), 195–205. https://doi.org/10.1016/j.ecss.2010.08.015

Thomas, Y., & Bacher, C. (2018). Assessing the sensitivity of bivalve populations to global warming using an individual-based modelling approach. Global Change Biology, 24(10), 4581–4597. https://doi.org/10.1111/gcb.14402

Thomas, Y., Flye-Sainte-Marie, J., Chabot, D., Aguirre-Velarde, A., Marques, G. M., & Pecquerie, L. (2018). Effects of hypoxia on metabolic functions in marine organisms: Observed patterns and modelling assumptions within the context of dynamic energy budget (DEB) theory. Journal of Sea Research, 143, 231–242. https://doi.org/10.1016/j.seares.2018.05.001

Turko, A. J., Firth, B. L., Craig, P. M., Eliason, E. J., Raby, G. D., & Borowiec, B. G. (2023). Physiological differences between wild and captive animals: A century-old dilemma. Journal of Experimental Biology, 226, 1–11. https://doi.org/10.1242/jeb.246037

Valentin, A. E., Penin, X., Chanut, J., Power, D., & Sévigny, J. (2014). Combining microsatellites and geometric morphometrics for the study of redfish (*Sebastes spp.*) population structure in the Northwest Atlantic. Fisheries Research, 154, 102–119. https://doi.org/10.1016/j.fishres.2014.02.008

Vaquer-Sunyer, R., & Duarte, C. M. (2008). Thresholds of hypoxia for marine biodiversity. Proceedings of the National Academy of Sciences of the United States of America, 105(40), 15452–15457. https://doi.org/10.1073/pnas.0803833105

Volkoff, H., & Rønnestad, I. (2020). Effects of temperature on feeding and digestive processes in fish. Temperature, 7, 307–320.

Wallace, D. W. R., Jutras, M., Nesbitt, W. A., & Donaldson, A. (2023). Can green hydrogen production be used to mitigate ocean deoxygenation? A scenario from the Gulf of St. Lawrence. Mitigation and Adaptation Strategies for Global Change, 28(8), 1–15. https://doi.org/10.1007/s11027-023-10094-1

Wang, Y., Gharouni, A., Friedland, K. D., & Melrose, D. C. (2021). Effect of environmental factors and density-dependence on somatic growth of eastern Georges Bank haddock (*Melanogrammus aeglefinus*). Fisheries Research, 240, 105954. https://doi.org/10.1016/j.fishres.2021.105954

Wang, T., Lefevre, S., Thanh Huong, D. T., Cong, N. van, & Bayley, M. (2009). The effects of hypoxia on growth and digestion. Fish Physiology, 27. https://doi.org/10.1016/S1546-5098(08)00008-3

Ward, P., & Myers, R. A. (2005). Shifts in open-ocean fish communities coinciding with the commencement of commercial fishing. Ecology, 86(4), 835–847.

Wood, S. (2017). Generalized additive models: An introduction with R (2nd ed.). Chapman and Hall/CRC.

Wu, R. S. S. (2002). Hypoxia: From molecular responses to ecosystem responses. Marine Pollution Bulletin, 45(1–12), 35–45. https://doi.org/10.1016/S0025-326X(02)00061-9

Yang, E. J., Zhang, J. D., Yang, L. T., Amenyogbe, E., Wang, W. Z., Huang, J. S., & Chen, G. (2021). Effects of hypoxia stress on digestive enzyme activities, intestinal structure and the expression of tight junction proteins coding genes in juvenile cobia (*Rachycentron canadum*). Aquaculture Research, 52(11), 5630–5641. https://doi.org/10.1111/are.15438

Yoon, G. R., Bozai, A., & Porteus, C. S. (2024). Could future ocean acidification be affecting the energy budgets of marine fish? Conservation Physiology, 12, 1–13. https://doi.org/10.1093/conphys/coae069

Zhang, W., Cao, Z. D., Peng, J. L., Chen, B. J., & Fu, S. J. (2010). The effects of dissolved oxygen level on the metabolic interaction between digestion and locomotion in juvenile southern catfish (*Silurus meridionalis* Chen). Comparative Biochemistry and Physiology Part A: Molecular and Integrative Physiology, 157, 212–219.

Zhang, Y., Gilbert, M. J. H., & Farrell, A. P. (2019). Finding the peak of dynamic oxygen uptake during fatiguing exercise in fish. Journal of Experimental Biology, 222.

Zhang, Y., So, B. E., & Farrell, A. P. (2021). Hypoxia performance curve: Assess a whole-organism metabolic shift from a maximum aerobic capacity towards a glycolytic capacity in fish. Metabolites, 11, 1–16.

Zhu, C. D., Wang, Z. H., & Yan, B. (2013). Strategies for hypoxia adaptation in fish species: A review. Journal of Comparative Physiology B, 183(8), 1005–1013. https://doi.org/10.1007/s00360-013-0762-3